Biomedical Sciences ETDs   Electronic Theses and Dissertations

5-1-2011

Live cell kinetics of erbB dimerization reveals influences of activation state and membrane organization

Shalini Low-Nam

Follow this and additional works at: https://digitalrepository.unm.edu/biom_etds

Recommended Citation

Shalini T. Low-Nam
Candidate

Biomedical Sciences
Department

This dissertation is approved, and it is acceptable in quality
and form for publication:

Approved by the Dissertation Committee:

Bridget Wilson   , Chairperson

Janet M Oliver

Kim Self

Diane Lidke

Jim A Tile

LIVE CELL KINETICS OF ERBB DIMERIZATION REVEALS INFLUENCES OF ACTIVATION STATE AND MEMBRANE ORGANIZATION

BY

SHALINI T. LOW-NAM

B.S. Molecular and Cellular Biology/French
The Johns Hopkins University, 2004

DISSERTATION

Submitted in Partial Fulfillment of the
Requirements for the Degree of

**Doctor of Philosophy
Biomedical Sciences**

The University of New Mexico
Albuquerque, New Mexico

May 2011

DEDICATION

I dedicate this work to my wonderful G&G, who know why words fail me. Thank you, Gypsy, for always reminding me to smile and relax, even after the longest and hardest days. You have taught me about spontaneity, going big, unconditional love, and grace. To my husband, Geoffrey, I do not have an adequate way to express my love and gratitude for the ways in which you challenge and inspire me. You have been so patient and kind during these years and have been my collaborator in everything. I value our partnership immensely and am proud that this document reflects our shared contributions.

I am also happy to share this dissertation with my family. To my sister, Dr. Nisha Cavanaugh, I am honored to be your baby sister and have learned so much from you. To my mother, Dr. Margaret Asirvatham, thank you for playing the most prominent role in my formative years as a scientist. To my father, Simon Low-Nam, thank you for years of support and for encouraging me to continually learn new skills. Craig, thanks for teaching me to climb; this outlet has been the perfect intellectual and athletic endeavor for us to maintain our sanity and share with friends. Hannah, thanks for allowing us to live vicariously through you and for keeping us young. To Janet and Steve Graff, thank you for fostering our creativity and independence and being willing to try new things with us.

Finally, I will always remember those who could not be here to share this with us. Amma, Joseph Uncle, Vesalius and others, you have a special place in my heart and I hope to represent you well.

ACKNOWLEDGEMENTS

There are numerous people for whose mentorship, advice, friendship, and kindness I am grateful. First and foremost are my co-mentors, Dr. Bridget Wilson and Dr. Diane Lidke. To Bridget, I will always be grateful for your enthusiasm for science and discussing results. I hope to learn to wear as many hats as you do with as much success. To Diane, thank you for teaching me so many techniques and, especially, for keeping up an invaluable dialogue on science, teaching, and many other topics. For you, I affectionately subtitle this dissertation, "It Takes Two to Tango." I thank both of these women for inspiring me and giving me a high standard to aspire to. I am grateful for their kindness in participating in my scientific education, my wedding, and will continue to look forward to their guidance in the future.

I have also been fortunate to have an invaluable Committee on Studies. I thank Dr. Keith Lidke for his ongoing participation in the development of analytical software and tools and for teaching me so much about MatLab. Furthermore, I have enjoyed his creative speculations about phenomena and appreciate his willingness to discuss confounding results. Dr. Debi Evans has been an important presence on my committee who provides me with an outlet to use my tendency to approach questions from a chemistry perspective. She has also given an opportunity to teach with her, which was a great interdisciplinary experience. Dr. Jeremy Edwards has taught me about the power of mathematical modeling and I look forward to the application of parameters from our measurements being implemented into his group's computational models. Finally, Dr. Janet Oliver has provided wisdom and invaluable expertise in preparing manuscripts

and in brainstorming ideas for my projects. I also thank Dr. Jeri Timlin for serving as an external reviewer for my dissertation defense.

The next person who I have to acknowledge is Geoffrey Graff, principal of ideo**craft**. He has helped me to develop wonderful visuals that make the communication of difficult concepts much more accessible.

The post-doctoral fellows and research assistant professors who have always treated me like a colleague have made a strong impression on me; I am grateful for their contributions to my project and to my career development. Dr. Amanda Carroll-Portillo, Dr. Heather Ward, and Dr. Mara Steinkamp have always engaged me in stimulating discourse and I have really enjoyed our interactions.

I am also grateful to the members of the OWL lab, past and present, who have aided in my projects. The opportunity to work in a large research group has been invaluable. First, to the technicians Marina Martinez, Christy Tarleton, Sheli Ryan, Janet Pfeiffer, Mary Raymond-Stintz, Angela Welford, and Anna Holmes, thank you for teaching me techniques and assays and, particularly, for helping me to learn about being a good lab citizen. To my fellow students and colleagues, especially Patrick Cutler and Jason Byars, I have learned a lot from working with you. There are many other members of the lab who have made the environment a productive one – I will try to remember all the lessons I learned from each of you.

I am grateful for colleagues in the Biomedial Sciences and NanoScience and Microsystems programs with whom have I have shared memorable times arguing with and learning from. Foremost among them are Nick Andrews, Ryan Brunsing, Jessica Seidel, and Samantha Schwartz.

LIVE CELL KINETICS OF ERBB DIMERIZATION
REVEALS INFLUENCES OF ACTIVATION STATE
AND MEMBRANE ORGANIZATION

BY

SHALINI T. LOW-NAM

ABSTRACT OF DISSERTATION

Submitted in Partial Fulfillment of the
Requirements for the Degree of

Doctor of Philosophy
Biomedical Sciences

The University of New Mexico
Albuquerque, New Mexico

May 2011

LIVE CELL KINETICS OF ERBB DIMERIZATION REVEALS INFLUENCES OF ACTIVATION STATE AND MEMBRANE ORGANIZATION

by

Shalini T. Low-Nam

B.S., Molecular and Cellular Biology/French, The Johns Hopkins University, 2004

Ph.D., Biomedical Sciences, 2011

ABSTRACT

The erbB1 receptor regulates cellular programs including proliferation, migration, and differentiation and is the prototypical receptor tyrosine kinase (RTK). The erbB family consists of four homologous transmembrane receptors (erbB1/HER1/EGFR, erbB2/HER2, erbB3/HER3, erbB4). Canonically, ligand binding leads to an extracellular conformational change that promotes the formation of a receptor-mediated back-to-back dimer, asymmetric orientation of the catalytic kinase domains, and downstream transphosphorylation of cytoplasmic tyrosine residues. Exceptions to this paradigm are the orphan erbB2 and the kinase defective erbB3. The erbB receptors are implicated in mechanisms of carcinogenesis and are, thus, important therapeutic targets. Antibodies and small molecule inhibitors have been used to target cancer cells expressing erbB1 and erbB2, however, tumors often become resistant to treatment. Recent evidence implicates erbB3 in escape from erbB1- and erbB2-targeted pharmacological agents. Therefore, understanding the function of these receptors and their interactions with each other is important for designing better therapeutics.

Here, we investigated erbB dimer formation and lifetime using live cell imaging and an analytical three-state Hidden Markov Model (HMM). First, multi-color quantum dot (QD) based probes that label resting or activated receptors were used to directly

observe dimerization and quantify diffusion and correlated motion. Second, pairwise analyses of single particle trajectories in our HMM are used to characterize transition rates between free, confined, and dimerized states. We examined preformed, unliganded erbB1 homodimers and demonstrate that these do not display correlated motion and that observed dimers are short lived. Interestingly, liganded erbB1 dimers have the same off rate regardless of the activation status of the kinase domain. We further describe features of membrane organization, in particular demonstrating differential partitioning of activated receptors that alters mobility and permits repeated interactions within domains.

Important mechanistic insight comes from our novel observations of short lived erbB2-erbB3 heterodimers and long lived erbB3 homodimers. Prior biochemical studies suggested that the erbB2-erbB3 heterodimer was the functional signaling unit. Our single particle tracking results are consistent with a new model for an active erbB3 kinase domain that is dependent on interactions with erbB2. Furthermore, our data indicate that erbB3 dimers and, ultimately, oligomers may be the principal signaling complex. This work demonstrates the importance of membrane architecture and reorganization in signal transduction and sheds new light on mechanisms of erbB activation with unprecedented spatial and temporal resolution.

Table of Contents

x

List of Figures

List of Tables

CHAPTER 1: INTRODUCTION

1.1 Overview

Cells must finely tune their responses to environmental cues in order to survive, promote differentiation and proliferation, and modulate other essential mechanisms. This is accomplished through transduction of extracellular signals through the plasma membrane into the cytoplasm and nucleus, controlling enzymatic activity and genetic programs. Although stringent regulation of cell signaling is necessary to maintain homeostasis, the details of the spatiotemporal control of these pathways are still poorly understood. *The dynamics of cell surface receptors, including diffusive characteristics, spatial distribution, and interactions with binding partners must be better characterized to understand how these parameters impact signal integration.* In particular, studying these properties in the context of the cell membrane is essential to understand how membrane composition and fluidity affects protein-protein interactions and clustering (Singer and Nicolson, 1972; Metzger, 1992).

The work presented here addresses some of these important issues with a focus on the erbB family of receptors. The following sections of this introduction describe erbB signaling, with a focus on mechanisms of receptor dimerization and the role of membrane reorganization on signaling. Next, the specific biophysical and analytical techniques that are applied to studying receptor dynamics at the single molecule level are described. Finally, this section closes with an overview of results presented within this dissertation, including the central hypothesis and the significance of this body of work.

1

1.2 Quantitative approaches to erbB1 receptor activation, signaling, and regulation

1.2.1 Key Words

EGFR/erbB1, receptor tyrosine kinase, receptor-mediated dimerization, tetramer, single molecule fluorescence, FRET

1.2.2 Abstract

Due to its complexity, the spatiotemporal control of erbB receptor dynamics has been of longstanding interest and the subject of extensive investigation, innovation, and debate. As canonical models for signal transduction, these transmembrane proteins have provided the prototype for many other cellular pathways and mechanisms. Biophysical studies to investigate erbB activation, signaling, and regulation have used a variety of approaches from biochemical to microscopy techniques. Mechanisms of erbB receptor dynamics have largely relied on structural studies that suggest the sequential formation of a dimer with extracellular symmetry and intracellular asymmetry. Recent investigations into the structure of the domain-bridging juxtamembrane sequence reconcile some outstanding questions about erbB activation and highlight a role for this region to stabilize the kinase dimer. In addition, approaches based on fluorescence imaging have permitted live cell monitoring of erbB dynamics. Data from these new methods refine the model for erbB receptor activity and the reactions that occur proximal to the plasma membrane, from ligand binding to downstream phosphorylation and adaptor protein recruitment. In this chapter, we highlight the molecular mechanisms of erbB receptor activation that have emerged from biophysical approaches, with an emphasis on fluorescence-based techniques.

1.2.3 Introduction

The identification of oncogenic mutations in proteins has led to ongoing efforts to better characterize the subtleties of protein-protein interactions that lead to the aberrant phenotype (Zhang et al., 2007). Under physiological conditions, receptor tyrosine kinase (RTK) receptors are implicated in normal growth, differentiation, adhesion, and cellular migration events. These transmembrane receptors are found in a variety of cell lineages and coordinate normal development. In the disease state, aberrant signaling by RTKs is often associated with poor outcomes. Despite decades of investigation into RTK function, many fundamental questions about the spatiotemporal regulation of receptor signaling dynamics remain unanswered.

The erbB family of RTKs is comprised of four homologous plasma membrane spanning receptors whose archetype member, the Epidermal Growth Factor Receptor (EGFR or erbB1 or HER1) is the main subject of this chapter. These ~170-180 kDa receptors share an architecture based on three principal domains: a ligand binding ectodomain, a transmembrane domain, and a cytoplasmic region associated with tyrosine kinase activity (Figure 1.1). The intracellular and extracellular domains are further subdivided into functional units that have been implicated in receptor activation and downstream signaling. Upon binding of the epidermal growth factor (EGF) ligand, the extracellular domain of erbB1 undergoes a conformational change from a tethered configuration to an extended one. In this conformation, the ectodomain of the receptor is poised to form the characteristic back-to-back dimer that serves as the activated and signaling competent complex (Mattoon et al., 2004). A family of structurally similar ligands potentiates the signaling of erbB receptors, leading to combinatorial complexity

3

in the formation of homo- and heterodimers, and, ultimately, clusters of receptors. The erbB2 and erbB3 members are exceptions to the general architecture and activity of these RTKs; the former has no cognate ligand and the latter was formerly believed to have limited, if not absent, intrinsic kinase activity (Yarden and Sliwkowski, 2001).

Dimerization of erbB receptors is classically considered as the initiating event in signal transduction by these RTKs and involves substantial domain rearrangements in the extracellular domain upon ligand activation. Domains I and III contain the ligand recognition motifs, whereas domains II and IV contain critical cysteine residues involved in the formation of disulfide bonds that stabilize the dimer. Domain II, in particular, contains a dimer arm motif that is occluded during normal tethering. Upon activation and release of the intermolecular tether, domain II is exposed and can interact with other receptors. Dynamic untethering permits the exposure of the dimer arm in absence of ligand, due to a small energy barrier that has been calculated for the reorientation of domains I and III that is associated with ligand binding (Ferguson et al., 2003; Mattoon et al., 2004) (Figure 1.1).

4
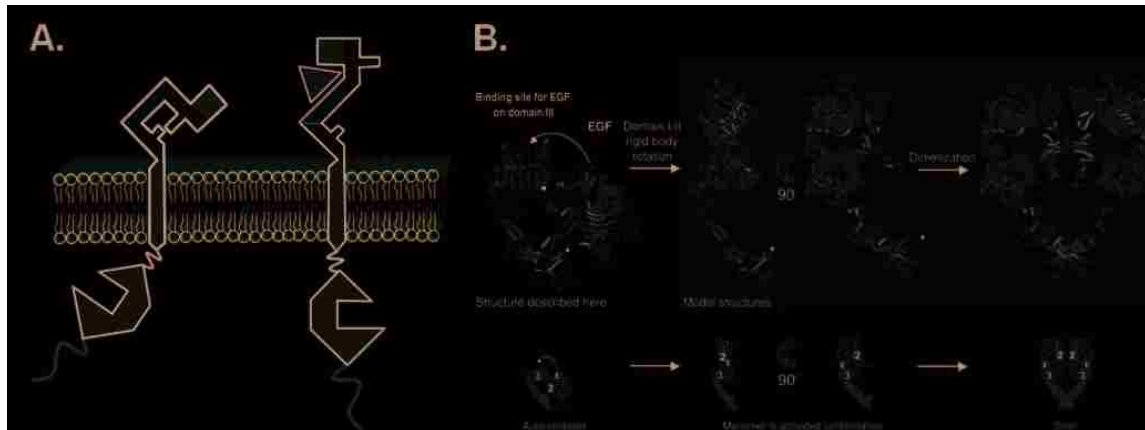
Figure 1.1 – Major domain rearrangements take place upon activation of erbB receptors. A. Binding of epidermal growth factor (EGF; yellow) to erbB1 brings domains I and III into close apposition (red, green, respectively) and permits intermolecular interactions of cysteine residues in domains II and IV of the extracellular domain (blue, purple, respectively). The dimer arm of domain II contributes the majority of the stability to the dimer. The transmembrane domains of receptors (orange) are thought to interact through the GXXXG motifs during dimerization (Lemmon et al., 1994). The cytoplasmic domain has three components: the juxtamembrane domain (black) which forms coiled coils upon dimerization, the catalytic kinase domain (pink; shown oriented with the N-lobe pointing toward the inner leafleft of the plasma membrane and the C-lobe toward the cytoplasm) involved in the asymmetric dimer, and the cytoplasmic tail (brown). Each of these three components contains tyrosine residues that may become phosphorylated upon receptor activation. B. Domain reorientation and rotation in response to ligand binding (Ferguson et al., 2003).

Ferguson provides a very thorough review of the insights that high resolution crystal structures have provided in understanding erbB signaling mechanisms (Ferguson, 2008). In that article, structural changes that occur upon receptor activation are extensively discussed. In the absence of a structure of the intact receptor, a comprehensive model of the domain rearrangements associated with signaling is difficult to assemble. Most importantly, erbB1 has been shown to differ from other RTKs

in the formation of a 2:2 EGF:erbB1 dimer, rather than the 1:2 ligand:receptor dimers that had been shown for closely related RTKs such as the insulin receptor (Burgess et al., 2003; De Meyts, 2008). For the latter, divalent ligands may crosslink receptors and activate downstream signaling, including autophosphorylation of tyrosine residues in the cytoplasmic tail and recruitment of adaptor proteins. The phosphorylated tyrosine residues serve as docking sites for adaptor proteins containing the Src homology domain 2 (SH2) (Pawson, 2004).

Upon the formation of an extracellular dimer, the erbB1 cytoplasmic tails reorient to form an asymmetric intracellular dimer. The N- and C- lobes of the kinase domain associate in an antiparallel fashion that is favorable for transphosphorylation (Figure 1.1). This configuration leads to an activation mechanism analogous to that seen in the interactions of cyclins (Zhang et al., 2006b) and their activators, leading to the use of the terms, "activator" and "receiver" to specify the enzyme and substrate components of the complex.

Structural studies of RTK activation form the basis of our understanding of mechanisms of activation and signaling initiation. However, newer methods have been developed to further detail erbB receptor regulation. Here, we highlight efforts to observe the intact receptor within the cellular membrane as a means of understanding real time receptor dynamics. This chapter focuses on biophysical characterization of membrane-proximal events in erbB1 activation and signaling including:

i.   Ligand-induced conformational changes and receptor dimerization

ii. Membrane environment rearrangements

iii. Tetramerization, oligomerization, and clustering

iv. Structural dimerization conferred by juxtamembrane domain interactions

v. Phosphorylation of cytoplasmic erbB1 residues

vi. Interactions with adaptor proteins

vii. Endocytosis

The concepts presented here, while focused on erbB1 may be applicable to other members of the erbB family and, more generally, to other transmembrane receptors whose signaling is driven by dimerization and clustering.

1.2.4 Structural insights into juxtamembrane domain activation

A substantial recent advance in our understanding of erbB signaling is the characterization of the juxtamembrane (JM) domain by two independent groups (Jura et al., 2009a; Red Brewer et al., 2009). This domain is divided into part A, that contains a helical motif, and part B that interacts directly with the kinase domain (Figure 1.1). Phosphorylation of a threonine residue (Thr654) within the A sequence leads to reduced internalization of erbB1 (Lund et al., 1990). This finding is consistent with a model for inhibition of catalytic activity of the cytoplasmic domain that precludes adaptor protein and endocytic machinery recruitment.

The juxtamembrane domains are autoinhibitory in other members of the RTK family (Hubbard, 2004). Jura, et al. analyzed the cytoplasmic domain of erbB4, including its JM, and Brewer, et al. crystallized a construct of erbB1 containing the entire JM domain (Jura et al., 2009a; Red Brewer et al., 2009). Mutations analysis was used by both groups. In the case of the erbB4 cytoplasmic tail, the JM-A segments could form a coiled-coil as shown using nuclear magnetic resonance. Furthermore, deletion of the JM-A led to diminished kinase activity, suggesting its role in stabilizing the activated

7

dimer. Unexpectedly, the erbB1 crystal by Brewer, et al. does not demonstrate the JM-A dimer expected from the Jura model, which may be explained by the different construct lengths used in these studies. One important caveat is that measurements in the absence of the intact receptor are difficult to equivocate.

Results of Jura, et al. suggest that the formation of a symmetric kinase domain dimer may represent a *non-signaling* complex. The C-terminal tail may block the C-lobe, preventing the activating phosphorylation event. This could explain the lack of signaling in preformed dimers that have been reported (Jura et al., 2009a; Hofman et al., 2010). The transition that takes place to transform an autoinhibitory, symmetric dimer to a signaling competent, asymmetric one remains unclear. The role of the JM segment in the activation mechanism of erbB1 remains incompletely elucidated but the potential for this bridging sequence to control events in erbB1 signaling seems considerable.

1.2.5 Negative cooperativity

Just as the soluble extracellular domain of erbB1 (sEGFR) was important to early crystallographic studies of receptor homodimerization, this recombinant construct has also been invaluable in the early investigations of EGF ligand binding affinity and the kinetics of dimerization (Lemmon et al., 1997; Dawson et al., 2005). Furthermore, these kinds of studies have been invoked to understand the concave up Scatchard plots that are characteristic for EGF binding to sEGFR (Lemmon et al., 1997). Such plots derived from biochemical measurements suggest bimodal ligand binding affinity states (high and low). Based on structure alone, an increased ligand binding affinity is expected upon dimer formation due to accessibility of domains I and III in the membrane proud conformation. Importantly, the curvature of Scatchard plots implies negative

cooperativity in ligand binding to erbB1 and suggests that the transition from 1:2 ligand:receptor hetero-complex to a 2:2 homodimer should be entropically unfavorable (Wofsy et al., 1992; Lemmon et al., 1997; Klein et al., 2004).

The formation of the asymmetric tail dimer may be interpreted to correlate structure, mechanism and the Scatchard plot characteristics. In this case, inside-out regulation of signaling could take the form of altered conformation that promotes or impairs ligand binding. Negative cooperativity has been argued in models for receptor dissociation that lead to signal amplification (Macdonald and Pike, 2008). The loss of affinity in a 1:2 ligand:receptor dimer could alter downstream interactions with adaptor proteins and molecules within the membrane.

Evidence for positive cooperativity has been suggested by an amplified phosphorylation response that exceeds a 1:1 stoichiometric ratio with ligand added (Ichinose et al., 2004). However, it is unclear if a second ligand binding event occurs in the immediate vicinity of the first. Furthermore, this phenomenon may relate to the monomer-dimer equilibrium, rather than simply accounting for receptor affinity for ligand. The argument for positive cooperativity is based on the energetic contribution that the kinase dimer may make to extracellular conformational stability.

1.2.6 ErbB1 dimers, tetramers, and higher-order oligomers

The formation of erbB1 complexes through homoassociation has been characterized using biochemical approaches including chemical crosslinking, immunoprecipitation, small angle x-ray scattering, and sucrose gradient centrifugation (Boni-Schnetzler and Pilch, 1987; Sherrill and Kyte, 1996; Lemmon et al., 1997; Moriki et al., 2001). From these studies, the formation of erbB1 homodimers suggests that

9

these species constitute the minimal signaling unit (Lemmon et al., 1997; Ferguson et al., 2003). However, direct mechanistic evidence of dimer formation and function using the full-length protein and the live cell context remained elusive until the development of sophisticated imaging approaches.

Fluorescence imaging has revolutionized cell biology by providing a toolbox to observe cellular phenomena *in situ* (Lidke and Wilson, 2009). In particular, single molecule approaches have pushed the resolution of imaging well beyond the Rayleigh limit and permitted observation of individual proteins with nanometer accuracy. These high precision imaging approaches have bridged the atomic level information of crystal structures with molecular level details of receptor behaviors and spatial distributions. Several fluorescent probes can be employed in single molecule measurements. Organic dyes and genetically expressed protein tags are useful in monitoring the entire population of erbB receptors simultaneously. Paired dyes that have overlapping spectral properties are useful in approaches that demonstrate the spatial relationship between closely apposed species and will be explained in greater detail in a subsequent section. Complementation assays using fluorescent markers have also been used to provide a high throughput method for screening erbB1 interaction partners (Blakely et al., 2000). Quantum dots (QDs) are particularly important probes due to their bright signal and optical characteristics, which permit long-term observation of individually labeled macromolecules. The combination of ensemble and single molecule approaches has provided both insight and controversy in understanding erbB signal activation and transduction.

10

Lidke, et al. demonstrated successful derivitization of biotinylated EGF ligand with QDs to create a novel probe to detect and monitor the behavior of activated erbB1. In addition to using EGF-QDs to monitor the diffusion of receptors, Lidke, et al. were the first to describe a mechanism for retrograde transport of erbB1 receptors along filopodial projections toward the cell body using a mechanism that is coupled to actin dynamics (Figure 1.2). Using a potent inhibitor of erbB1 kinase activity, PD153035, this work further demonstrated that the signaling competent 2:2 dimer is the fundamental signaling unit (Lidke et al., 2004; Lidke et al., 2005a). Diffusion measurements based on mean squared displacement (MSD) on the filopodia are consistent with other coefficients reported for erbB1 (Appendix A) (Lidke et al., 2005a).
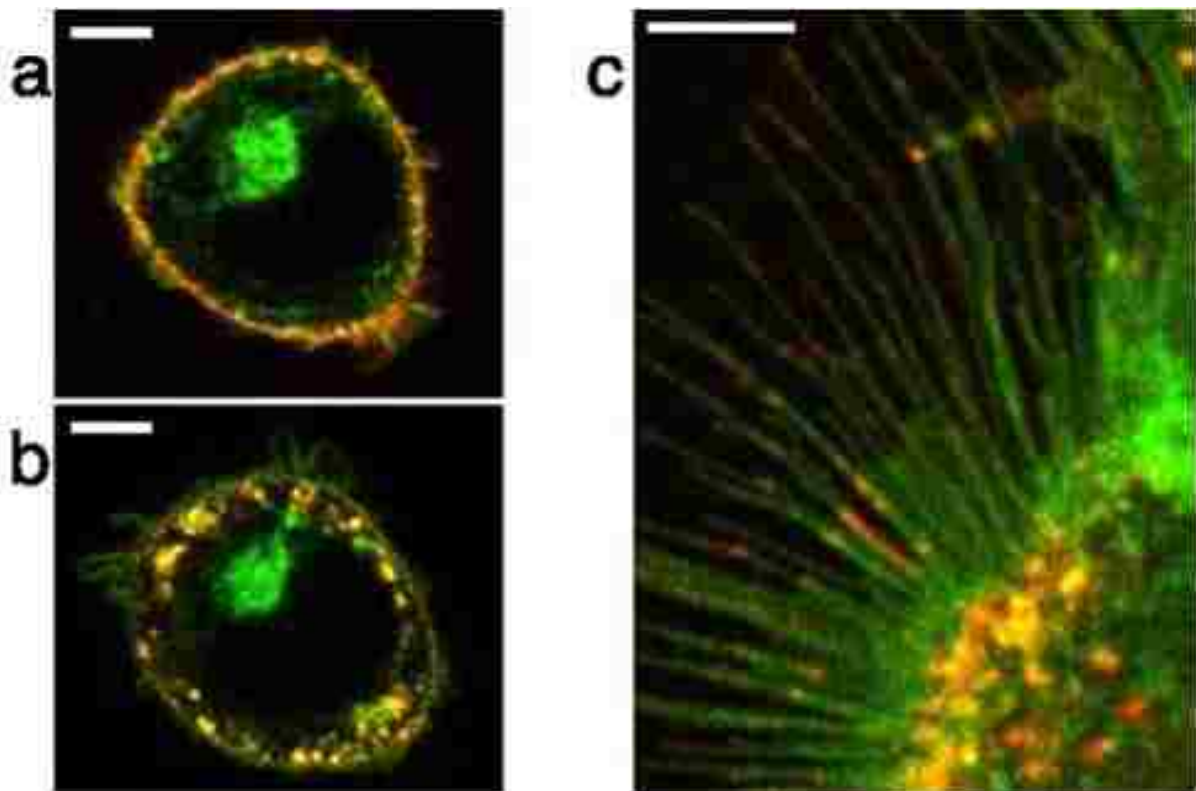
Figure 1.2. Binding of QD-EGF to cell surface erbB1 leads to activation. A. QD-EGF ligand binds to erbB1 receptors and colocalizes with GFP-erbB1. B. Activated receptors

11

are internalized. C. erbB1 receptors are visualized on cell projections called filopodia using QD-EGF (Arndt-Jovin et al., 2006).

An intriguing feature of erbB1 diffusion is the effect of dimerization and signaling on its magnitude. Some reports indicate that a two-fold slowing in receptor mobility reflects successful dimerization, however this parameter was not directly measured (Xiao et al., 2008; Chung et al., 2010). Single-color QD tracking of erbB1 using a cumulative squared displacement approach (CSD) to monitor the K721M mutant that lacks catalytic activity highlighted kinetic stability conferred to dimers by the domain II dimer arm (Chung et al., 2010). Work in our group implementing a multi-color QD tracking method demonstrates that a two-fold decrease in diffusion is observed for liganded receptors that enter a membrane microdomain and that an ultimate 6-fold decrease in mobility marks the formation of a signaling competent dimer. Furthermore, this diffusional slowing is dependent on kinase domain function. In the presence of PD153035, ligand-bound receptors form dimers whose mobility decreases by only a factor of two compared to the monomeric form of the occupied, inhibited erbB1. Importantly, these observations were based on direct visualization of erbB1 homodimerization and diffusion characterized on state-dependent analysis of single molecule trajectories resulting from fitting using a 3-state Hidden Markov Model (HMM). This approach has also permitted extrapolation of receptor interaction kinetics and direct measurement of resting receptor behavior.

Dimers have been detected in the absence of ligand binding and a role for so-called preformed dimers, or predimers, is the subject of some debate (Gadella and Jovin, 1995; Moriki et al., 2001). In particular, the existence of predimers at steady state

12

(Burgess et al., 2003), or as a function of receptor overexpression, has been queried to understand basal activation and signaling as well as a source of hyperactivity and a sensitized calcium response (Uyemura et al., 2005). ErbB1 receptors observed by total internal reflection fluorescence (TIRF) microscopy showed almost instantaneous two-fold increases in intensity at sites of soluble, fluorescent ligand binding, suggesting activation was promoted by the initial presence of 0:2 or 1:2 dimers. This would also provide some support for the positive cooperativity model since the binding of the first ligand in the dimer permitted rapid binding of a second ligand and, thus, the increased collected emission. These ligand bound dimers demonstrated downstream activity based on the binding of a fluorescently labeled antibody recognizing a phosphotyrosine residue on the cytoplasmic tail of erbB1 (Sako et al., 2000). Preformed resting complexes were also suggested to be enriched in the periphery of cells observed under TIRF illumination with the potential to sensitize the cellular response to ligand activation in an erbB1 density-dependent manner (Chung et al., 2010). The effect of receptor number on the formation of preformed dimers was also argued using the number and brightness (NB) approach that uses fluorescence signals within a region to quantify the total receptors within the focal area (Nagy et al., 2010). On the contrary, preformed dimer complexes have also been argued to represent non-signaling receptor units whose distribution and behavior changes upon activation (Hofman et al., 2010). These studies have taken advantage of another spectroscopic tool, Förster resonance energy transfer (FRET).

FRET is a potent technique to demonstrate distances between molecules (Lidke and Wilson, 2009). The non-radiative exchange of energy between two fluorophores

13

from a donor of shorter wavelength to an acceptor of longer wavelength requires that a small separation distance, r, of less than 10 nanometers (Energy $\propto 1/r^6$). Measurements of energy transfer between erbB1 receptors using fluorescent ligand suggest both dimerization and larger order clustering. Comparisons of homo-FRET between endogenous proteins on live cells with those on vesicle preparations indicate energy transfer that is dependent on oligomerization, rather than dimerization (Whitson et al., 2005). This contrasts with two-color FRET detection that suggests dimers, despite the anticipated separation of two ligands in the dimer having a separation exceeding 10 nm (Sako et al., 2000). In addition to FRET approaches, image correlation studies suggested that resting complexes comprised of at least two receptors per cluster increase in number to approximately four proteins per cluster following stimulation (Clayton et al., 2005). The efficiency of energy transfer suggests an equilibrium between activated dimers and tetramers that may represent a transition between the monomer-dimer steady state for resting receptors. Another study found that two FRET distances can be detected between fluorescent ligand molecules (of approximately 8 and 5.5 nm). This is consistent with a model using the crystal structures of back-to-back dimers uniting with two other receptors, possibly interacting as another dimer, to form a tetramer (Webb et al., 2008). These orientations may relate to the affinity status of the receptor and could provide an activation cascade that depends on correct interactions between the quaternary elements of the complex. While these kinds of studies provide interesting mechanistic insight, ligand-bound receptors are observed in the presence of unlabeled ones, making the findings difficult to interpret.

14

In addition to forming dimeric and tetrameric complexes, erbB1 and its homologues combine to form larger order oligomeric clusters. Mapping of receptors and adaptor proteins by transmission electron microscopy (TEM) highlighted the role of clustering and membrane patches in signal transduction (Wilson et al., 2004; Yang et al., 2007). The rotational mobility of receptors has been shown to slow as cluster size increases (Zidovetzki et al., 1986). This may relate to ligand binding affinity, which is suggested to be higher in oligomeric complexes (Uyemura et al., 2005) and could result from stimulation of resting clusters (Saffarian et al., 2007; Yang et al., 2007). The roles of membrane components in clustering, endocytosis and microdomain organization have been extensively studied and are the subject of section 1.1.8. Increases in receptor cluster size are correlated with signaling, as demonstrated by studies showing tyrosine kinase dependent clustering of erbB1 (Ariotti et al., 2010; Hofman et al., 2010). The large-scale reorganization that takes places upon ligand stimulation has led to a model for signal propagation that does not require all receptors within an oligomer to be occupied with ligand.

1.2.7 Lateral signaling propagation

A model for the spreading of erbB signaling has been proposed that relies on lateral propagation of phosphorylation along the membrane in a manner that cannot be explained by diffusion of receptors alone. This spread is observed as early as 60 seconds following activation and persists for up to 15 minutes. The phosphorylation status of receptors was monitored using a FRET-based technique that shows the degree of phosphorylation exceeds the concentration of the stimulus in both whole cells and semi-intact cellular membranes (Verveer et al., 2000; Ichinose et al., 2004).

Furthermore, the phosphorylated sites are spatially separated from the locations of stimuli as the EGF ligands in these assays are immobilized on beads (Verveer et al., 2000). This supports a role for transient dimers in perpetuating activation signals but it remains unclear if the interactions and signaling of singly liganded dimers differs from that of preformed, unoccupied dimers (Figure 1.3).

The conclusion that erbB receptors alone spread the phosphorylation signal is supported by studies using the Src family kinase inhibitor PP2 (Ichinose et al., 2004). Large scale recruitment of cytoplasmic Grb2 may require as few as 20% of erbB1 receptors to be ligand bound (Reynolds et al., 2003). Normal erbB signaling is regulated by the balance of phosphorylation and dephosphorylation by kinases and phosphatases, respectively. The production of hydrogen peroxide may be the normal result of erbB1 activation, leading to inhibition of phosphatase activity and promote the signaling cascade. This is supported by evidence that inhibition of hydrogen peroxide activity abolishes the lateral signaling mechanism (Reynolds et al., 2003). Mathematical models also demonstrate that equilibrium favors a high degree of receptor phosphorylation (Reynolds et al., 2003).
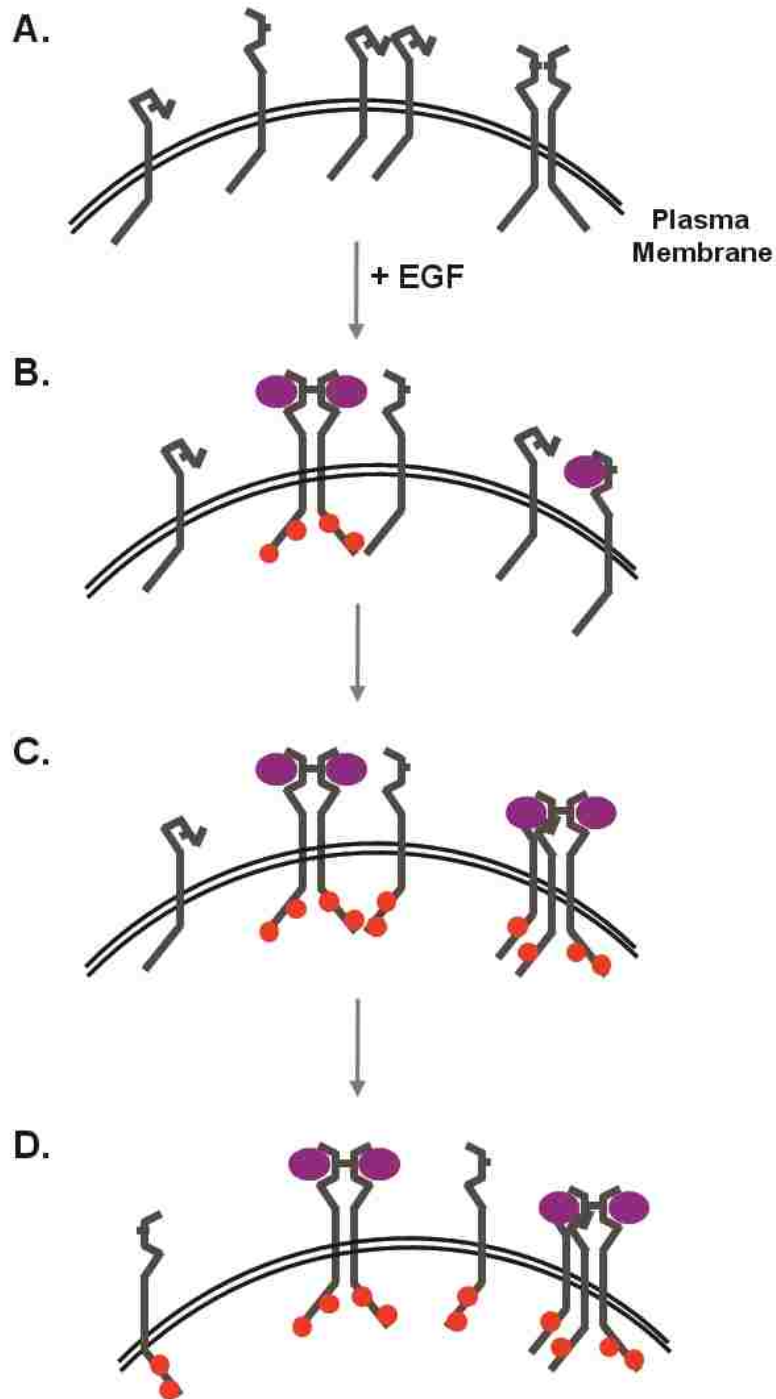
Figure 1.3. Lateral signaling propagation provides a mechanism to explain widespread erbB phosphorylation after minimal stimulation by ligand. A. At rest, erbB1 is present on the plasma membrane in the tether or extended conformation and preformed dimers can occur in the absence of ligand. B. Following addition of EGF, signaling dimers form and transphosphorylate tyrosine residues (shown as red circles). C. In lateral signaling

propagation, activated receptors can phosphorylate nearby receptors, even without ligand stimulation of those neighbors. D. After minutes, and as a consequence of diffusion, the phosphorylated receptors may outnumber the ligand bound and dimerized receptors.

The dynamics of clustering and signal propagation could have a more pronounced importance in the disease state. In the case of aberrant signaling, conformational stability of the extracellular domain could promote dimerization or altered kinase activity. Another feature of lateral propagation could include a role for negative cooperativity in dissociating activated receptors to diffuse to adjacent erbBs and relay the stimulatory signal. Understanding the kinetics of dimerization can offer some insight into this mechanism. The lifetime of singly liganded dimers is less than that of the 2:2 dimer, suggesting that this erbB1 complex would require very rapid phosphorylation in order to signal (Low-Nam, et al., Chapter 3). The kinetics of phosphatase and kinase activities need to be better understood in order to fully comprehend the role for lateral signaling in erbB activation.

1.2.8 ErbB1 endocytosis and membrane organization

The localization of resting erbB1 and the redistribution of the receptor upon activation have been of broad interest and highlight the significance of the local environment in modifying receptor behavior. Studies involving inhibition or depletion of membrane components have demonstrated the complexity of erbB receptor partitioning. Receptor clusters may be detected in so-called membrane rafts (Keating et al., 2008) and erbB1 mobility is affected by cholesterol depletion, possibly through an actin-mediated mechanism (Orr et al., 2005; Ariotti et al., 2010). The role of actin in

18

modulating receptor behavior has been previously demonstrated (Andrews et al., 2008) and may link activation to endocytosis.

A principal mechanism for the downregulation of signaling involves the internalization of receptors and degradation or recycling to the surface. The route of receptor endocytosis is unclear. Evidence suggests both clathrin- and caveolin-mediated internalization that may be dependent on the extent of activation (Keating et al., 2008; Xiao et al., 2008). Internalization may also play a role in signaling based on evidence of erbB1 activity from endosomes (Wang et al., 2002). Direct evidence to corroborate receptor activation state with recruitment of endocytic machinery and the route of internalization remains elusive.

1.2.9 Outstanding questions and future directions

Extensive investigations into erbB receptor dynamics have detailed mechanisms for receptor activation, diffusion, interaction, and signaling. Microscopy, in particular, has informed our understanding of receptors on live cells and has reconciled some of the questions that biochemistry and structure alone cannot address. However, a number of issues remain in order to assemble a comprehensive model of erbB signaling. Some of these questions are listed below:

• Are dimers that interact for a few seconds actively signaling?

• What other downstream molecules can be observed to monitor signaling in real time?

• What is the relationship between the affinity states of the receptor and the conformation, density of erbBs?

19

• Can activator and receiver kinases in a single dimer exchange roles in order to allow phosphorylation to occur in all combinations of cis- and trans-?

As tools to investigate receptor dynamics continue to be developed and increase our molecular level understanding of cellular signaling, we hope to reconcile some of these questions. Importantly, many of these mechanisms are not mutually exclusive and may contribute to cellular homeostasis and control of erbB behaviors. The advent of fluorescence techniques to more directly observe these phenomena has provided great progress and provides avenues for further discovery.

1.3 Single Particle Tracking and Hidden Markov Models

1.3.1 Single Particle Tracking Background

High spatial resolution is required to fully investigate and appreciate the dynamics of erbB diffusion and protein-protein interactions. While ensemble measurements provide valuable information about average properties of proteins, single molecule data provide information on the full range of heterogeneous behaviors exhibited by cellular macromolecules. A variety of single molecule techniques have been established in order to monitor cellular behaviors in the sub-diffraction limited regime imposed by conventional light microscopy approaches (Saxton and Jacobson, 1997). Single particle tracking (SPT), in particular, provides both the spatial and temporal resolution necessary (Anderson et al., 1992) to study the diffusion and dimerization of erbB receptors on live cells. Single molecule methods take advantage of individual labeling of a target with a polystyrene bead, gold particle, or fluorescent dye or protein. We take

20

advantage of fluorescence approaches, based on the simple mechanism shown in Figure 1.4.
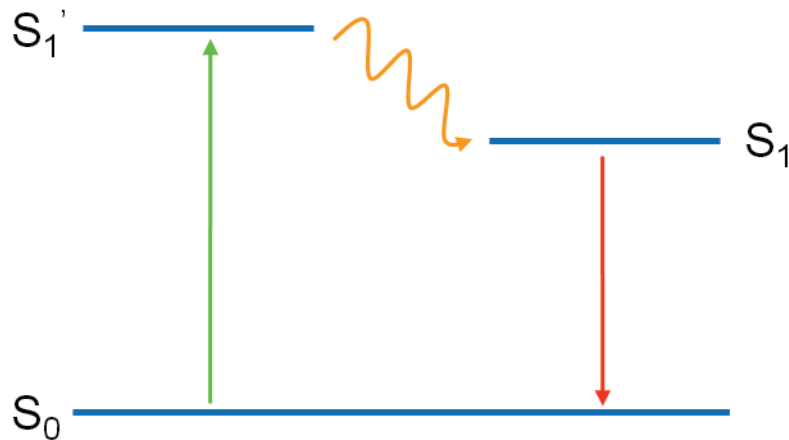
Figure 1.4. Jablonski diagram of the mechanism of fluorescence. The promotion of an electron to an excited state ($S_1^{'}$) occurs through the absorption of a high energy photon. From this excited state, the electron undergoes relaxation which dissipates some energy (to energy state S_1) before the electron, ultimately, returns to the ground state (S_0). This final step results in the emission of a photon of longer wavelength.

Specific conjugation schemes are used to control the stoichiometry of fluorescent labeling of proteins and are explained in greater detail in Chapter 2. Visualization of labeled targets is achieved using a variety of microscopy approaches. For SPT, target proteins are labeled at a low density in order to resolve each probe with very high precision (Saxton and Jacobson, 1997) and permit the tracking of particles over time. Importantly, a high degree of sampling is required in order to capture the heterogeneity characteristic of biological systems.

Live cell SPT is accomplished by imaging probes over time using either transmitted light or fluorescent illumination. The advent of high-speed cameras has permitted rapid acquisition of data at rates up to thousands of frames per second (Murase et al., 2004).

Despite this capability, most data is collected at slower speeds to allow for sufficient signal collection from probes at each frame in order to optimize fitting and tracking during post-processing. This trade off between acquisition rate and signal-to-noise is a delicate balance that must be optimized for each system of probes and cells. The signal from polystyrene beads and gold is very high and does not diminish as a function of time. However, these nanoparticles are very large and carry the disadvantage of perturbing the normal dynamics of the labeled target (Saxton and Jacobson, 1997). On the other hand, the smaller size of fluorescence-based probes is advantageous in preserving normal molecular behaviors, but the photophysical properties of these probes vary widely. Fluorescent dyes, proteins, and nanoparticles are imaged at slower rates (equivalent to long integration times) in order to collect more signal and improve localization accuracy, with theoretical precision of less than 1 nm (Jonas et al., 2006). Lower intensity of illumination is also ideal in order to prevent loss of signal from photobleaching. Another confounding feature of fluorescent probe emission is intermittency ("blinking") due to trapping of an electron in the so-called dark state (Nirmal et al., 1995). Ongoing efforts are aimed at improving fluorescent tags to optimize signal-to-noise and overcome the negative effects on probes associated with prolonged imaging.

As explained in greater detail in Chapter 2, inorganic quantum dots (QDs) have come to the forefront as superior single molecule probes. Conventional QDs are nanometer-scale semiconductor crystals composed of a cadmium selenide core and zinc sulfide coating (Michalet et al., 2005). Compared to typical organic dyes, QDs provide a high signal-to-noise ratio, even under widefield illumination. These

22

nanoparticles display an array of useful photophysical properties, including high photostability, a high absorption cross-section, high quantum yield, and tunable emission. They can be imaged at a rapid rate for long periods. All of these characteristics are ideal for single particle tracking and provide the molecular scale resolution needed for understanding erbB biology.

Analysis of single-particle tracking data requires fitting each QD to the point-spread-function of the optical system followed by subsequent estimation of particle coordinates at each time step (Anderson et al., 1992; Schutz et al., 1997; Cheezum et al., 2001). Trajectories are assembled from high precision short tracks that are determined to have a high probability of forming spatially and temporally independent sequences of coordinates. Long trajectories are required to detect changes in diffusivity within tracks, to sample different regions of the membrane, and to increase precision in determining relative behaviors of pairwise tracks. The approaches that we employ to analyze point emitters are detailed in Chapters 2 and 3 (Smith et al., 2010).

Analysis of SPT data within single trajectories or across data sets is used to extract results that describe underlying biochemical and cellular processes. Of particular interest is detection of space- or time-dependent behaviors that can manifest as shifts in mobility or reflect changes in local environment or protein-protein interactions. Typical parameters derived from single particle trajectories include diffusion coefficient and estimation of confinement zone sizes (Kusumi et al., 1993). Vectorial displacement of trajectories of different colors can be implemented to assess correlated motion on interacting species (Andrews et al., 2008). Unfortunately, the aforementioned analyses are insufficient to acquire kinetic on and off rates for individual dimerization events. As

previously discussed, these parameters have been of great interest to erbB biologists and modelers as a measure of receptor dynamics. We extend SPT data processing in order to extrapolate characteristics of erbB dimerization directly from our live cell measurements.

1.3.2 Hidden Markov Model Background

Hidden Markov Modeling (HMM) is a form of statistical analysis in which parameters for the behaviors of "hidden" states are extracted from a set of observables. It is based on a Markov process, which models the evolution of a memoryless system. An HMM is defined by a number of model and observable states and the parameter set that describes the probabilities of state transitions (Rabiner, 1989). It is not necessary to identify the state at each time step; instead, an overall kinetic model is assumed for the underlying process and its transitions. Previous applications of HMM approaches to single particle datasets include analysis of DNA looping and actin cytoskeletal dynamics. Monitoring DNA looping by excursion of a tethered polystyrene bead required filtering of data due to diffusion of the bead that was independent of the nucleic acid dynamics (Beausang et al., 2007). Our data sets do not necessitate this pre-processing because movement of the QDs is small compared to the protein diffusion.

In this work, an HMM is developed and implemented to interrogate erbB receptor dimerization and dimer lifetime, as measured by two spectrally distinct QDs overlapping for varied time periods. Long observation times are also important in permitting discrimination of mechanisms with slow kinetics. For dimerization of erbB receptors under physiological and oncogenic conditions, we anticipated a range of interaction rates. The distance between particles at each time step serves as the essential

parameter in the model, with the ability to resolve the molecular-scale formation of a dimer complex. The probability of protein-protein interactions is further modulated by protein mobility and membrane microenvironment. The implementation of a three-state HMM (free, domain-confined, and dimer states) is explained in Chapter 3.

1.4 Hypothesis

1.4.1 Hypothesis

This dissertation focuses on members of the erbB receptor tyrosine kinase (RTK) family and investigates protein diffusion, dimer lifetimes and interactions within the cell membrane using novel biophysical and computational approaches. This work addresses the prior lack of mechanistic information about dimer formation, as well as a paucity of quantitative parameter values for dimerization kinetics on live cells.

At the beginning of this project, I proposed the hypothesis *that diffusional and conformational dynamics of erbB receptors regulate homo- and hetero- dimerization, initiating signal transduction. I further hypothesized that these important parameters are perturbed by both mutation and inhibitory drugs.*

To test this hypothesis, I set about to study erbB dynamics in both wild type and mutant cells. Carefully planned experiments included pretreatments with erbB-targeted therapeutic agents (laptinib, therapeutic antibodies). HMM analysis of single particle tracking data suggested three interaction states for erbB receptors: free, confined, and dimerized. As a result, I propose the following refinements to my central hypothesis: 1) *that differential levels of ligand occupancy affect erbB dimer off rates, influencing signal initiation and duration; 2) that the local membrane environment impacts receptor*

25

encounter frequency; and 3) state-dependent changes in diffusional dynamics reflect a modest contribution from the increase in size of dimers and a larger contribution due to recruitment of cytoplasmic signaling partners. The molecular-level understanding that results from these studies has addressed erbB signaling in ways that previous approaches have not accomplished. Taken together, these experiments are expected to demonstrate the complexity of erbB signal initiation and provide a means of investigating these dynamics with high spatial and temporal resolution.

The structure of this work is shown in Figure 1.5. Chapter 2 provides details of experimental approaches that have been developed in the laboratory and further refined in order to address the problems of erbB dynamics and dimerization. The first section explains the development and characterization of probes used in fluorescence microscopy and single particle tracking. The second provides the approaches used in acquiring SPT data and, in particular, the image processing methods used to quantify receptor behaviors. Chapter 3 details the studies that have been performed to characterize erbB1 homodimerization on A431. Chapter 4 applies the approaches developed for erbB1 dimerization studies to erbB2 and erbB3. In this section, our approaches provide particular insight into erbB3 biology and argue that this receptor is an active kinase that is sequentially controlled by erbB2-erbB3 heterodimerization and erbB3 homodimerization. Finally, Chapter 5 provides a discussion of all the studies presented and focuses on the impact of our approaches to the field of membrane biology.
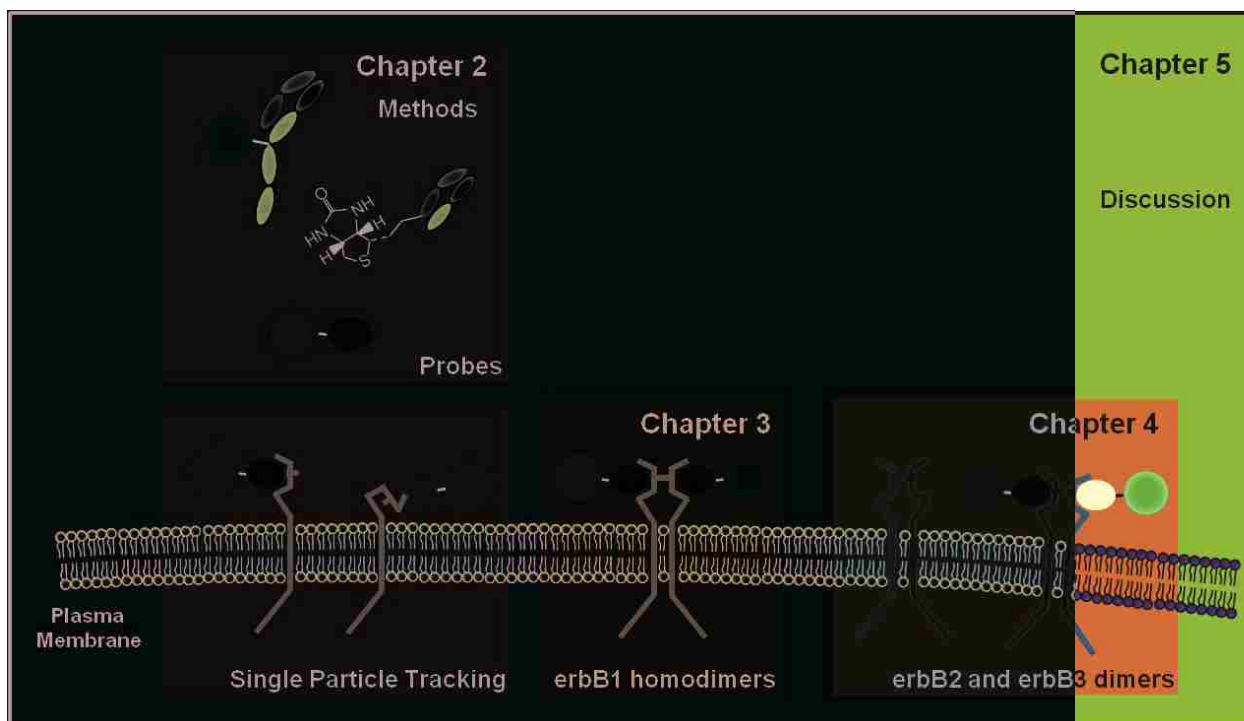
Figure 1.5. Overview of chapters in dissertation. Chapter 2 focuses on tools that are developed and improved in this work. Dissection of erbB1 homodimerization follows in Chapter 3. Extensions of these approaches to address questions related to erbB2 and erbB3 dimerization are the subject of Chapter 4. Finally, discussion in Chapter 5 summarizes findings and highlights the insights into membrane biology, in particular.

CHAPTER 2: PROBE DEVELOPMENT AND METHODOLOGY

2.1 Specific contributions

The following chapter details the methods that have been implemented, refined, and developed during the course of this dissertation project. The first section on probe development was written by the author. I made Fab fragments with help from Dr. Walter Kisiel and the NHS ester labeling section was developed with contributions from Dr. Amanda Carroll-Portillo and Samantha Schwartz. The biotin quantitation section is excerpted from a chapter in *Methods in Molecular Biology* written by Diane Lidke, myself, Patrick Cutler, and Keith Lidke. All of the other protocols in this section were generated from my own notes and experiments.

The section on single particle tracking and data analysis using the Hidden Markov Model includes parts of the *Methods in Molecular Biology* chapter, but I have modified it for specific labeling and observation of erbB receptors. Furthermore, I composed the HMM section at the end of the chapter, including generating example data sets shown in the figures. The MatLab code provided in Appendix D was compiled by me, but includes contributions from Keith Lidke and Patrick Cutler. The *Notes* sections in each part of this chapter were mainly contributed by myself, but also include information from the *Methods in Molecular Biology* chapter.

2.2 Antibody fragmentation and probe conjugation chemistries

2.2.1 Summary

Antibody labeling through covalent chemical crosslinking is a common strategy used to specifically tag and monitor proteins of interest. There are several

bioconjugation chemistries that permit antibodies and antibody fragments to be linked to fluorophores for use in fluorescence microscopy. Here, protocols are described to: 1) cleave antibodies to produce Fab fragments, 2) label using an NHS-ester linkage, 3) reduce and label using thioether chemistry, and 4) characterize probes.

Keywords: antibody, VHH, NHS-ester, maleimide thioether, biotin, streptavidin

2.2.2 Introduction

Epitope-specific antibodies are commonly used to label proteins of interest and provide a useful tool that is used to observe subcellular localization and behavior with a high degree of specificity. Canonical immunoglobulins (IgG) are produced by immune cells and are raised against many foreign molecules. A typical IgG molecule forms an antigen-recognition cleft through the combination of heavy (VH) and light (VL) chain variable regions (Figure 2.1). Variation in the genes encoding the VH and VL regions confers a high degree of diversity to the IgG repertoire.

The generation of monovalent antibodies and antibody fragments is essential to measurements requiring a 1:1 stoichiometry of labeling. In particular, studies involving the dimerization of two individual proteins can be confounded by artificial crosslinking induced by bivalent antibodies. The structure of an IgG is shown in Figure 2.1, with its essential interchain disulfide bonds at the hinge region. These bonds can be cleaved using enzymes and the use of the cysteine protease, papain, to produce Fab fragments is described below. In addition to monovalent labeling using Fab fragments, the arm of a heavy chain only Camelid antibody (VHH) can be used to singly label proteins and has increased stability in the absence of paired heavy and light chains. Nanobody (VHH) molecules have been shown to have high thermal stability and dissociation constants

29

comparable to intact antibodies (Muyldermans et al., 2001; Dumoulin et al., 2002; Holliger and Hudson, 2005; Harmsen and De Haard, 2007; Roovers et al., 2007). Another strategy for labeling cell surface receptors is to conjugate ligands to probes; the example of specifically tagging the erbB1ligand, epidermal growth factor (EGF) is explained here.

Reactive groups are required to conjugate dyes and other macromolecules to erbB probes. Despite the diversity of the amino acid building blocks that proteins are comprised of, only a few have the tunable characteristics that are useful for conjugation schemes. The reactive primary amine groups that are found on Lysine (K) residues are attractive candidates for linking protocols because side chain reactivity is pH-dependent. These positively charged groups are usually outward-facing in the globular structure of proteins and, thus, easy to access. The typical crosslinking involving K residues uses reactive NHS esters to form peptide bonds (Figure 2). However, since many proteins contain multiple K residues, control of labeling stoichiometry using this approach can be very difficult. An attractive alternative modification approach takes advantage of the reactivity of sulfhydryl groups found exclusively on cysteine (C) residues. In higher-order protein conformations, cysteine residues are typically involved in bridging polypeptide sequences through the formation of disulfide bonds, making these groups inaccessible. However, these bridges are made available through reduction procedures, making the use of this reactive group problematic in the case of excess reduction that leads to protein denaturation (see Note 2.1). In this case, linkages through sulfhydryls use reactive maleimides to create thioether crosslinks (Figure 2.2).

A useful strategy to link to probes is through the high affinity interaction between biotin and avidin proteins. Biotin is a naturally occurring, small molecule, vitamin H and is 244 Daltons (Da) in size. Its affinity for tetravalent avidin glycoproteins (67 kDa) is on the order of 10^{15} M^{-1}, conferring a very high degree of stability to probes crosslinked using this chemistry (Chapman-Smith and Cronan, 1999). Due to its high avidity, conjugations based on biotin-streptavidin linkages require carefully regulated protocols in order to achieve the desired 1:1 stoichiometry. The flexibility permitted by biotinylating probes and introducing streptavidin Quantum Dots (QDs) on demand increases the shelf life of these labels. Biotinylation can be achieved using either of the chemistries described above and will be detailed in the subsequent protocols.
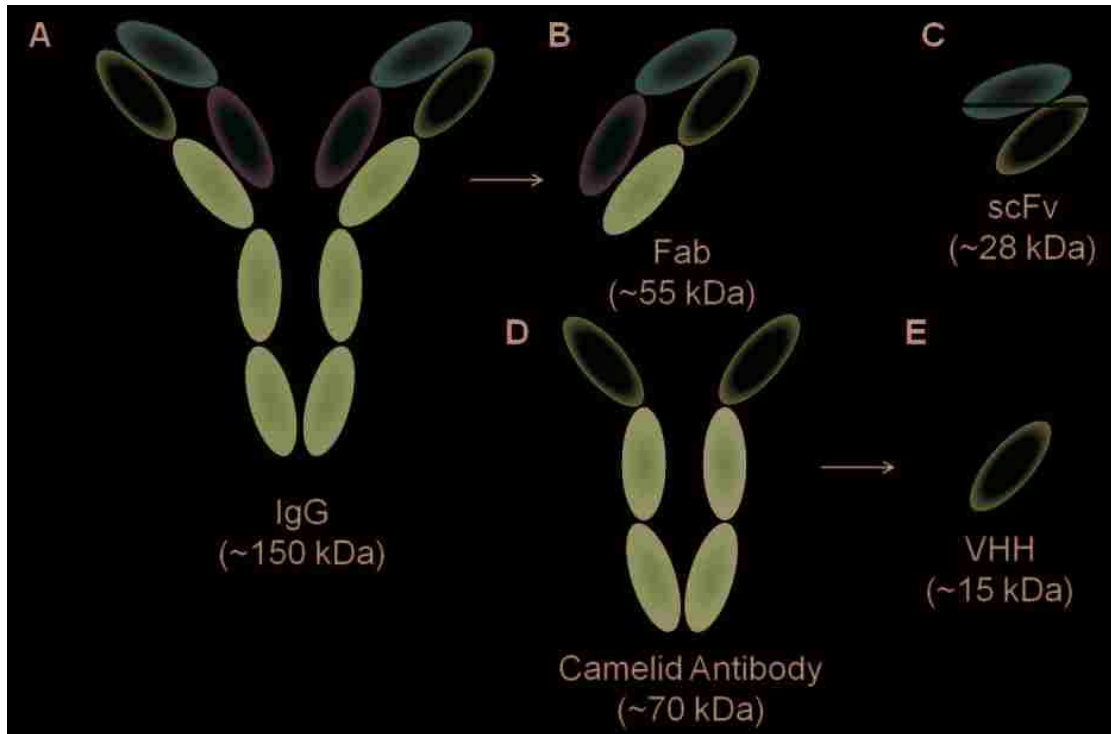
Figure 2.1. Antibodies and antibody fragments used in fluorescent labeling. A. Canonical IgGs are comprised of paired heavy and light chains. B. Upon fragmentation at the hing region by papain, fragments retaining epitope recognition clefts are produced (Fabs). C. A protein engineering approach to the production of monovalent antibody fragments involves the linking of the variable domains of the heavy and light chains to produce single chain antibodies (scFvs). D-E. An alternative form of antibody found in llamas is the heavy-chain only, camelid antibody, whose monovalent fragment is a nanobody (VHH).

A.
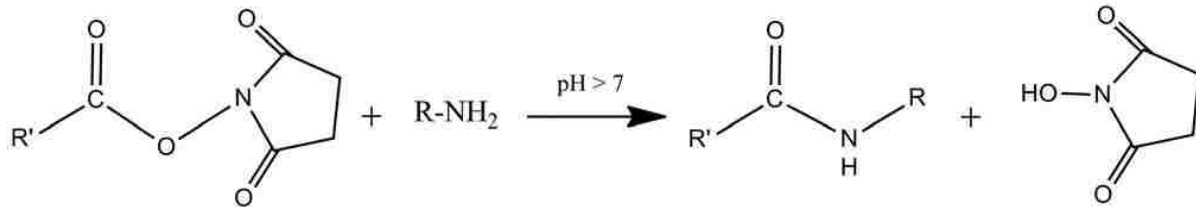
R' = dye or label to conjugate to protein of interest

B.
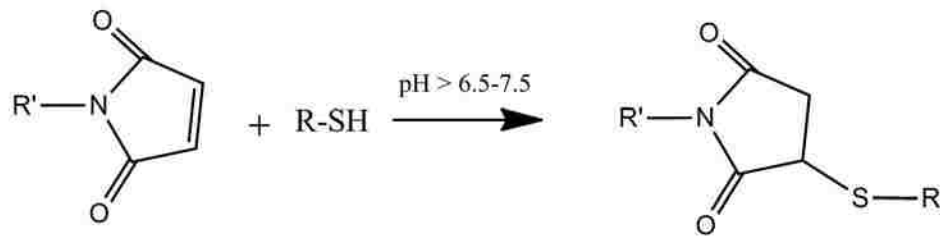
R' = dye or label to conjugate to protein of interest

Figure 2.2. Conjugation chemistries. A. NHS ester conjugation using reactive primary amines. B. Maleimide thioether crosslinking using reactive thiols that are exposed by protein reduction.

2.2.3 Materials

1. Microcon Centrifugal Filter Devices (Millipore, Ultracel YM-10 (10,000 MWCO))

2. PD Spin Trap G-25 Columns (GE 28-9180-04)

3. Pierce Slide-A-Lyzer MINI Dialysis Units (2000 MWCO; #69580)

4. Antibody ([1 mg/mL]; antibody = IgG, reduced antibody = rIgG)

5. 6-((6-((biotinoyl)amino)hexanoyl)amino)hexanoic acid, succinimidyl ester (Biotin-XX-SE, Invitrogen B-1606, Carlsbad, CA)

6. Maleimide-PEG$_2$-biotin (200 mM in DMSO)

7. 0.5 M Iodoacetamide (in diH$_2$0; made fresh)

8. 0.3 M Dithiothreitol (in diH$_2$0; made fresh)

9. 1X Phosphate Buffered Saline, pH 7.2

10. 7.5% SDS-PAGE gel

11. Non-denaturing loading buffer

   * Add solid SDS (tip of a scoopula) to the bottom of an eppendorf tube

   * Add 18-19 µL of 1x PBS

   * Add 2-1 µL of sample (for total volume of 20 µL)

   * Boil at 95˚C for 3-5 min

   * Immediately add a few crystals of solid sucrose; mix and melt

   * Load on gel

12. 1M NaHCO$_3$ (84.01 g/mol), dissolved in 1X PBS

13. Dye, in DMSO, at as high a concentration as possible (Stocks typically kept at [10 mM] in DMSO, -20°C)

14. IgG or ligand, minimum of 20 ug, at a concentration of 1 mg/mL in reaction

34

15. Tyrode's live cell imaging buffer (also called Rab): 135 mM NaCl, 10 mM KCl, 0.4 mM $MgCl_2$, 1 mM $CaCl_2$, 10 mM Hepes, pH 7.2. On the day of use, supplement this solution with 20 mM glucose and 0.1% BSA.

16. Agarose (Amresco 9012-36-6)

17. 1x TBE buffer: 0.89 M Tris, 0.02M EDTA-Na_2-salt, 0.89M Boric acid

2.2.4 Methods

2.2.4a General information

Proteins, particularly antibodies, may be purchased with carriers in solution for storage. Removal of components like azides is essential to prevent competing side reactions. Determination of protein concentration and methods for desalting and purification may be necessary precursors to conjugation procedures. A summary of available probes can be found in Appendix A.

1. Take Nanodrop® A_{280} reading of antibody to be used (to determine concentration) and run small sample on a non-denaturing gel (to determine if antibody is degraded)

    a. A 1 mg/mL concentration is desired – use Centricon concentrators (10,000 MWCO for full size antibodies) if necessary

        i. Centricon concentrators:

            1. Insert the Microcon reservoir (white section down) into provided 1.5ml tube for waste collection.

            2. Add sample (500 µL max) to reservoir without touching membrane.

            3. Spin sample at 14,000 x g for up to 30 min at RT (5-10 minute increments are recommended)

4. Remove reservoir and place inverted into a new collection tube.

5. Collect concentrated sample by spinning at 1000 x g for 3 min at RT

b. Spectrophotometry calculations (Beer-Lambert Law); for more useful information, refer to: www.piercenet.com/files/TR00006-Extinction-coefficients.pdf

    i. $A = \varepsilon c l$

    ii. $\varepsilon_{IgG} \approx 210{,}000 \ M^{-1}cm^{-1}$

    iii. $\therefore \varepsilon_{rIgG} \approx 105{,}000 \ M^{-1}cm^{-1}$

c. To eliminate unwanted carrier molecules (BSA, Thimerosol, Azide), exchange buffer using PD Spin Trap Columns or dialyze with MINI Dialysis units against 1x PBS

    i. PD Spin Trap Columns:

        1. Vortex Microcon column briefly to resuspend column matrix and break bottom closure off

        2. Insert the Microcon column into provided 1.5ml tube for waste collection, and unscrew cap slightly

        3. Balance in microcentrifuge and spin at 800 x g for 1 min

        4. Add 300 μL buffer (1x PBS) to equilibrate column without touching matrix and spin again at 800 x g for 1 min

        5. Repeat equilibration step (#4) for a total of 5 times

6. Transfer column to 1.5 mL eppendorf tube and add sample (<130 µL) to center of column without touching matrix; elute with 800 x g for 2 min

7. Return sample to column and repeat spin to ensure all of sample moves through column

2.2.4b Generating Fab fragments

Papain digestion cleaves the uppermost disulfide bond in the IgG hinge region and produces 2 Fab fragments per catalytic event. Digestion of the IgG can be optimized by changing the pH, duration, and temperature of the reaction. Cleavage using pepsin will produce the bivalent $F(ab')_2$ fragment that can be further reduced to attain Fab' fragments that have two reactive sulfhydryl groups, however, this approach will not be discussed.

IgG Cleavage

1. Overnight dialysis of the IgG to 1x PBS is carried out if the IgG is in another buffer or comes with carriers like azide that can interfere with the reaction. A final concentration of 2 mg/mL IgG is preferred for the enzymatic cleavage step.

2. A 1 mg/mL papain solution made from lyophilized powder is activated with 2 mM EDTA and 10 mM DTT for 15 minutes at 37°C.

3. Digest enzyme using a 100:1 enzyme:substrate stoichiometric ratio for 1 hour at 25°C. A total volume of 2 mL is typically used.

4. Terminate the digestion reaction using iodoacetamide (ICH_2CONH_2, Sigma Pg 1350). A final concentration of 20 mM is needed to arrest the papain reaction.

5. Dialyze the sample overnight against 1x PBS to remove the iodoacetamide. Use small dialyzer (Pierce Slide-A-Lyzer, 10,000 MWCO)

2.2.4c NHS-ester conjugation

Conjugation using reactive primary amines is attractive because of the ability to increase the availability and reactivity of a target protein by modulating the pH. NHS-ester bioconjugation is typically performed at basic pH in a phosphate buffer (see Note 2.2). The protocol for biotinylation using this scheme is highlighted below; however, this general approach can be implemented to derivatize a protein of interest with a fluorophore or other linking group (see Note 2.3).

Biotinylation

QD-EGF may be purchased (Molecular Probes, Invitrogen, E3477) at a 1:1 stoichiometry and the EgB4 VHH can be produced as a singly biotinylated fragment using the BirA expression system (Howarth et al., 2006; Roovers et al., 2007). A protocol is provided below that can be used for biotinylation of proteins and has been successfully implemented for the labeling of the erbB3 ligand, Neuregulin.

1. Add 20 μg of 1 mg/mL protein to a 2 mL reaction tube that contains a micro-magnetic stir bar. Add 1M NaHCO$_3$ 1:10 to reaction's final volume to raise the pH > 8.

2. Make a 4 mg/mL (7 mM) solution of biotin-XX-SE in DMSO. DMSO stocks of Biotin-XX-SE can be stored at -20°C for later use. Biotin-XX-SE can be dissolved in aqueous buffer, but should be made immediately prior to the conjugation process, as solutions of these compounds will gradually hydrolyze in water (See Note 2.4).

3. While gently stirring the solution, add the biotin-NHS solution to the reaction tube for a 1:1 stoichiometric reaction ratio.

38

4. Allow reaction to stir for 20 min at room temperature.

5. Prepare PD SpinTrap G-25 columns (GE Healthcare) spin columns at room temperature as directed. Complete this step so that the final wash coincides with the end of the reaction time (extended reaction will increased the labeling stoichiometry of the final product). Ensure that the resin does not dry out. We have found that separation performed at room temperature increases recovery from the column.

   a. Resuspend resin by vortexing.

   b. Remove storage buffer by centrifugation for 1 minute at 800 x g.

   c. Wash column with 300 μL of appropriate buffer (1X PBS) and spin for 1 minute at 800 x g; dispose of flow through and replace column in collection tube; repeat these washes 5 times.

   d. Apply 70-130 μL of sample to the center of the column, in a fresh collection tube.

   e. Elute by centrifugation for 2 minutes at 800 x g; the final conjugate is in the collection tube. This elution step should be repeated by taking the first run-through and repeating the 2 minute centrifugation in order to increase recovery of the labeled product.

6. Transfer the contents of the collection tube to a 0.5 mL centrifuge tube. Store at 4 °C.

7. Determine protein concentration: $C=A_{280} / \varepsilon L$; where A_{280} is the absorbance at 280 nm, ε is the extinction coefficient for the protein, and L is the cuvette path length (1 cm).

2.2.4d Maleimide thioether conjugation

Reactive sulfhydryl groups are less numerous in proteins than primary amines, permitting advantageous specificity in conjugation. The ability to label the hinge region of a reduced antibody permits a convenient approach for 1:1 labeling with only two reactive groups at the hinge. A competitive reaction using iodoacetamide permits labeling and capping of the monovalent form of the antibody that precludes reformation of the bivalent IgG (see Note 2.5). The typical crosslinking through reactive maleimide reagents involves the activation and use of either homo- or hetero-bifunctional crosslinkers.

Conjugation using reactive hinge sulfhydrls

Proteins can be hinge-labeled using fluorescent dyes or, as described below, biotin. The protocol described here is generally applicable to other thioether reactions.

1. Reduce antibody with 1 mM DTT for 30 min at room temp (100 μL reaction volume), agitating periodically (avoid producing bubbles)

   a. Final volume at end of complete protocol can be 130 μL

   b. Example reaction:

      98 μL 1 mg/mL antibody to be reduced

      2 μL 50 mM DTT (diluted from 0.3M)

   c. Desalt reaction using PD Spin Trap G-25 column equilibrated with PBS or dialyze with MINI Dialysis columns for 4 hours against PBS

      a. Remove all DTT as it will inhibit maleimide reaction

   d. Incubate with Maleimide-PEG$_2$-biotin (3:1 ratio) with 20 μM iodoacetamide for 1 hour on ice with occasional agitation (flick tube gently)

40

a. Low level of iodoacetamide competes for free thiols helping to accomplish 1:1 rIgG:biotin ratio

　　　b. Example reaction:

　　100 µL rIgG antibody

　　1 µL 2 mM maleimide-PEG$_2$- biotin (diluted)

　　1 µL 2 mM Iodoacetamide (diluted)

　e. Add excess Iodoacetamide to bring the final concentration up to 20 mM and leave on ice for another hour to complete capping process; again use occasional agitation

　　　a. Example reaction:

　　102 µL solvent

　　4.2 µL 500 mM Iodoacetamide

　f. Clean up conjugate with PD Spin Trap G25 column equilibrated with PBS (or with dialysis) and take A$_{280}$ reading of sample on Nanodrop$^{®}$

2.2.5 Characterization of probes

2.2.5a Determination of degree of labeling

Most labeling requires quantification of the degree of labeling (DOL) of probes, with a 1:1 stoichiometry as the preferred ratio. The determination of DOL using spectrophotometric absorption measurements is described below. The calculation is based on absorption changes in the labeled protein that reflect contributions by the dye or other moiety. The correction factor is related to the extinction coefficient of the label at a given reference wavelength and the values for Alexa Fluor dyes are shown in Table 2.1 (see Note 2.6).

- Protein Concentration (M) = $[A280 - (A_{dye\ conjugate} * Correction\ Factor)]/\varepsilon_{protein}$

Table 4. Physical characteristics of the Alexa Fluor® dyes.

Dye	Molecular Weight	λ_{max} *	Em *	ε †	CF_{280} ‡	CF_{260} §
Alexa Fluor® 350	410	346	442	19,000	0.19	0.25
Alexa Fluor® 405	1028	401	421	34,000	0.70	0.23
Alexa Fluor® 430	702	434	541	16,000	0.28	ND
Alexa Fluor® 488	643	495	519	71,000	0.11	0.30
Alexa Fluor® 500	700	502	525	71,000	0.18	0.32
Alexa Fluor® 514	714	517	542	80,000	0.18	0.31
Alexa Fluor® 532	721	532	554	81,000	0.09	0.24
Alexa Fluor® 546	~1260	554	570	112,000	0.12	0.21
Alexa Fluor® 555	~1250	555	565	150,000	0.08	0.08
Alexa Fluor® 568	792	578	603	91,300	0.46	0.45
Alexa Fluor® 594	820	590	617	90,000	0.56	0.43
Alexa Fluor® 610-X	1285	602	624	132,000	0.44	0.43
Alexa Fluor® 633 **	~1200	632	647	100,000	0.55	ND
Alexa Fluor® 647 **	~1300	650	665	239,000	0.03	0.00
Alexa Fluor® 660 **	~1100	663	690	132,000	0.10	0.00
Alexa Fluor® 680 **	~1150	679	702	184,000	0.05	0.00
Alexa Fluor® 700 **	~1400	702	723	192,000	0.07	0.00
Alexa Fluor® 750 **	~1300	749	775	240,000	0.04	0.00
Alexa Fluor® 790 **	~1750	785	810	260,000	0.08	0.09

* Fluorescence absorbance and emission maxima, in nm, conjugated to an IgG antibody. † Extinction coefficient at λ_{max} in $cm^{-1}M^{-1}$. ‡ Correction factor for absorption readings (A_{280}) at 280 nm; e.g., $A_{280,actual} = A_{280,observed} - (CF_{280} \times \lambda_{max})$. § Correction factor for absorbance readings (A_{260}) at 260 nm; e.g., $A_{260,actual} = A_{260,observed} - (CF_{260} \times \lambda_{max})$. ** Human vision is insensitive to light beyond ~650 nm, and therefore it is not possible to view the far-red–fluorescent dyes by looking through the eyepiece of a conventional fluorescence microscope. ND = Not determined.

Table 2.1. Characteristics of Alexa dyes from Invitrogen.

-Moles of dye per mole protein = $A_{dye\ conjugate}/(\varepsilon_{dye} * Concentration_{Protein})$;

remember to multiply by dilution factor

2.2.5b Biotin quantitation

A kit is available to quantify the degree of IgE biotinylation (FluoReporter® Biotin Quantitation Assay) using a 96-well format fluorescence reporter assay. The FluoReporter® system uses a fluorescent avidin reagent that is bound to quenching

ligands. Biotin displaces the quencher, resulting in a fluorescent signal that is proportional to the concentration of biotin added.

1. *Optional*: The IgE may be proteolytically cleaved to expose the biotin molecules completely. If this step is included, use a biotinylated IgG that is included as a control. We do not typically include this digestion step in our experiment.

2. Using a volume of 50 µL per well, serially dilute the biotinylated lysine standard to cover the range of 0-80 pmol standard; repeat in triplicate.

3. Aliquot 50 µL of two-fold serially diluted the biotinylated IgE to get concentrations within the sensitivity range of the assay.

4. Add the Biotective Green reagent to initiate the reaction; incubate for 5 minutes, covered, at room temperature.

5. Immediately after the incubation, read fluorescence using 485 nm excitation and 530 nm emission using a fluorescent plate reader.

6. Biotinylated lysine data is fit to a quadratic equation to generate a standard curve from which the concentration of biotin in the IgE samples can be determined.

7. The ratio of biotin concentration to that of IgE is the degree of labeling (DOL).

2.2.5c Immunofluorescent labeling

To test the probes that are made using NHS-ester and maleimide thioether conjugation, labeling directly on cells can be implemented to ensure that ligands or antibodies recognize their correct epitopes. However, this approach does not reflect exact stoichiometry and other approaches (like spectrophotometric ones) are needed to quantify degree of labeling. The general process of immunofluorescent (IF) labeling is

43

outlined below, but each step can be modified in duration and concentration of reagents in order to optimize results:

1. Cells are seeded on coverslips or in an 8-well chamber at a 50% confluency. Wash 3 times with live cell imaging buffer (Tyrode's).

2. For live labeling, add a low concentration of fluorescent probe (for EGF ligand, a 100 nM concentration will be saturating for most cell lines) diluted in Tyrode's buffer for 5 minutes. Exposure at room temperature or 37^oC will permit internalization as early as 5 minutes; to retain erbB receptors at the membrane, perform this step on ice.

3. Wash cells 3 times with Tyrode's buffer.

4. Fix cells using 4% PFA in 1 x PBS, Ph 7.4 for 15 minutes at room temperature.

5. Wash cell 3 times with 1 x PBS.

6. Add DAPI nucleic acid dye in 1 x PBS (1:5000 dilution is typical) in order to visualize the nucleus.

7. Image using epifluorescence or confocal microcopy. The latter is especially useful to observe the membrane staining that is expected for receptors at the membrane. Some examples of labeling using fluorescent probes are show in Figures 2.3 and 2.4.
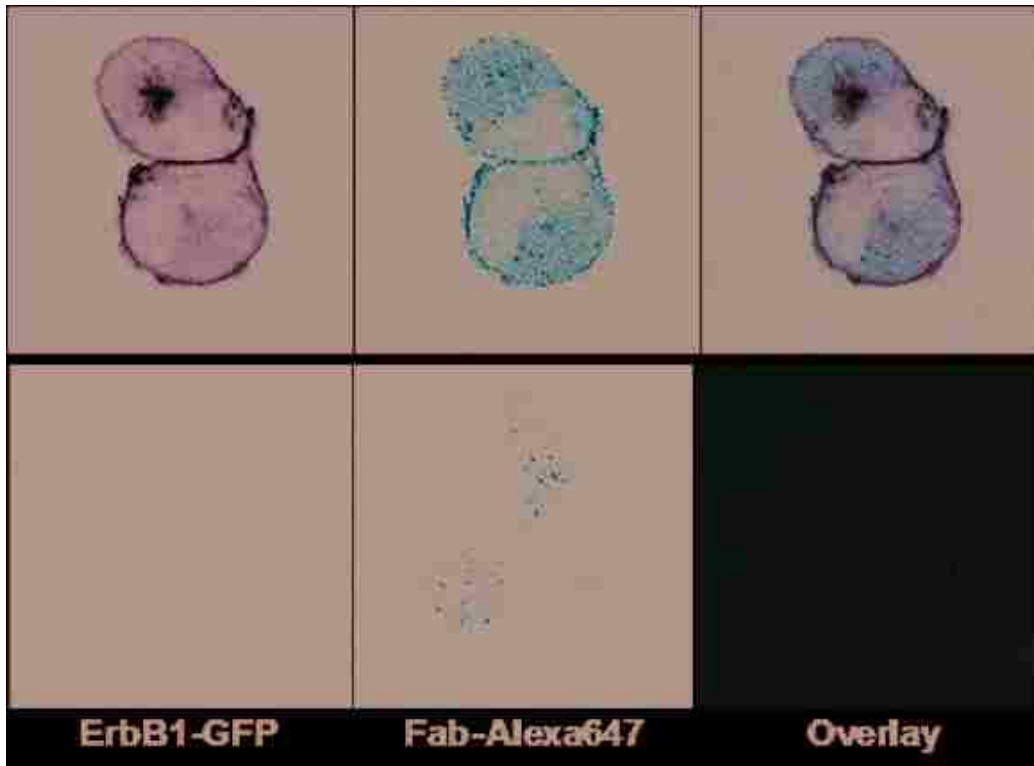
Figure 2.3. Fluorescence microscopy images of whole cells. Cells are labeled with fluorescent probes prepared by papain cleavage of an anti-erbB1 antibody and conjugation to Alexa 647 dye using NHS-ester chemistry. a) CHO cells transfected with GFP-erbB1, labeled with Fab fragments conjugated to Alexa 647 dye, and overlay. These two rows show that there is some amount of Fab that can passively diffuse through the plasma membrane, when labeled with this dye. b) A431 cells labeled with VHH (Nanobody) fragments conjugated to QD647 colocalize with EGF QD585. This panel shows colocalization at the cell surface and some cotransport of the QD probes during endocytosis.
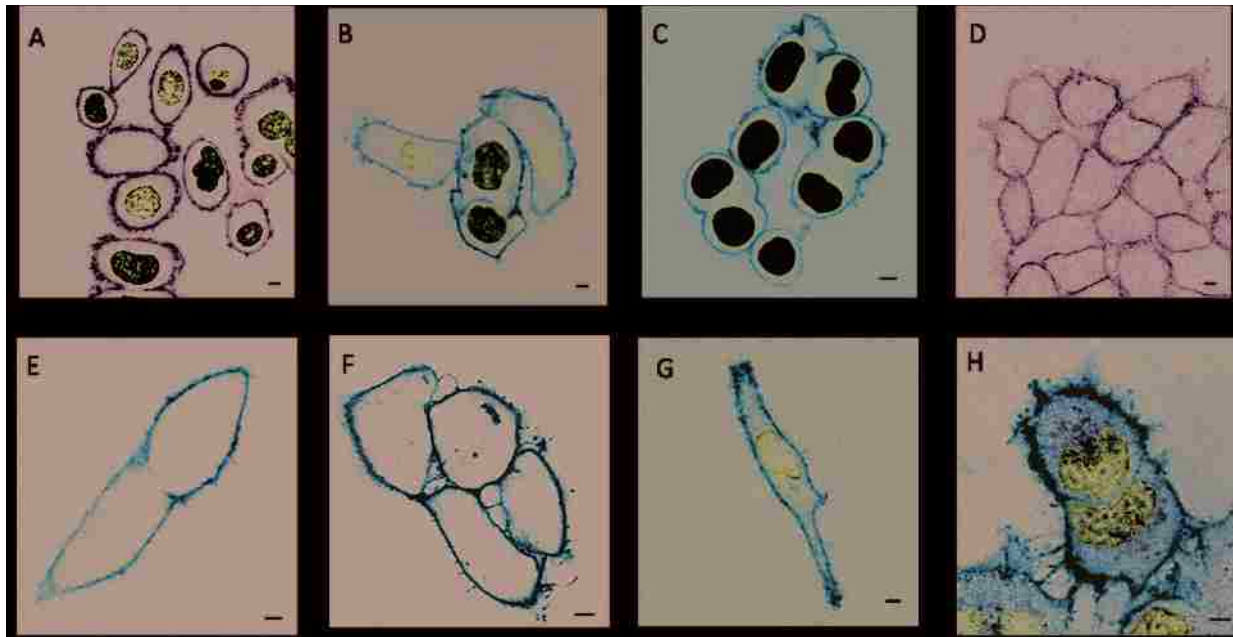
Figure 2.4. Fluorescent labeling of cell lines. A) Monovalent Alexa488- and B) Alexa647-Herceptin labeling of erbB2 SKBR3 cells. C) Herceptin QD655 labeling oferbB2 SKBR3 cells. D) Nanobody (Anti-erbB1 VHH IIIa42) Alexa488 and E) Alexa647 labeling of A431 cells, 4°C. F) Nanobody Alexa647 labeling of A431 cells, 37°C. Some internalization is observed. G) Reduced EGF (rEGF) QD655 labeling of A431 cells. H) Labeling of A431 cells with rEGF QD655 and EGF QD585 shows colocalization and some internalization after 5 minutes at 37°C. Nuclei stained with DAPI. Scale bar = 5 nm. Images taken on Zeiss LSM 510-META. Contrast enhanced.

2.2.5d Fluorescent protein SDS-PAGE

Fluorescent constructs can be visualized using standard chromatographic approaches. Separation of labeled probes on gels is useful in determining purity of proteins, especially after reduction. An example gel is shown in Figure 2.5.

1. Save some untreated antibody to run on SDS-PAGE gel

2. After DTT and desalting (rIgG), remove some sample to run on SDS-PAGE gel

3. At completion of protocol (rIgG-biotin), remove some sample to run on SDS-PAGE gel and for biotin quantitation

4. After incubation with streptavidin (rIgG-biotin-fluorophore), remove some for SDS-PAGE gel

5. Gel = Antibody, rIgG, rIgG-biotin, rIgG-biotin-fluorophore

- o Two 7.5% SDS-PAGE gels

- o Stain one gel with Sypro Ruby (show protein bands) and scan with Fuji Phosphorimager (show fluorescence)

- o Transfer other gel to nitrocellulose and perform western blot with α-biotin HRP antibody (1:100 dilution; Cell Signaling, #7075)

47
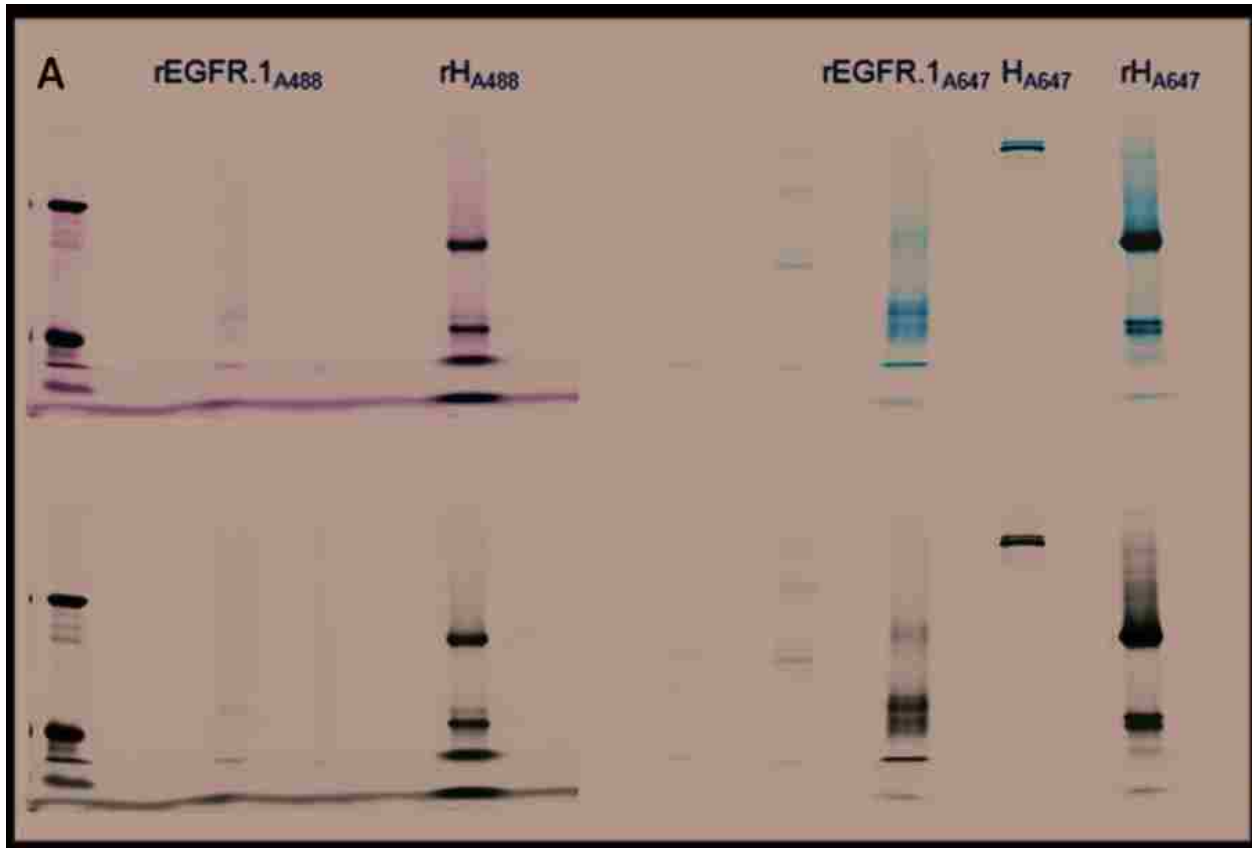
Figure 2.5. Electrophoretic mobility of probes. A) SDS-PAGE of reduced labeled antibodies. Alexa488- and Alexa647- labeled reduced anti- erbB1 (clone EGFR.1, labeled as rEGFR.1) shows poor labeling and the susceptibility to reduction mentioned above. Reduced Herceptin (rHerceptin, labeled as rH) shows a principle band at 75kDa, indicative of hinge-reduced fragments. Black and white images coincide with laser-imaged figures above them, respectively.

2.2.5e Fluorescent QD agarose PAGE

QD probes can also be observed by determining relative shift on a discontinuous agarose gel (Nehilla et al., 2005; Pons et al., 2006; Liu and Vu, 2007). An example of QDs run on a gel is shown in Figure 2.6.

1. Cast a 1.75% agarose gel (w/v) in 100 mL 1x TBE by gently boiling the solution to solubilize the agarose

2. After the 1.75% resolving gel sets, cut off a portion of the top of the gel to cast a 0.5% agarose stacking gel.

3. Run agarose gel in 1x TGS buffer at 120 V for approximately 45 minutes using samples as prepared for SDS-PAGE (described previously).
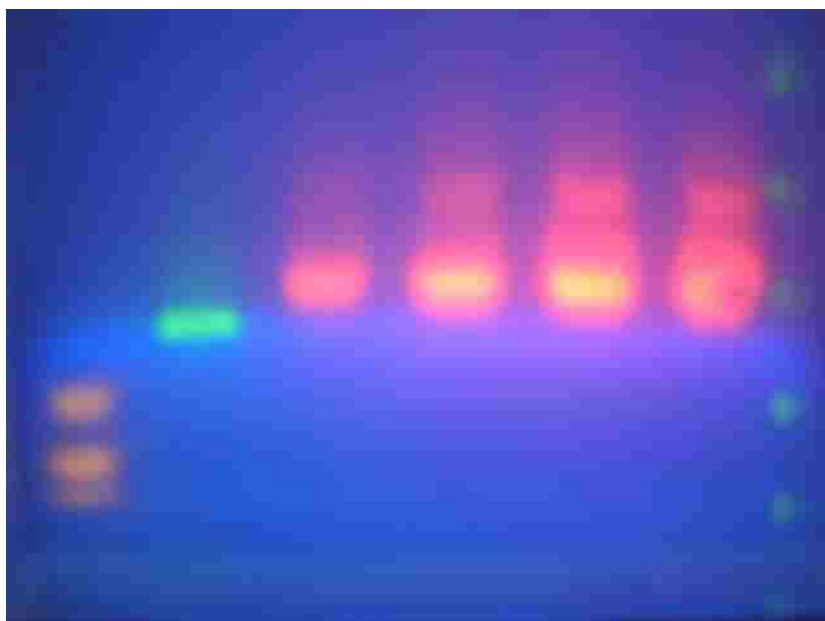
Figure 2.6. Relative mobility of QDs. QD-based probes were separated on a discontinuous agarose gel. Samples, loaded from left to right are: Molecular Weight Markers (Bio-Rad Precision Plus Standards), QD525, QD585, QD605, QD655, and QD705.

2.2.6 Notes

2.1. Using a concentration of 10 mM DTT, reduction occurs at the hinge of an IgG. A higher concentration (100mM or higher) will fully reduce heavy and light chains.

2.2. Buffer pH and temperature can be modified in order to optimize degree of labeling. TRIS buffers should be avoided when performing amine reactive conjugations. This molecule contains reactive amine groups that can compete with the reaction.

2.3. NHS ester fluorescent dyes can be purchased from Invitrogen. An alternate chemistry for the NHS reactive group is based on tetrafluorophenyl (TFP) moieties. This other conjugation scheme may be applied using similar protocols and also works well for linking to reactive primary amines.

2.4. Dissolving reactive groups and dyes in DMSO will permit longer storage. Solubilizing in water is not recommended since hydrolysis occurs readily and precludes further conjugations. Storage at -20°C in DMSO can be useful for up to 6 months. Ultimately, reagents in DMSO must be diluted prior to incorporation in reactions. The desired final concentration of DMSO is much less than 1% in order to avoid interference with the conjugation.

2.5. DTT powder (Sigma 43815) is water soluble up to 50 mg/mL (0.3 M); can buy DTT in solution at 1 M concentration (Sigma 646563); store at -20°C. Iodoacetamide (Sigma I1149) is water soluble up to 0.5 M; store at -20°C. An alternative approach to biotin-maleimide is to reduce and cap antibody with iodoacetamide and then conjugate antibody with NHS ester dye/biotin conjugates at a 1:1 ratio. Current use of this protocol in our lab has indicated that the desalt columns retain some protein during use. While we are testing to determine if running the sample through the column multiple times

alleviates this problem, we are currently unsure if this is a feasible solution. As such, minimizing the amount of columns used in the protocol, dialysis, and alternative cleaving reagents (TCEP and βME) are being explored. Labeling using maleimide chemistry should be performed at pH between 6.5 and 7.5. Basic pH can cause competing reactions with primary amines. Thiols should be excluded from the reaction, but can be used to quench the crosslinking and halt further labeling.

2.6. If spectrophotometric measurements are made, the dilution factor should be included in this calculation.

2.3 Single quantum dot tracking and Hidden Markov Model analysis of erbB dimerization

Modified from: Lidke, Low-Nam, Cutler, and Lidke, Determining FcεRI diffusional dynamics via single quantum dot tracking. *Methods Mol. Biol*. Submitted.

2.3.1 Summary

Single particle tracking using fluorescent quantum dots (QDs) provides high resolution spatial-temporal information on receptor dynamics that cannot be obtained through traditional biochemical techniques. In particular, the high brightness and photostability of QDs make them ideal probes for single particle tracking on living cells. We use QD-labeled ligand- and antibody-based probes to investigate the dynamics of erbB receptors. Herein are protocols for 1) coupling QDs to proteins that bind to erbB receptors, 2) tracking individual QD-bound receptors and 3) analysis of one- and two-color tracking data using several analytical approaches, including a three-state Hidden Markov Model.

Keywords: erbB receptors, single particle tracking, quantum dots

2.3.2 Introduction

Many events in cellular growth and development are initiated by the erbB family of receptor tyrosine kinases (RTKs). There are four homologous members of the erbB family: erbB1/EGFR/HER1, erbB2/HER2, erbB3, and erbB4. Canonical activation of receptors requires ligand binding to the extracellular domain to stabilize the untethered conformation and promote the formation of back-to-back dimers. A cascade of signal transduction proceeds with the formation of an asymmetric dimer of the kinase domain tails, transphosphorylation of cytoplasmic tyrosine residues and the recruitment of adaptor proteins. Ultimately, downstream interactions lead to changes in the genetic programs that control events like growth, differentiation, adhesion, and migration (Lemmon and Schlessinger, 2010). Ligand-stabilized activation of erbB receptors is associated with changes in receptor dynamics and cellular topography, suggesting important roles for diffusion and interactions in signaling.

Single particle tracking (SPT) is a powerful tool for studying the subtleties of protein behaviors and interactions. By measuring the motions of individual proteins, SPT can reveal details of protein dynamics at the molecular level. Proteins of interest are labeled at a sufficiently low density in order to resolve their individual positions with high precision (Saxton and Jacobson, 1997). The use of bright and photostable Quantum Dots (QDs) for SPT has extended the capabilities of this technique by allowing for longer tracking times and facilitating multi-color measurements (Dahan et al., 2003; Lidke et al., 2004; Lidke et al., 2005a; Andrews et al., 2008; Roullier et al., 2009). Simultaneous multi-color tracking allows for direct comparison of protein dynamics when different species are labeled with distinct QDs and can provide

52

information about protein-protein interactions. We have previously shown that QD-labeled EGF ligand can bind erbB1 and can be used to track receptor dynamics in the activated state (Lidke et al., 2004; Lidke et al., 2005a). The use of a monovalent antibody fragment of a heavy-chain only antibody, called a nanobody (VHH), that does not activate the receptor or compete for ligand binding is useful for studies of the dynamics of the resting receptor. Here we describe methods collection and analysis of SPT data. Information on the generation of erbB probes useful for tracking each member of the family may be found in the chapter, "Antibody fragmentation and probe conjugation chemistries."

2.3.3 Materials

1. Phosphate-buffered saline (PBS), pH 7.4 (Gibco 10010-023, Carlsbad, CA)

2. Streptavidin-conjugated QDs (SAvQD) (Molecular Probes, Eugene, OR)

3. Tyrode's live cell imaging buffer (also called Rab): 135 mM NaCl, 10 mM KCl, 0.4 mM $MgCl_2$, 1 mM $CaCl_2$, 10 mM Hepes, pH 7.2. On the day of use, supplement this solution with 20 mM glucose and 0.1% BSA.

4. LabTek eight well cover slip chambers (Nunc 155411, Rochester, NY)

5. Dulbecco's Minimum Essential Medium (DMEM, Gibco 21063-045, Carlsbad, CA) supplemented with 10% Fetal Bovine Serum (MEM/FBS) or other appropriate serum for cells.

6. Biotinylated protein in 1 X PBS, pH 7

7. FluoReporter® Biotin Quantitation Assay (Molecular Probes F30751, Carlsbad, CA)

8. Two color image splitter such as Cairn Optosplit (Faversham, UK), Optical Insights Dual View (Santa Fe, NM), or four color QuadView image splitter (Optical Insights).

9. Appropriate emission filters and dichroics for QDs of interest (Chroma, Rockingham, VT or Semrock, Rochester, NY)

10. erbB expressing cells (A431, MCF7, MCF7 Her2 18, SKBR3, HeLa, and others)

2.3.4 Methods

2.3.4a Preparation of QD probes

A kit is available for SMCC activated QD conjugation to reactive thiols on reduced proteins (Invitrogen, Carlsbad, CA). This kit works very well for hinge labeling of antibodies that have been reduced between the heavy chains, as well as ligands that have been reduced by DTT. The latter are gently reduced so that some refolding occurs and permits binding to erbB receptors, but generally precludes activation (Diagaradjane et al., 2008).

This protocol describes methods for conjugation to commercial SAvQDs (see Note 2.7). Singly biotinylated EGF ligand is purchased or can be prepared using bioconjugation of reactive primary amine groups with biotin-SE (see Chapter 2.1 for details). Monovalent 1:1 biotinlyated VHH is produced using the BirA expression system.

3.1.2 QD-protein conjugation

1. Dilute SAvQDs to 90 nM in 100 µl of PBS+1%BSA.

2. Dilute Biotin-EGF or Biotin-VHH to 30 nM in 100 µl of PBS+1%BSA.

3. Add Biotin-protein to the SAvQD and gently mix several times with a micropipette, being careful to avoid generating bubbles.

4. Incubate for at least 60 min at 4 °C with gentle agitation. The result is a 30 nM stock of QD-Probe that can be stored at 4 °C for up to 2 weeks (see Note 2.8).

54

2.3.4b Cell labeling and microscopy

Single particle tracking using the QD probes is performed in combinations in order to observe 0:2, 1:2, and 2:2 ligand:erbB1 complex formation using the VHH and EGF conjugates (see Note 2.9).

3.2.1 Labeling Cells

1. erbB expressing cells are plated in 8-well chambers 1 to 2 days prior to the experiment in DMEM/FBS (or other appropriate media, see Note 2.10). An initial density of 50,000 cells/well or 25,000 cells/well results in an appropriate density after 1 or 2 days, respectively.

2. Wash cells 2-3 times with 350 µl Tyrode's live cell imaging buffer.

3. Label cells at a final concentration of 20 pM EGF-QD or 2-10 pM VhH in Tyrode's.

    a. For two-color QD tracking, label cells by simultaneously with a mixture of the two QD probes (see Note 2.11).

4. *Optional*: Wash cells after 30 seconds to 1 minute in order to remove unbound QDs. Ensure that there is at least 350 µL of imaging buffer in each well during imaging.

5. *Optional*: Add this step after QD-IgE labeling in cases where saturating non-fluorescent EGF(dark EGF) is required (i.e. for maximal activation of receptors). Add 100 nM EGF to each chamber.

Fiducial data acquisition

1. 5 uL of 1:10 dilution (in PBS or live cell imaging buffer) of 0.2 µm Tetraspeck beads are dropped onto one well of an 8-well chambers slide and allowed to settle for 2 minutes. This well is washed 2-3X with live cell imaging buffer and left in buffer for

imaging. Using one well of an 8-well slide with cells in the center four wells increases efficiency during imaging.

2. Take a *Background* image sequence (100 frames) without light going to the CCD. The knob has light going to the eyepiece and all lights should be off. (Once at the beginning of each imaging session)

3. Take a *Beads* photon calibration sequence (100 frames) using at least 4 beads in a field of view. The sequence is taken with the beads out-of-focus to sample the dynamic range of the detector. Using the Tetraspeck beads, longer integration times can be used. (Once at the beginning of each imaging session)

4. Take a fiducial calibration series using the Tetraspeck beads using the MatLab function fiducial_beads. (performed at the beginning and end of each chamber, see Note 2.12)

5. A beads sequence is acquired to permit imaging with a live overlay. The sequence of 100 frames is summed and a border is used to frame each channel for input into the function aligncrop.

Script:

```
bd = sum(sequence,[ ],3);

beads = aligncrop(bd,4,80);

%use calculate live overlay button in andorixon GUI
```

Single particle tracking

1. Place 8-well chamber containing erbB expressing cells on the microscope stage and allow time for temperature equilibration. We use an inverted wide field microscope (Olympus IX71) equipped with an objective heater (Bioptechs) to maintain

temperature at 34-36 °C. Excitation is from a mercury lamp (436/10 nm BP filter) and emission is collected by an electron multiplying CCD camera (emCCD, Andor iXon). For two-color imaging, an image splitter that projects two color channels simultaneously on the emCCD is used with appropriate QD emission filters. For example, we use an OptoSplit II (Cairn Research) equipped with a 600 nm dichroic and 655/40 nm and 585/20 BP emission filters (Chroma) (see Note 2.13). Locate a single cell and focus on the apical membrane. A 60x water, 1.2 NA objective is recommended to avoid aberrations induced by oil/water index of refraction mismatch.

2. Begin acquisition of time series. Data is typically collected at 20-33 frames per second. Longer exposure times give better signal-to-noise at the expense of temporal resolution.

3. A single well can be imaged for up to 7 minutes in the presence of activating EGF but should not be imaged longer than this as receptor internalization confounds data acquisition.

2.3.5 Analysis

2.3.5a Single QD tracking

A 2D Gaussian is used to represent the microscope point spread function (PSF), with σ_{PSF} values measured for each color channel using immobilized fluorophores on a cover slip. See Figure 2.7 for more PSF details. Localization accuracy is limited primarily by the microscope PSF, the number of photons collected from the fluorophore, and the background count rate (Smith et al., 2010). For image processing, we use and recommend MATLAB (The MathWorks, Natick, MA) in combination with the freely available DIPimage toolbox (Delft University of Technology, http://www.diplib.org/).

57

Raw data is cropped into left and right channels using the function splitImage. All tracking is done on unshifted data.

1) Convert CCD image data to photon counts (Lidke et al., 2005c).

 a) Subtract the camera offset pixel-wise for each image frame. The camera offset image is the mean image of ~ 1000 frames taken with no light on the CCD.

 b) Divide the offset corrected images by the CCD gain. The gain can be found as the slope of the variance vs. intensity plot generated from a stack of ~20 images of an identical object. The variance and intensity are calculated along the 3rd dimension. Slightly out of focus fluorescent beads mounted on a cover slip make a good, photostable test object. Gain calculation is implemented as DIPimage function 'cal_readnoise.'

2) Find coordinates of QDs.

 a) Identify areas of interest. Initial segmentation of each image is performed by subtracting a Gaussian filtered image with filter kernel $\sigma_k = 2*\sigma_{PSF}$ from a filtered image with $\sigma_k = \sigma_{PSF}$. A threshold of the standard deviation across the resulting image is used to identify candidate fit regions.

 b) Maximum Likelihood Estimate of QD position, emission rate and background count rate (Smith et al., 2010). A box of ~ 6 * σ_{PSF} pixels centered around the center of mass of each contiguous area found in part a) is used as a fitting region for a single molecule fit.

 c) Reject objects that are not single molecules. Objects that do not pass a shape test or do not pass an emission rate threshold are removed from further analysis.

3) Build trajectories from QD coordinates (Andrews et al., 2008)

58

a) Compile short, continuous trajectories. Starting with the first frame, all coordinates found in the subsequent frame are compared to each set of coordinates from the current frame. If they pass a threshold probability given by $P(r,\Delta t)=\exp[-r^2/(4D\Delta t)])$, where P is typically 0.01, D is an estimated diffusion constant, and r is the distance between coordinates, they are connected to build a trajectory. If more than one particle passes this threshold, the coordinate with the highest P value is selected (see Note 2.14).

b) Connect short trajectories. The x,y,t coordinates at the beginning and end of each short trajectory are used to repeatedly connect short trajectories into final trajectories. Using the same equation as above, the threshold probability for this step is typically 10^{-4}. We also give an upper limit for the distance and time interval between coordinates in order for two short trajectories to be joined into a longer trajectory.
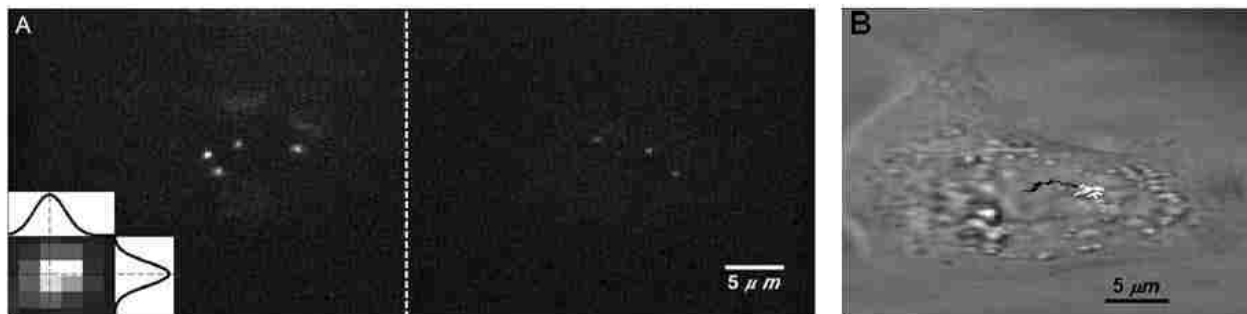
Figure 2.7. Example of Single QD-EGF Tracking. A) Images from one frame of two-color QD-EGF tracking on the surface of SKBR3 cells showing each channel (QD655 on the left, QD585 on the right) as projected by the Optosplit. Inset on the lower left shows the PSF fits of a single QD655. These images were acquired with excitation intensity of 4.7 W/cm^2 (436/10 BP), results in average photon counts of 314 and 172 for QD655 and QD585, respectively. The localization error is then 24 nm for QD655 and

36nm for QD585. B) Selected trajectories of erbB1 labeled with QD655-EGF (white) or QD585-EGF (black) overlaid on the transmission image.

2.3.5b Calculation of diffusion coefficients

Once trajectories have been obtained from the time series, diffusion coefficients (D) can be extracted. Here we outline the generation of mean square displacement (MSD) plots, which can then be fit to models of diffusion (Andrews et al., 2008). The best fit model reveals the type of motion (i.e. free, restricted, directed diffusion or immobile) and the diffusion coefficients for each molecule (Figure 2.8A,B). Using trajectories from GPUSPT, diffusion coefficients (D) are extracted using the function D1_3. From diffusion coefficients, cumulative probability analysis (CPA) permits comparisons of the distribution of D values for different conditions by sorting and binning measured D values. Median D is reported as the representative diffusion rate of receptors tracked under each condition.

1. For each trajectory, generate an MSD plot (see Figure 2.8).

2. Fit to the appropriate model to obtain diffusion coefficient (D)

Free: MSD = *offset* + 4*DΔt;*

Restricted: MSD = *offset* + (L^2/3)*(1-exp(-Δt / τ); τ=L^2/12D;*

Directed diffusion: MSD = *offset* + 4*DΔt* +$v^2\Delta t^2$;*

where *offset* is the y-axis offset and related to the localization accuracy, Δt is time interval, *L* is the length of one side of the area that the molecule is restricted in, and *v* is transport velocity.   The statistical error increases with large time intervals, therefore no more than the first 25% of the MSD plot should be considered for fitting.

3. To compare aggregate data, generate a Cumulative Probability Analysis (CPA) plot (see Figure 2.8C). Due to the spread in values for SPT data, diffusion coefficients are better represented by a CPA than by an average value (Ehrensperger et al., 2007). Comparison of CPA plots for different conditions immediately reveals differences in diffusional dynamics (Figure 2.8C). A CPA plot can be generated from fits to the above models. To remove the influence of restricted diffusion from the calculation of D, fitting the free diffusion model to the first few points of the MSD is often used. The number of points used can vary; we use D_{1-3} while others report D_{2-4} or D_{1-5}.

In particular, the example in Figure 2.8C shows relative diffusion for erbB1 receptors on A431 cells, tracked using QD-EGF, in the presence or absence of PD153035 tyrosine kinase inhibitor and, furthermore, in the presence or absence of pretreatment with the matrix metalloprotease (MMP) inhibitor, Batimastat. This drug is used to prevent autocrine shedding of ligand from the cell surface. Results shown in this plot demonstrate that autocrine shedding is not a marked factor in A431 cell behavior, as seen in the high degree of similarity in receptor mobility in the presence or absence of this treatment. As a result of this analysis, Batimastat was not used in A431 studies.
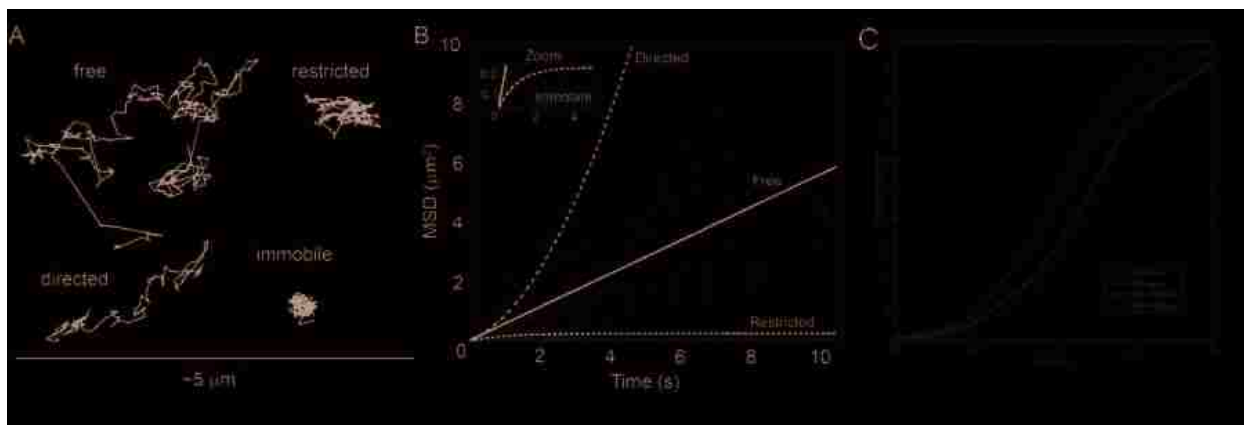
Figure 2.8. Example of analysis of Single Particle Trajectories. A) Example trajectories showing the four modes of motion that are observed for erbB receptors (Free, Restricted, Directed, Immobile). B) An MSD plot for a single particle trajectory (grey circles) shows that free diffusion (i.e. linear fit, solid black line) best represents the data. Also shown are the shapes of curve obtained from restricted diffusion (--), immobile molecules (ıı) and directed diffusion (-|-). The inset highlights the differences between the fits. C) CPA plot comparing QD-EGF behavior in the presence (red line) or absence (blue line) of PD153035, where dashed lines are in the absence of Batimastat and solid lines represent data following pretreatment with the MMP inhibitor. The leftward shift of diffusion coefficients seen in the presence of QD-EGF indicates activation and slowing of erbB1 receptors. The blue and red lines overlay almost perfectly, showing that autocrine shedding of ligand is not a significant contributor to A431 erbB1 activation.

2.3.5c Two-channel overlay

To properly analyze two-color single QD tracking data   (i.e. differentiating between dimers and colocalized QDs), optimal interchannel registration is required.   Using software to directly overlay data from each channel using just an image shift will result in suboptimal interchannel colocalization since an image splitter may introduce non-uniform chromatic aberrations into the separate images projected onto the detector.

1. Collect calibration image(s) (see Note 2.15) A calibration image should consist of single point sources spanning the field of view. Fiducial calibration data is optimal

due to its well distributed sampling of the entire field of view and the ability to optimize the localization accuracy of the point source(s) (Churchman et al., 2005) (see Figure 2.9). It is important to obtain a test and training image for calibration in order to define the localization accuracy achieved using an independent test set.

2. Localize calibration points in each channel using a 2D Gaussian PSF fit model. The width of the microscope PSF is proportional to wavelength and therefore the PSF for each channel will be different. Since localization accuracy is essential for optimal colocalization, identifying the sigma for the 2D Gaussian PSF model for each channel is recommended.

3. Train and test the calibration model

    a. Identify a proper calibration model for your instrumental setup. We use a polynomial (specifically a+bx+cy+dxy where a,b,c,d are coefficients and x,y are spatial coordinates) to describe the relationship between positions in each channel. Other calibration models are also available (Churchman et al., 2005).

    b. Use a training calibration image to build the model (find coefficients) and test the calibration image to estimate the prediction accuracy of the calibration. See Figure 2.9 for more details on channel transformation. If calibration images are acquired before and after data acquisition, then train the model with the pre-acquisition calibration and test it with the post-acquisition calibration data. This will give insights into the instrument stability during the acquisition of experimental data.

4. Apply calibration model to QD data. The coordinates obtained from single particle tracking of raw data are corrected to correspond with the reference channel using

www.manaraa.com

the calibration model.   Trajectories should always be obtained from un-shifted

images
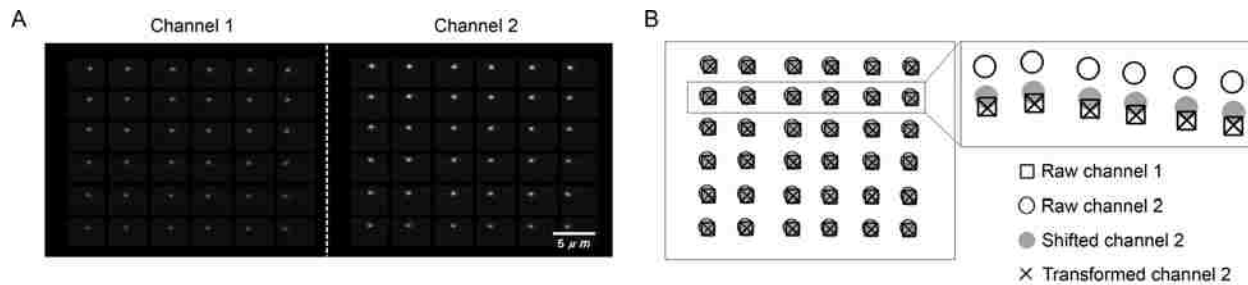
Figure 2.9. Fiducial Calibration Data Set. A) Fiducial bead data shown for each channel
using a single broad spectrum bead (200 nm Tetraspec Bead from Invitrogen) imaged
by stepping the stage (5 μm) to sample the entire emCCD. B) Analysis of the calibration
image shows the imaged positions for each channel, the linearly shifted channel 2 data,
and the transformed channel 2 data. This transformation vector is then used to
transform the channel 2 SPT data to allow overlay with channel 1 trajectories.

2.3.5d Correlated motion analysis

Pair-wise comparisons of two-color trajectories permit further description of receptor

behaviors, namely the presence of interactions whose lifetimes are longer than the

imaging acquisition time. This analysis shows the degree of correlated motion by

determining parameters for each candidate pair in sequential frames. The trajectories of

receptors during an interaction will be coordinated, as seen in a decrease in the

uncorrelated jump distance parameter (see Figure 2.10).

1. Determine initial separation between two trajectories; if this is less than a specified

    cutoff (i.e. 500 nm), continue to analyze the candidate pair.

2. Uncorrelated jump distance is determined for all candidate pairs at each time step

    using: $D_i = \left| J_i - J_i (J_i \cdot J_j) / (|J_j||J_i|) \right|$, where $J1_i = r1_{i+1} - r1_i$ and $J2_i = r2_{i+1} - r2_i$. $|J_i|$

    represents the magnitude of the displacement during a time step and r_i is the

64

position of a QD at time *i* (Andrews et al., 2008). The uncorrelated jump distance

parameters are averaged and binned in 50 nm separation intervals for plotting.
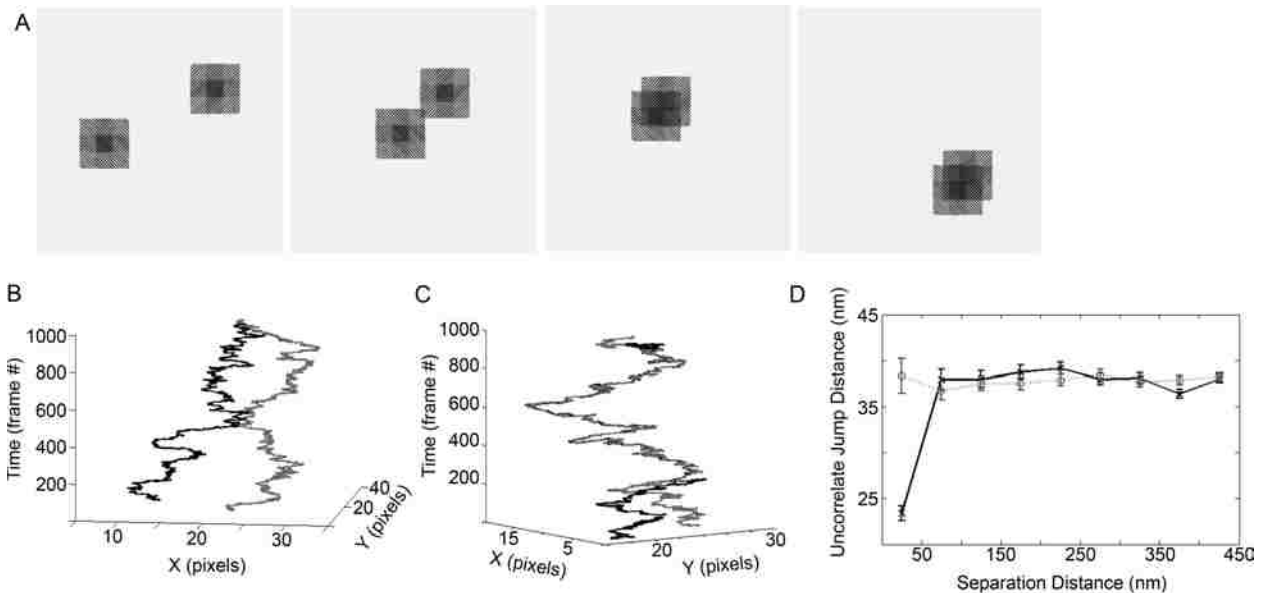
Figure 2.10. Pairwise Correlated Motion Analysis of Simulated Single Particle Trajectories. A) A schematic of two-color QD tracking shows single molecules that are initially separated, but in frame 3 form a dimer and continue to move in a coordinated manner, reflecting the interaction between the receptors. B) and C) Simulated two particle trajectories of receptors demonstrating uncorrelated and correlated motion, respectively. Particle trajectories are plotted in three dimensions using coordinates and time frame. D) Global analysis of many simulated trajectories demonstrates the trends seen in the cases of correlated (black) and uncorrelated (grey) motion. In the former case, as particles come within the interaction distance and move together, the uncorrelated jump distance parameter markedly decreases. Simulation conditions included 10 particles for each QD color, 5000 frames, diffusion coefficient = 0.07 μm^2/s, and a 25 nm interaction distance. Correlated motion analyses of erbB receptors can be found in Chapters 3 and 4.

2.3.5e Movies

Color overlays can be made using cropped data; the true overlay is generated

using the transform from the fiducial calibration, but is very slow. This is done by looping

over each frame using the function ch2_2_ch1. Rudimentary overlays can be made using a simple lateral shift vector, determined using alignsplitim.

Script:

```
resultsdir='Z:\Shal\SPT Data\100108_A431_PD\Chamber1\';

codir='Z:\Shal\SPT Data\100108_A431_PD\Chamber1\ColorOverlays\';

mkdir(codir);

tformdir='Z:\Shal\SPT Data\100108_A431_PD\Chamber1\';

tformfile='FiducialCalibrationStart';

load([tformdir tformfile]);

Lfiles=dir([resultsdir 'L*']);

Rfiles=dir([resultsdir 'Ru*']);


for kk=1:size(Lfiles,1)

        clear coloroverlay

        load([resultsdir Lfiles(kk).name])

        fn=Lfiles(kk).name;

        load([resultsdir Rfiles(kk).name]);

        for tt=0:999

                ch1=squeeze(L(:,:,tt));

                ch2=squeeze(Ru(:,:,tt));

                [temp_ch1_out temp_ch2_out] = ch2_2_ch1(ch1,ch2,tform,0);   %
                changed last input from 1 to 0 so that plots aren't generated every
                time - should be faster.
```

```
        if tt == 0

                ch1_out = newim([size(temp_ch1_out) size(L,3)]);

                ch2_out = newim([size(temp_ch2_out) size(Ru,3)]);

        end

        ch1_out(:,:,tt) = temp_ch1_out;

        ch2_out(:,:,tt) = temp_ch2_out;

    end

    co = joinchannels('RGB',stretch(ch1_out,50,100),stretch(ch2_out,50,100));

    % you want to save this as you go through the loop or else will simply
    overwrite it.

    save([codir 'co_' fn],'co');

end
```

It is often easiest to view movies in .avi format. The coloroverlays can be converted, en masse to .avi using the function writedisplayavi.

Script:

```
codir='Z:\Shal\SPT Data\100109_A431\Chamber1\ColorOverlays\';

cofiles=dir([codir 'co*']);

avidir='Z:\Shal\SPT Data\100109_A431\Chamber1\ColorOverlays\Avis\';

mkdir(avidir);

for kk=1:size(cofiles,1)

    clear co

    load([codir cofiles(kk).name]);

    fn=cofiles(kk).name;
```

```
co

writedisplayavi(1,[avidir fn '.avi'],20,'Cinepak');

close all

end
```

2.3.6 Hidden Markov Model data analysis

Pairwise trajectories from two-channel data are analyzed using a modified three-state Hidden Markov Model (HMM). Using this approach, the underlying state behavior of interacting receptors can be fit using the known separation distances at each timepoint. Initially, a simple, two-state model for monomeric or dimeric receptors was employed to analyze data sets. After thorough analysis and the visualization of idealized dimers from the bleedthrough of QD625 signals into both imaging channels simultaneously, we determined that the two-state HMM could not comprehensively explain our observations (for further details, please see Appendix C from Low-Nam, et al.). The final HMM consists of three states (free or monomeric, domain co-confined, or dimeric) for erbB receptors on cells. Our observations of single receptors on cells permits not only determination of the interaction kinetics of dimerization, but also points out the significant influence of domain arrangement and membrane architecture on complex formation, molecular collisions, and signaling. A more complete explanation of this approach and its derivation can be found in our manuscript, Low-Nam, et al., Chapter3.

2.3.6a HMM data structure

For data to be evaluated in the HMM, it is helpful to reorganize the files so that all the data of the same type (ie 2-color EGF) are in the same folder. Unlike the model developed by Beausang and Nelson, we do not implement a transition matrix (Beausang et al., 2007). The data are organized into a structure that includes path information to the raw data, calibration files, and tracking results. This data structure is augmented with each analysis step so that the pertinent information is linked and can be retraced. The HMM functions are described below. A comprehensive script and all of the functions needed for analysis are included in Appendix D.

HMM_LinkData:

Creates the HMMData format (.HMMDATA file type) and connects data files for each acquisition (raw data, background and beads image, fiducial data sets). An example of the data structure is seen in Figure 2.11.

HMM_Track

This function tracks data of the type HMMData using the SPT tracking functions previously explained (Smith et al., 2010). Fiducial calibration and channel registration are also performed. For further analysis data of the type HMMData_raw_ch1_tracks and HMMData_shifted_ch2_tracks are on a common coordinate system and can be directly compared (refer to Figure 2.11).

Data preprocessing and fitting

Dimer candidates are found using the function HMM_PreprocessStates. This filtering determines which tracks come within a minimum distance cutoff (1 μm, currently) and have at least 3 simultaneously valid frames – both characteristics are

necessary for an interaction to be considered. To handle so much data, this pairwise analysis is done in cycles, to prevent running out of memory. For pairs of trajectories that meet the cutoffs, a vector of coordinates, valids, and localization accuracies is saved along with a PairID number. A plot of the distances between the trajectories can be generated, if desired; alternately, the distancepath parameter can be passed in as an empty vector (for the two-state model only). A data type HMM_PreProcessData (.HMMPP file type) is created. This structure is augmented in subsequent analyses and an example of the results can be seen in Figure 2.11.

Candidate pairs are passed into the function PMatrix to determine the probabilities of transitions using the function Pbr1r2. The likelihood of the current state, given state the preceding one and the separation distance between the particles during that time step, is determined, where receptors can only enter the bound state when they are within the interaction distance (see Note 2.16). The Diffusive Hidden Markov Model is run using the function HMM_FindRates. This only fits in the forward direction for a range of Tau_BF and Tau_BB values (we do not employ the forward-backward algorithm as we found that it did not improve the rate fits); plots are generated for the maximum likelihood values of the rates and a mesh plot can be shown (for the two-state model only).

Viterbi algorithm and plotting

After the reaction rates have been solved, the Viterbi algorithm (Viterbi, 1967) is implemented in order to determine where sets of trajectories exhibit each type of state behavior. The functions HMM_FindStates and HMM_StatesDist are used to assign state values (3-free, 2-domain, 1-dimer) to each trajectory at each time step and ensure

the filling of the State Matrix for further analyses. The function HMM_PlotCandidates_3state can be used to plot candidate pairs. Plots for trajectories in 3D, distance between tracks with a state trace overlay, and others are generated. These plots can be useful to look through in order to find ideal pairs for making movies or figures. An example of plots can be viewed in Figure 2.12. However, this can be a time-intensive step because all candidate plots will be created and saved; plotting can also be performed at a subsequent time and examples of plotting scripts can be found in Appendix D.

A.

```
HMM_Data =
          TreeDir: 'Z:\Shal\SPT Data\GroupedData_A431_Final\'
         DataFile: '\EGF\100611\Chamber1\EGF-2010-6-11-14-6.mat'
           BGFile: [1x51 char]
       Bead_Align: '\EGF\100611\Chamber1\fiducial-2010-6-11-14-1.mat'
      Bead_Align1: '\EGF\100611\Chamber1\fiducial-2010-6-11-14-32.mat'
          SaveDir: [1x58 char]
           FigDir: [1x66 char]
        Bead_Gain: '\EGF\100611\Chamber1\Beads-2010-6-11-13-59.mat'
        PixelSize: 2.6667e-001
         TimeStep: 5.0000e-002
           ch_bin: [1 1]
   DataConditions: 'QD EGF'
         Dconvert: 7.0312e-001
            tform: [1x1 struct]
   raw_ch1_tracks: [23x1000x2 double]
   ch1_intensities: [23x1000 double]
       ch1_valids: [23x1000 logical]
          ch1_LA: [23x1000 double]
       ch1_sigma: [23x1000 double]
   raw_ch2_tracks: [16x1000x2 double]
   ch2_intensities: [16x1000 double]
       ch2_valids: [16x1000 logical]
          ch2_LA: [16x1000 double]
       ch2_sigma: [16x1000 double]
  shifted_ch2_tracks: [16x1000x2 double]
```

B.

```
HMM_PreProcessData =
         StartFrame: {1x135 cell}
           EndFrame: {1x135 cell}
             PairID: {1x135 cell}
             FileID: {1x135 cell}
           D_Thresh: 2.0000e-001
             IntDis: 1.8750e-001
                  L: 3.7500e+000
         MinOverlap: 10
            MinPath: 50
          DutyCycle: 5.0000e-001
            MinTime: 10
            Nstates: 3
           P_states: {1x135 cell}
           V_states: {1x135 cell}
         DomainSize: 5.6250e-001
      K_matrix_found: [3x3 double]
   K_matrix_found_err: [6x1 double]
  K_matrix_found_Hessian: [6x6 double]
                InP: 4.2920e+004
         StateMatrix: {1x135 cell}
            PViterbi: {1x135 cell}
        FilledStates: {1x135 cell}
         StateLength: [12x1 double]
```

Figure 2.11. Analysis structures include sub-structures, vectors, and paths. A. The HMM_Data type is created in order to keep track of raw data and results from tracking. B. The HMM_PreProcessData type shows the results of preprocessing, fitting, and subsequent HMM analyses.
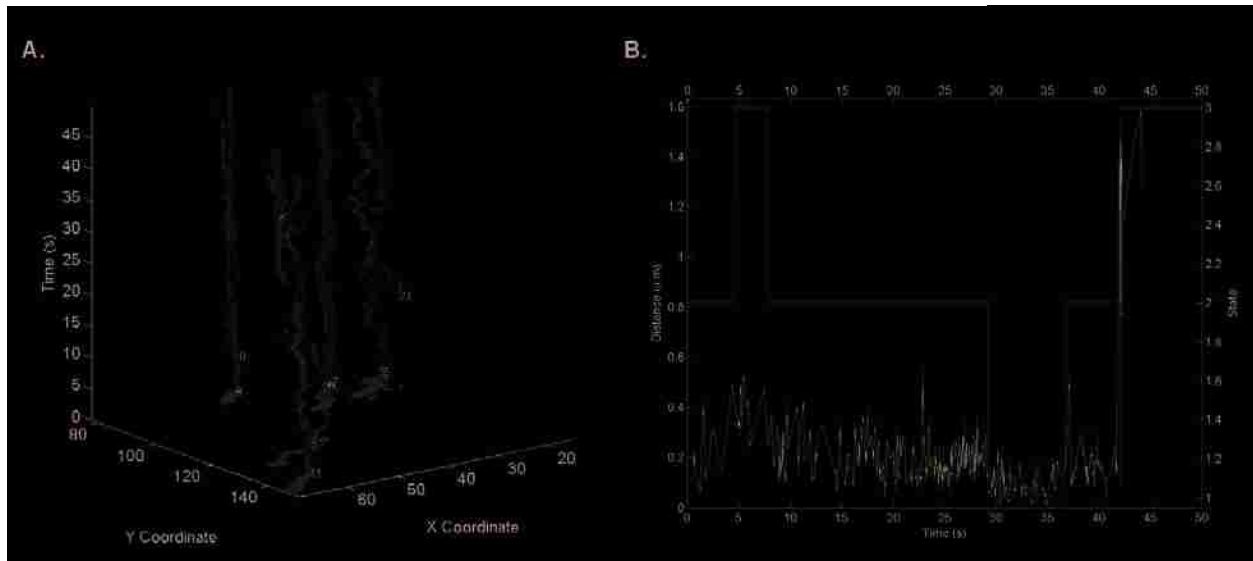
Figure 2.12. Plotting of HMM results. A. 3D trajectories for all candidate pairs in a single movie. Tracks are shown in red and green for QD655 and QD585, respectively. State colors are overlayed for domain (magenta) and dimer (blue). When no state information exists, the tracks are considered to be free. B. An example of a distance and state trace for a pair see in 6A. The state trace shows all three states: free (red), domain (magenta), and dimer (blue) over the black distance between tracks (in µm) for the 50 second acquisition.

Diffusion by state

Once the states have been determined, diffusion analysis can be performed, using the Filled State information to separate mobility by state. D1_3 analysis cannot be implemented due to insufficient information for short tracks. Instead, diffusion is determined using Square Displacement analysis that uses all values for squared displacement for a given time interval and fits the distribution, using a two-component least squares regression (de Keijzer et al., 2008). Results shown in Figure 2.13 are obtained using Pr2_3State.
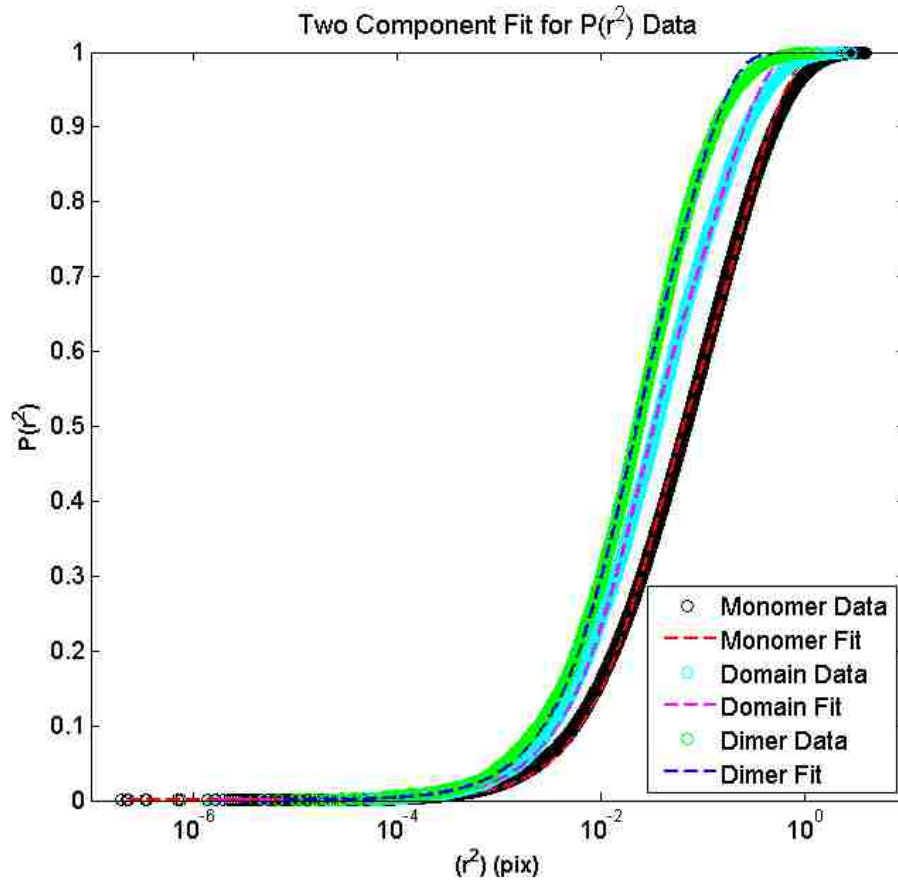
Figure 2.13. State-dependent diffusion analysis of HMMData tracks. Data from the QD655 channel is analyzed using the Square Displacement approach. Using the state matrix from HMM_StatesDist, the data are sorted by state and plotted as a cumulative probability distribution of square displacements (r^2). A two-component fit to the distribution is used to determine the diffusion coefficient. As expected, the QD-EGF data shown in this example display slowed diffusion from monomer-to-domain-to-dimer states, observed as a leftward shift in the data.

2.3.7 Notes

2.7. Labeling conditions can be optimized by first using a fluorescent (rather than biotin) derivative of succinimidyl ester, such that the conjugation chemistry is the same and the dye-to-protein ratio can be easily determined by spectrophotometric absorption measurements.

2.8. QD-protein probes should be diluted to appropriate concentrations in imaging buffer just before use since buffers containing divalent cations can cause SAvQD aggregation over time.

2.9. Typical QD tracking is performed using two colors of the same protein. However, the heterodimer is monitored using one color conjugated to VHH and the other to EGF. It can be useful to check that the color choice does not alter the measured diffusion or interactions, but evidence from our data suggests that the QD color does not affect the measurement.

2.10. Cells are typical grown in media that does not contain the pH indicator, phenol red. In the absence of this indicator, it is important to monitor the pH occasionally to ensure that there are not substantial changes in this parameter. In particular, serum starving cells in phenol free media is useful in minimizing cellular autofluorescence that can often result from the retention of phenol red as small packets inside cellular vesicles.

2.11. Although simultaneous addition of QDs to cells is often preferable in tracking of erbB receptors, sequential labeling can be used to optimize density of labeling. When adding QD solutions to a well for imaging, it is preferable to slowly add 50 µL of probe

solution to 300 µL of cells in Tyrode's in order to prevent a response elicited simply by mechanical response to the solutions mixing.

2.12. For analysis, the first fiducial trn image should be used for calibration and the second tst image for testing and error analysis. It is beneficial to acquire fiducial calibration as often as is feasible within the experimental conditions. If beads appear to go out of focus during the acquisition of a fiducial image, then the microscope needs to be refocused and the fiducial calibration image needs to be reacquired.

2.13. While QDs are highly photostable, illumination with intense light can increase QD blinking and even lead to blue-shift and photodegredation of the QD emission. Therefore, optimal illumination power (typically controlled through neutral density filters) that maximizes QD signal but does not lead to blue-shifting should be determined for each system. Channels are aligned and allowed to sit at least four hours (preferably overnight) before imaging. The springs relax over time and are allowed to reach equilibrium prior to data acquisition. The camera is controlled using the andorixon GUI and data is saved using the lasercontroller GUI.

2.14. In single particle tracking, the parameters for single molecule thresholds and trajectory connection probability thresholds should be optimized on a sub-set of data and checked manually before proceeding with an automated analysis of larger data sets.

2.15. We have observed sporadic instrumental drift when using an image splitter; therefore, it is important to investigate stability when performing experiments in which nanometer overlay accuracy is important. We have found it good practice to obtain a calibration image both before and after data acquisition to ensure instrument stability.

2.16. Two distances are involved in state characterizations using the HMM. The interaction distance (ID) is defined by the crystal structure size of the erbB dimer, including accounting for the size of the QD probes used to visualize the interaction. On the other hand, the confinement zone size (domain distance, DD), is fit within the HMM itself and requires looping the fitting routine over a range of DD values (typically 50:50:500; that is 50 to 500 nm at 50 nm intervals). Thus, domain sizes are not predetermined, but extrapolated from the raw data.

CHAPTER 3: ERBB1 DIMERIZATION IS PROMOTED BY DOMAIN CO-CONFINEMENT AND STABILIZED BY LIGAND

Shalini T. Low-Nam[1], Keith A. Lidke[2], Patrick J. Cutler[1], Rob C. Roovers[3], Paul M.P. van Bergen en Henegouwen[3], Bridget S. Wilson[1], Diane S. Lidke[1*]

[1]Department of Pathology and Cancer Research and Treatment Center, [2]Department of Physics, University of New Mexico, Albuquerque, NM; [3]Department of Cellular Dynamics, Institute of Biomembranes, Utrecht University, The Netherlands

* To whom correspondence should be addressed. E-mail: dlidke@salud.unm.edu

3.1 INTRODUCTION, RESULTS AND DISCUSSION

Ligand-induced signaling by the epidermal growth factor receptor (EGFR/HER1/erbB1) drives cell growth, adhesion and survival (Schlessinger, 2002). Structural studies suggest that ligand binding stabilizes the extended extracellular domain conformation, permitting formation of a back-to-back homodimer (Ferguson et al., 2003) and initiating signaling. Outstanding questions in the field include the role of preformed, unliganded dimers, (Chung et al., 2010; Hofman et al., 2010) relative stability of dimers with different ligand-receptor stoichiometries (Sako et al., 2000; Lidke et al., 2005a; Macdonald and Pike, 2008), and the receptor reaction kinetics within the context of the membrane (Orr et al., 2005; Hsieh et al., 2008). Here, two-colour quantum dot (QD) tracking is used to directly visualize erbB1 homodimerization on living cells. Kinetic parameters were extracted from pairwise trajectories using a 3-state Hidden Markov Model (HMM) that identifies transition rates between free, domain-confined, and dimer states. We present evidence that co-confinement in membrane microdomains promotes repeated encounters between receptors, enhancing dimer formation. We find that dimers composed of 2 ligand-bound receptors are long-lived and their off rate (k_{off}) is independent of kinase activity, while unliganded dimers have >4-fold faster off rates. Mobility decreases >6-fold when ligand-bound receptors form dimers. Large changes in diffusion are not observed in the absence of ligand or presence of kinase inhibitors, pointing to reduced mobility as a feature of signal propagation.

Early estimates of erbB1 dimerization parameters relied on solution-based measurements and the use of recombinant extracellular domains. *In vitro* approaches,

including chemical crosslinking and small-angle x-ray scattering, have been coupled to mathematical modeling for estimation of homodimer equilibrium dissociation constants in the absence and presence of ligand (Sherrill and Kyte, 1996; Lemmon et al., 1997; Kholodenko et al., 1999). The effects of receptor number and density on dimerization behavior have also been considered by computational approaches (Shankaran et al., 2006; Hsieh et al., 2008), supported by indirect evidence such as tyrosine phosphorylation kinetics as well as recent fluorescence correlation analyses (Nagy et al., 2010). These prior studies considered the ensemble, steady state behaviors of erbB1 but do not address the stochastic nature of receptors encountering each other in the fluid and dynamic landscape of the plasma membrane. In particular, they fail to address accumulating evidence that the membrane is composed of heterogeneous microdomains that can serve as transient confinement zones (Kusumi et al., 1993; Simson et al., 1995) with the potential to influence the signaling process.

Sophisticated fluorescence imaging techniques have been used to investigate features of erbB1 behavior, including receptor diffusion and clustering (Sako et al., 2000; Ichinose et al., 2004; Lidke et al., 2004; Lidke et al., 2005a; Orr et al., 2005; Nagy et al., 2010). EGF-bound quantum dots have permitted tracking of ligand-bound erbB1 homodimers and heterodimers on live cells, with an early focus on filopodial transport and internalization kinetics (Lidke et al., 2004; Lidke et al., 2005a). These photostable fluorescent nanoprobes have useful photophysical properties, such as broad excitation and narrow emission spectra, permitting extended periods of observation and facilitating simultaneous two-colour single particle tracking (SPT) (Lidke et al., 2005a; Andrews et al., 2008; Roullier et al., 2009). Prior QD-EGF studies revealed that a 2:2 EGF:erbB1

dimer was the predominant signaling competent complex (Lidke et al., 2005a). Here new analytical methods were developed to quantify receptor dynamics, with an emphasis on differences in diffusion and dimerization off rates related to receptor occupancy and activation state.

Figure 3.1A illustrates our experimental approach using two-colour QD tracking to follow the dynamics of endogenous erbB1 receptors on the apical surface of live A431 cells. Receptors were labeled with QDs conjugated to either EGF (Lidke et al., 2004) or a non-activating, monovalent camelid anti-erbB1 antibody fragment (VHH) that does not compete for EGF binding (bottom plane) (Hofman et al., 2008). Simultaneous, two-colour imaging was achieved using a beam splitter that projects QD655 (magenta) and QD585 (green) emissions onto the emCCD (middle plane). Finally, a custom-designed image registration method is used to map the relative positions of 585 and 655 QDs over the time course of data acquisition (top plane). As described in the Supplementary Information, image registration was based on fiducial calibration of pairwise images of immobilized, two-colour fluorescent beads(Churchman et al., 2005). Fast computation of single molecule trajectories was accomplished using a GPU-based approach, which identifies single molecule locations and builds trajectories using post-processing algorithms (see Supplementary Information, Fig. S3.1 online) (Smith et al., 2010). These data sets provided two types of information about receptor behavior. First, diffusion coefficients were extracted from the trajectories of individual receptors using well-established methods(de Keijzer et al., 2008). Second, novel computational analyses of two-colour imaging data permitted measurement of dimerization and state-dependent behavior .

Figure 3.1B reports global changes in diffusion properties of erbB1 receptors under different experimental conditions, represented as the probability distribution of squared displacements (de Keijzer et al., 2008). Each curve is derived from single QD tracking of thousands of diffusing receptors and shows the broad range of diffusional behaviors for a given receptor state, with left-shifted plots being the slowest (see Supplementary Information, Table S3.1 online). Ligand-bound receptors were tracked using either QD-VHH probes in the presence of saturating concentrations of nonfluorescent EGF (10 nM) or picomolar concentrations of QD-EGF. These data show a strong relationship between diffusion and activation state, with the resting receptors (QD-VHH, orange) having a higher mobility than ligand-bound (QD-EGF, black) receptors. In the presence of PD153035 that inhibits erbB1 kinase activity (Fry et al., 1994), ligand-bound receptors displayed fast mobility (green), similar to resting diffusion. The slowed lateral motility of ligand-bound receptors is thus linked to tyrosine phosphorylation, possibly through protein scaffolding or signaling-induced changes in the local environment. Importantly, the addition of dark EGF to QD-VHH-labeled cells results in slower diffusion of the receptors, confirming that the QD-VHH does not interfere with ligand binding or dimerization.
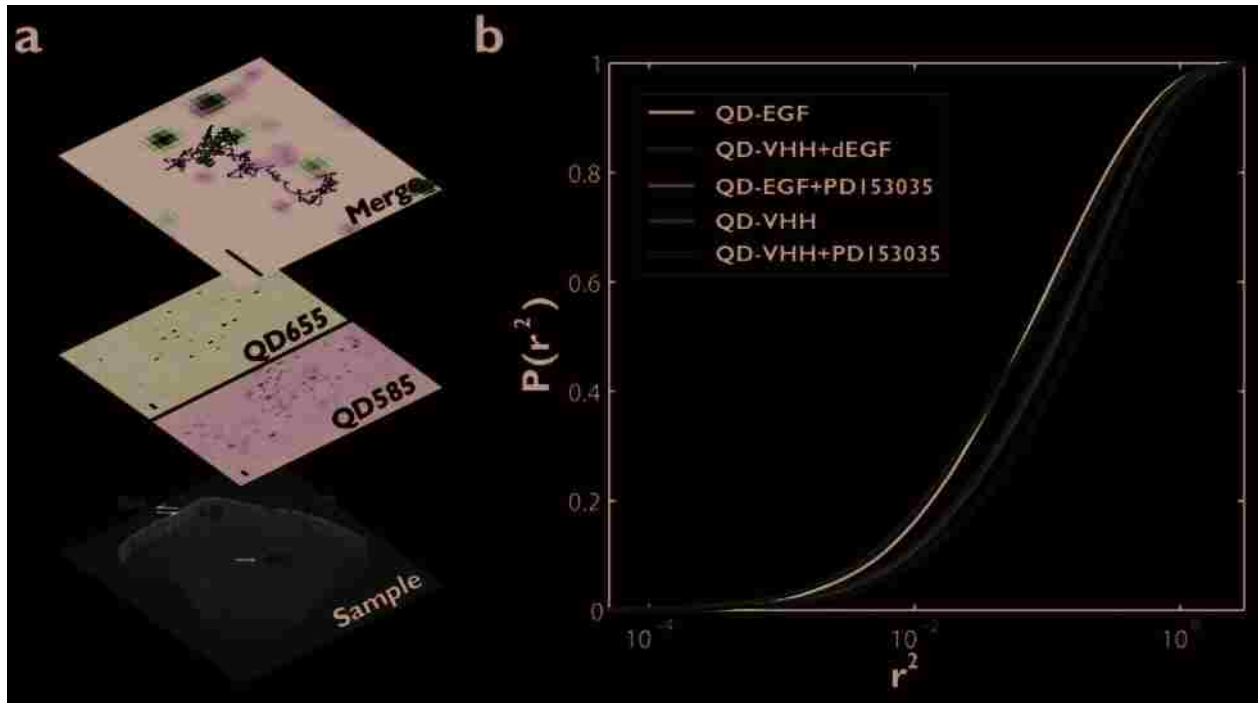
Figure 3.1. Slowed diffusion as a function of receptor activation is revealed by single QD tracking on the apical surface of A431 cells. (a) Following 4 hours of serum starvation in the absence or presence of 1 μM PD15035, the activated and resting erbB1 receptor were labeled and tracked on live A431 cells with either two colors of 2 pM QD-EGF, 20 pM QD-VHH, or a combination of each at 37°C, respectively. Bottom plane: ErbB1 receptor cartoons (blue, not to scale) on the surface of an adherent cell on a coverslip, with probes recognizing the tethered and extended conformations (EGF ligand, blue; VHH, orange; QD655, magenta; QD585, green). Middle plane: Single molecules were visualized in a QD655 or QD585 channel for up to 7 minutes after stimulation. Top plane: Following SPT and image registration, trajectories are plotted on the same coordinate system. Scale bar, 2 μm. (b) Cumulative probability plot of squared displacement for each condition: QD-EGF (black), QD-VHH + non-fluorescent EGF (purple), QD-VHH (orange), QD-VHH + PD153035 (green), and QD-EGF + PD153035 (blue). A rightward shift in distribution indicates increased diffusion. Fits for two-component square displacement analyses are provided as Supplementary information (Table S3.3).

Imaging of spectrally-distinct QDs allowed direct observation of receptor associations. As receptors approach each other, their relative motion reveals insights into their interactions and the constraints imposed by membrane architecture. In Fig. 3.2A, QD-EGF585-erbB1 (green) and QD-EGF655-erbB1 (magenta) complexes are observed to diffuse in close proximity for ~30 s before forming a stable dimer (white) that persists until the end of the acquisition (see Supplementary Information, Video S3.1 online). Plots in Fig. 3.2B show the trajectories of each receptor (middle), as well as their separation distance (bottom) over time. Note the sharp drop to a separation distance of ~50 nm that marks the dimerization event is accompanied by correlated motion of the trajectories starting around t=30 s. This 40-50 nm offset is consistent with an estimate of the spacing between the centres of two QDs attached to the back-to-back, ligand-bound erbB1 homodimer crystal (see Supplementary Information, Fig. S3.4 online). Figures 3.2C-D show a representative encounter between one ligand-bound and one resting erbB1. These receptors experience long durations of close proximity (<500 nm), demonstrating the ability of membrane microdomains to co-confine receptors (Kusumi et al., 1993; Andrews et al., 2008; Roullier et al., 2009). After 5-10 s of co-confinement, the receptors move far apart as they escape from the domain. These data show that dimerization events can be captured in real-time and also illustrate the need to develop analytical tools that distinguish between close approach and *bona fide* dimer events.

Correlated motion analysis offers a means to validate dimerization across large data sets of two-colour trajectories (Fig. 3.2E-F; see Supplementary Information, Fig. S3.2 online) (Andrews et al., 2008). This method reports receptor displacement (jump

magnitude, red) and the degree of uncorrelated motion (blue) between receptors in the population as a function of separation distance. Dimerized receptors are expected to move together, exhibiting correlated motion. For ligand-bound receptors (Fig. 3.2E,F), this is seen as a reduction in uncorrelated jump distance at close distance. This behavior is not altered by PD153035 treatment, confirming that EGF binding strongly promotes dimer formation that is independent of kinase activity. We further address this interesting observation in Figure 3.3 below. Of note, despite observations of close approach between QD-VHH-erbB1 complexes, this analysis method showed no correlated motion in the absence of ligand (Fig. 3.2G). These data indicate that dimers between unliganded receptors must be of short duration compared to the time-scale of these measurements (0.05 s). In contrast, interactions between one EGF-bound and one unliganded receptor do demonstrate correlated motion (Fig. 3.2H).

84
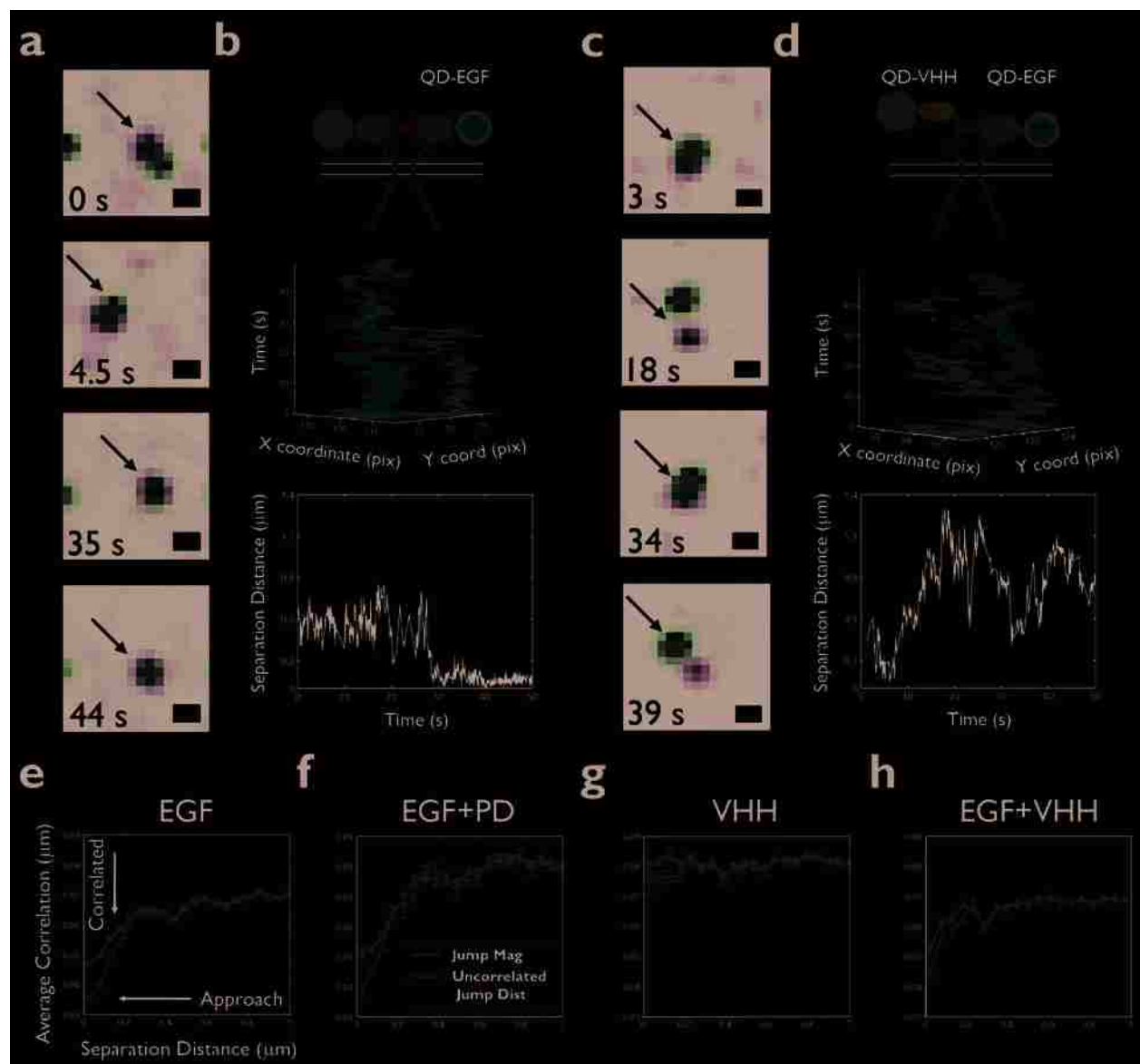
Figure 3.2. Direct visualization of erbB1 dimerization is captured by two-color SPT. (a) Sample time series showing dimer formation (white) between QD585-EGF-erbB1 (green) and QD655-EGF-erbB1 (magenta). (b) Cartoon of tracking condition (top), 3D trajectories (middle), and distance between receptors (bottom) as a function of time are shown for the indicated receptors in (a). (c) Sample time series for QD655-EGF-erbB1 and QD585-VHH-erbB1 shows interactions for a 1:2 EGF:erbB1 dimer. (d) Cartoon of tracking condition (top), 3D trajectories (middle), and distance between receptors (bottom) as a function of time are shown for the receptors in (c). Scale bar, 0.5 μm. (e-h) Ensemble correlated motion plots summarize all two-color data for EGF, EGF+PD, and

VHH conditions. A decrease in uncorrelated jump distance (blue) at short separations indicates that receptors are moving together. A concurrent drop in jump magnitude (red) demonstrates decreased diffusion.

To extract dimerization kinetics, we developed a mathematical model based upon a Hidden Markov Model (HMM) approach (Rabiner, 1989).   This method generates a maximum likelihood estimate of the kinetic rate constants for transitions between states. For a set of observables, in this case separation between two receptor trajectories, the HMM is used to identify hidden states that reflect the underlying behaviors of the proteins.   In order to accurately represent the data, we implemented a three-state model: free, domain-confined and dimer (see Fig. 3.3A,B and   Supplementary Information, Fig. S3.5 online). Domains are considered to be cell surface regions that may be mobile and provide a barrier to free diffusion, causing receptors to deflect off the boundaries and facilitate repeated interactions between resident proteins. Although domain composition is not explicitly considered in our model, these microdomains are consistent with prior work describing "actin corrals" (Kusumi et al., 1993; Andrews et al., 2008), "lipid rafts" (Chen et al., 2004) or "protein islands" (Lillemeier et al., 2006). The model provides an objective fit for the size of confinement zones by optimizing error terms.   QD-EGF-bound receptors are the most constrained, with a Gaussian sigma of 150 nm (see see Supplementary Information,and Table S3.2 online).

Results in Figure 3.3C provide, for the first time, accurate measurement of intact receptor dimer off rates. A summary of kinetic parameters derived from these data is reported in Supplementary Information, Table S3.2.   Notably, k_{off} for ligand-bound homodimers are similar, regardless of treatment with the kinase inhibitor.   Dimers that

form between receptors in the absence of ligand (QD-VHHs) exhibit a >4 fold higher off rate (see Supplementary Information, Video S3.2 online). We conclude that preformed dimers are highly transient. Finally, dimers composed of one ligand-bound erbB1 and one unoccupied receptor were also relatively unstable, with a 2-fold larger off rate than dimers composed of two EGF-bound erbB1. Thus, EGF binding to both receptors in a dimer is required for the most stable complex formation.
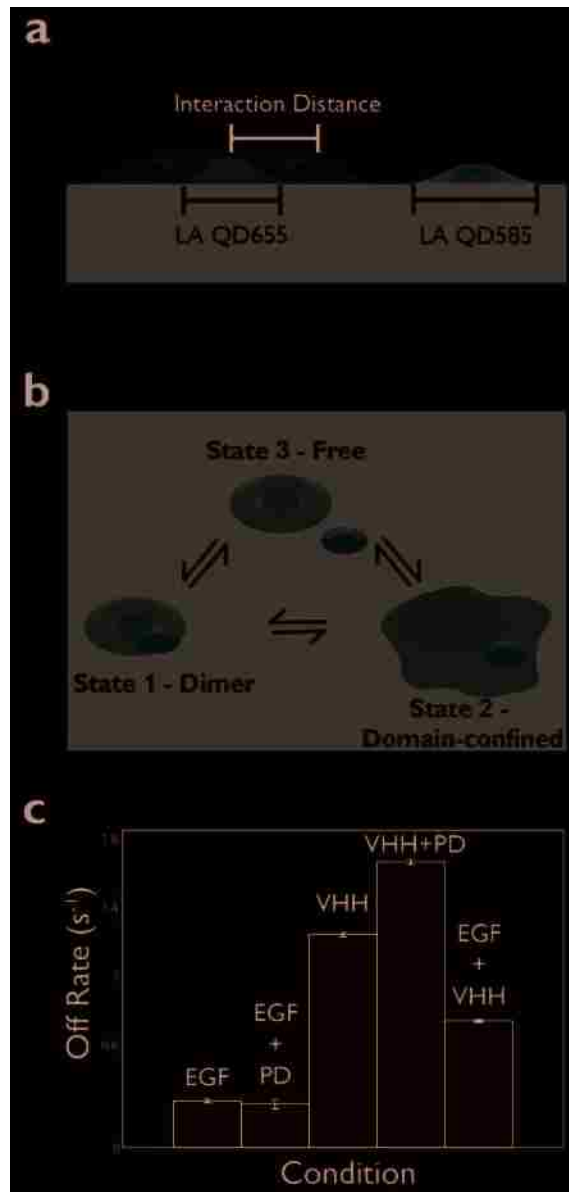
Figure 3.3. Kinetics of homodimerization characterized by a three-state HMM reveal activation state dependent off rates. (a) Definition of a dimer. Two-color receptors are fit with localization accuracies (LA) for each channel; the white probability surface represents the area within which a dimer is identified. The interaction distance (ID) is defined by the crystal structure of the back-to-back erbB1, EGF bound dimer and the diameters of the QDs (40-50 nm). (b) The three states are defined as Free, Domain-Confined, and Dimer, based on observed separation. Six kinetic rates are fit for the transitions between these states. (c) Off rates (s^{-1}) for dimers fit using the three-state

HMM. Off rate is defined as the sum of the rates of transitions between the dimer-to-domain confined and dimer-to-free states.

As a final analysis step, the Viterbi algorithm was used to identify states within candidate pair trajectories (see Supplementary Information, Fig. S3.5 online) based on the kinetic parameters returned from the HMM (Forney, 1973). An example of such a state path is shown in Fig. 3.4A. Here, two ligand-bound erbB1 are observed to explore the same domain (magenta line) for up to 50 seconds, interspersed by multiple 10-15 second periods of dimer formation (blue line). This type of behavior was observed in multiple experiments (see Supplementary Information, Fig.S3.5 and Videos S3.3,S3.4 online), underscoring the importance of co-confinement to foster repeated interactions between the same pair of receptors. It would be exceedingly rare to observe these types of rebinding events in a well-mixed environment. A second type of behavior is shown in Fig. 3.4B, where two receptors form a stable dimer at 28 sec that lasts throughout the remainder of the acquisition period. We next determined the duration of individual dimer events observed in our entire data set. Fig. 3.4C reports the distribution of dimer lifetimes for ligand-bound (QD-EGF) versus unoccupied (QD-VHH) receptors. Note that less than 6% of dimers between unoccupied receptors last longer than 4 s (Fig. 3.4C inset). In contrast, long-lived dimers are a striking feature of two liganded receptors (>34% exceed 4 s).

From our state information, we were also able to determine the diffusion coefficient for receptors identified as monomers, domain-confined or dimers under each experimental condition (Fig. 3.4D, see Supplementary Information, Table S3.3 online). Consistent with the correlated motion analysis (Fig. 3.2G), unoccupied receptors retained fast mobility in all states. The most dramatic change in mobility is seen with

89

signaling competent QD-EGF-bound dimers. These complexes often become immobile, with an average >6-fold reduction compared to the unconfined monomer state. In the presence of PD153035, QD-EGF-erbB1 dimers only slow down by two-fold, demonstrating that dimer diffusion is dependent on tyrosine kinase activity (see Supplementary Information, Video S3.6 online).
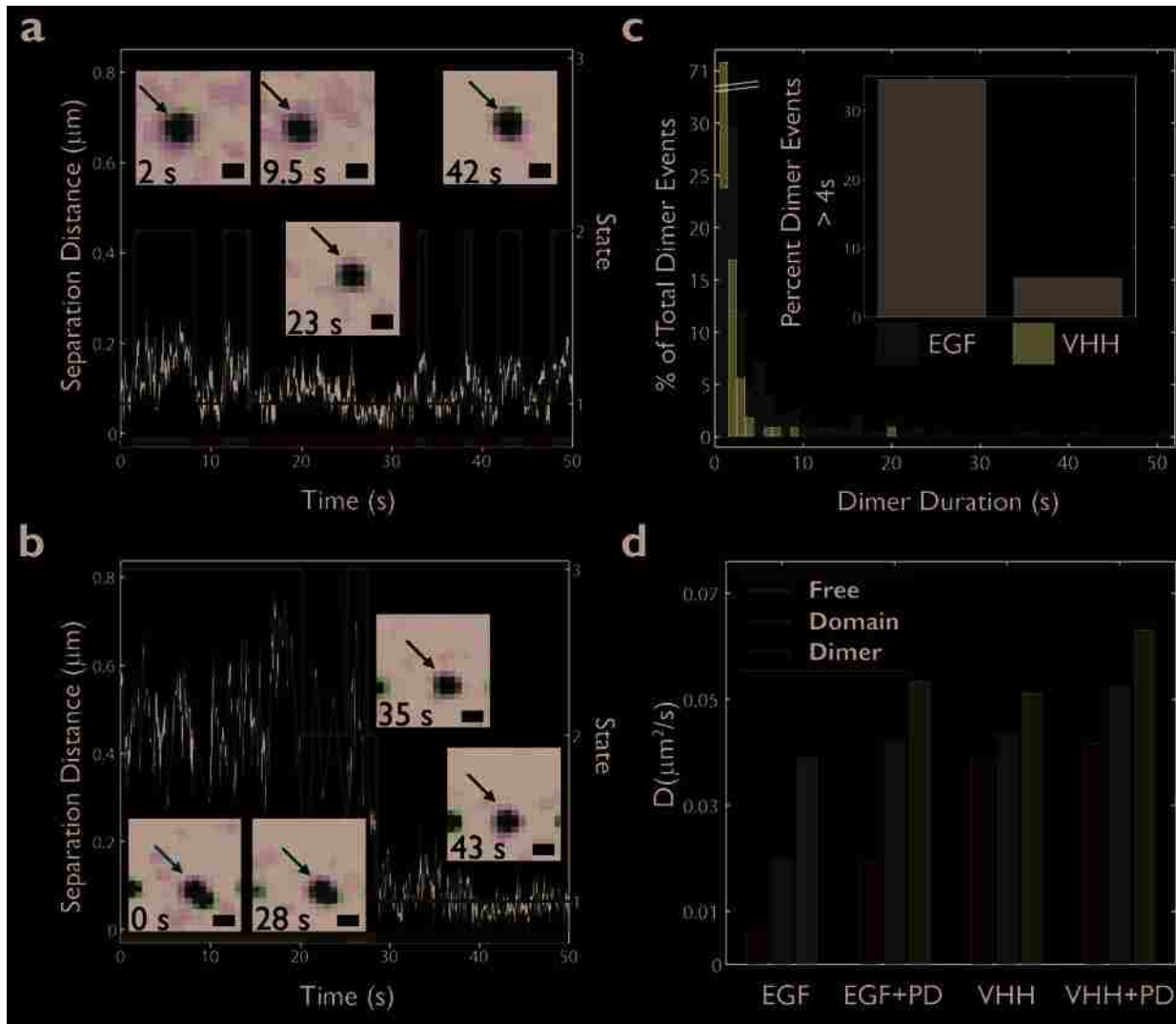
Figure 3.4. State-dependent analysis of erbB1 behavior after HMM fitting reveals underlying interaction mechanisms. (a) An example distance trace (black) for two QD-EGF-bound receptors shows close approach punctuated by periods of excursion. Domain state (2, purple) and dimer state (1, blue) are connected by green segments to

show state path. This path is projected onto the x-axis to show the timeline of states explored. Stills of the receptors involved in the interaction are inset. (b) Distance and state trace for two QD-EGF bound receptors shows formation of a dimer (Free state in red and others as aforementioned) that persists until the end of the acquisition. Scale bars, 0.5 µm. (c) Normalized histogram of erbB1 dimer lifetimes for QDEGF (red) or QD-VHH (yellow) homodimers, determined from Viterbi analysis. Inset shows the raw number of long-lived dimers for each condition. Note that the long-lived dimer duration may be underestimated due to the finite length of the time series. (d) Summary of diffusion coefficients for EGF, EGF+PD, VHH, and VHH+PD conditions following characterization of states by HMM and Viterbi analyses.

The mechanism of erbB1 homodimer immobilization, seen only for signaling competent complexes, is unknown. However, analysis of diffusional behavior within domains suggests a receptor-dependent change in the local environment. Ligand-bound erbB1 monomers slow by a factor of 2 when in the domain state. While this is consistent with earlier reports of slower protein diffusion within microdomains (Daumas et al., 2003; Douglass and Vale, 2005; Roullier et al., 2009), the distinction here is that HMM analysis specifically identifies pairs of receptors that are co-confined. Notably, ligand-bound but kinase-inhibited monomers do not demonstrate as dramatic a change in diffusion when co-confined. These data suggest that domains containing signaling competent erbB1 have subtly different properties and, further, that the short but repeated dimer events observed within domains (Fig. 3.4A) may generate signals. These signals could influence diffusion through creating barriers (ie, protein scaffolding), promoting cytoskeletal assembly or by lipid raft coalescence(Hofman et al., 2008)

The technical advantages afforded by two-colour quantum dot tracking have permitted us to resolve several outstanding questions related to erbB1 biology. First, we

91

show that there is not a simple relationship between diffusion and dimer status. SPT using probes that distinguish between unoccupied and ligand-bound receptors revealed the full range of diffusive behavior for monomers and dimers under all experimental conditions (Fig. 3.1B, Fig. 3.4D). By distinguishing between different states, we calculate a diffusion rate for unoccupied erbB1 monomers of 0.05 μm^2/s. There is only a slight change in diffusion for the short-lived dimers that form between two unoccupied receptors (0.038 μm^2/s). Importantly, we are able to report that signaling competent, ligand-bound dimers slow dramatically (0.005 μm^2/s) compared to ligand-bound dimers whose kinase domains are inhibited by PD153035 (0.019 μm^2/s). These data contradict the primary assumption of Chung et al (Chung et al., 2010) that 2-fold changes in erbB1 diffusion can be used as the sole criteria for identifying dimers. Thus, reduced mobility is a complex reflection of stability and size of the protein aggregate as well as signaling-mediated changes in the local environment.

Second, we are now able to compare off rates for dimers formed on the surface of live cells. We show that dimers composed of 2EGF:2erbB1 are the most stable, confirming predictions based a large prior body of evidence (Schlessinger, 2002). This is inconsistent with at least one important aspect of the negative cooperativity model recently proposed by others (Macdonald and Pike, 2008), which predicts that two EGF-bound monomers should have the lowest interaction affinity. Furthermore, we see that dimers composed of 1EGF:2erbB1 are short lived (k_{off} = 0.738 s^{-1}) while dimers between unoccupied receptors are even more transient (k_{off} = 1.24 s^{-1}). Considering the short lifetime, we predict that these complexes are relatively weak at initiating signal transduction. This is consistent with reports of inactive, unliganded dimers (Jura et al.,

2009a; Hofman et al., 2010). Since homodimers of EGF-bound receptors demonstrate the longest lived interactions and the ability to remodel their local environment, we suggest that dimers constitute the minimal signaling competent unit, consistent with other reports (Lemmon et al., 1997; Lidke et al., 2005a; Zhang et al., 2006b).

Finally, this work addresses a long standing debate about roles for membrane organisation in promoting signal initiation (Chen et al., 2004). We show that EGF-bound monomer pairs can repeatedly encounter each other within surface domains, with sequential periods of dimerization. Since encounters between proteins are diffusion-limited, stochastic processes, this cannot be explained without evoking contributions of membrane compartmentalization. EGF-bound monomers exhibit reduced mobility within domains only in the absence of kinase inhibitors. We speculate that repeated dimer events can achieve a degree of signaling that alters the local environment, which in turn slows receptors and promotes rebinding.

The new quantitative methods described here capture dynamic receptor interactions at the single molecule level, providing detail that is averaged out in traditional methods. Since dimerization is a common mechanism for signal initiation, our approach can be applied across many receptor systems to further our understanding of dimerization kinetics, receptor mobility and membrane structure influences on regulating signal transduction.

3.2 MATERIALS AND METHODS

3.2.1 Reagents

Biotinylated EGF was purchased at a 1:1 stoichiometry (Invitrogen, Carlsbad, CA) and singly biotinylated VHH fragment EGb4 was produced using the BirA expression system (Roovers et al., 2007). Biotin-EGF or biotin-VHH were conjugated to Qdot® 655 or Qdot® 585 streptavidin conjugate (Invitrogen, Carlsbad, CA) in PBS + 1% BSA to generate stock solutions of 30 nM 1:1 monovalent QD-conjugates (Lidke et al., 2004). Stock solutions were stored at 4°C and used for up to two weeks. Biotin-EGF was conjugated to Qdot® 625 streptavidin for bleedthrough experiments. Experiments with PD153035 (Tocris Bioscience, Ellisville, MO) were performed at a final concentration of 1 µM inhibitor.

3.2.2 Cell culture

A431 Human Epithelial carcinoma cells were cultured in Dulbecco's Modified Eagle's Medium without phenol red (Sigma-Aldrich, St. Louis, MO) supplemented with 10% fetal bovine serum (FBS; Invitrogen, Carlsbad, CA) and penicillin and streptomycin. For live cell imaging, cells were plated in 8-well Lab-Tek chambers (Nunc, Rochester, NY) and allowed to reach up to 50% confluency before experimentation.

3.2.3 Cell treatment for SPT experiments.

Cells in Lab-Tek chambers were imaged in Tyrode's supplemented with 0.1% BSA and 20 mM glucose. Prior to imaging, cells were serum starved in Dulbecco's Modified Eagle's Medium lacking FBS for four hours. Experiments with PD153035 were performed after serum starvation including 1 µM inhibitor and live cell imaging buffer also included 1 µM PD153035.

3.2.4 Fluorescence Microscopy

Wide field imaging for SPT was performed using an Olympus IX71 inverted microscope equipped with a 60× 1.2 N.A. water objective. Wide field excitation was provided by a mercury lamp with either a 436 /10 nm BP excitation filter and a 50/50 neutral density filter. Emission was collected by an electron multiplying CCD camera (Andor iXon 887) using a QuadView image splitter (Optical Insights) to simultaneously image two spectrally distinct QDs. QD emission was collected using a 600 nm dichroic and the appropriate emission filters, 655/40nm and 585/20 BP (Chroma, Rockingham, VT). A single pixel is equivalent to 267 nm. The sample temperature (34-36 °C) was maintained by an objective heater (Bioptechs, Butler, PA).

3.2.5 Image Processing

All image processing was performed using Matlab (The MathWorks, Inc., Natick, MA) in conjunction with the image processing library DIPImage (Delft University of Technology). For descriptions of specific analysis routines see Supplementary Information.

3.2.6 GPU Single Particle Tracking and Track Elongation

Images were acquired at 20 fames/s for a total of 1,000 frames. Single molecule localization and trajectory connection were carried out as previously described(Smith et al., 2010). Complete derivation of the track elongation algorithm is provided in Supporting Online Text.

To elongate short tracks, the positions (p_i and p_{i+j}) with the smallest Δt for temporally independent tracks are compared using equation 6. Temporally independent tracks with the best p-value that pass a user-defined cutoff are augmented for form an

elongated trajectory. Due to temporal independence of short trajectories, the cutoff and Δt for track elongation can be relaxed slightly from those used in the initial connection algorithm without introducing artifacts. This process is repeated until no temporally independent tracks that pass the cutoff remain. An example comparison of short and elongated trajectories is shown in Supplemental Figure S1.

3.2.7 Square Displacement Analysis

Diffusion analysis of trajectories was performed by square displacement analysis and two-component fitting, as previously described(de Keijzer et al., 2008).

3.2.8 Correlated Motion Analysis

The degree of correlation between pairwise trajectories was determined as previously described(Andrews et al., 2008).

3.2.9 Fiducial Data Acquisition and Image Registration

See supplemental text for mathematical details. Images were registered using a calibration image of multi–fluorophore fluorescent beads (0.2 μm Tetraspeck, Invitrogen, Carlsbad, CA) that have an emission spectrum covering the two spectral windows. The camera was sampled by moving a single bead across the field of view using a mechanical stage (Prior Pro Scan II, Rockland, MA) to obtain good sampling over the field of view. A fiducial data set was acquired at the beginning and end of each chamber tested. Corresponding beads are identified in each channel and fit to a polynomial calibration model. (Churchman et al., 2005).

3.2.10 Hidden Markov Model

See supplemental text for mathematical details. We use a three state model: 1) Dimer; 2) Domain; 3) Free. The observed parameter in the hidden Markov model is the

separation. For the dimer and domain model, the distribution of the displacements between the QDs is modeled by a zero mean Gaussian distribution in each (x,y) dimension using σ_{dimer} and, σ_{domain} respectively. The resulting observed distribution of displacements is a convolution of the actual displacements and the errors in measurement, which are also assumed to contribute as unbiased Gaussian distributions. The value σ_{dimer} is taken as that expected from combining information from crystal structure measurements and the size of QDs, whereas σ_{domain} is varied to find the best fit across all data sets of a specific condition. For the Free model, the probability density is calculated as a function of the observed distance in the previous frame and a characteristic diffusion constant.

The set of rate constants is found by maximizing the likelihood over all interactions of two QDs for a specific condition, The errors on each parameter are given as standard errors and are calculated as $(H_{i,i}^{-1})^{-1/2}$ where H is the Hessian matrix of the negative log-likelihood and i denotes one of the estimated rate constants. Given the set of rate parameters found in the estimation step, the Viterbi algorithm(Forney, 1973) is used to identify the most likely state within individual QD interactions.

3.2.11 Statistical Analysis

Errors in two-component fits for square displacement are reported as 95% confidence intervals.

3.3 ACKNOWLEDGEMENTS

CHAPTER 4: ERBB3 IS AN ACTIVE KINASE DRIVEN BY SEQUENTIAL HETERODIMER AND HOMODIMER INTERACTIONS

Mara Steinkamp*[#], Shujie Yang*^[#], Shalini Low-Nam*,

Xiangbing Meng*^, Marilyn S. Smith[+¤], Diane S. Lidke* and Bridget S. Wilson*[||]

*Department of Pathology & Cancer Research & Treatment Center,

University of New Mexico, Albuquerque, New Mexico 87131

[+] [¤]Department of Microbiology, Immunology, and Molecular Genetics,

University of Kansas Medical Center, Kansas City, KS 66160

Present Addresses: ^University of Iowa, Department of OB/GYN, Iowa City, Iowa

52242

[¤]IBT Laboratories, Lenexa, KS 66219

# Contributed equally to this work

[||] To whom correspondence should be addressed. E-mail: bwilson@salud.unm.edu

4.1 Specific contributions

This chapter is a manuscript submitted to *Molecular Biology of the Cell* by co-authors Dr. Mara Steinkamp and Dr. Shujie Yang. The focus of the paper is evidence for catalytic activity by the kinase domain of erbB3. Biochemical studies were carried out by the co-authors that demonstrate the ability for erbB3 immunocomplexes to phosphorylate an exogenous substrate and the dependence of such activity of erbB3 ligand binding and interactions with erbB2. A new hypothesis was developed that suggested that erbB3 catalytic activity may result from the series of interactions involving ligand-induced conformational changes and heterodimer formation.

I contributed single particle tracking probe development, experiments and analysis to demonstrate the formation of erbB2/erbB3 and erbB3/erbB3 complexes on live cells. Specifically, I developed the protocols to biotinylate the heregulin ligand for labeling of erbB3 with streptavidin-QD-ligand complexes and refined the maleimide thioether protocol labeling of reduced Herceptin as a monovalent label for erbB2. With Dr. Mara Steinkamp, we characterized these probes biochemically to ensure no perturbation of normal physiology. Single particle tracking experiments, mainly on SKBR3 cells, were carried out by Dr. Mara Steinkamp and myself. I completed all tracking, computational analysis, and plotting of live cell data. The observation of these erbB complexes on cells provides evidence in support of the model from biochemical data and further demonstrates the stability of erbB3 homodimers.

4.2 SUMMARY

Previously considered a "dead" kinase, erbB3 is implicated in escape from erbB-targeted cancer therapies. ErbB3 phosphorylation is shown to be largely erbB2-dependent, based on studies in SKBR3 cells treated with antibodies that block the erbB2 dimerization arm or with lapatinib. Intact, phosphorylated erbB3 has significant tyrosine kinase activity as measured in immune complexes from HRG-stimulated cells. ErbB3 kinase activity was confirmed in transfected CHO cells expressing gain-of-function (erbB3^{E933Q}) or ATP-binding (erbB3^{R819A}) mutants. Novel mechanistic insight comes from live cell, two-color single particle tracking experiments using quantum dot (QD) probes. These studies document short-lived erbB2/erbB3 heterodimers and long lived erbB3 homodimers. We propose a model in which transient heterodimers permit transphosphorylation of erbB3 by erbB2. Persistent signaling is likely sustained by stable erbB3 homodimers that scaffold PI 3-kinase and phosphorylate cellular substrates. The model is supported by electron microscopy studies showing that erbB3/PI-3K signaling patches have disproportionally low amounts of erbB2.

4.3 SIGNIFICANCE

ErbB3 expression is implicated in the failure of EGFR and erbB2-targeted cancer therapies. This finding was surprising since erbB3 has classically been thought of as kinase dead and dependent on an active family member for its function. Our work reveals that intact erbB3 has independent kinase activity. Furthermore, single particle tracking data suggest that erbB2/erbB3 heterodimers, originally thought to be the functional signaling unit, are transient, while erbB3 homodimers are stable. Thus during

erbB2-targeted therapy, ErbB3 might still form signaling competent homodimers that encourage tumor growth. Identification of a novel gain-of-function mutation in a breast cancer cell line also indicates that erbB3 function could be enhanced by mutations in cancer. Therefore, directly targeting erbB3 may be of great therapeutic value.

4.4 HIGHLIGHTS

- ErbB3 requires erbB2 to become activated.
- Once activated, immunoprecipitated erbB3 can independently phosphorylate a substrate.
- ErbB3 forms short lived heterodimers with erbB2, while erbB3 homodimers are long lived.

4.5 INTRODUCTION

Epidermal growth factor receptor (EGFR/erbB1) and erbB2 genes are often amplified or mutated in cancers, particularly non-small cell lung cancer and breast cancer, making these receptors important molecular targets for cancer therapy (Wieduwilt and Moasser, 2008). Lung adenocarcinomas harboring erbB1 kinase domain mutations strongly correlate with clinical response to gefitinib (Iressa) and erlotinib (Tarceva) (Paez et al., 2004). However, tumors often become refractory to treatment. ErbB3, a closely related family member, is often co-expressed in these cancers and has been implicated in escape from both EGFR and erbB2-targeted therapies (Engelman et al., 2007; Sergina et al., 2007).

102

ErbB3 was previously thought to be catalytically inactive and thus only able to function as a heterodimer (Guy et al., 1994; Sierke et al., 1997). In the classic view of erbB3 signaling, ligand binding to erbB3 leads to heterodimerization with "kinase-competent" erbB family members (e.g. erbB2) or even members of other receptor tyrosine kinase families (e.g. MET) (Engelman et al., 2007). The dimerizing partner is then considered to be solely responsible for transphosphorylation of YXXM motifs in erbB3 with subsequent recruitment of PI3-kinase and other erbB3 binding partners (Yarden and Sliwkowski, 2001). However, a recent report by Lemmon and colleagues challenged the notion that erbB3 is a "dead" kinase by demonstrating that the isolated erbB3 intracellular domain (ICD) is capable of weak autophosphorylation (Shi et al., 2010). These data support the hypothesis that erbB3 homodimers are functional signaling complexes. In this report, we provide the first evidence for ligand-mediated upregulation of erbB3 kinase activity measured in immune complexes containing intact erbB3 receptors. We further show that SKBR3 breast cancer cells harbor a gain-of-function erbB3 somatic mutation in the kinase domain, which is particularly significant because the substitution occurs on a cytoplasmic dimerization interface where it enhances erbB3 kinase activity and sensitivity to ligand. Our results strengthen the argument that erbB3 is itself a legitimate therapeutic target {Sithanandam, 2008; VanHook, 2010} and yet raise new and important questions. Foremost of these is the relative importance of erbB3 heterodimers and homodimers to both signal initiation and signal propagation.

We approach these questions using a combination of single molecule tracking and electron microscopy, technologies that together provide nanoscale information about

the dynamics of receptor-receptor interactions (SPT) and the changes in spatial organization over time (EM). Bright, photostable QD probes were used for single particle tracking of erbB3 and erbB2 receptors (Lidke et al., 2004; Andrews et al., 2008; Andrews et al., 2009), capturing the diffusion-limited interactions between individual proteins in real time. ErbB2-erbB3 heterodimers are shown to be relatively short-lived, compared to more stable erbB3 homodimers. This sub-second temporal information is complemented by nanometer-scale spatial resolution of erbB3 signaling patches in native membranes, obtained using immunoelectron microscopy techniques (Yang et al., 2007). Results are consistent with a model where transient interactions between erbB3 and erbB2 are followed by heterodimer dissociation and formation of signaling domains composed predominantly of erbB3 homodimers and downstream signaling partners, such as PI 3-kinase.

4.6 RESULTS

4.6.1 ErbB3 immune complexes contain HRG-induced tyrosine kinase activity

The SKBR3 breast cancer cell line expresses EGFR, erbB2 and erbB3, providing an appropriate model system to study erbB family interactions. We previously reported levels of erbB surface expression in this cell line by flow cytometry (~200,000 erbB1, 2 million erbB2, 70,000 erbB3 per cell) and developed a non-radioactive, microplate-based peptide substrate assay to measure kinase activity in EGFR and erbB2 immune complexes (Yang et al., 2007). Figure 4.1A (top panel) reports results using erbB3 immune complexes, documenting significant tyrosine kinase activity that reached maximal levels within 2 minutes of stimulation with the erbB3 ligand, heregulin (HRG).

104

Increased kinase activity with HRG treatment was accompanied by an increase in erbB3 phosphorylation (Figure 4.1A, lower panel). Remarkably, when identically prepared erbB3 immune complexes were subjected to SDS-PAGE and blotted for erbB1 or erbB2, no significant co-precipitation of either receptor was detected (Figure 4.1B). ErbB1 or erbB2 immunoprecipitates served as positive controls in these experiments.

4.6.2 Kinase activity in ErbB3 immune complexes is not attributed to associated ErbB2, EGFR or Src kinases

We next used a pharmacological approach to characterize tyrosine kinase activity present in erbB3 immune complexes, by adding known ATP-binding competitive inhibitors directly to the *in vitro* kinase reaction. Marked inhibition of erbB3 kinase activity was seen with the broad specificity inhibitor, staurosporine (Figure 4.1C) (Fabian et al., 2005), but not with the selective EGFR inhibitor AG1478, the erbB2 inhibitor AG879, the dual EGFR/erbB2 inhibitor PD153035, the Src family inhibitor PP2 (data not shown).
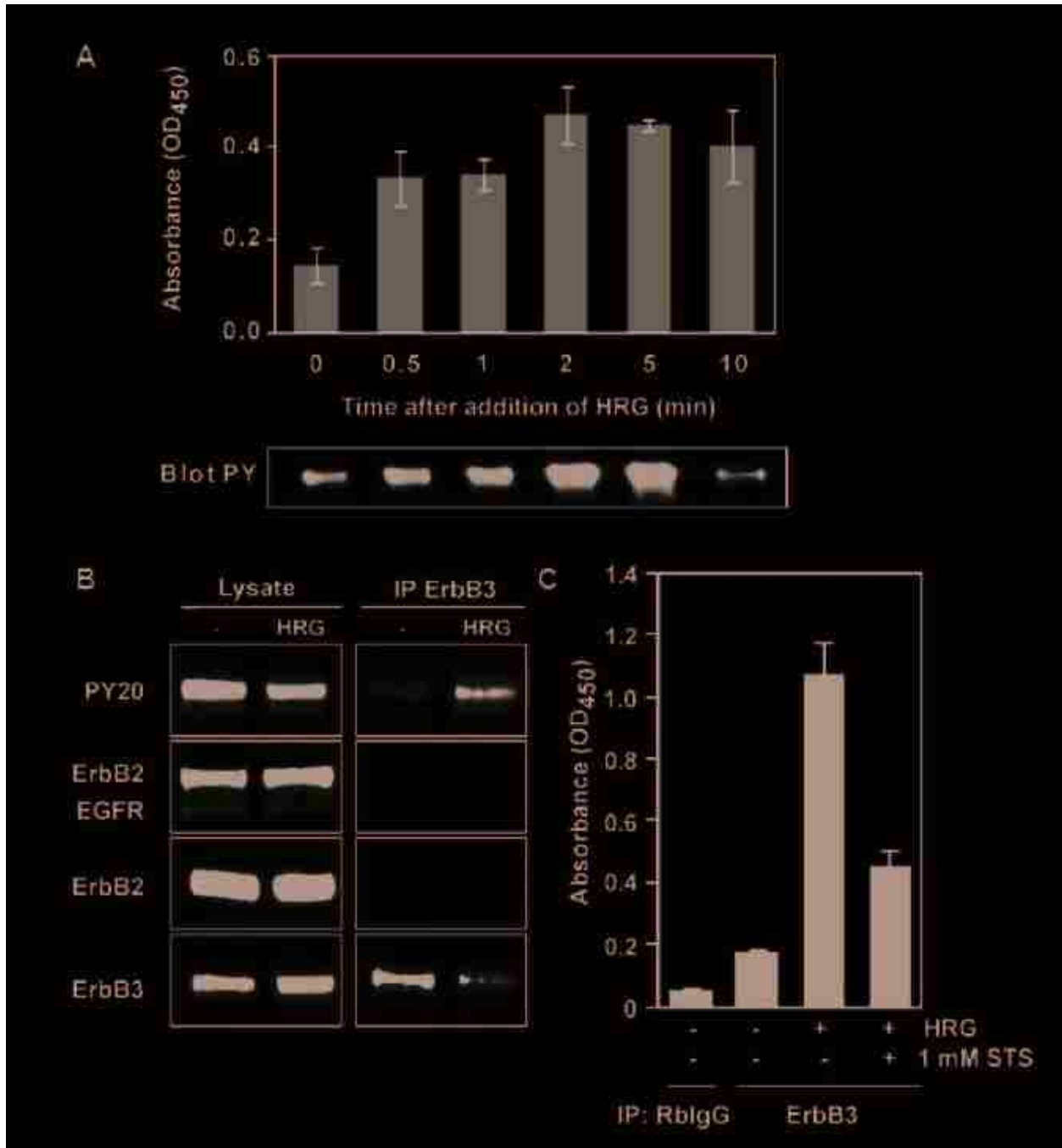
Figure 4.1. Robust tyrosine kinase activity in erbB3 immune complexes correlate with erbB2-dependent HRG-induced erbB3 phosphorylation. (**A**) ErbB3 was immunoprecipitated from SKBR3 cells after 2 hr serum starvation (0) with or without the indicated treatment interval with 12 nM HRG. Immune complexes were evaluated for

kinase activity by *in vitro* K-LISA using an EAY peptide substrate (top panel) or subjected to SDS-PAGE, followed by immunoblotting with PY antibody (lower panel). Bars are the mean of three replicates +/- standard deviation. (**B**) Other erbB family members are not present in erbB3 immunoprecipitates. Where indicated, cells were stimulated with 3.2 nM HRG, lysed using 1% NP-40 and immunoprecipitated using ErbB3-specific antibodies. Samples were subjected to SDS-PAGE, followed by immunoblotting with an anti-EGFR antibody that recognizes both EGFR and erbB2 (Santa Cruz sc-O3), erbB2-specific (RB9040-P, Neomarkers, Fremont CA) or erbB3-specifc (Santa Cruz sc-285) antibodies. (**C**) Treatment with staurosporine reduces erbB3 kinase activity. erbB3 was immunoprecipitated from SKBR3 cells after 2 hr serum starvation and left untreated (-HRG) or treated with HRG (3.2 nM) for 2 min. *In vitro* kinase activity of erbB3 immune complexes was then measured by K-LISA. 1 µM staurosporine was added directly to the kinase reaction. Rabbit IgG was used as a negative control to determine levels of non-specific kinase activity contributed from protein lysates in the K-LISA assay. See also Figure S1.

We considered the possibility that activity in erbB3 immune complexes might be explained by SH2-mediated recruitment of cytoplasmic tyrosine kinases. To address this, we used a commercial SH2 protein array to screen for potential phospho-erbB3 binding partners in SKBR3 cells that might be pulled down with erbB3 in immunoprecipitates (Supplemental Figure 4.1). This array includes SH2-domains derived from thirteen cytoplasmic tyrosine kinases (Abl, Csk, BTK, Zap-70 and all Src-family members). Arrays were incubated with cell lysates prepared from HRG-activated

SKBR3 cells, followed by antibody-based probing of the membranes for detection of erbB3 or erbB2. None of the SH2-domains derived from cytoplasmic tyrosine kinases bound to phospho-erbB3 (Supplemental Figure 4.1). Only the SH2-domain of the p85 subunit of PI 3-kinase, already well established as the primary binding partner for phospho-erbB3 (Hellyer et al., 2001), captured erbB3 to a significant amount. To rule out any contributions from associated PI 3-kinase, which has serine kinase activity (Dhand et al.), we directly added wortmannin (10 nM) directly to the erbB3 kinase reaction; this irreversible inhibitor of Class I PI 3-kinases had no effect on erbB3 kinase activity (data not shown). Together, these results strongly support the conclusion that potential candidates (EGFR, erbB2, Src kinase, PI3K) are *not* responsible for the tyrosine kinase activity present in erbB3 immune complexes and that this activity is likely due to erbB3 itself.

4.6.3 SKBR3 cells express both erbB3(WT) and a kinase domain mutant erbB3^{E933Q}

Oncogenic mutations in erbB1, erbB2 and erbB4 are well established (Paez et al., 2004; Lee et al., 2006; Soung et al., 2006), leading us to speculate that the high erbB3 kinase activity in SKBR3 cells could be due to a mutant form of erbB3. Using PCR-based sequencing of cDNA, we found that SKBR3 cells express two alleles of erbB3, the wild type (WT) erbB3 and a mutant form with a single kinase domain substitution (E933Q) (Figure 4.2A). This mutation lies within the C-lobe dimerization surface of the kinase domain (Figure 4.2B) (Zhang et al., 2006a). Site-directed mutagenesis was used to introduce this substitution into an existing expression vector for an erbB3-mCit

fusion protein. Wildtype erbB3-mCit or E933Q erbB3-mCit were stably transfected into CHO (Chinese Hamster Ovary) cells and colonies were selected based on surface expression of erbB3-mCit (Supplemental Figure 4.2).

4.6.4 ErbB3^{E933Q} is a novel gain-of-function mutant

Characterization of the CHO transfectants showed that erbB3^{E933Q}-mCit was more sensitive to lower concentrations of ligand than erbB3^{WT}-mCit, as evidenced by increased levels of phospho-erbB3, coprecipiation of PI 3-kinase and by increased phosphoAkt levels at the lowest HRG doses (Supplemental Figure 4.2). Figure 4.2D also demonstrates that the erbB3^{E933Q} mutation also enhances kinase activity. In this experiment, erbB3 immune complexes were isolated from CHO cells expressing either erbB3^{WT}-mCit or erbB3^{E933Q}-mCit and used as a source of receptor for the *in vitro* kinase activity. Western blots show comparable amounts of erbB3 in the immune complexes. Wildtype erbB3, isolated from the CHO transfectants, showed significant basal activity, typically with little or no increase in activity after HRG-induced phosphorylation. Overall activity in erbB3^{E933Q}-mCit immune complexes was consistently higher than wildtype, with modest upregulation following the addition of HRG (erbB3^{E933Q}-mCit +HRG showed activity 1.5 fold above WT, p-value = 0.01by Student's t-test).

4.6.5 ErbB3^{R819A} has diminished kinase activity

If erbB3 is a *bona-fide* kinase, then mutating key residues in the kinase domain should reduce erbB3 kinase activity. Alignment of the catalytic domains of the four erbB receptors shows the divergence of erbB3 from the other family members, but also highlights conserved motifs that remain intact (Figure 4.2C). The conserved catalytic

aspartic acid has been altered to an asparagine in erbB3 (D813 in EGFR to N815 in erbB3). However, Shi et al. recently demonstrated that erbB3 can compensate for loss of the catalytic base by using an alternate reaction pathway to catalyze phosphoryl transfer (Shi et al., 2010). Other features important for kinase activity are conserved in erbB3, including an AAR motif that is important for ATP binding. In EGFR, mutation of the arginine at position 817 to alanine reduced ATP binding and kinase activity (Chan and Gill, 1996). We engineered a mutation of the homologous arginine (R819) to alanine in the erbB3-mCit expression vector and developed stably-transfected CHO cells expressing erbB3^{R819A}-mCit at the surface. Lysates from erbB3^{WT}-mCit and erbB3^{R819A}-mCit cell lines were prepared with or without HRG stimulation, normalized based upon mCit fluorescence, and used for preparation of anti-erbB3 immune complexes and *in vitro* kinase assays. Although phosphorylation of erbB3^{R819A}-mCit in response to HRG treatment was comparable to WT erbB3 (Figure 4.2E), there was markedly reduced kinase activity in the erbB3^{R819A}-mCit immune complexes. These results are again consistent with the conclusion that the kinase activity in erbB3 immune complexes can be attributed to erbB3 itself.
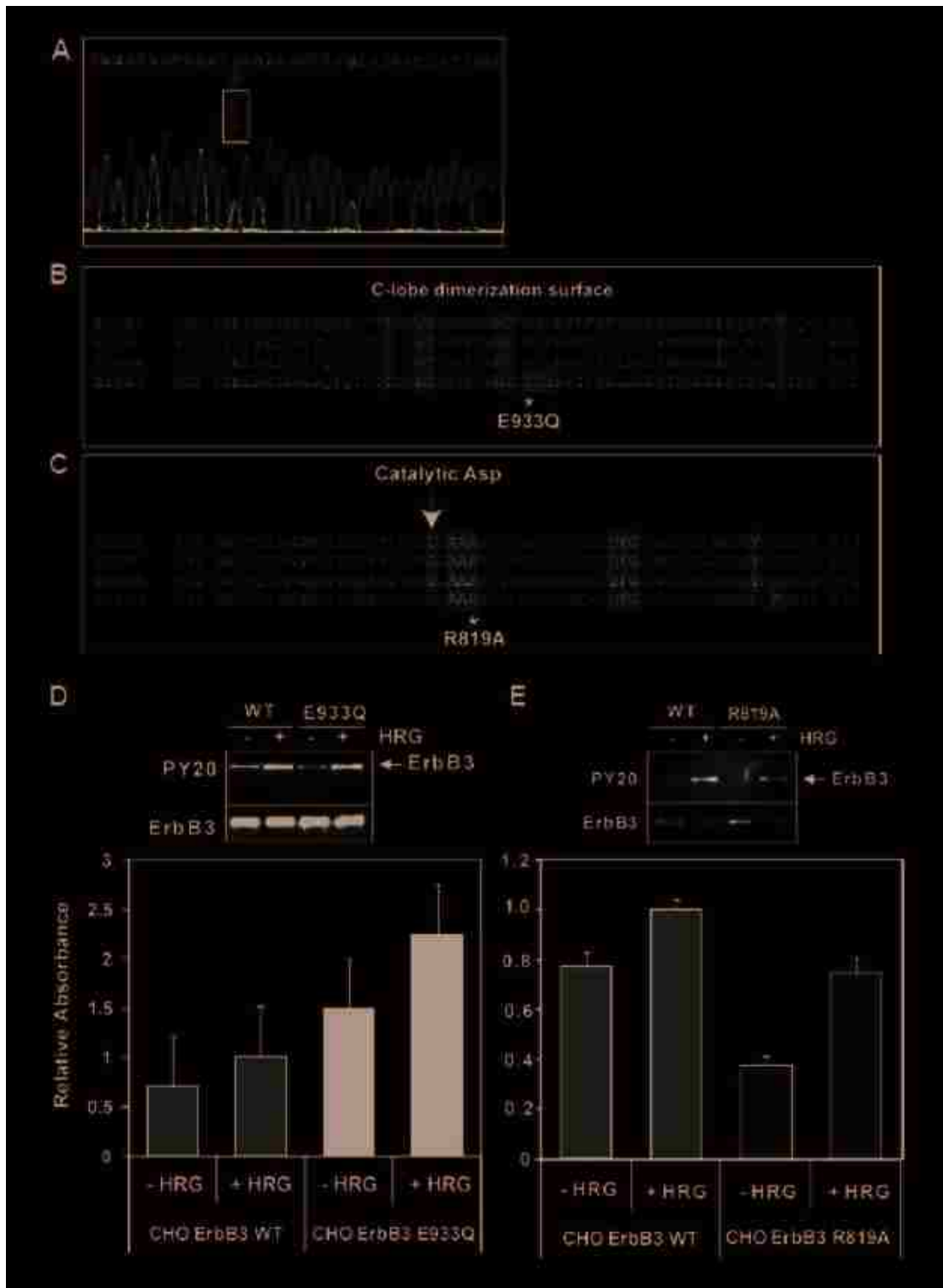
Figure 4.2. SKBR3 cells carry a heterozygous mutation in the kinase domain of erbB3, which affects downstream signaling. (**A**) DNA sequencing of erbB3 in SKBR3 cells

revealed a heterozygous G to C mutation at position 3047 of erbB3 (Genbank ID: NM_001982); this results in an amino acid substitution E933Q in the erbB3 kinase domain. (**B,C**) Alignment of two segments of the erbB family kinase domains. (**B**) Aligned sequence containing the C-lobe dimerization surface where the SKBR3 mutation E933Q is located. Hydrophobic residues predicted to lie on the surface are highlighted in blue (Zhang et al., 2006b). Three residues including E933 that differ between erbB3 and EGFR or erbB4 are highlighted (yellow). (**C**) Sequence surrounding the catalytic site of the kinase domain. Conserved bases shown to affect EGFR kinase activity are highlighted in green. The catalytic D813 in EGFR is substituted with asparagine in erbB3 (arrow). The AAR and DFG motifs are conserved in all four family members. The R819A mutation introduced into ErbB3 is shown (asterisk). (**D, E**) *In vitro* erbB3 tyrosine kinase activity in CHO transfectants. ErbB3 activity was measured by K-LISA in erbB3 immunoprecipitates prepared from cell lysates before or after 2 min stimulation with 3.2 nM HRG. Western blots in these panels show the phosphorylation status of erbB3 protein in IP samples from the same experiment. Values represent the mean value of immunoprecipitates assayed in triplicate and error bars indicate standard deviation. ErbB3 E933Q expressed in CHO cells shows increased kinase activity in the K-LISA assay (**D**) while erbB3 R819A has reduced basal activity (**E**). See also Figure S2.

4.6.6 ErbB2 mediates activation of ErbB3

Since erbB2 is a known dimerizing partner for erbB3, we next treated SKBR3 cells with three distinct erbB2 inhibitors to evaluate their effects on HRG-induced erbB3 phosphorylation. Thirty minute pretreatment of SKBR3 cells with lapatinib, a dual EGFR/erbB2 small-molecule tyrosine kinase inhibitor, dramatically lowered HRG-induced erbB3 phosphorylation (PY1289) (Figure 4.3A), indicating that erbB3 phosphorylation is largely dependent on erbB2. Lapatinib treatment also reduced erbB2 phosphorylation (PY1248). Pretreatment of cells with lapatinib also reduced erbB2 and

erbB3 kinase activity (Figure 4.3B). ErbB2 kinase activity was only reduced by ~50%

possibly due to the reversible nature of lapatinib inhibition. However, erbB3 kinase

activity was essentially abolished. These data support the concept that erbB3 requires

erbB2 for activation.

We next compared results after 1 hr pretreatment with 100 nM 2C4, the mouse

monoclonal antibody from which the drug Pertuzumab was derived(Adams et al., 2006).

This antibody, which blocks the erbB2 dimerization arm (Franklin et al., 2004), is shown

here to block HRG-mediated upregulation of erbB3 phosphorylation (PY1289) by ~75%

(Figure 4.3C). Note that 2C4 treatment had negligible effects on erbB2

phosphorylation. We speculate that erbB2 homodimers may actually be *stabilized* by

the bivalent antibody and further, that the dimer can be active despite the bulky antibody

bridging the two dimerization arms.

It should be noted that the relative expression levels of the two erbB receptors

differ significantly in the two cell lines used for these studies, providing a useful

comparison for possible effects of receptor density. SKBR3 cells express at least 30

fold *more* erbB2 than erbB3, while the CHO transfectants express many fold *fewer*

erbB2 than erbB3 (Yang et al., 2007). To establish dependency of erbB3 activation on

erbB2, even when erbB2 is in low abundance, CHO transfectants were also pretreated

with the 2C4 antibody prior to HRG stimulation. Here again, 2C4 treatment blocked

phosphorylation of tyrosine 1289 in both WT and E933Q forms of erbB3 by at least 50%

(Supplemental Figure 4.3). It also substantially reduced activation of the PI3K pathway,

as evidenced by diminished phosphorylation of Akt. Thus, erbB2 participates in erbB3

activation even when it is largely outnumbered by erbB3.

113

Figure 4.3D reports data comparing another erbB2-specific therapeutic antibody, Trastuzumab (also known as Herceptin) (Carter et al., 1992). The binding site for Trastuzumab is distinct from 2C4, in that it binds to the juxtamembrane region of the erbB2 extracellular domain (Cho et al., 2003) and therefore is less likely to interfere with dimerization. SKBR3 cells were pretreated for 30 minutes with either intact (bivalent) trastuzumab or reduced (monovalent) trastuzumab linked to a QDot to determine whether this antibody would alter erbB3 activation under our experimental conditions. Unlike 2C4, trastuzumab in either form failed to significantly affect HRG-induced erbB3 phosphorylation (Figure 4.3D). These data are in close agreement with previous studies on trastuzumab (Agus et al., 2002; Diermeier et al., 2005). This lack of inhibition by trastuzumab is important for the experiments shown in Figure 4.4.

114
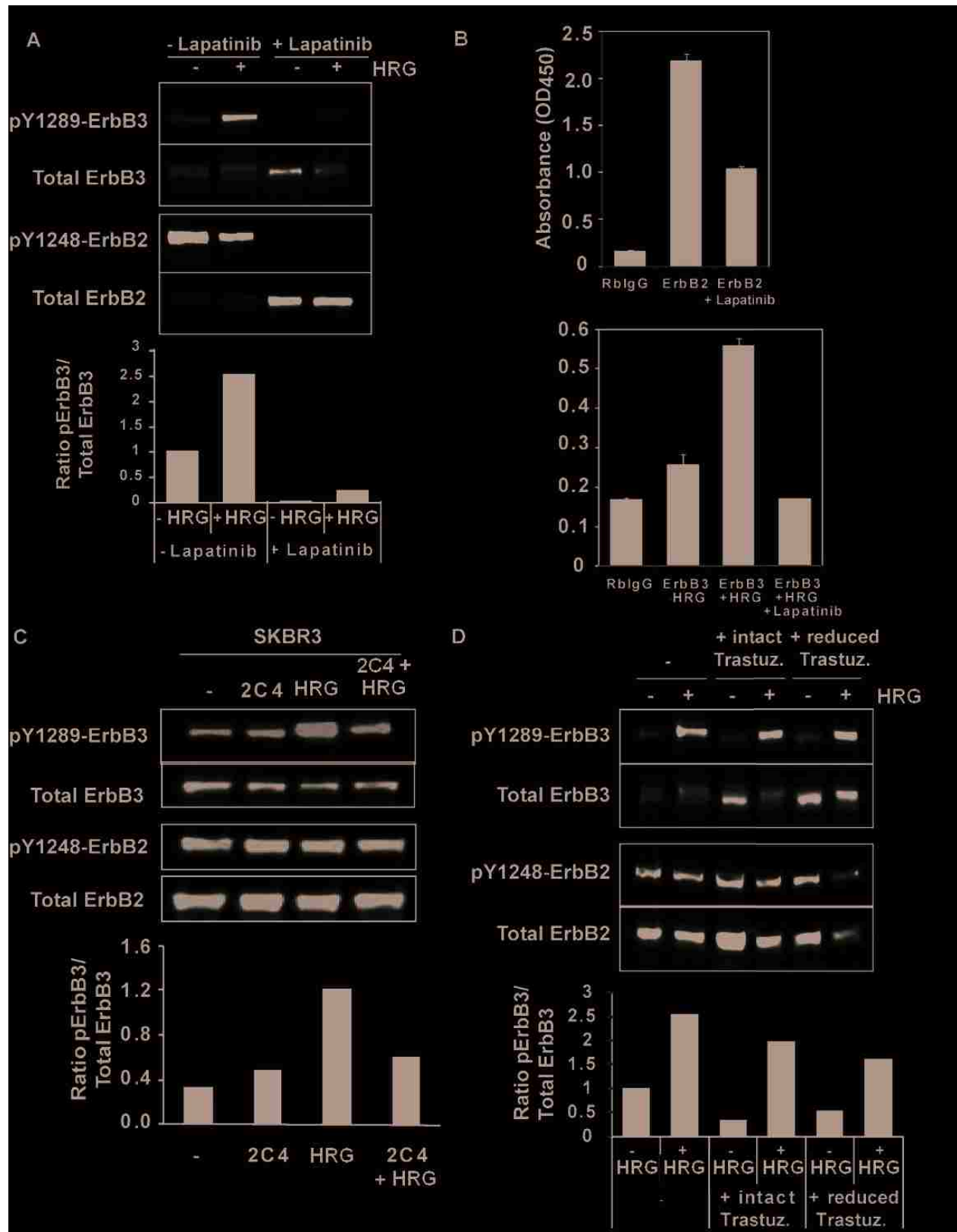
Figure 4.3. ErbB3 activation is ErbB2 dependent. (A) Lapatinib inhibition of ErbB3 phosphorylation in SKBR3 cells. SKBR3 cells were serum-starved for 4hr then treated +/- 500 nM Lapatinib for 30 minutes then +/- 12 nM HRG for 2 min. Aliquots of lysates were separated by SDS-PAGE, followed by immunoblotting with PY1289-erbB3 or PY1248-erbB2 phospho-specific antibodies or antibodies to detect total erbB3 or erbB2 as indicated. (B) Pretreatment of SKBR3 cells with Lapatinib reduces erbB2 and erbB3 kinase activity in the K-LISA assay. SKBR3 cells were serum-starved for 4hr +/- 500 nM Lapatinib, followed by immunoprecipitation with anti-erbB2 or erbB3 antibodies. Washed beads were used as a source of enzyme for K-LISA, where kinase activity is reported as changes in 450nm absorbance of the chromagen substrate. (C) The anti-erbB2 antibody, 2C4, reduces HRG-dependent erbB3 phosphorylation in SKBR3 cells. SKBR3 cells were serum-starved for 2hr prior to treatments. The key is as follows: untreated (-); treated for 1 hr with 100 nM 2C4 (2C4); stimulated with 12 nM HRG for 2 min. (+ HRG); or treated for 1hr with 100 nM 2C4 and stimulated with 12 nM HRG for 2 min. (2C4 + HRG). Aliquots of lysates were separated by SDS-PAGE, followed by immunoblotting with phospho-specific antibodies or antibodies to detect total erbB3 and erbB2. (D) Pretreatment of cells with the anti-erbB2 antibody Trastuzumab has little effect on HRG-dependent erbB3 phosphorylation in SKBR3 cells. SKBR3 cells were serum-starved for 4 hr and treated with intact or reduced (monovalent) Trastuzumab for 30 min before stimulation with 12 nM NRG. Quantification of the band intensities was performed and the ratio of perbB3 to total erbB3 is shown in the graphs below the westerns in A, C and D.

4.6.7 Single particle tracking reveals short lived ErbB2/ErbB3 heterodimers and long lived ErbB3 homodimers.

Although most consider the active signaling complex for erbB3 to be an erbB2/erbB3 heterodimer, the *in vitro* kinase assays above suggest that erbB3 can form active homodimers. As a first step in measuring dimer composition on the surface of live cells, we designed a novel set of single particle tracking probes. To prepare probes

for ligand-bound erbB3, we biotinylated HRG for coupling to commercial streptavidin-QDs (emission peaks at 585 or 655nm). The HRG QDot probe behaved similarly to unlabeled NRG, increasing phophorylated erbB3 in SKBR3 cells when they were stimulated with ligand for 2 minutes (Supplemental Figure 4.4). To detect individual erbB2 receptors, we directly conjugated QDs to reduced trastuzumab using maleimide thioether chemistry. It should be noted that we found the reduced form of trastuzumab, prepared according to published methods (Tada et al., 2007), to be more stable than the Fab form of the antibody. Importantly, as shown in Figure 4.3D, this monovalent reagent binds erbB2 but does not block its ability to activate erbB3.

Representative experiments using these probes to capture homo- and heterodimer events are shown in Figure 4.4A,B. Each plot shows the fluctuating distance between a nearby pair of receptors during the observation period, as they diffuse across the surface of live SKBR3 cells. Dotted lines mark the theoretical distance between two QDs in a dimer complex. This estimate ranges from 45-48 nm, based on the published structural information for the erbB extracellular domains when bound to ligand or to trastuzumab (Supplemental Figure 4.5). The plot in Figure 4.4A documents the formation of an erbB3 homodimer, which occurs approximately 6 seconds into the image acquisition period. Insets in Figure 4A show that spectral overlap of the 2 QDs occurs at the onset of dimer formation. The dimer is persistent, maintaining an average 50 nm separation distance throughout the remainder of the time series (>45 seconds). Additional examples are shown in Supplemental Figure 4.6A. Importantly, erbB3 homodimerization was readily observed with the majority of events persisting beyond

the end of the acquisition period. Thus, erbB3 homodimers are common events and their interaction times are long.

In contrast, Figure 4.4B illustrates representative examples of erbB3/erbB2 heterodimers, which were predominantly short-lived. The stochasticity of these interactions is apparent from comparisons with additional dimer events, illustrated in Supplemental Figure 4.6B.

The image series in Figure 4.4A,B provide visual, real-time documentation of individual dimer events. For quantitation of entire datasets for the two distinct conditions, each containing thousands of 2-color trajectories, we applied two independent methods of measuring receptor interactions as a function of separation distance (Figure 4.4 C,D) (Andrews et al., 2008). In the first analysis method (blue line), we report the magnitude of the uncorrelated jump distance (UJD) vector for each pair of receptor trajectories as a function of their proximity. This method is based on the concept that, when two receptors form a dimer, their motion becomes correlated and UJD decreases. Thus, in the top panel, the sharp decrease in the UJD (blue line) at short separation distance (<100 nm) is compelling evidence for erbB3 homodimerization. This phenomenon is much less dramatic for analysis of the two-color erbB2/erbB3 dataset (Figure 4.4D), consistent with the short duration of the heterodimers.

The red line in these plots reports analysis of a second criteria for dimerization, which is the jump magnitude (ie, mobility) of receptors as a function of proximity between pairs. As expected, 2-color tracking of erbB3 bound to QD ligand shows a sharp decrease in mobility at short separation distances, consistent with prior reports of

slower mobility for dimerized receptors (Roullier et al., 2009). The reduction in jump magnitude for 2-color tracking of erbB3-erbB2 is very slight at short distances. This also supports our conclusion that individual erbB2 molecules interact transiently with erbB3.

A

ErbB3 Homodimer

ErbB3 ErbB2 Heterodimer

ErbB2 Homodimer

Time (sec)

expected dimer distance

1 micron scale bar

B

ErbB3

ErbB2/ErbB3

ErbB2

Average Correlation (μm)

Separation Distance (μm)

uncorrelated jump distance
jump magnitude
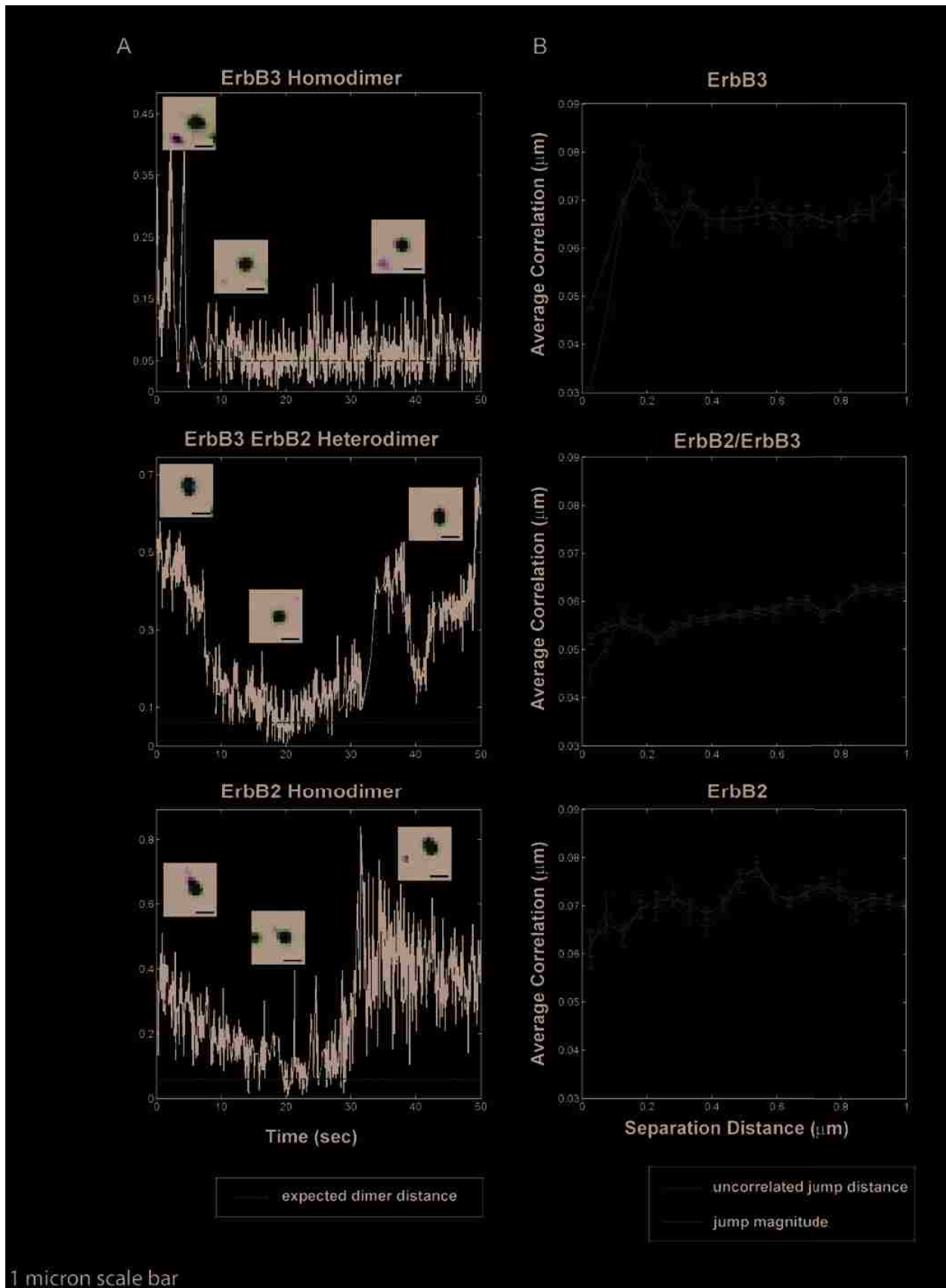
Figure 4.4. Single particle tracking detects long lived ErbB3 homodimers and short lived ErbB2/ErbB3 heterodimers and ErbB2 homodimers. (A-C) Receptor dimerization behavior can be seen by monitoring the distance between two QD-tagged proteins over time. Shown are representative examples for erbB3 homodimers (A), erbB2/erbB3 (B) and erbB2 heterodimers (C). Further examples can be found in Supplemental Figure 4.6. The dashed line represents the estimated dimer separation distance (50 nm, see Supplemental Figure 4.5). Insets show the images of the nearby pairs at specific time frames. Scale bar, 1 micron. (D-G). Uncorrelated jump distance (red) and jump magnitude (blue) are plotted as a function of separation distance for each of the 3 datasets, comprised of thousands of 2-color trajectories for each experimental condition.

4.6.8 Heregulin treatment leads to formation of ErbB3-PI3K signaling clusters, with limited recruitment of ErbB2.

Prior work in SKBR3 cells first demonstrated that HRG treatment leads to reorganization of erbB3 in the plasma membrane, seen as a transition from singlets and small clusters (2-7 receptors) to large signaling patches containing tens to hundreds of receptors (Yang et al., 2007). This result is highly reproducible, as shown in Figure 4.5A, where a large cluster of erbB3 can be observed after double labeling of a plasma membrane sheet ripped from an activated SKBR3 cell. In this image, erbB3 is labeled with large (10 nm) immunogold particles while erbB2 is labeled with small (5 nm) gold particles. The relative distributions of these two labels are depicted in the corresponding 2-color distribution map (Figure 5B; erbB2 red, erbB3 green). Although there are a small number of ErbB2 gold particles within the erbB3 patch, application of the Ripley's bivariant test indicates that their colocalization is not significant (Figure 4.5C). Figure 4.5D shows that erbB3 also forms large signaling patches after

transfection into CHO cells, where expression levels exceed that of endogenous erbB2 several fold. The Hopkins statistic (accompanying plot) confirms that erbB3 clustering is statistically significant in HRG-stimulated CHO cells.   Images in Figure 4.5E,F show results after double labeling of activated CHO cell membranes for erbB3 (10 nm) and the p85 subunit of PI 3-kinase (5 nM). PI3K is strongly recruited to the erbB clusters in both erbB3^{WT}-mCit and erbB3^{E933Q}-mCit transfectants.   Colocalization of ErbB3 and PI3K in HRG-treated membranes was confirmed using the Ripley's bivariant statistic (plots corresponding to Fig 4.5E,F) .

122
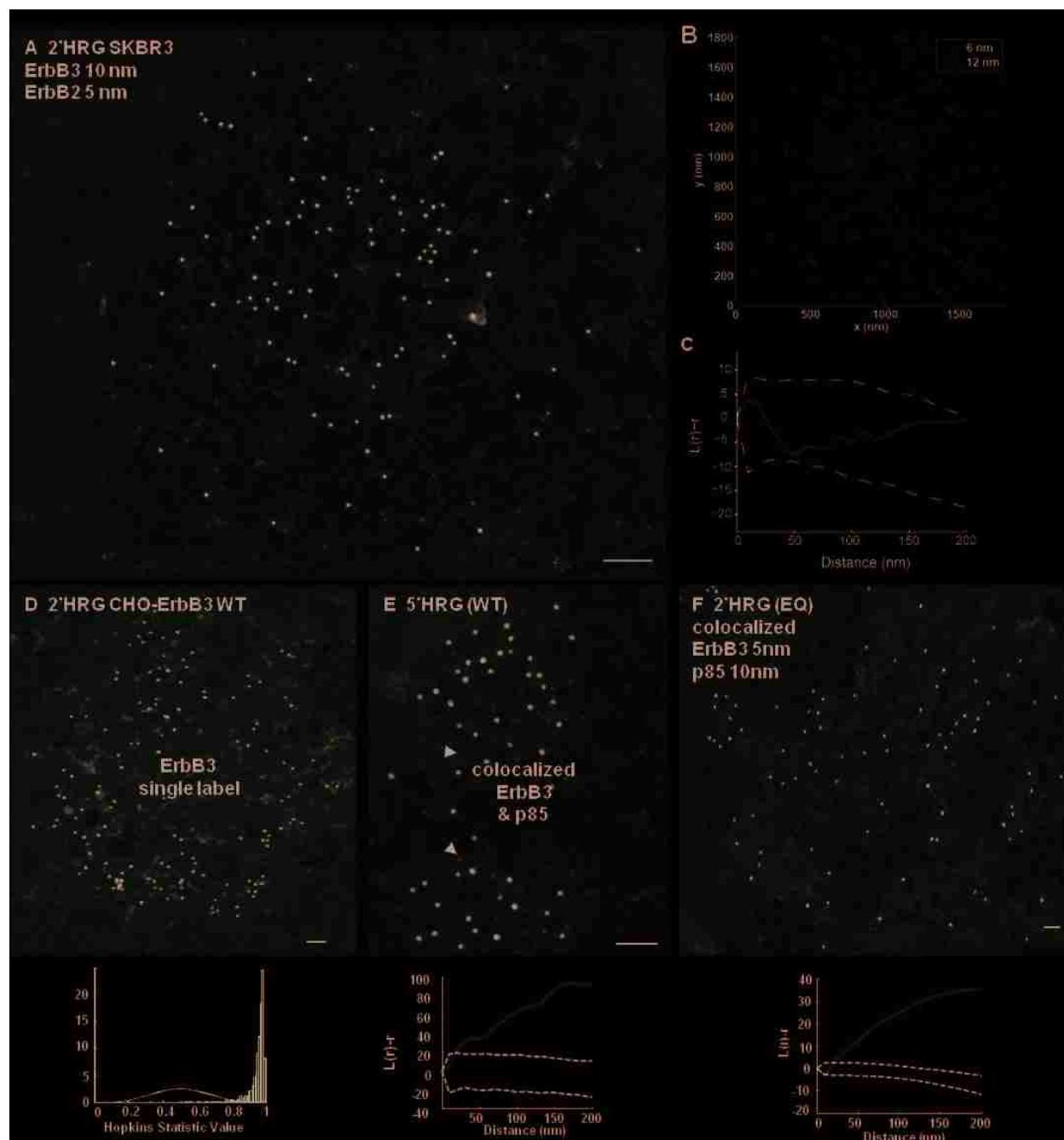
Figure 4.5. Colocalization of membrane-associated ErbB3 with ErbB2 and p85. (A) EM image of a membrane sheet prepared from SKBR3 cells that were serum starved for 4hr and then stimulated with 12 nM HRG for 2 min. After fixation, sheets were labeled from the inside with antibodies to the cytoplasmic tails of erbB3 (10 nm gold) and erbB2 (5 nm gold). (B) Two-color representation of the different distribution of erb3 (green) and erbB2 (red), corresponding to immunogold particle positions in the image shown at left

in (A). Particle distributions were captured using a plug-in for ImageJ (Zhang et al., 2006a). (C) Ripley's bivariate analysis indicating a lack of co-localization for Erb2 and ErbB3 in the image in (A). (D-F) Transfected CHO cells were serum-starved for 2 hrs. Cells were then stimulated with 3.2 nM HRG for 2 or 5 min. Membrane sheets were prepared from CHO-ErbB3 (WT) cells or CHO-erbB3^{E933Q} as indicated, fixed and then labeled with immunogold reagents against erbB3 alone (D) or in combination with immunogold reagents against the p85 subunit of PI 3-kinase (E, F). Bars = 0.1µm. Plots below show results of spatial statistics tests for clustering (Hopkins) and co-localization (Ripley's bivariate analysis), as applied to images in D-F. Hopkins analyses for erbB3 confirm that clusters in HRG-stimulated cells are significantly different from random. The Ripley's test confirms co-clustering of erbB3 and PI 3-kinase after HRG.

4.7 DISCUSSION

ErbB3 has been considered a unique member of the erbB family based upon reports of negligible tyrosine kinase activity (Guy et al., 1994; Sierke et al., 1997). However, this conclusion was based on studies that either occurred before the discovery of erbB3 ligands, preventing evaluation of ligand-induced changes in erbB3 activity (Carraway et al., 1994);(Guy et al., 1994), or that assessed HRG-dependent effects in the absence of other erbBs (Sierke et al., 1997). Our study uniquely evaluates ligand-dependent activation for endogenous erbB3, expressed in combination with other erbB family members and with direct measurement of tyrosine kinase activity in immune complexes bearing the intact erbB3 receptor. Our finding that the intact erbB3 has the ability to phosphorylate an exogenous substrate follows very recent proof of autophosphorylation activity of the erbB3 (ICD) when clustered in vesicles (Shi et al., 2010). It differs from both Shi et al (2010) and Jura et al (2009), who found the erbB3 ICD to be incapable of phosphorylating an exogenous substrate (Jura et al., 2009b; Shi

et al., 2010).   Methodology is clearly a key component to our success, since the data strongly support the conclusion that the intact erbB3 receptor is catalytically competent once activated in the membranes of live cells that co-express erbB3 dimerization partners.

We further describe the novel discovery of a naturally occurring erbB3 gain-of-function mutation, E933Q, expressed in the aggressive SKBR3 breast cancer cell line. This amino acid occupies a key position in the C-lobe of the erbB3 kinase domain, lying on the surface precisely where the C-lobe of one monomer contacts the N-lobe of another monomer in the asymmetrical dimerization model (Monsey et al.).   Mutation of the sequence [933]ENI[935] to ADS enhanced its ability to activate erbB4, leading to the hypothesis that mutations at this interface enhance allosteric activation of the receiving partner in the dimer (Monsey et al.).   We note that E933Q has increased sensitivity to low levels of ligand and increased kinase activity (Fig. 4.3; Fig. S4.2) when transfected into CHO cells, which express low levels of hamster erbB2.   It is tempting to think that this mutation may similarly promote erbB2/erbB3 interactions or erbB3 homodimerization to enhance erbB3 activity.   Although oncogenic mutations in ErbB1, erbB2 and erbB4 are well established (Paez et al., 2004; Lee et al., 2006; Soung et al., 2006), erbB3 kinase domain mutations appear to be relatively rare (Jeong et al., 2006). The most extensive study to date, based upon a tyrosine kinase "transcriptome" analysis of 254 established tumor cell lines, found only a few amino acid substitutions which were outside of the erbB3 kinase domain (Ruhe et al., 2007).   Considering the discovery of this new gain-of-function mutation, a more extensive evaluation of erbB3 kinase domain mutations in epithelial tumors may be worthwhile.

In this study, we take advantage of our capabilities in single particle tracking (Lidke et al., 2005b; Andrews et al., 2008; Andrews et al., 2009) to provide definitive evidence that erbB3 forms stable homodimers. This approach is one of several powerful new imaging technologies that enable the acquisition of quantitative information about protein-protein interactions and spatial organization (Lidke and Wilson, 2009; Dehmelt and Bastiaens, 2010).   Based upon this new evidence, we propose a modification of the traditional erbB3 signaling model that relies solely on signaling through erbB2/erbB3 heterodimers (Figure 4.6). We propose that transient heterodimerization enables erbB3 activation through trans-phosphorylation, but the bulk of signaling may occur through erbB3 homodimers that form after dissociation of the heterodimer partners. This proposal is compatible with the lateral signaling hypothesis proposed by others (Graus-Porta et al., 1997).
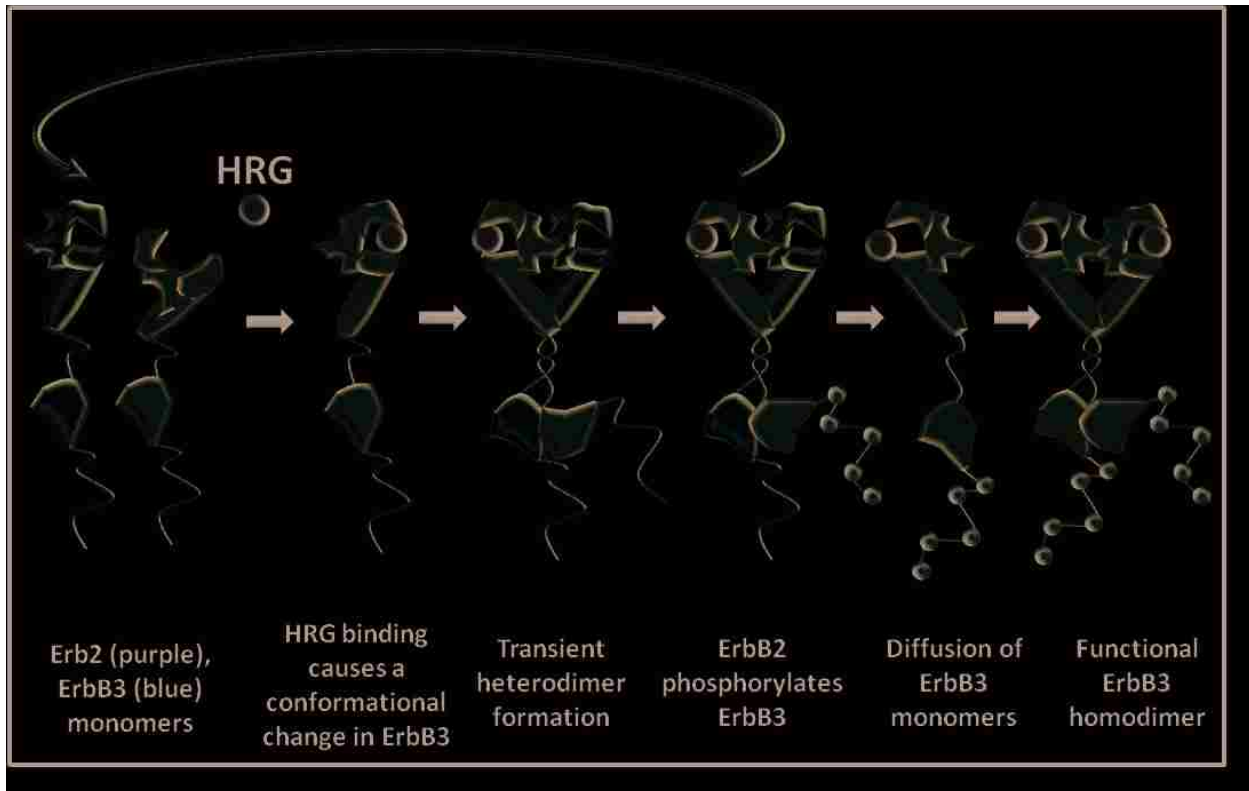
Figure 4.6. A model of ErbB2/ErbB3 interactions leading to activated ErbB3 homodimers. In the absence of HRG, both erbB2 and erbB3 exist primarily as monomers and erbB3 rests in a tethered conformation. Upon stimulation with HRG, erbB3 undergoes a conformational change which frees its dimerization arm and facilitates transient heterodimerization with erbB2. ErbB2 activates erbB3 through phosphorylation of erbB3's cytoplasmic tail. Following dissociation from erbB2, activated erbB3 monomers then diffuse and form functional homodimers. Because phosphorylated erbB3 has increased kinase activity, erbB3 is capable of activating other erbB3 receptors and/or phosphorylating cytoplasmic signaling partners.

It is likely that erbB2 is not the only heterodimerizing partner capable of activating erbB3 in transient complexes, since coupling with another transmembrane tyrosine kinase receptor, Met, has also been reported (Beerli et al., 1995; Campiglio et al., 1999; Engelman et al., 2007). One important aspect of the new transient interaction model is the reduced reliance on equivalent (or greater) levels of expression of erbB3 dimerizing

www.manaraa.com

partners, since multiple erbB3 receptors could potentially be activated by a single e4.rbB2 receptor. For example, we observed that erbB3 activation is significant in transfected CHO cells where it is several times more abundant than endogenous erbB2. The erbB2-blocking antibody (2C4) inhibits HRG-induced erbB3 phosphorylation to a similar degree (about 75%) in CHO cells and in SKRB3 cells where the several million erbB2 outnumber erbB3 many fold. The humanized anti-erbB2 therapeutic antibody, Pertuzumab, was derived from 2C4 (Adams et al., 2006). We speculate that residual erbB3 activation, in the absence of ErbB2 as e heterodimerizing partner, may possibly be attributed to erbB3's own kinase activity providing one possible mechanism for tumor resistance.

Another unique feature of our studies is the direct visualization of erbB3 "signaling clusters" by immunoelectron microscopy of membrane sheets ripped from cells after 2-5 min. stimulus with HRG. The images in Figure 4.5 show that erbB3 is the predominant erbB receptor species in these signaling patches, lending additional support for the concept that persistent signaling occurs through erbB3 homointeractions. These studies call for a revision of the erbB3 pre-oligomerization model of Landgraf and colleagues, where *preexisting* inactive erbB3 oligomers were proposed to *dissociate* upon ligand binding to promote heterodimerization (Landgraf and Eisenberg, 2000; Kani et al., 2005). Instead, we observed that erbB3 clusters were small in resting cells, ranging in size up to seven receptors, while HRG treatment resulted in formation of clusters with hundreds of erbB3 receptors(Yang et al., 2007). If inactive erbB3 oligomers exist, they must be composed of dimers or limited to only a few receptors per oligomer. We note that erbB2-erbB3 patches are morphologically unlike other known

128

membrane domains, such as caveolae that have previously been implicated as destinations for signaling proteins (Yamabhai and Anderson, 2002). These "dark patches" may represent pre-existing membrane domains with properties that are attractive to activated receptors and are consistent with the "protein islands hypothesis", stemming from prior work in T cells (Lillemeier et al., 2006). The molecular profile of these patches remains unidentified to date, although we found strong labeling for the p85 subunit of PI3K in the patches following HRG treatment (Figure 4.4C and 4.4E).

In summary, we demonstrate that intact erbB3 immune complexes have HRG-dependent kinase activity that catalyzes the phosphorylation of an exogenous substrate *in vivo*. This kinase activity correlates with erbB3 phosphorylation, which is dependent on an active erbB2. However, erbB2/erbB3 heterodimers are not the source of catalytic activity since erbB2 is not present in erbB3 immunoprecipitates used as a source of enzyme in the assay. Also, erbB2 is not required in a 1:1 ratio since erbB3 signals robustly to the PI3K-Akt cell survival pathway even when artificially introduced into CHO cells that express a small amount of endogenous erbB2 and no other members of the erbB family. HRG-dependent erbB3 signaling requires erbB2 participation for activation of erbB3, but may thereafter form kinase-active, signaling-competent erbB3 homodimers. ErbB3 signaling output can be amplified by a novel gain-of-function substitution in the erbB3 kinase domain or reduced by mutagenesis of the AAR motif in the catalytic region. These results suggest that erbB3 may have both co-dependent and independent roles in tumor survival and is itself a potential therapeutic target in some cancers.

4.8 MATERIALS AND METHODS

4.8.1 Cell Lines, Reagents

SKBR3 cells were cultured in McCoy's media, 10% FBS with penicillin/streptomycine and 2 mM L-glutamine. For live cell imaging, cells were plated in 8-well Lab-Tek chambers (Nunc, Rochester, NY) and allowed to reach up to 50% confluency before experimentation. CHO cells were cultured in DMEM, 10% FBS (Hyclone) with penicillin-streptomycin, 2 mM L-glutamine. EGF was from Biomedical Technologies (Stoughton, Massachusetts). For western and K-LISA experiments, Heregulin 1-β1 from US Biological (Swampscott, Massachusetts) was used to stimulate cells in culture. Staurosporine and EGFR antibodies were from Calbiochem (La Jolla, California). Lapatinib was from LC laboratories (Woburn, Massachusetts). Anti-EGFR SC-03 was from Santa Cruz Biotechnology (Santa Cruz, California). ErbB2 antibodies RB9040 and MS-325 were from Labvision (Fremont, California); erbB3 antibodies SC-285 and SC-415 and p85 antibodies SC-1637, SC-423 were from Santa Cruz; p85 06-497 antibody was from UBI (Lake Placid, New York). Antibodies for phospho-(Y1248)-erbB2, phospho(Y1289)-erbB3, phospho(S473)-Akt and total Akt (#9272) were from Cell Signaling (Danvers, Massachusetts); HRP-conjugated PY20 antibodies were from BD Biosciences (San Jose, California). For single particle tracking, recombinant human NRG1-beta 1/HRG1-beta 1 extracellular domain (R&D Systems) was singly biotinylated using NHS-ester conjugation chemistry (Biotin-XX, sulfosuccinimidyl ester, Invitrogen). Biotinylated HRG was conjugated to Qdot® 655 or Qdot® 585 streptavidin conjugate (Invitrogen) in PBS + 1% BSA to generate stock solutions of 30 nM 1:1 monovalent QD-

130

conjugates. Reduced Herceptin-Qdot® 655 or Qdot® 585 were produced using maleimide chemistry with commercial Antibody Conjugation Kits (Invitrogen).

4.8.2 Sequencing ErbB3

mRNA was extracted from SKBR3 cells using the RNeasy Mini Kit (QIAGEN, Chartsworth, California). Pairs of primers were designed to span the ErbB3 tyrosine kinase domain:

5'-CTCTGGACCCCAGTGAGAAG-3' and 5'-GGGAGTACAAATTGCCAAGG-3';

5'-GGTCAGCCACACCAAAATCT-3' and 5'- CAGATACCGTGGTGGGTCTC-3'.

After amplification using a QIAGEN One-step RT-PCR kit, PCR products were separated by agarose gel electrophoresis, extracted with the QIAquick gel extraction kit, and sequenced using the above primer sets.

4.8.3 Site-directed mutagenesis and transfection

The human v-erb-b2 homolog 3 (erbB3) WT gene fused to mCitrine (mCit; a monomeric YFP variant) was previously introduced into the pcDNA6 vector (Lidke et al., 2004). The E933Q and R819A mutations were introduced into pcDNA6 ErbB3 mCitrine by site-directed mutagenesis using the Quick-Change Site Directed Mutagenesis kit (Stratagene, Santa Clara California). PAGE-purified mutagenesis primers and their reverse compliment were obtained from Invitrogen or Integrated DNA Technologies (Coralville, Iowa). Sequence of the sense primers were:

E933Q: 5'-CAAGTGTTGGATGATTGATCAGAACATTCGCCCAAC-3'

R819A: 5'-CATAGAAACCTGGCTGCCGCAAACGTGCTACTCAAGTC-3'

Plasmids were transfected into CHO cells using Lipofectamine 2000 (Invitrogen). Blasticidin-resistant transfectants expressing visible erbB3-mCit were sorted by Moflo

131

(UNM Flow Cytometry facility), followed by colony selection in 96 well plates and visual inspection of clones expressing erbB3-mCit on the cell surface.

Alignment of the kinase domains of the EGFR family utilized the program ClustalW available on the EMBL-EBI website (Larkin et al., 2007).

4.8.4 Western blotting and immunoprecipitation analyses

Cells were serum-starved (2-4 hours) then stimulated with ligands -/+ inhibitors as reported in legends. Cells were solubilized in cold NP-40 lysis buffer (Yang et al., 2007). Protein concentrations in cleared lysates were measured by BCA assay (Pierce, Rockford, Illinois). For the kinase assay in Figure 2D, relative amounts of erbB3-mCit protein per sample were measured using the Qubit fluorometer (Invitrogen). For immunoprecipation, supernatants were preincubated with Protein A-beads (Amersham GE Healthcare, Chicago, Illinois) followed by incubation at 4°C with primary antibodies. Proteins in washed immune complexes were denatured and separated by SDS-PAGE, transferred to nitrocellulose membranes, probed with primary and HRP-conjugated secondary antibodies and detected by the ECL method (Pierce).

4.8.5 *In vitro* tyrosine kinase assay

Kinase activity in bead-bound immune complexes was measured using commercially available K-LISA EAY kits (Calbiochem, La Jolla, California) or ELISA plates coated in-house with 1 µg/ml EAY peptide and blocked with BSA. Beads bound to rabbit IgG, incubated under identical conditions with cell lysates and subsequent washes, served as a negative control. Aliquots of precipitate/slurry were transferred in triplicate to wells of K-LISA strips, followed by incubation +/- inhibitors according to the manufacturer's

protocol. Significance of data from six independent experiments was determined using Student's t-test.

4.8.6 SH2-domain array capture assay

Lysates were prepared from serum-starved SKBR3 cells after stimulation with HRG (12nM, 2min). TranSignal phosphotyrosine profiling arrays (Panomics, Redwood City, California) were sequentially incubated with clarified lysates, erbB3 or erbB2 specific antibodies, and HRP-conjugated second antibodies. Reactive spots were visualized by the ECL method (Pierce) and reported in the Supplement.

4.8.7 Single particle tracking (SPT), Image Registration and Analysis

Cells in 8-well Lab-Tek chambers (Nunc, Rochester, NY) were imaged in Tyrode's buffer supplemented with 0.1% BSA, 20 mM glucose. Prior to imaging, cells were serum starved for 4 hr in McCoy's Medium lacking FBS. Experiments with lapatinib (Eton Biosciences Inc., San Diego, CA.) were performed after an additional 30 min incubation in serum-free media with 500 nM inhibitor; drug was also present during imaging. Images were acquired at 20 frames/s using an Olympus IX71 inverted microscope equipped with a 60x 1.2 N.A. water objective and objective heater (Bioptechs, Butler, PA) to maintain sample temperature at 34-36 °C. Wide field excitation was provided by a mercury lamp with a 436 /10 nm BP excitation filter. Emission was collected by an electron multiplying CCD camera (Andor iXon 887) using a QuadView image splitter (Optical Insights) to simultaneously image the QD585 (585/20) BP and QD655 (655/40nm) probes. Image processing was performed using Matlab (The MathWorks, Inc., Natick, MA) functions in conjunction with the image processing software DIPImage (Delft University of Technology). Single molecule

localization and trajectory elongation were performed as previously described (Smith et al., 2010). Two channel images were registered as described previously (Churchman et al., 2005). Pairwise trajectories were analyzed to determine the degree of correlated motion as previously described (Andrews et al., 2008).

4.8.8 Electron Microscopy

Detailed methods have been described (Wilson et al., 2000; Wilson et al., 2007). Cells on glass cover slips were incubated +/- stimuli (37°C), fixed with 0.5-2% PFA and membrane sheets were prepared as in (Yang et al., 2007). At least two experiments were performed for each condition, for which at least ten images were acquired on a Hitachi H-7500 transmission electron microscope. Spatial statistical analyses used the Hopkins test for clustering and Ripley's K bivariate function for co-clustering (Haase, 1995; Wilson et al., 2004; Zhang et al., 2006a).

4.9 ACKNOWLEDGEMENTS

CHAPTER 5: DISCUSSION AND IMPLICATIONS

5.1 SUMMARY

The studies shown here address the roles of diffusion and dimerization kinetics in regulating erbB receptor signaling. ErbB dimer formation and local membrane reorganization are critical features of signal initiation, but have been difficult to resolve, especially in the live cell context. We developed a suite of tools that specifically address the roles of diffusion, interaction kinetics, and membrane topography in erbB receptor dynamics. Most importantly, these approaches exceed the capabilities of previous approaches through improved spatial and temporal resolution. A number of studies have been conducted on intact erbB receptors at the single molecule level but have been unable to directly visualize the formation of dimers and use these events to characterize the reaction kinetics (Sako, 2000 Orr, 2005, Lidke, 2004, Lidke, 2005, Chung, 2010).

5.1.1 Significance of new HMM Method

The Hidden Markov Model extracts rate constants for receptor transitions between free, domain-confined, and dimerized states. The novelty of this approach is that the HMM assumes a kinetic model for the underlying biological progress whose rate constants are unknown. By using our large data sets from SPT, we can determine a maximum likelihood estimate of the kinetics of the system. This represents an important methodological advance for quantitation of state-dependent behaviors. The off rate is a useful parameter that reflects the full range of physiologically relevant dimer lifetimes. The potential of improved computational models to inform our mechanistic

136

understanding of erbB dynamics, using parameters from live cell measurements, is discussed in section 5.2.3.

Another useful feature of this approach is the determination of the confinement zone using changes in state behavior. This is an improvement over the traditional mean square displacement (MSD) analysis (Kusumi, 1993). The large sample size analyzed by the HMM approach better approximates the size of these regions of the membrane than typical MSD calculations, which rely on behaviors of individual trajectories. In the emerging era of single molecule biochemistry, this method clearly demonstrates the potential of SPT to determine the dynamic interactions between species. The HMM represents a statistically rigorous approach that addresses the challenges of studying live cell protein-protein dynamics.

5.1.2 Significance of erbB1 results

In work focused on the formation of erbB1 homodimers, we demonstrate that ligand binding determines dimer stability, regardless of the activation status of the kinase domain. The importance of local environment composition and organization is underscored by our unique observation of repeated dimer events between two receptors. Kinase-inhibited receptors do not show a significant change in mobility when co-confined, regardless of ligand addition. We show that 2 EGF:2 erbB1 homodimers display slowed mobility in the domain state, highlighting the role for membrane partitioning at the onset of signaling. Immobilization appears to be a feature of signal propagation as seen in signaling competent, ligand-bound dimers whose mobility slows more than 6-fold compared to the monomer state.

This work also addresses many of the important hypotheses that remain unresolved in the erbB1 field. First, the presence of dimers in the absence of ligand was detected, which supports the concept that preformed dimers can and do occur. However, these species displayed the shortest lifetime and did not demonstrate correlated motion. These results suggest that such 0 ligand:2 erbB1 complexes are weakly associated and are unlikely to initiate signaling, consistent with reports for nonsignaling predimers (Hofman, 2010). Signaling by preformed dimers may be highly receptor density dependent (Clayton, 2005, Gadella, 1995, Chung, 2010, Nagy, 2010).

Second, we observe that dimers that are composed of two liganded receptors are the most stable. This calls for reinterpretation of the negative cooperativity model, which suggests the lowered binding affinity of a 1:2 ligand: erbB1 dimer for ligand (MacDonald, 2010). Our results of short lived 1:2 dimers suggest that, if negative cooperativity exists, the contribution to erbB1 signaling may be limited due to the short duration of this state (Figure 5.1). In addition, dimers are the result of occupied monomers that encounter one another in a manner that is promoted by membrane confinement. Dimers with a single ligand will be expected to dissociate and upon binding of a second ligand, will form the more stable 2:2 dimers.

138
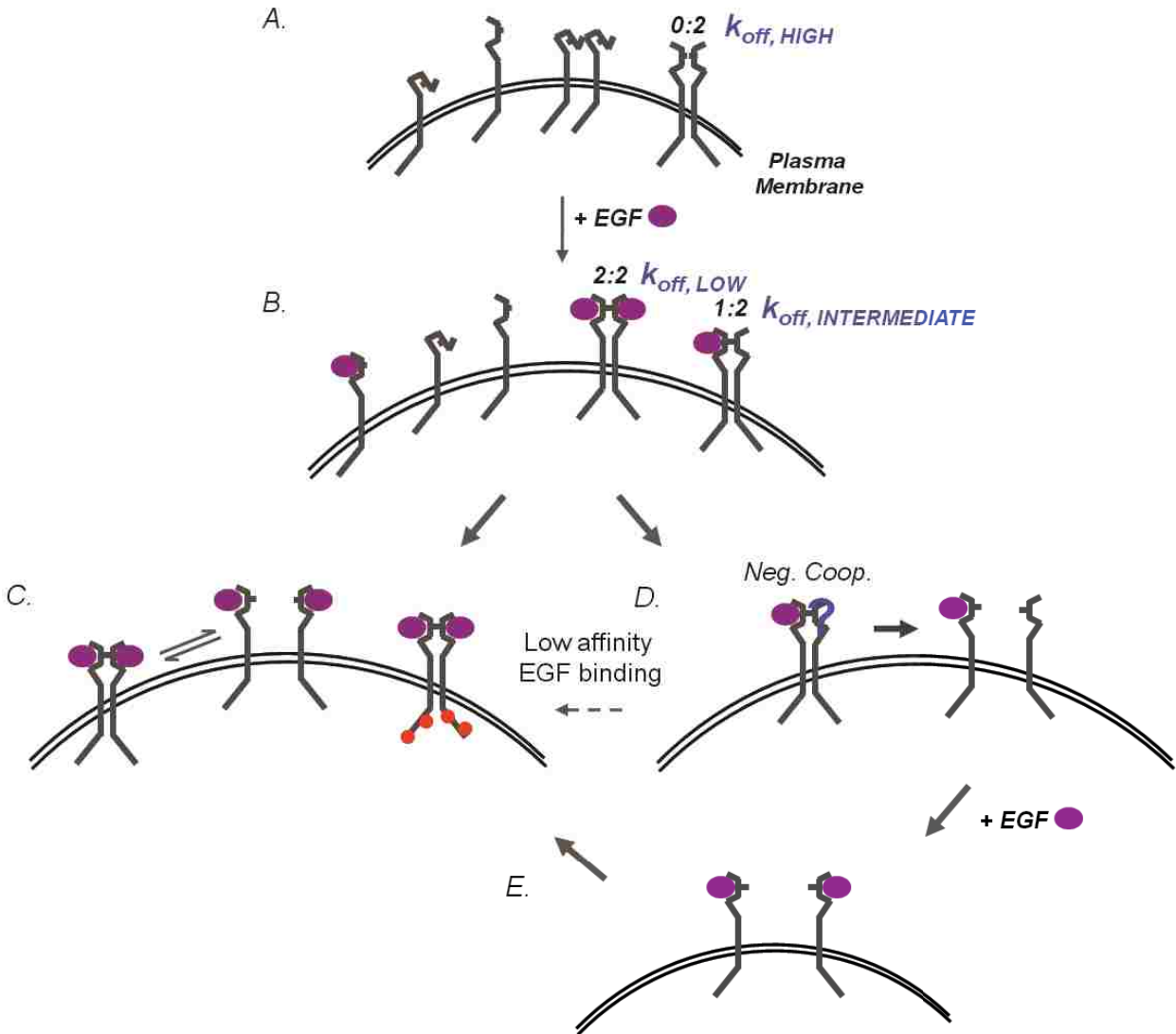
Figure 5.1. Dynamics of erbB1 receptors on cells are affected by dimer off rates and ligand activation. **A)** In the resting state, receptors are on the surface in the tethered or extended conformation. Preformed dimers (0:2 ligand:erbB1) may also be present in the absence of the ligand, but k_{off} is high for this complex. **B)** Following addition of ligand, occupied monomers, unoccupied receptors, and dimeric complexes exist. The 2:2 dimer has the smallest off rate, whereas the 1:2 dimer has an intermediate k_{off}. **C)** Liganded dimers may demonstrate repeated encounters within a domain and multiple dimer events. Alternately, long lived dimers undergo transphosphorylation (red circles) and signal downstream through adaptor proteins. **D)** Negative cooperativity suggests that 1:2 dimers will have a lowered affinity for the second ligand binding event. Our data

139

shows that these dimers have an intermediate off rate, suggesting that dissociation is favored over binding of a 2nd ligand. **E)** If the unliganded receptor from the 1:2 complex binds another ligand, these receptors may exhibit the behavior shown in **(C).**

5.1.3 Significance of erbB2 and erbB3 results

We also used our new Hidden Markov Model approach to study the misfits of the erbB family: erbB2 and erbB3. These members have been of great interest, especially for their putative roles in mechanisms of carcinogenesis. Colleagues in the laboratory (Yang and Steinkamp) demonstrated that erbB3 complexes catalyze the phosphorylation of a peptide substrate, in an erbB2- and ligand-dependent manner. Importantly, this activity is not associated with other erbB receptors or other co-precipitated proteins. These results alone constitute a paradigm shift in erbB signaling with kinase activity directly associated with erbB3 receptors.

From our single particle tracking measurements, the model of short lived erbB2-erbB3 heterodimers preceding the formation of signaling competent, long lived erbB3 homodimers is supported by both dimer event lengths from HMM and correlated motion analyses (Figure 4.6). A feature of this model that may carry disease significance is that a 1:1 ratio of erbB2:erbB3 receptors is not requisite, suggesting that even a small number of erbB2 receptors can effect a robust erbB3 signaling response. Our ability to characterize the kinetics of these dimer events points to the potential of this approach to understanding erbB-related mechanisms of oncogenesis. We expect to apply these techniques, in particular, to understanding the molecular basis of erbB3-mediated escape from erbB-targeted therapies.

5.2 PERSPECTIVE AND FUTURE STUDIES

5.2.1. erbB receptor homo- and hetero-dimer formation and signaling

Despite decades of study, the erbB receptors remain the focus of ongoing research. As early as the 1980s, the erbB1 gene was shown to be overexpressed in primary brain tumors (Libermann, 1985) and the hyperactivity associated with high receptor density is implicated in poor clinical outcomes (Slamon, 1989). The roles of these membrane proteins as regulators of important cellular functions have motivated detailed investigations of the molecular mechanisms that govern their function. Since the discovery of ligand-induced dimerization as the first step in erbB signal transduction (Ullrich, 1990), the formation of these complexes has been a subject of keen interest. Using the approaches we have developed, the combinatorial complexity of dimer formation can be interrogated in a variety of cell types, including those expressing erbB mutants. In particular, density dependent effects of receptor ratios on diffusion and interaction kinetics could provide insight into fundamental mechanisms of aberrant erbB signaling.

The studies presented here provide previously unattainable molecular detail of erbB receptor dimerization. An essential question remains regarding the threshold lifetime for a dimer before successful transphosphorylation, adaptor protein recruitment (Pawson, 2004, Schlessinger, 2003), and signaling occur. Some short dimer lifetimes were observed, as well as repeated interactions of receptors for variable times. The short lifetime associated with erbB2-erbB3 heterodimers may require rapid phosphorylation in order to activate the erbB3 kinase. It is important to understand if these short or punctuated interactions actively signal. A possibility is that the activity of

phosphatases leads to dephosphorylation of tyrosine residues, precluding downstream events. The timescale of this feedback could determine the productivity of short lived dimers. Additionally, the downregulation of signaling through endocytosis may be occurring during the events that are observed. This mechanism has been demonstrated to occur in response to ligand stimulation, using both clathrin-dependent and clathrin-independent entry routes (Sadowski, 2009, Sorkin, 2009, Xiao, 2008). It will be important to determine if 1:2 and 2:2 ligand:receptor dimers have equivalent internalization kinetics.

The need to specifically correlate the kinase activity of the receptor with the dimerization event is a significant challenge. As a starting place to address this question in intact cells, techniques using fixation can be employed to monitor the phosphorylation status of dimerized receptors. The Lidke laboratory is developing an approach based on combining imaging and microfluidic technologies to quickly flow in a fixative and crosslink a cell following the observation of dimerization by our standard QD protocol. Using this method, cells can be halted in time, permeabilized, and fluorescently labeled antibodies can be flowed into the chamber and show not only the phosphorylation status of the receptor, but can also be used to detect which, if any, adaptor proteins have been recruited to the site of receptor interaction. Unfortunately, this approach precludes the correlation of ongoing dimerization events and receptor diffusion with downstream signaling in real time. Regardless, this is an important first step in characterizing the dimers we observe using SPT techniques.

Ultimately, the ability to report kinase activity in real time will be the preferred means to corroborate dimerization with receptor phosphorylation. Some efforts have

been made to overcome the requirement to make *ex post facto* observations of kinase activity. An example is the use of biosensors based on the incorporation of a synthetic fluorophore whose optical properties are modulated by the phosphorylation status of its associated protein (Sharma et al., 2008). As probes, labels, and imaging modalities continue to advance, this goal may be realized and will permit the concurrent observation of dimers and phosphorylation, providing unequivocal mechanistic evidence for the activation of these complexes. This will also be invaluable in verifying or disproving the mechanism of lateral signaling propagation as the spread of phosphorylated residues may be more directly associated with the erbB receptors involved.

5.2.2 Membrane organization and receptor partitioning

The results presented in this work have significant implications for understanding erbB receptor dynamics, with particular insights into the impact of the cell membrane on protein-protein interactions. The features of receptor diffusion and interaction kinetics are critically influenced by the lateral organization of the plasma membrane. The viscosity of this complex environment has led to diffusion measurements of transmembrane proteins that are an order of magnitude slower than those observed in artificial membranes (Kusumi, 2005, Bacia, 2004). This decreased mobility could be due to protein-protein interactions (Douglass, 2005), cytoskeletal confinement (Kusumi, 1993, Jacobson, 1995, Andrews, 2009), or lipid microdomains (Simons, 1997). A role for residency time in membrane domains of specific composition to regulate receptor signaling is of great interest to the cell biology community.

In SPT studies of erbB receptors, Orr, et al. found that perturbation of actin and cholesterol has differential effects on erbB1 and erbB2. Depletion of cellular cholesterol induced confinement of both receptors, but actin depolymerization only affected erbB1, increasing its diffusion (Orr, 2005). These result suggest differential partitioning of the orphan receptor, erbB2 from erbB1, which may have important functional consequences. My colleagues in the Wilson laboratory have used membrane sheets and immunoelectron microscopy to show that large patches of erbB3 receptors following stimulation with heregulin. The exclusion of erbB2 from these patches further indicates membrane reorganization as a critical feature of signaling. This is consistent with earlier results that show cell surface microdomains that co-confine erbB1 receptors and whose composition is affected by the activation status of the complex. Taken together, these results indicate a special role for membrane components in providing unique environments for the members of the erbB family. Receptor clustering upon activation may precede signaling and internalization; the reconciliation of the sequence of events that lead to the formation of these patches on the membrane remains a topic of great interest.

In an ongoing effort to map the cell membrane, experiments to determine the effects of choleseterol depletion and actin disassembly on erbB dimerization kinetics should be explored. Actin treadmilling has already been shown to play a role in normal mechanisms of activated erbB1 function (Lidke, 2005) and may stabilize dimers through direct interactions. In fact, interactions with the cytoskeleton may lead to immobilization of the receptor for signaling and, ultimately, endocytosis (Rijken, 1995, Xiao, 2008). The tools we developed in this dissertation project can be readily applied to these studies.

144

One potential approach is to use Latrunculin A to depolymerize actin. Partial extraction of cholesterol with methyl-beta-cyclodextrin is another approach that avoids the complications resulting from the total depletion of cholesterol (Owen et al., 2006).

5.2.3 Implications for erbB-target therapies

Current therapies targeting the erbB receptors fall into two broad classes: small molecule tyrosine kinase inhibitors and monoclonal antibodies that interfere with receptor activation. The single molecule approaches we developed provide a unique framework to characterize the mechanism of action for these kinds of pharmacological agents. We demonstrated the use of an ATP competitive inhibitor, PD153035, in the erbB1 studies. These efforts not only showed effects of the drug on receptor diffusion, but also furthered our understanding that an active kinase domain plays a minimal role in erbB1 homodimer stability. The analysis of drugs can be extended to other receptor antagonists. Two engineered antibodies of interest are MM-111 and MM121 that target erbB3. Efforts to label and study these agents are underway and are expected to provide mechanistic insight into their function. Our results also suggest an important therapeutic avenue for treating erbB related diseases, namely through the development of agents that affect receptor localization. A role for agents that disrupt the changes in lateral organization associated with signaling dimers could have great clinical value.

5.2.4 Computational modeling – a useful next step

Computational models of erbB network behaviors can be useful in predictions of signaling outcomes. A number of models already exist and have provided insight into the effects of network components on signaling outcomes (Kholodenko et al., 1999; Hsieh et al., 2008; Dehmelt and Bastiaens, 2010). However, these models may fall

145

short when using parameters derived from only solution-based measurements (Rates from literature are summarized in Appendix F). The diffusive and kinetic parameters we have extrapolated from live cell observations of erbB receptors will improve the potential of these models. Systems biology models that are motivated by our parameters have utility as platforms to test hypotheses difficult to execute in the lab, as well as to simulate therapeutic paradigms.

In collaboration with the Edwards group and other colleagues at the UNM STMC, we plan to use the values from our measurements to improve an existing stochastic computational model for erbB1 signaling and, ultimately, extend its variables to include erbB2 and erbB3 components. The benefit of using this *in silico* approach is in the abilities to allow simulations to reach equilibrium and to observe the entire receptor population, not simply those that are QD labeled in SPT experiments. We are interested in how receptors behave at steady state, following activation, and in monitoring the downstream outputs. One goal is to test the predictions of the new model in this chapter (Figure 5.1), by populating a stochastic simulation with receptors and providing a stimulus. We expect that, at equilibrium, the system will be minimally affected by negative cooperativity. Receptors are expected to have the most productive interactions when both monomers in a dimer are bound to ligand.

146

5.3 CONCLUSIONS

In this work, we have described erbB diffusion and dimerization kinetics with mechanistic details that were previously unattainable. In particular, these measurements were made on live cells, under physiologically relevant conditions. We have elucidated new features of erbB signaling, including the repeated interactions of erbB1 receptors and the successful formation of long lived erbB3 homodimers. The sophisticated approaches we developed and implemented, both experimental and analytical, provide the spatial and temporal resolution necessary to visualize and quantify receptor mobility, dimer off rates, and state-dependent behaviors. These techniques have addressed a number of questions in the erbB field and permit the detailed investigation of many other interesting cellular phenomena.

APPENDIX A: REPORTED ERBB RECEPTOR DIFFUSION COEFFICIENTS

Cell Line	Technique(s)	Temperature of Experiments (°C)	Diffusion Coefficient (µm²/s)	Percent Immobile	Notes	Citation
A431	FRAP	5; 37	0.028; 0.085	?	Based on abstract	Hillman et al., *Biochem.*, 1982.
COS	FRAP	25	0.01	30-50	Receptor and C-tail mutants diffuse similarly	Livneh et al., *JCB* 1986.
Mouse keratinocyte	FRAP; SPT using 40 nm colloidal gold	36.5	0.011-0.02	2-17	Cytoskeletal fences; range of D: 0.0046-0.1 µm²/s	Kusumi et al., *BJ*, 1993.
A431	SPT using Cy3-EGF	25	?	?	Intensity spikes (factor of 2). P-Y detected using mAb74	Sako et al., *Nat. Cell Biol*, 2000
A431, HeLa, MCF7	SPT using EGF-QD; FRAP	23	+PD: 0.0038 +CytoD: 0.0042 FRAP on cell body: 0.06, 0.04 (EGF)	?	Transport along filopodia requires a dimer	Lidke et al., *JCB*, 2005.
Human Mammary Epithelia	FRAP using mAb13A9 and mAB7C2 Fab's	25	0.023 erbB1; 0.035 erbB2; +CytoD: 0.027 erbB1	?	Effects of F-actin and cholesterol on D; heterodimers; cholesterol→confinement	Orr et al, *BJ*, 2005.
HeLa	SPT using C-term. EGFR-GFP	25	0.049; 0.024 (EGF)	20-25	Both clathrin and caveolin enodocytosis	Xiao et al., *Biochem. & Biophys. R Comm.*, 2008.
CHO, A431, BT20, A549, H460	SPT, cumulative square displacement	Unreported	0.06-0.33 (αerbB1 Fab)	?	Transfected and endogenous intack erbB1	Chung, et al., *Nature*, 2010

APPENDIX B – FLUORESCENT PROBES

Probe	Epitope	Fluorophore & Chemistry	Activity
EGF QD585	erbB1 ligand	SAvQD585	erbB1 activating
EGF QD625	erbB1 ligand	SAvQD625	erbB1 activating
EGF QD655	erbB1 ligand	SAvQD655	erbB1 activating
EGF QD705	erbB1 ligand	SAvQD705	erbB1 activating
rEGF QD585	reduced erbB1 ligand	maleimide QD585	erbB1 non-activating
rEGF QD655	reduced erbB1 ligand	maleimide QD655	erbB1 non-activating
13A9 A488	erbB1	Alexa488 C5 maleimide	Non-EGF Competing
ERBB1.1 A488	erbB1	Alexa488 NHS ester	Non-EGF Competing
ERBB1.1 A647	erbB1	Alexa647 NHS ester	Non-EGF Competing
VHH(EGb4) A488	erbB1 (domain I)	Alexa488 NHS ester	Non-EGF Competing
VHH(EGb4) A647	erbB1 (domain I)	Alexa647 NHS ester	Non-EGF Competing
VHH(EGb4) QD585	erbB1 (domain I)	SAvQD585	Non-EGF Competing
VHH(EGb4) QD655	erbB1 (domain I)	SAvQD655	Non-EGF Competing
Herceptin A488	erbB2	Alexa488 NHS ester	erbB2 Inhibitor
Herceptin A647	erbB2	Alexa647 NHS ester	erbB2 Inhibitor
rH A488	erbB2	Alexa488 C5 maleimide	Reduced erbB2 Inhibitor
rH QD585	erbB2	maleimide QD585	Reduced erbB2 Inhibitor
rH QD655	erbB2	maleimide QD655	Reduced erbB2 Inhibitor
Heregulin A647	erbB3 ligand (8 kDa)	Alexa647 NHS ester	erbB3 activating (EGF-like domain of ligand)
Heregulin QD585	erbB3 ligand (8 kDa)	SAvQD585	erbB3 activating (extracelluar domain)
Heregulin QD655	erbB3 ligand (8 kDa)	SAvQD655	erbB3 activating (extracelluar domain)
VHH(EGa) A488	erbB1 (domain III)	Alexa488 NHS ester	EGF Competing
VHH(EGa) A647	erbB1 (domain III)	Alexa647 NHS ester	EGF Competing
VHH(EGa) QD585	erbB1 (domain III)	SAvQD585	EGF Competing
VHH(EGa) QD655	erbB1 (domain III)	SAvQD655	EGF Competing

APPENDIX C: SUPPLEMENTARY INFORMATION FOR CH. 3

Abbreviations

EGF, epidermal growth factor; erbB1, erythroblastic leukemia viral oncogene homolog 1 or epidermal growth factor receptor; HMM, Hidden Markov Model; SD, square displacement; QD, quantum dot; SPT, single particle tracking; VHH, nanobody

Materials and Methods

Reagents. Biotinylated EGF was purchased at a 1:1 stoichiometry (Invitrogen, Carlsbad, CA) and singly biotinylated VHH fragment EGb4 was produced using the BirA expression system (Roovers et al., 2007). Biotin-EGF or biotin-VHH were conjugated to Qdot® 655 or Qdot® 585 streptavidin conjugate (Invitrogen, Carlsbad, CA) in PBS + 1% BSA to generate stock solutions of 30 nM 1:1 monovalent QD-conjugates (Lidke et al., 2004). Stock solutions were stored at 4°C and used for up to two weeks. Biotin-EGF was conjugated to Qdot® 625 streptavidin for bleedthrough experiments. Experiments with PD153035 (Tocris Bioscience, Ellisville, MO) were performed at a final concentration of 1 μM inhibitor.

Cell culture. A431 Human Epithelial carcinoma cells were cultured in Dulbecco's Modified Eagle's Medium without phenol red (Sigma-Aldrich, St. Louis, MO) supplemented with 10% fetal bovine serum (FBS; Invitrogen, Carlsbad, CA) and penicillin and streptomycin. For live cell imaging, cells were plated in 8-well Lab-Tek chambers (Nunc, Rochester, NY) and allowed to reach up to 50% confluency before experimentation.

Cell treatment for SPT experiments. Cells in Lab-Tek chambers were imaged in Tyrode's supplemented with 0.1% BSA and 20 mM glucose. Prior to imaging, cells

were serum starved in Dulbecco's Modified Eagle's Medium lacking FBS for four hours. Experiments with PD153035 were performed after serum starvation including1 µM inhibitor and live cell imaging buffer also included 1 µM PD153035.

Fluorescence Microscopy. Wide field imaging for SPT was performed using an Olympus IX71 inverted microscope equipped with a 60× 1.2 N.A. water objective. Wide field excitation was provided by a mercury lamp with either a 436 /10 nm BP excitation filter and a 50/50 neutral density filter. Emission was collected by an electron multiplying CCD camera (Andor iXon 887) using a QuadView image splitter (Optical Insights) to simultaneously image two spectrally distinct QDs. QD emission was collected using a 600 nm dichroic and the appropriate emission filters, 655/40nm and 585/20 BP (Chroma, Rockingham, VT). A single pixel is equivalent to 267 nm. The sample temperature (34-36 °C) was maintained by an objective heater (Bioptechs, Butler, PA).

Image Processing. All image processing was performed using Matlab (The MathWorks, Inc., Natick, MA) in conjunction with the image processing library DIPImage (Delft University of Technology). For descriptions of specific analysis routines see Supplementary Information.

GPU Single Particle Tracking and Track Elongation. Images were acquired at 20 fames/s for a total of 1,000 frames. Single molecule localization and trajectory connection were carried out as previously described (Smith et al., 2010). Complete derivation of the track elongation algorithm is provided in Supporting Online Text.

To elongate short tracks, the positions (p_i and p_{i+j}) with the smallest Δt for temporally independent tracks are compared using equation 6. Temporally independent

tracks with the best p-value that pass a user-defined cutoff are augmented for form an elongated trajectory. Due to temporal independence of short trajectories, the cutoff and Δt for track elongation can be relaxed slightly from those used in the initial connection algorithm without introducing artifacts. This process is repeated until no temporally independent tracks that pass the cutoff remain. An example comparison of short and elongated trajectories is shown in Supplemental Figure S1.

Squared Displacement Analysis. Diffusion analysis of trajectories was performed by square displacement analysis and two-component fitting, as previously described (de Keijzer et al., 2008).

Correlated Motion Analysis. The degree of correlation between pairwise trajectories was determined as previously described (Andrews et al., 2008).

Fiducial Data Acquisition and Image Registration. Images were registered using a calibration image of multi–fluorophore fluorescent beads (0.2 µm Tetraspeck, Invitrogen, Carlsbad, CA) that have an emission spectrum covering the two spectral windows. The camera was sampled by moving a single bead across the field of view using a mechanical stage (Prior Pro Scan II, Rockland, MA) to obtain good sampling over the field of view. A fiducial data set was acquired at the beginning and end of each chamber tested. Corresponding beads are identified in each channel and fit to a polynomial calibration model. (Churchman et al., 2005).

After direct experimental comparison, no significant difference between using a locally weighted method and the polynomial method discussed below was observed. The polynomial calibration model used is shown in equation 1 (eqn. 1).

$$
\begin{array}{c}
x_{1,1} \\
x_{1,2} \\
x_{1,3} \\
\vdots \\
x_{1,n}
\end{array}
=
\begin{array}{ccccc}
1 & x_{2,1} & y_{2,1} & y_{2,1}x_{2,1} \\
1 & x_{2,2} & y_{2,2} & y_{2,2}x_{2,2} \\
1 & x_{2,3} & y_{2,3} & y_{2,3}x_{2,3} \\
\vdots & \vdots & \vdots & \vdots \\
1 & x_{2,n} & y_{2,n} & y_{2,n}x_{2,n}
\end{array}
\times
\begin{array}{c}
a_{x,1} \\
a_{x,2} \\
a_{x,3} \\
a_{x,4}
\end{array}
\qquad \text{eqn. 1}
$$

In equation 1, the x location of the *nth* bead in channels 1 and 2 are indicated by $x_{1,n}$

and $x_{2,n}$.   Several polynomials were tested for the calibration and the polynomial shown

in equation 1 appeared to sufficiently describe the channel overlay without over fitting.

Equation 1 is shown in matrix notation in equation 2.

$$\mathbf{X}_1 = \mathbf{B}_{\mathbf{x}_2,\mathbf{y}_2}\mathbf{a}_x \qquad \text{eqn. 2}$$

The coefficients $\mathbf{a}_x$ can be solved for using equation 3.

$$\mathbf{a}_x = \mathbf{B}_{\mathbf{x}_2,\mathbf{y}_2} \setminus \mathbf{x}_1 \qquad \text{eqn. 3}$$

Similarly, the coefficients $\mathbf{a}_y$ for the y locations can be solved for using equation 4.

$$\mathbf{a}_y = \mathbf{B}_{\mathbf{x}_2,\mathbf{y}_2} \setminus \mathbf{y}_1 \qquad \text{eqn. 4}$$

Equation 2 can then be used to transform the localization of single molecules in channel

2 to the properly aligned coordinates in channel 1.

The fiducial calibration image acquired prior to the experiment is used to estimate

the model coefficients with equations 3 and 4. The fiducial registration error is shown in

equation 5.

$$\sqrt{\sum_{i=1}^{n}\left[\left(x_{1,i}-x_{2,i}\right)^2 + \left(x_{1,i}-x_{2,i}\right)^2\right]} \qquad \text{eqn. 5}$$

The fiducial registration error of the post experiment fiducial calibration image is used to

estimate the accuracy of the channel overlay. Using two independent calibration images

collected before and after experiments to train and test the model, allows for a more accurate estimate of the error in the channel overlay during the experimental acquisition. An example of a fiducial data set and the accompanying transformation can be found in fig. S1.

SUPPORTING TEXT

Optimizing SPT Trajectories

Optimized elongation of single particle trajectories provides the necessary temporal resolution for kinetic fitting. Longer tracks are necessary to correlate motion in separate channels over an extended period of time and in order to determine the duration of protein-protein association. In order to elongate optimized initial short tracks, temporally independent tracks are identified (fig. S1C).

Particles are fit using a 2 dimensional Gaussian estimate of the microscope point spread function. Algorithms for single molecule localization are implemented on the GPU architecture. Short tracks are connected using homemade software comparing positions (p_i) of all single particles in frame *i* with all single particles positions (p_{i+j}) in frame *i+j*. A probability of p_i and p_{i+j} being the same particle in different time frames is estimated using equation 6.

$$P(p_i \rightarrow p_{i+j}) = e^{\frac{(x_i - x_{i+j})^2 + (y_i - y_{i+j})^2}{4D\Delta t}} \qquad \text{eqn. 6}$$

D is an estimated diffusion constant, Δt is the time between the observation in frame *i* and frame *i+j*. In accordance with literature values (Lidke et al., 2005a; Orr et al., 2005) 0.1 was used for the estimated diffusion constant. Upper limits for the p-value and Δt are user-defined parameters utilized to facilitate temporal connectivity.

Hidden Markov Model

A two-state HMM is insufficient to describe observed erbB1 behaviors. Our first analytical model of erbB1 homoassociation was the simplest, two-state model for

protein-protein interactions in which the states were free (state = 0) or dimer (state = 1). The initial estimate of the Interaction Distance (ID) was based on the crystal structure of the back-to-back erbB1 homodimer (fig. S5) and set to 50 nm. Using this value for the dimer distance, many dimerization events were seen to be interrupted by short breaks, yet the same two receptors would return to the dimer state. This indicated the need for a third, domain-confined, state to completely describe the data (fig. S4).

To ensure that the apparent fluctuations in distance were due to receptor separation and not artifacts in the measurement, we performed two-color measurements using a QD625-EGF probe using whose emission is simultaneously registered in both 585 nm and 655 nm imaging channels (fig. S5). These "perfect dimer" single molecule events demonstrated consistent separation over time that was equivalent to the sum of the localization accuracies of the particles (40-60 nm). This shows that our image registration was very accurate and that the observed fluctuations in separation were genuine. This also confirms that the rigorous 50 nm definition of ID could be used in our analyses.

The three-state HMM permits fitting of transitions rates and domain size. The unexpected distance fluctuation behavior, taken together with the high precision image registration, led us to define a third, domain state. Using the three-state HMM, we can fit both the transition rates between states and the Gaussian sigma for the domain size. These fits are summarized in table S2 below. The domain is smallest for the ligand-bound and signaling competent receptors. Interestingly, there are not large differences between the other domain sizes, suggesting that reorganization and consolidation of the domain changes as a function of signaling propagation.

Using the three-state HMM, many states and types of interactions are observed. Examples of state traces are shown in figure S6, including a long lived QD-EGF (fig. S6A) dimer and the formation of a dimer that subsequently demonstrated the repeated reflection and return behavior previously discussed (fig. S6B). Other examples include exploration of all three interaction states, across several conditions (fig. S6D-F). Another interesting behavior is seen in figure S6C in which there is excursion and return of two ligand-bound receptors between the domain and free states, suggesting a second level of confinement.

A final advantage of our three-state HMM is the ability to take advantage of the state characterizations in order to determine the diffusion coefficients of erbB1 in each state, as shown in Figure 4. Complete results for this analysis under each tracking condition are summarized in table S3.

A complete derivation of the three-state HMM follows.

1 Mathematical Formalism of the HMM Analysis

1.1 Probability Densities of Observed Separations

We use a three state model:

I Dimer

II Domain

III Free

The observed parameter in the hidden Markov model is the separation, d. For the dimer and domain model, the distribution of the displacement between the reporting QDs is parameterized by a zero mean Gaussian distribution in each (x,y) dimension using σ_{dimer} and σ_{domain}, respectively. The value σ_{dimer} is taken as that expected from combining information from crystal structure measurements and the size of QDs, whereas σ_{domain} is varied to find the best fit across all data sets of a specific condition. The resulting observed distribution of displacements is then a convolution of the actual displacements and the errors in measurement, which are also assumed to contribute as unbiased Gaussian distributions, giving

$$\sigma_{\text{I},n}^2 = \frac{1}{2}\sigma_{1,n}^2 + \frac{1}{2}\sigma_{2,n}^2 + \sigma_{\text{overlay}}^2 + \sigma_{\text{dimer}}^2$$

$$\sigma_{\text{II},n}^2 = \frac{1}{2}\sigma_{1,n}^2 + \frac{1}{2}\sigma_{2,n}^2 + \sigma_{\text{overlay}}^2 + \sigma_{\text{domain}}^2$$

where σ_{overlay} is the potential error due to the registration of the two channels, and $\sigma_{i,n}$ is the localization error of QD i in frame n. The probability densities of the observed separations are then:

$$p_1(d_n) = \frac{d_n}{\sigma_{\text{I},n}^2} e^{-\frac{d_n^2}{2\sigma_{\text{I},n}^2}}$$

$$p_2(d_n) = \frac{d_n}{\sigma_{\text{II},n}^2} e^{-\frac{d_n^2}{2\sigma_{\text{II},n}^2}}$$

For the Free model, the probability density is calculated as a function of the observed distance in the previous frame and a characteristic diffusion constant, to give:

$$p_3(d_n|d_{n-1}) = \frac{d_n}{2\pi\sigma_{\text{III},n}^2} \int_0^{2\pi} e^{-\frac{1}{2\sigma_{\text{III},n}^2}(d_n^2 + d_{n-1}^2 - d_{n-1}d_n \sin(\theta))} d\theta$$

where

$$\sigma_{\text{III},n}^2 = \frac{1}{2}\sigma_{1,n}^2 + \frac{1}{2}\sigma_{2,n}^2 + \frac{1}{2}\sigma_{1,n-1}^2 + \frac{1}{2}\sigma_{2,n-1}^2 + \sigma_{\text{overlay}}^2 + 2D\Delta t_n$$

or in the case where there is no previous position information is given by:

$$p_3(d_0) = \frac{2d_0}{L^2}$$

which represents the probability density for separation for two particles that are randomly placed within a region of size, L, where L defines a maximum separation cut-off value for analysis.

1.2 Calculating the Likelihood

Given a set of rate constants $k_{i,j}$ for transitions from state i to state j and making the assumption that multiple transitions in the interval Δt are not allowed, the probability of making a transition from state i to j are given by the matrix $\mathbf{T_n}$ whose elements are by:

$$t_{i,j,(i\neq j)} = \frac{k_{i,j}}{\sum_{j=1,(j\neq i)}^{3} k_{i,j}}(1 - \exp(\Delta t_n \sum_{j=1,(j\neq i)}^{3} k_{i,j})$$

$$t_{i,i} = 1 - \sum_{j=1,(j\neq i)}^{3} t_{i,j}$$

Note that Δt_n is specific for the observation n since due to QD blinking, the time elapsed from the previous available observation of distance may be more than one frame. Using a diagonal matrix $\mathbf{P_n}$ with elements given by $P_{i,i} = p_i$ and a vector of initial probabilities $\pi = (p_1(d_0), p_2(d_0), p_3(d_0))$, The likelihood of an observed data set given the model parameters θ (which are the set of rate constants) is (9,10):

$$L(\theta) = \pi \mathbf{T_1 P_1 T_2 P_2}...\mathbf{T_N P_N} \cdot (1, 1, 1)^T \qquad (1)$$

The likelihood is calculated for all interactions of two QDs for a specific condition and the value

$$\sum_{\text{interactions}} \log L(\theta)$$

is maximized by varying parameters.

The errors on each parameter are given as standard errors and are calculated as $\sqrt{H_{i,i}^{-1}}$ where $\mathbf{H}$ is the Hessian matrix of the negative log-likelihood and i denotes one of the estimated rate constants. Elements of $\mathbf{H}$ are calculated numerically.

Given the set of rate parameters found in the estimation step, the Viterbi algorithm (11) is used to identify the most likely state within individual QD interactions.

1.3 Example Simulation

To illustrate the HMM analysis, we show the results of the analysis of a simulated receptor pair that make transitions between states with specified rates. The parameters of the simulation are similar to that of the system under study:

σ_{overlay}:	10 nm
σ_{dimer}:	50 nm
σ_{domain}:	150 nm
$\sigma_{1,n}, \sigma_{2,n}$:	30 nm
D:	0.05 μms^{-1}
Δt:	0.05 s

In fig. S3, the observed separation, the known state and the found states are shown. The table below shows the specified transition rates and the found rates along with the standard error.

	known (s^{-1})	found (s^{-1})
$k_{\text{II,I}}$	1.00e-002	8.48e-003 $\pm$ 1.84e-003
$k_{\text{III,I}}$	1.00e-005	3.03e-013 $\pm$ 3.97e-006
$k_{\text{I,II}}$	5.00e-003	5.78e-003 $\pm$ 1.34e-003
$k_{\text{III,II}}$	5.00e-003	2.90e-003 $\pm$ 9.54e-004
$k_{\text{I,III}}$	5.00e-004	7.10e-004 $\pm$ 5.07e-004
$k_{\text{II,III}}$	2.00e-003	2.97e-003 $\pm$ 1.13e-003

159
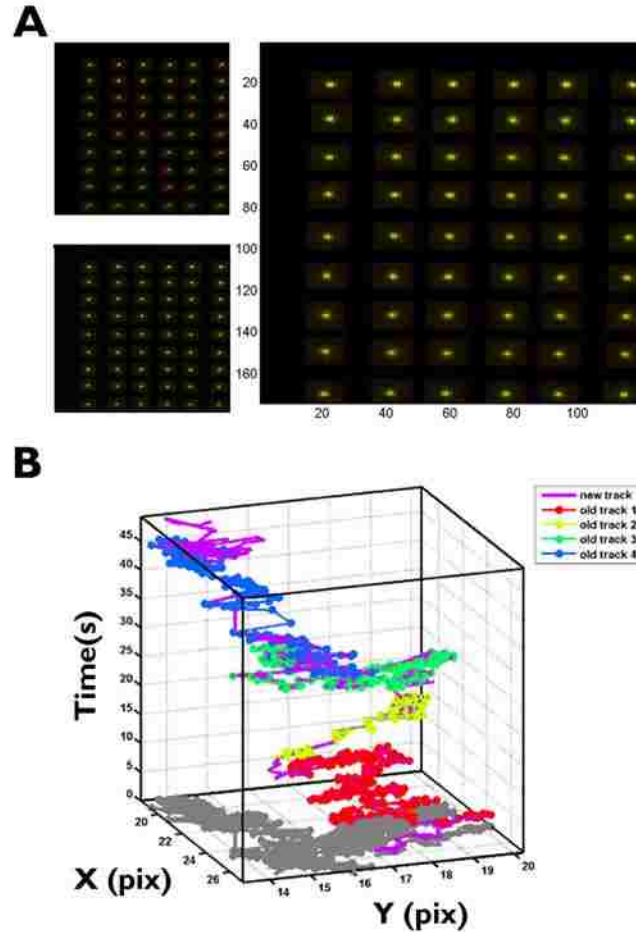
Figure S3.1. Calibration of alignment is performed routinely and optimized track elongation is achieved using spatial and temporal independence. (A) A fiducial calibration series is acquired using the two-channel set-up and is analyzed in order to determine the transformation vector. The subsequent fiducial data series is acquired following data collection and its error can be used to assess drift in the system during the elapsed time. Top left: Raw data; Bottom left: Lateral shift overlay (RMSE = 0.64 pixels = 171 nm); Right: Interpolated overlay (Fiducial registration error = 0.07 pixels = 18.6 nm). (B) A trajectory, shown in purple, from QD-EGF SPT is shown as connected from four shorter tracks, delineated in red, yellow, green, and blue.
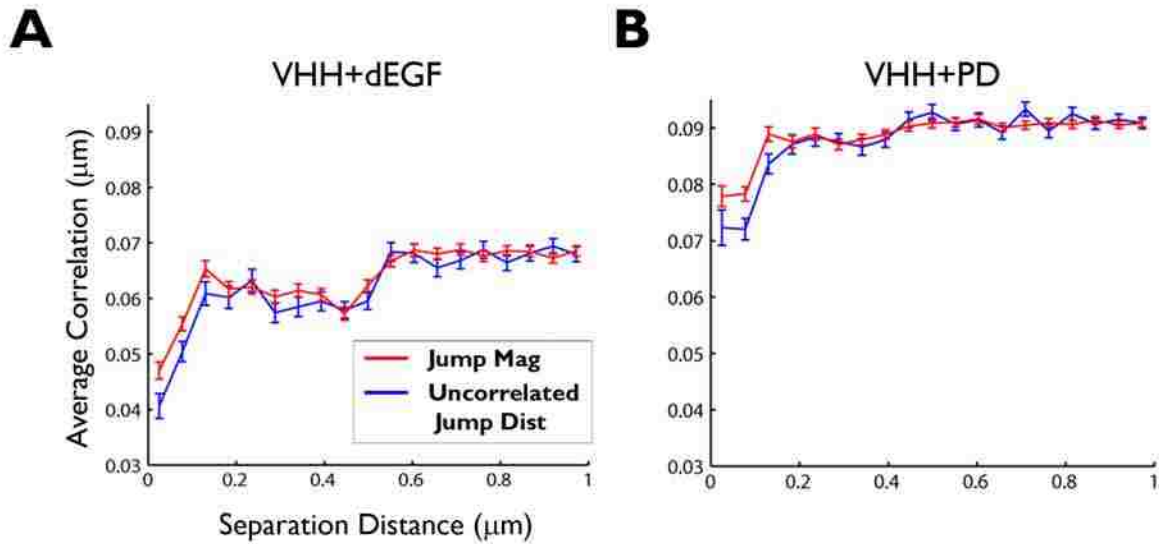
Figure S3.2. Correlated motion analysis of erbB1 shows activation state dependence. Results of correlated motion analyses for VHH + dark EGF (A) and VHH + PD153035 (B) conditions. A decrease in uncorrelated jump distance (blue) at short separations indicates that receptors are moving together. A concurrent drop in jump magnitude (red) demonstrates decreased diffusion. Although there were fewer candidate pairs and dimers observed for QD-VHH + dEGF, non-fluorescent ligand nevertheless induces correlated motion (A). The smaller number of candidate pairs is expected due to the low level of labeling and the saturating levels of ligand, precluding a high frequency of close approach of QD-labeled erbB1 receptors. Interestingly, resting receptors in the presence of the PD153035 inhibitor also showed a degree of correlated motion, even in the absence of ligand (B). These results are consistent with a mechanism for the small molecule drug that confers an intermediate affinity for ligand (9), suggesting a change in the extracellular conformation of erbB1.
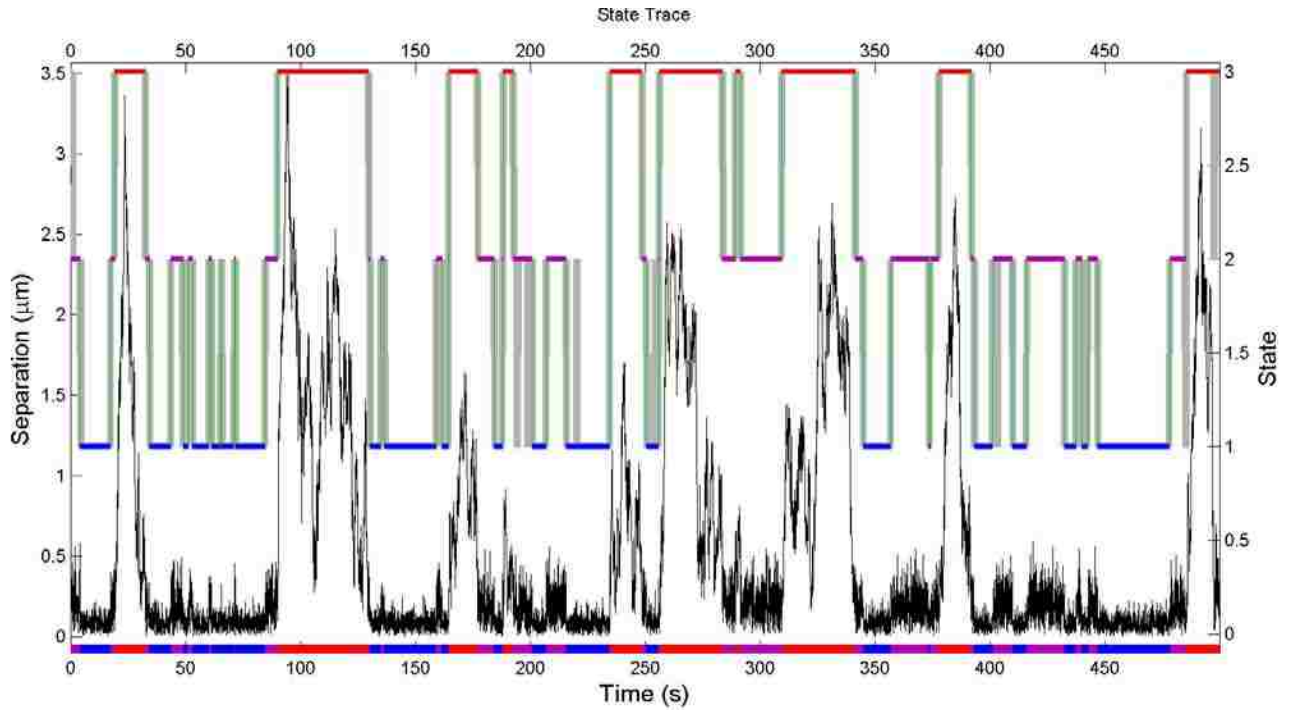
Figure S3.3. HMM analysis of a simulated receptor pair. The observed separation (black) is used to find the transition rate constants. The found rates are then used to find the most likely state at each time point. The found state, dimer, domain, or free are indicated by blue, magenta, and red, respectively. The known underlying state is shown in gray.
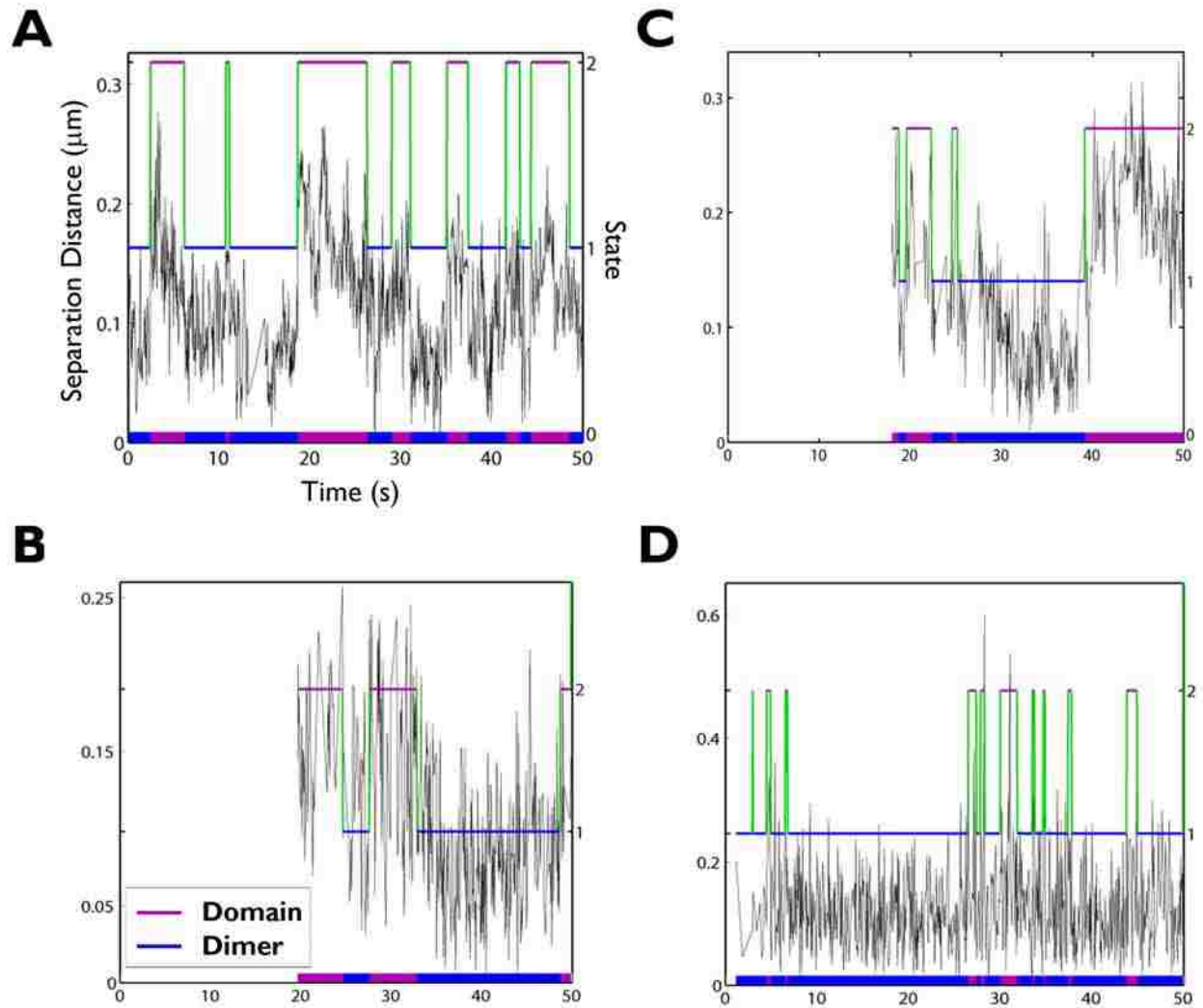
Figure S3.4. ErbB1 receptors experience periods of close approach, punctuated by episodes of separation of up to hundreds of nanometers. (A) and (B) Examples of two-color QD-EGF tracking show dimer events, interrupted periods of larger separation. (C) and (D) Examples of interaction, separation, and return were also detected in other conditions. QD-EGF in the presence of PD153035 and QD-VHH are shown, respectively. Domain (2, purple) and Dimer (1, blue) states are connected by green segments to show the state path. This path is projected onto the x-axis to show the timeline of states explored.
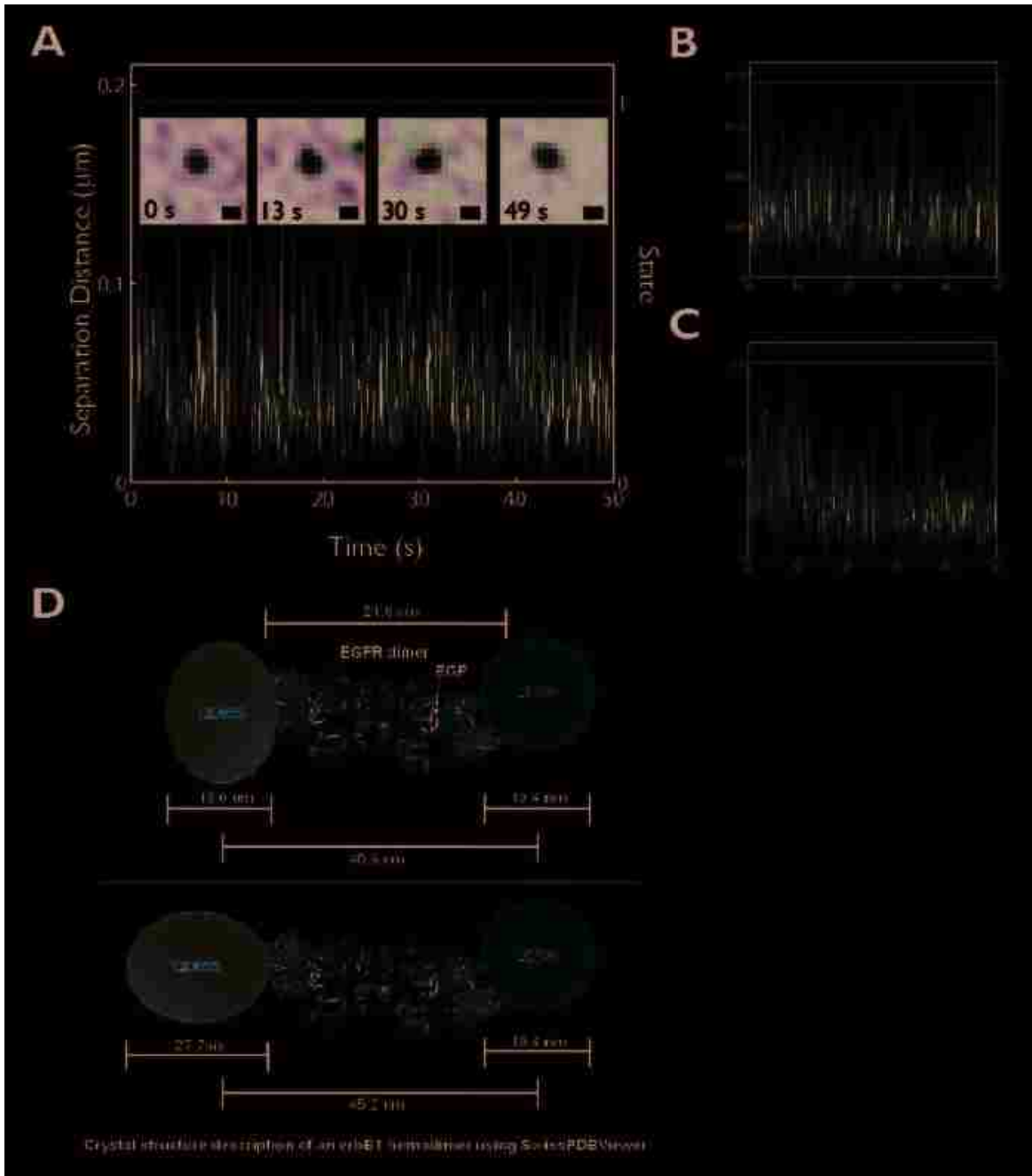
Figure S3.5. Optimized image registration is confirmed using bleedthrough of QD625 signal and permits strict definition of dimer distance. (A) Data collected using an QD625-EGF probe whose fluorescence signal appears simultaneously in both imaging channels demonstrates a "perfect dimer" (stills are inset; scale bar = 0.5 µm). The separation distance is constant over time and does not show the fluctuations observed in two-color tracking data sets. The observed offset of 40-60 nm reflects high precision channel registration; differences were only due to small errors in the single molecule

164

localization of each particle. (B) and (C) Further examples of "perfect dimers" observed using QD625-EGF in the presence of the PD153035 inhibitor show that there is no effect of diffusion or activation state on image registration. (D) The dimer distance is based on the 3.3 Å crystal structure of the erbB1 extracellular domain ligand bound dimer and estimates of QD radii from previous measurements (10,11).
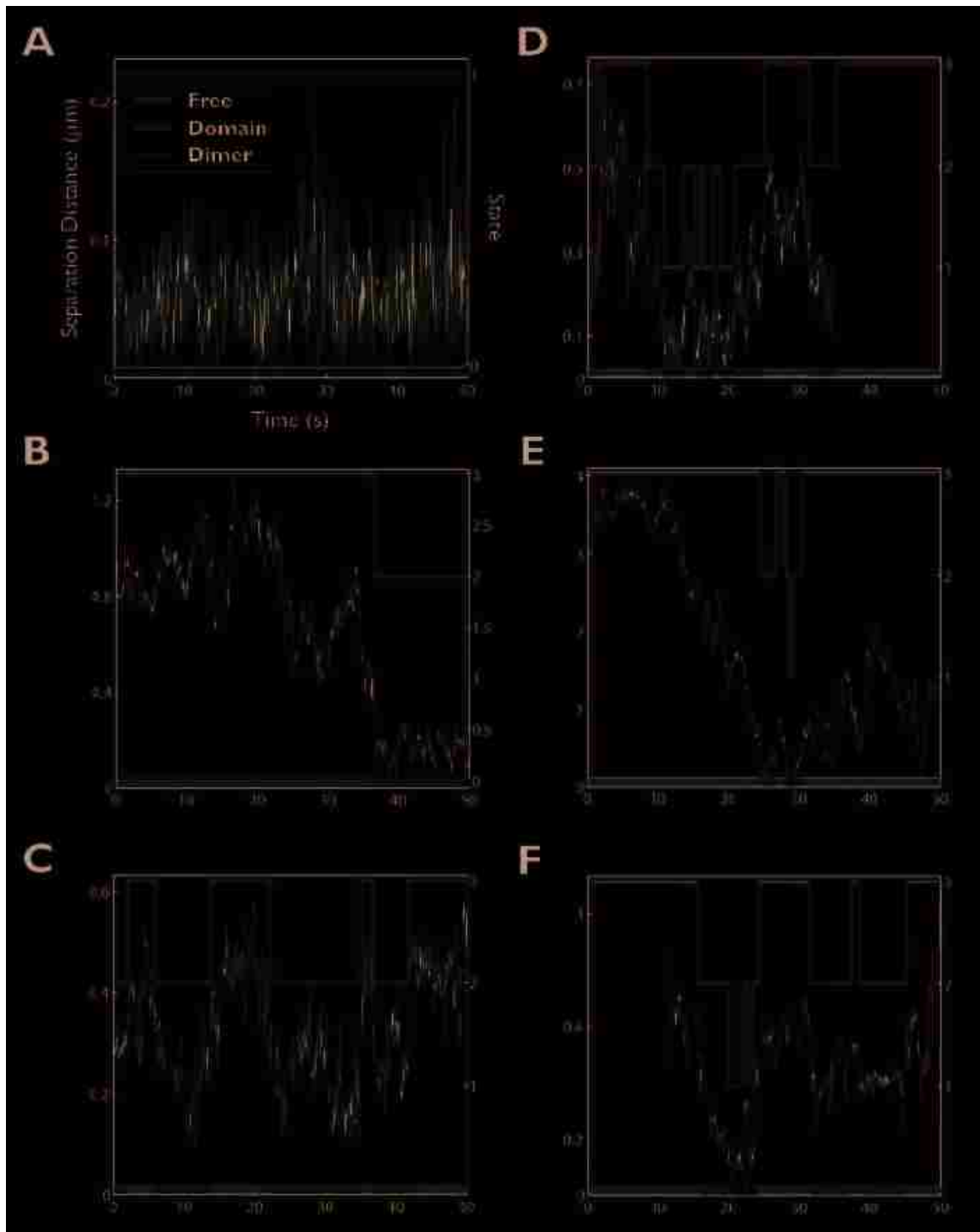
Figure S3.6. State characterization of erbB1 interactions shows formation of resting, activated, and signaling-incompetent homodimers. (A)-(D) Examples of QD-EGF tracking analyzed using the three-state HMM. In panel (B), the dimer that is observed at the end of the acquisition subsequently experiences punctuated interactions, as seen in Figure S9A. (E) and (F): Examples of interactions in other conditions. QD-EGF in the presence of PD153035 and QD-VHH are shown, respectively. Free (red), Domain

(purple) and dimer (1, blue) states are connected by green segments to show the state path. This path is projected onto the x-axis to show the timeline of states explored.

Label	Status of erbB1	D [* 1E-02] (µm^2/s)	95% Confidence Interval ([* 1E-02] µm^2/s)	N
QD-EGF	Activated	3.84	3.83-3.84	397546
QD-EGF +QD-VHH	Ligand bound receptor	3.60	3.60-3.61	93472
QD-VHH +dEGF	Excess ligand	3.97	3.96-3.97	109510
QD-EGF +PD	Ligand bound and inhibited	5.29	5.28-5.29	89223
QD-VHH	Resting	5.10	5.09-5.10	214007
QD-VHH +QD-EGF	Resting receptor	5.57	5.56-5.58	56943
QD-VHH +PD	Inhibited	6.28	6.28-6.28	197059
QD-EGF +QD-VHH	Combined ligand bound and resting receptors	3.85	3.85-3.86	228134

Table S3.1. Single color diffusion measurements of erbB1 under different conditions. Data for each condition shows tracking label (probe tracked in bold), the activation state of the labeled erbB1 receptors, diffusion coefficient (D) of the mobile component, the 95% confidence interval for the mobile component fit, and the number of square jumps used in the fit (N).

Probe	Additional Reagent(s)	Notes	Condition	Free → Dimer	Free → Domain	Domain → Dimer	Domain → Free	Dimer → Domain	Dimer → Free	k dimer off (s-1)
QD-EGF	None	ID=50; DD=**150**	Activated	4.78E-06	5.14E-03	8.45E-03	1.21E-02	1.36E-02	7.94E-13	2.73E-01
				3.02E-06	6.69E-04	9.44E-04	2.93E-04	6.11E-04	2.67E-05	1.22E-2
QD-VHH	None	ID=50; DD=**250**	Resting	3.15E-05	8.26E-03	5.42E-03	1.83E-02	6.19E-02	1.36E-04	1.24E+00
				1.00E-03	1.03E-03	6.49E-03	4.91E-04	6.36E-04	4.65E-05	1.28E-2
QD-EGF	1uM PD153035	ID=50; DD=**200**	Inhibited	1.40E-14	6.28E-03	6.93E-03	2.27E-02	1.22E-02	4.95E-04	2.53E-01
				7.04E-04	2.29E-03	2.41E-03	6.44E-04	1.30E-03	1.80E-06	2.60E-2
QD-VHH	1uM PD153039	ID=50; DD=**250**	Inhibited	3.55E-05	9.36E-03	7.58E-03	2.32E-02	8.32E-02	8.78E-12	1.66E+00
				1.91E-05	1.21E-03	7.60E-03	5.17E-04	7.62E-04	5.55E-05	1.53E-2
QD-EGF + QD-VHH	None	ID=50; DD=**250**	Activated and Resting	9.97E-15	6.13E-03	2.91E-03	8.74E-03	1.37E-02	2.32E-02	7.38E-01
				8.91E-03	7.22E-04	2.19E-03	4.97E-04	4.38E-04	1.45E-06	8.76E-3

Table S3.2. Three-state HMM fitting results. Domain size and HMM kinetic rates change by condition. Condition reflects the state of the erbB1 receptors that are being tracked by the probes, shown in bold. Transition rates are shown in units of frames^{-1}. The value of k dimer off is the sum of the transitions from dimer-to-domain and dimer-to-free. Error in fits is shown in red.

Free State

Label	Status of erbB1	D [* 1E-02] (µm^2/s)	95% Confidence Interval ([* 1E-02] µm^2/s)	N
QD-EGF	Activated	3.90	3.9-3.91	382897
QD-EGF **+QD-VHH**	Ligand bound receptor	3.12	3.12-3.12	168345
QD-VHH **+dEGF**	Excess ligand	4.00	3.99-4.00	107039
QD-EGF **+PD**	Ligand bound and inhibited	5.33	5.32-5.33	87117
QD-VHH	Resting	5.12	5.11-5.12	208720
QD-VHH **+QD-EGF**	Resting receptor	5.63	5.62-5.63	54414
QD-VHH **+PD**	Inhibited	6.32	6.31-6.32	191133

Domain State

Label	Status of erbB1	D [* 1E-02] (µm^2/s)	95% Confidence Interval ([* 1E-02] µm^2/s)	N
QD-EGF	Activated	1.99	1.98-2.00	8628
QD-EGF **+QD-VHH**	Ligand bound receptor	2.41	2.38-2.44	2361
QD-VHH **+dEGF**	Excess ligand	2.59	2.55-2.63	2080
QD-EGF **+PD**	Ligand bound and inhibited	4.23	4.15-4.30	1372
QD-VHH	Resting	4.32	4.30-4.34	4683
QD-VHH **+QD-EGF**	Resting receptor	3.94	3.91-3.97	2375
QD-VHH **+PD**	Inhibited	5.25	5.23-5.27	5345

Dimer State

Label	Status of erbB1	D [* 1E-02] (µm^2/s)	95% Confidence Interval ([* 1E-02] µm^2/s)	N
QD-EGF	Activated	0.563	0.555-0.571	6021
QD-EGF **+QD-VHH**	Ligand bound receptor	0.777	0.729-0.825	485
QD-VHH **+dEGF**	Excess ligand	0.977	0.822-1.13	391
QD-EGF **+PD**	Ligand bound and inhibited	1.91	1.88-1.94	734
QD-VHH	Resting	3.88	3.84-3.94	604
QD-VHH **+QD-EGF**	Resting receptor	1.80	1.58-2.01	154
QD-VHH **+PD**	Inhibited	4.18	3.74-4.63	581

Table S3.3. State-dependent diffusion of erbB1 by condition demonstrates slowing upon entering domain and dimerization. Data for each condition shows tracking label (probe tracked in bold), the activation state of the labeled erbB1, diffusion coefficient (D)

168

of the mobile component, the 95% confidence interval for the mobile component fit, and the number of square jumps used in the fit (N).

Supporting Movies

Movie 3.1. Formation of a QD-EGF ligand bound 2:2 erbB1 homodimer that approaches, interacts, and remains together for the remainder of the acquisition. This movie accompanies the interaction shown in Fig. 3.2A and 3.2B and the state trace and stills in Fig. 3.4B. The coordinate for each single molecule fit is shown as a green (QD585) or magenta circle (QD655) within the fluorescent spot. A colored tail for each particle shows a track of the previous 15 coordinates. The final frame shows the entire trajectory for each receptor of interest. Movies have been Gaussian filtered (sigma = 0.7) and contrast enhanced. Playback speed is 40 frames per second (fps) and is equivalent to 2 times real time.

Movie 3.2. A short lived resting 1:1 erbB1 homodimer visualized using two-color QD-VHH. The movie corresponds to the state trace shown in Fig. S3.6F. Color scheme, comet tail, filtering, and payback speed are as previously mentioned for Movie 3.1.

Movie 3.3. Formation of a ligand bound 2:2 erbB1 homodimer. The movie corresponds to the state trace shown in Fig. S3.6B. Notice that the two receptors remain separated for the majority of the movie, before initial overlap of the signals. Color scheme, comet tail, filtering, and payback speed are as previously mentioned for Movie 3.1.

Movie 3.4. Continued observation of the dimer formed in Movie 3.3 shows ligand bound erbB1 receptors that experience periods of separation and return. Notice that sustained spectral overlap is not apparent and magenta and green signals can be distinguished as the receptors diffuse. Color scheme, comet tail, filtering, and payback speed are as previously mentioned for Movie 3.1.

Movie 3.5. A long lived QD-EGF labeled 2:2 erbB1 homodimer that persists for the entire 50 second acquisition. The movie corresponds to the state trace shown in Fig. S3.6A. Color scheme, comet tail, filtering, and payback speed are as previously mentioned for Movie 3.1.

Movie 3.6. Interactions between QD-EGF labeled receptors in the presence of 1 mM PD153035. The movie corresponds to the state trace shown in Fig. S3.6E. Notice the

large region explored by the green receptor, in particular, and the very brief spectral overlap toward the end of the sequence. Color scheme, comet tail, filtering, and payback speed are as previously mentioned for Movie 3.1.

APPENDIX D – MATLAB SCRIPTS AND FUNCTIONS

```
%Dissertation Appendix
%MatLab scripts and functions for SPT analyses
%Shalini Low-Nam

%The scripts and functions contained in this appendix were principally written by S.
Low-Nam, P. Cutler, and K. Lidke. Many components of this code reflect the effort of
multiple authors and are the subject of ongoing edits. This code represents the state of
analyses at the time of the publication of this dissertation. Author contributions are
documented for most functions.

%Example: EGF analysis for A431 cells data
%%
%% Tracking

% Create tracking and saving directories (change these each time)
topdir='Z:\Shal\SPT Data\GroupedData_A431_Final';
saveDir = [topdir '\HMM Final\HMM EGF\'];
figDir = [saveDir 'figures\'];

mkdir(saveDir)
mkdir(figDir)

%%Link Data to create HMM_Data structure
%%Each structure contains paths to raw data, calibration files, etc
%%Results from later analyses can be appended onto the structure`
clear all
close all

%Folders of raw data
topdir='Z:\Shal\SPT Data\GroupedData_A431_Final';
saveDir = [topdir '\HMM Final\HMM EGF\'];
figDir = [saveDir 'figures\'];
condition = 'QD EGF';
fileCondition = 'EGF';
datadir{1}=[topdir '\EGF\091214\Chamber3\'];
datadir{2}=[topdir '\EGF\091214\Chamber4\'];
datadir{3}=[topdir '\EGF\091214\Chamber5\'];
datadir{4}=[topdir '\EGF\091216\Chamber1\'];
datadir{5}=[topdir '\EGF\091216\Chamber3\'];
datadir{6}=[topdir '\EGF\100611\Chamber1\'];
datadir{7}=[topdir '\EGF\100611\Chamber2\'];
datadir{8}=[topdir '\EGF\100614\Chamber1\'];

count = 0;
```

```matlab
for jj = 1:length(datadir)
    Files=dir([datadir{jj} fileCondition '*.mat']);
    bgFile = dir([datadir{jj} 'Background-*.mat']);
    bgn = [datadir{jj} bgFile.name];
    bdFile = dir([datadir{jj} 'Beads*.mat']);
    bdn = [datadir{jj} bdFile.name];
    bdAlignFiles = dir([datadir{jj} 'fiducial-*.mat']);
    bdAlign = [datadir{jj} bdAlignFiles(1).name];
    bdAlign1 = [datadir{jj} bdAlignFiles(2).name];
    for ii=1:size(Files,1)
        fn=[datadir{jj} Files(ii).name];
        disp(fn)
        try
            HMM_Data(ii)                                         = 
HMM_LinkData(topdir,saveDir,figDir,fn,bgn,bdAlign,bdAlign1,bdn,0.266667,0.05,[1 
1],condition);
        catch ME
            count = count+1;
            HMM_Error(count).ME = ME;
            HMM_Error(count).fileNum = ii;
            save([saveDir 'HMM_Error.HMM_Error'],'HMM_Error')
        end
    end
end

%%Tracking script:
clear all
close all

%Create parameters for tracking and use SPTracking (Smith, et al., Nature Methods
2009)
topdir='Z:\Shal\SPT Data\GroupedData_A431_Final';
saveDir = [topdir '\HMM Final\HMM EGF\'];

psf1 = 0.7382;
psf2 = 0.7021;
D = 0.05;
MinPhotons1 = 100;
MinPhotons2 = 100;
MinTrackLength = 10;
MaxJump = 10;
MaxTjump = 20;
cutoff1 = 0.1;
cutoff2 = 0.1;
iDiv = -1.5;
cmaxjump = 10;
```

172

```matlab
cmaxTjump = 40;
coverlap = 5;
cpValue = 0.01;
cnstd = 4;
cplotflag = 0;

HMM_Params = HMM_CreateParams([psf1 psf2],D,[MinPhotons1 MinPhotons2],...
    MinTrackLength,MaxJump,MaxTjump,cutoff1,cutoff2,iDiv,cmaxjump,cmaxTjump,...
    coverlap,cpValue,cnstd,[saveDir 'Params.HMMParams']);

Files=dir([saveDir '*.HMMData']);
if exist([saveDir 'HMM_Error.HMM_Error'],'file')
    load([saveDir 'HMM_Error.HMM_Error'],'-mat')
    count = length(HMM_Error);
else
    count = 0;
end
save([saveDir 'tempFiles'])
for ii=1:size(Files,1)
    try
        close all
        clear HMM_Data
        fn=[saveDir Files(ii).name]
        disp('making short tracks')
        HMM_Data = HMM_Track(fn,[saveDir '\Params.HMMParams']);
        close all
        save(fn,'HMM_Data')
    catch ME
        count = count+1;
        HMM_Error(count).ME = ME;
        HMM_Error(count).fileNum = ii;
        disp(Files(HMM_Error(count).fileNum).name);
        disp(getReport(HMM_Error(count).ME));
        save([saveDir 'HMM_Error.HMM_Error'],'HMM_Error')
        close all
        clear all
        topdir='Z:\Shal\SPT Data\GroupedData_A431_Final';
        saveDir = [topdir '\HMM Final\HMM EGF\'];
        load([saveDir 'tempFiles'])
        load([saveDir 'HMM_Error.HMM_Error'],'-mat')
        count = length(HMM_Error);
    end
end

function varargout = HMM_LinkData(varargin)
% HMM_LinkData  create HMM_Data file for HMM_Track
```

```
%
% HMM_Data = HMM_LinkData(topdir,saveDir,figDir,DataFile,bgn,bdAlign,bdAlign1,...
%          bdn,pixelSize,TimeStep,ch_bin,condition);
%
% INPUTS
%   TreeDir - main directory SaveDir, FigDir, DataFile, and all ather
%           associated files must be within TreeDir or a subfolder of
%           TreeDir
%   SaveDir - directory in which to save HMM_Data file
%   FigDir - directory in which to save resultant figures
%   DataFile - raw data file
%   BGfile - file containing backgroud sequence
%   Bead_Align - file containing pre experiment fiducial data
%   Bead_Align1 - file containing post experiment fiducial data
%   Bead_Gain - file containing gain calibration sequence of beads
%   PixelSize - size of pixels in image (microns). Default 0.266667.
%   TimeStep - time between each frame. Default 0.01
%   ch_bin - binary vector corresponding to channels (length 1,2 or 4).
%           Default [1 1].
%   DataConditions - string with on of the conditions defined on the first
%               line of HMM_LinkData code. Indicates experimental treatment.
% OUTPUTS
%   HMM_Data - HMM_Data structure. Data structure also saved in
%           HMM_DataFile
%
% see also HMM_CreateParams and HMM_Track

conditions ={'QD EGF','QD Nanobody','QD EGF + PD','QD Nanobody + PD',...
    'QD Nanobody + dEGF','QD Nanobody + dEGF + PD','QD EGF + dEGF',...
    'QD EGF + dEGF + PD','QD EGF + QD VhH','QD EGF + QD VhH + PD','QD EGF +
    PFA','QD Neu','Sim','QD625','QD rH'};

d = struct('menu','HMM',...
    'display','HMM Link Data',...

'inparams',struct('name',{'TreeDir','Save_Dir','Fig_Dir','DataFile','BGFile','Bead_Align','Bead_Align2','Bead_Gain','PixelSize','TimeStep','ch_bin','DataConditions'},...
    'description',{'Top Tree Directory','Save Directory','Figure Directory','Raw Data File','Background File',...
    'Bead Alignment File Before','Bead Alignment File After','Bead Gain File','PixelSize','TimeStep','binary vector corresponding to channels (length 1,2 or 4)','Data Conditions'},...
    'type',
{'indir','indir','indir','infile','infile','infile','infile','infile','array','array','array','option'},...
    'dim_check',  {0,0,0,0,0,0,0,0,0,0,{[1 1],[1 2],[1 4]},0},...
    'range_check',{'*.*','*.*','*.mat','*.mat','*.mat','*.mat','*.mat','*.mat',[],[],[],conditions},...
```

```matlab
    'required',    {0,0,0,0,0,0,0,0,0,0,0,0},...
    'default',     {'','','','','','','','',16/60,.01,[1 1],conditions{1}}...
    ),...
    'outparams',struct('name',{'HMM_Data'},...
    'description',{'HMM Data Structure'},...
    'type',{'strct'}...
    )...
    );
if nargin == 1
    s = varargin{1};
    if ischar(s) & strcmp(s,'DIP_GetParamList')
        varargout{1} = d;
        return
    end
end
try
    [TreeDir, SaveDir, FigDir , DataFile , BGFile , Bead_Align , Bead_Align1 , Bead_Gain
,PixelSize,TimeStep, ch_bin, DataConditions ] = getparams(d,varargin{:});
catch
    if ~isempty(paramerror)
        error(paramerror)
    else
        error(firsterr)
    end
end
```

```matlab
%% Parse Inputs
n=size(TreeDir,2)-1;
HMM_Data.TreeDir=TreeDir;
if ~strcmp(TreeDir(end),'\')
    HMM_Data.TreeDir=[TreeDir '\'];
end
HMM_Data.DataFile=DataFile(n+2:end);
HMM_Data.BGFile=BGFile(n+2:end);
HMM_Data.Bead_Align=Bead_Align(n+2:end);
HMM_Data.Bead_Align1=Bead_Align1(n+2:end);
HMM_Data.SaveDir=SaveDir;
if ~strcmp(SaveDir(end),'\')
    HMM_Data.SaveDir=[SaveDir '\'];
end
HMM_Data.FigDir=FigDir;
if ~strcmp(FigDir(end),'\')
    HMM_Data.FigDir=[FigDir '\'];
end
HMM_Data.Bead_Gain=Bead_Gain(n+2:end);
HMM_Data.PixelSize=PixelSize;
```

175

```matlab
HMM_Data.TimeStep=TimeStep;
HMM_Data.ch_bin=ch_bin;
HMM_Data.DataConditions=DataConditions;
HMM_Data.Dconvert = 1/PixelSize^2*TimeStep;

%% Calculate Gain and Background
% Performed in HMM_Track using GainBGCorrectFile  PJC 03/19/10

% maxframes=20;
% bg=load([HMM_Data.TreeDir HMM_Data.BGFile]);
% gain=load([HMM_Data.TreeDir HMM_Data.Bead_Gain]);
%       out      =        cal_readnoise(gain.sequence(:,:,0:min([size(gain.sequence,3)
maxframes])),bg.sequence,100,-1,0);
%
% close all
% HMM_Data.BGImage=mean(bg.sequence,[],[3]);
% HMM_Data.CCDGain=out(2);
% clear bg gain

%% Calculate Shift
% align=load([HMM_Data.TreeDir HMM_Data.Bead_Align]);
if sum(HMM_Data.ch_bin) == 1
    HMM_Data.tform = [];
else
    options=set_im_transformOptions;
    options = set_im_transformOptions(options,'meritcutoff',.9);
    [ostd,tform]                    =                    chOverlaySTD([HMM_Data.TreeDir
HMM_Data.Bead_Align],[HMM_Data.TreeDir
HMM_Data.Bead_Align],HMM_Data.ch_bin,options);
    % tform = im_transform_gauss(align.trn,options);
    % options=set_im_transformOptions(options,'tform');
    HMM_Data.tform=tform;
    temp = findstr('\',HMM_Data.Bead_Align);
    if isempty(temp)
        temp=0;
    end
    saveas(1,[HMM_Data.FigDir HMM_Data.Bead_Align(temp(end)+1:end-4)],'fig')
    saveas(1,[HMM_Data.FigDir HMM_Data.Bead_Align(temp(end)+1:end-4)],'png')
    saveas(2,[HMM_Data.FigDir HMM_Data.Bead_Align1(temp(end)+1:end-4)],'fig')
    saveas(2,[HMM_Data.FigDir HMM_Data.Bead_Align1(temp(end)+1:end-4)],'png')
    close all
end
%% Write output
tmp=max(strfind(HMM_Data.DataFile,'\'));
if isempty(tmp) tmp=0; end
    tmp=tmp+1;
```

176

```matlab
save([HMM_Data.SaveDir HMM_Data.DataFile(tmp:end-4) '.HMMData'] , 'HMM_Data');

varargout{1}=HMM_Data;

function varargout = HMM_CreateParams(varargin)
% HMM_CreateParams  create HMM_Params file for HMM_Track
%
%                              HMM_Params                                  =
HMM_CreateParams(GPUSPT_PSF,GPUSPT_Dest,GPUSPT_MinPhotons,...
%    GPUSPT_MinTrackLength,GPUSPT_MaxJump,GPUSPT_MaxTimeJump,...
%    GPUSPT_Cutoff1,GPUSPT_Cutoff2,GPUSPT_iDiv,CONNECT_MaxJump,...
%    CONNECT_MaxTimeJump,CONNECT_Overlap,CONNECT_Cutoff,...
%    CONNECT_nstd,HMM_Param_File);
%
% INPUTS
%  GPUSPT_PSF - vector of sigmas for all channels. Default [1 1].
%          (psfsigma input for GPUSPT)
%  GPUSPT_Dest - estimated diffusion coefficient um^2/s. Default 0.05.
%           (D input for GPUSPT)
%  GPUSPT_MinPhotons - vector of min photons allowed for each channel.
%               Default [100 100]. (Ncutoff for GPUSPT)
%  GPUSPT_MinTrackLength - minimum number of coordinates for a good track.
%               (goodframes input for GPUSPT)
%  GPUSPT_MaxJump - max spatial (pixel) jump between 'on' frames.
%           Default 10. (maxjump input for GPUSPT)
%  GPUSPT_MaxTimeJump - maximum allowed 'off' frames. Default 20.
%            (maxTjump input for GPUSPT)
%  GPUSPT_Cutoff1 - initial diffusion cutoff. Default 0.1. (diffcutoff1
%           input for GPUSPT)
%  GPUSPT_Cutoff2 - secondary diffusion cutoff. Default 0.1. (diffcutoff2
%           input for GPUSPT)
%  GPUSPT_iDiv - minimum acceptace of particle for log likelihood value.
%           Default -1. (iDiv input for GPUSPT)
%  CONNECT_MaxJump - max spatial (pixel) jump between 'on' frame. Default 10.
%            (maxjump input for connectTracks)
%  CONNECT_MaxTimeJump - maximum allowed 'off' frames. Default 40.
%             (maxTjump input for connectTracks)
%  CONNECT_Overlap - temporal overlap allowed. Default 5. (overlap input
%            for connectTracks)
%  CONNECT_Cutoff - diffusion cutoff. Default 0.01. (input for connectTracks)
%  CONNECT_nstd - number of standard deviations to use in connecting
%           tracks. Default 4. (nstd input for connectTracks)
%  HMM_Param_File - file in which to save HMM_Params structure.
% OUTPUTS
%  HMM_Params - HMM_Params structure. HMM_Params structure also saved in
%        HMM_Param_File
```

```
%
% Note: for testing or simple usage HMM_Param_File can be set to [cd
'\Params.HMMParams']
%
% see also GPUSPT, HMM_LinkData, and HMM_Track

%updated by Pat Cutler 4/1/10 for ability to handle 1,2, or 4 ch data

d = struct('menu','HMM',...
    'display','HMM Create Parameter Set',...
    'inparams',struct('name',{'GPUSPT_PSF','GPUSPT_Dest','GPUSPT_MinPhotons',...

'GPUSPT_MinTrackLength','GPUSPT_MaxJump','GPUSPT_MaxTimeJump','GPUSPT_
Cutoff1',...

'GPUSPT_Cutoff2','GPUSPT_iDiv','CONNECT_MaxJump','CONNECT_MaxTimeJump','
CONNECT_Overlap',...
    'CONNECT_Cutoff','CONNECT_nstd','HMM_Param_File'},...
    'description',{'GPUSPT_PSF','GPUSPT_Dest','GPUSPT_MinPhotons',...

'GPUSPT_MinTrackLength','GPUSPT_MaxJump','GPUSPT_MaxTimeJump','GPUSPT_
Cutoff1',...

'GPUSPT_Cutoff2','GPUSPT_iDiv','CONNECT_MaxJump','CONNECT_MaxTimeJump','
CONNECT_Overlap',...
    'CONNECT_Cutoff','CONNECT_nstd','HMM_Param Output File'},...
    'type',      {'array','array','array','array','array','array','array','array',...
    'array','array','array','array','array','array','outfile'},...
    'dim_check',  {{[1 1],[1 2],[1 4]},0,{[1 1],[1 2],[1 4]},0,0,0,0,0,0,0,0,0,0,0,0},...
    'range_check',{[],[],[],[],[],[],[],[],[],[],[],[],[],[],'*.HMMParams'},...
    'required',   {0,0,0,0,0,0,0,0,0,0,0,0,0,0,0},...
    'default',    {[1 1],.05,[100 100],10,10,20,.1,.1,-1,10,40,5,0.01,4,''}...
    ),...
    'outparams',struct('name',{'HMM_Params'},...
    'description',{'HMM Parameter Structure'},...
    'type',{'strct'}...
    )...
    );
if nargin == 1
    s = varargin{1};
    if ischar(s) & strcmp(s,'DIP_GetParamList')
        varargout{1} = d;
        return
    end
end
try
```

178

```matlab
   [GPUSPT_PSF,GPUSPT_Dest,GPUSPT_MinPhotons,...

GPUSPT_MinTrackLength,GPUSPT_MaxJump,GPUSPT_MaxTimeJump,GPUSPT_Cu
toff1,...

GPUSPT_Cutoff2,GPUSPT_iDiv,CONNECT_MaxJump,CONNECT_MaxTimeJump,CO
NNECT_Overlap,...
   CONNECT_Cutoff,CONNECT_nstd,HMM_Param_File] = getparams(d,varargin{:});
catch
   if ~isempty(paramerror)
      error(paramerror)
   else
      error(firsterr)
   end
end


HMM_Params.GPUSPT_PSF=GPUSPT_PSF;
HMM_Params.GPUSPT_Dest=GPUSPT_Dest;
HMM_Params.GPUSPT_MinPhotons=GPUSPT_MinPhotons;
HMM_Params.GPUSPT_MinTrackLength=GPUSPT_MinTrackLength;
HMM_Params.GPUSPT_MaxJump=GPUSPT_MaxJump;
HMM_Params.GPUSPT_MaxTimeJump=GPUSPT_MaxTimeJump;
HMM_Params.GPUSPT_Cutoff1=GPUSPT_Cutoff1;
HMM_Params.GPUSPT_Cutoff2=GPUSPT_Cutoff2;
HMM_Params.GPUSPT_iDiv=GPUSPT_iDiv;
HMM_Params.CONNECT_MaxJump=CONNECT_MaxJump;
HMM_Params.CONNECT_MaxTimeJump=CONNECT_MaxTimeJump;
HMM_Params.CONNECT_Overlap=CONNECT_Overlap;
HMM_Params.CONNECT_Cutoff=CONNECT_Cutoff;
HMM_Params.CONNECT_nstd=CONNECT_nstd;
save(HMM_Param_File,'HMM_Params');

varargout{1}=HMM_Params;

function varargout = HMM_Track(varargin)
% HMM_TRACK  track data in linked in HMM_Data using HMM_Params
%
% HMM_Data = HMM_Track(HMM_DataFile,HMM_ParamsFile);
%
% INPUTS
%   HMM_DataFile - name of HMM_Data file. Created using HMM_LinkData
%   HMM_ParamsFile - name of HMM_Params file. Created using HMM_CreateParams
% OUTPUTS
%   HMM_Data - HMM_Data structure. Data structure also saved in
%           HMM_DataFile
%
```

```matlab
% see also HMM_LinkData and HMM_CreateParams


% updated by Pat Cutler 4/1/10 for ability to handle 1,2, or 4 ch data
% !!!point transformation is no longer performed within this function!!!
% changed by Shalini Low-nam 08/40/2010 so that all HMM functions are
% consistent: transformation done within this function (not done in SPTData
% functions)

d = struct('menu','HMM',...
    'display','HMM Track Data',...
    'inparams',struct('name',{'HMM_Data','HMM_Params'},...
    'description',{'HMM Data File','HMM Parameter File'},...
    'type',      {'infile','infile'},...
    'dim_check',  {0,0},...
    'range_check',{'*.HMMData','*.HMMParams'},...
    'required',   {0,0},...
    'default',    {'',''}...
    ),...
    'outparams',struct('name',{'HMM_Data'},...
    'description',{'Modified HMM Data Structure'},...
    'type',{'strct'}...
    )...
    );
if nargin == 1
    s = varargin{1};
    if ischar(s) & strcmp(s,'DIP_GetParamList')
        varargout{1} = d;
        return
    end
end
try
    [HMM_Data,HMM_Params] = getparams(d,varargin{:});
catch
    if ~isempty(paramerror)
        error(paramerror)
    else
        error(firsterr)
    end
end

%% Load, Split and Background, Gain correct
load(HMM_Data,'-mat');
load(HMM_Params,'-mat');

% Usage of GainBGCorrectFile updated  PJC 03/19/10
```

```matlab
% rawdata=load([HMM_Data.TreeDir HMM_Data.DataFile]);
%
% try
%     bgim=HMM_Data.BGImage;
% catch
% bg=load([HMM_Data.TreeDir HMM_Data.BGFile]);
% bgim=mean(bg.sequence,[],[3]);
% end
% s=GainBGCorrect(rawdata.sequence,bgim,HMM_Data.CCDGain);

if strcmp(HMM_Data.DataConditions,'Sim')
    temp=load([HMM_Data.TreeDir HMM_Data.DataFile]);
    s=temp.sequence;
    clear temp
else
    s=                                         GainBGCorrectFile([HMM_Data.TreeDir
HMM_Data.DataFile],[HMM_Data.TreeDir  HMM_Data.Bead_Gain],[HMM_Data.TreeDir
HMM_Data.BGFile]);
end

close all

if length(HMM_Data.ch_bin) == 2
[ch{1},ch{2}] = splitImage(s,5,HMM_Data.ch_bin,0);
else if length(HMM_Data.ch_bin) == 4
    [ch{1},ch{2},ch{3},ch{4}] = splitImage4ch(s,5,0);
  else
    ch{1} = s;
  end
end
```

%% Tracking

```matlab
HMM_Params;

D=HMM_Params.GPUSPT_Dest;
PSF=HMM_Params.GPUSPT_PSF;
iDiv=HMM_Params.GPUSPT_iDiv;
GF=HMM_Params.GPUSPT_MinTrackLength;
Psz=HMM_Data.PixelSize;
TS=HMM_Data.TimeStep;
MaxJ=HMM_Params.GPUSPT_MaxJump;
MaxTJ=HMM_Params.GPUSPT_MaxTimeJump;
mask=0;
Nc=HMM_Params.GPUSPT_MinPhotons;
```

```matlab
dc1=HMM_Params.GPUSPT_Cutoff1;
dc2=HMM_Params.GPUSPT_Cutoff2;
srange=[.5 1.5];

idx = find(HMM_Data.ch_bin);
for ii = idx
    clear GPUgaussMLE connectcoords
    disp(['making short tracks ch' num2str(ii)])
    %%June 1, 2010; call GPUSPT_sigma to get out sigma at each coordinate
    [tracks,intensities,valids,LL,LA,Sigma] = GPUSPT_sigma(ch(Paez et al.),...

D,PSF(ii),HMM_Params.GPUSPT_iDiv,GF,Psz,TS,MaxJ,MaxTJ,mask,Nc(ii),dc1,dc2,sr
ange);
    disp(['connecting short tracks ch' num2str(ii)])
    [tracks,LA,intensities,Sigma] = connectTracks(tracks,LA,intensities,Sigma,...

HMM_Params.GPUSPT_Dest*HMM_Data.Dconvert,HMM_Data.TimeStep,HMM_Para
ms.CONNECT_MaxJump,...

HMM_Params.CONNECT_MaxTimeJump,HMM_Params.CONNECT_Overlap,...
        HMM_Params.CONNECT_Cutoff,HMM_Params.CONNECT_nstd,0);
    valids = logical(tracks(:,:,1));
%     intensities(~valids) = 0;
%   [ch1_tracks,ch1_intensities,ch1_valids,ch1_iDiv,ch1_LA,co1] = GPUSPT(ch1,...
%       D,PSF,iDiv,GF,Psz,TS,MaxJ,MaxTJ,mask,Nc,dc1,dc2,srange);
    eval(['HMM_Data.raw_ch' num2str(ii) '_tracks=tracks;'])
    eval(['HMM_Data.ch' num2str(ii) '_intensities=intensities;'])
    eval(['HMM_Data.ch' num2str(ii) '_valids=valids;'])
    eval(['HMM_Data.ch' num2str(ii) '_LA=LA;'])
    eval(['HMM_Data.ch' num2str(ii) '_sigma=Sigma;'])
%     if length(size(LA))==3
%         eval(['HMM_Data.ch' num2str(ii) '_LA=LA(:,:,1);'])
%     else
%         eval(['HMM_Data.ch' num2str(ii) '_LA=0;'])
%     end
    close all
end
plotHMM_Data(HMM_Data,1);
% PSF=HMM_Params.GPUSPT_PSF_R; %%August 4 - What are these?
% Nc=HMM_Params.GPUSPT_MinPhotons_R;

clear GPUgaussMLE connectcoords

% [raw_ch2_tracks,ch2_intensities,ch2_valids,ch2_iDiv,ch2_LA] = GPUSPT(ch2,...
%     D,PSF,iDiv,GF,Psz,TS,MaxJ,MaxTJ,mask,Nc,dc1,dc2,srange);
% [ch2_tracks,ch2_intensities,ch2_valids,ch2_iDiv,ch2_LA,co2] = GPUSPT(ch2,...
```

```matlab
%      D,PSF,iDiv,GF,Psz,TS,MaxJ,MaxTJ,mask,Nc,dc1,dc2,srange);

close all

% co1
% co2
% HMM_Data.ch1_tracks=ch1_tracks;
%
% HMM_Data.raw_ch1_tracks=ch1_tracks;
% HMM_Data.ch1_intensities=ch1_intensities;
% HMM_Data.ch1_valids=ch1_valids;
% HMM_Data.ch1_coloroverlay=co1; %Shal

% if length(size(HMM_Data.ch1_LA))==3 %check
%     HMM_Data.ch1_LA=HMM_Data.ch1_LA(:,:,1);
% else
%     HMM_Data.ch1_LA=0;
% end

for jj=1:size(HMM_Data.raw_ch2_tracks,1)
   Rxch2=HMM_Data.raw_ch2_tracks(jj,:,1)';
   Rych2=HMM_Data.raw_ch2_tracks(jj,:,2)';
   [x y]=point_transform(Rxch2,Rych2,HMM_Data.tform);
   x(~HMM_Data.ch2_valids(jj,:)) = 0;
   y(~HMM_Data.ch2_valids(jj,:)) = 0;
   HMM_Data.shifted_ch2_tracks(jj,:,:)=[x y]; % this might need re-arrangement
end

% HMM_Data.shifted_ch2_tracks=s_ch2_tracks;
% HMM_Data.ch2_intensities=ch2_intensities;
% HMM_Data.ch2_valids=ch2_valids;
%HMM_Data.ch2_coloroverlay=co2; %Shal

% length(size(HMM_Data.ch2_LA)) %check
% pause
% if length(size(HMM_Data.ch2_LA))==3
%     HMM_Data.ch2_LA=HMM_Data.ch2_LA(:,:,1);
% else
%     HMM_Data.ch2_LA=0;
% end

tmp=max(strfind(HMM_Data.DataFile,'\'));
if isempty(tmp) tmp=0; end
tmp=tmp+1;
save([HMM_Data.SaveDir HMM_Data.DataFile(tmp:end-4) '.HMMData'] , 'HMM_Data');
```

183

varargout{1}=HMM_Data;

```
function varargout = GPUSPT_sigma(varargin)
%GPUSPT uses fast GPU localization for single particle tracking (output sigma)
%
[tracks,intensities,valids,iDiv,LA,Sigma,coloroverlay]=GPUSPT_sigma(in,D,psfsigma,iDi
v,goodframes,pixelsize,timestep,maxjump,maxTjump,mask)
%
% INPUT:
% in:        3D time series (required)
% D:         Estimated diffusion constant in micron^2/s (default=1)
% psfsigma:   2D Gaussian PSF sigma (default=1)
% iDiv:       Minimum accepted log liklihood value (default=-1)
% goodframes:  minimum number of coordinates in a returned track (default=100)
% pixelsize:  Linear pixel size in microns (default=1)
% timestep:   Timestep in seconds (default=1)
% maxjump:    Maximum allowed spatial jump between nearest 'on' frames
% maxTjump:   Maximum allowed 'off' frames in a trajectory (default=10)
% mask:       2D binary mask
% Ncutoff     [min_photons max_photons]
% diffcutoff1  initial diffusion cutoff
% diffcutoff2  secondary diffusion cutoff
% sigmarange   range of allowed, fitted sigma values default=[0.5 1.5]
% OUTPUT:
% tracks:     Coordinate array  in pixels and frames [particle#,time,coords]
% intensities: Estimated emission rate (photons/frame) [particle#,time]
% valids:      [particle#,time]
% iDiv:        [particle#,time]
% LA:          [particle#,time]
% Sigma:      psf for each coordinate [particle#,time]
% coloroverlay:   Green:data, Red: found emitters
%
% EXAMPLE:
%
%
% Dependencies:
% GPUgaussMLEFinal
% connectcoords
% GaussianSeries
% cMakeSubregions

% (C) Copyright 2008      Department of Physics and Astonomy
%    All rights reserved     University of New Mexico
%                    Albuquerque, New Mexico
%                       USA
%
```

184

```
% Keith Lidke, December 2008

%%Shal, 02.16.2010 to get sigmas at each coordinate

d = struct('menu','Tracking',...
    'display','GPU Tracking',...
    'inparams',struct('name',{'in','D','psfsigma','iDiv','goodframes','pixelsize','timestep',...
    'maxjump','maxTjump','mask','Ncutoff','diffcutoff1','diffcutoff2','sigmarange'},...
    'description',{'Input Series (blank for test)','Estimated Diffustion Const.
(um^2/s)','Gausian PSF sigma','iDivergence Threshold',...
    'minimum length of track to return','Pixel size (um)','Time step (s)',...
    'max allowed jump (pixels)','max allowed time jump (frames)','mask',...
    'Min allowed object photons','threshold probablity 1','threshold probablity 2','Sigma
Range'},...
    'type',
{'image','array','array','array','array','array','array','array','array','image','array','array','array
','array'},...
    'dim_check',  {0,0,0,0,0,0,0,0,0,0,0,0,0,0,-1},...
    'range_check',{[],[],[],[],[],[],[],[],[],[],[],[],[],[]},...
    'required',   {1,0,0,0,0,0,0,0,0,0,0,0,0,0,0},...
    'default',    {'',1,1,-1,100,1,1,10,33,'0',50,.01,.001,[0.5 1.5]}...
    ),...

'outparams',struct('name',{'tracks','intensities','valids','iDiv','LA','Sigma','coloroverlay'},...
    'description',{'Found coordinates','track intensities','track
validity','iDivergences','Calculated Accurcacies','psf for each coordinate','color
overlay'},...
    'type',{'array','array','array','array','array','array','image'}...
    )...
    );
if nargin == 1
    s = varargin{1};
    if ischar(s) & strcmp(s,'DIP_GetParamList')
        varargout{1} = d;
        return
    end
end
try

[in,D,psfsigma,iDiv,goodframes,pixelsize,timestep,maxjump,maxTjump,mask,Ncutoff,dif
fcutoff1,diffcutoff2,sigmarange] = getparams(d,varargin{:});
catch
    if ~isempty(paramerror)
        error(paramerror)
    else
        error(firsterr)
```

185

```
    end
end

clear varargin

if isempty(in)
    in=noise(gaussf(noise(newim)>3)*200);
    goodframes=1;
end


%% find how may regions
if length(size(in))<3

in=repmat(in,[1 1 1]);
end

fprintf('finding candidates...\n')
tic
x=0;
y=0;
z=0;
s=std(in);
T=size(in,3);
for ii=1:size(in,3)
    tmp=in(:,:,ii-1);
    tmp=gaussf(tmp,[1 1 0]*psfsigma)-gaussf(tmp,[1 1 0]*2*psfsigma);
    tmp=tmp>(.5*s);
    msr = measure(squeeze(tmp),squeeze(in(:,:,ii-1)),{'Gravity','Size'},[],1,0,0);
    if isempty(msr);continue;end
    c=msr.Gravity';
    SZmask=(msr.Size>3)';
    x=cat(1,x,c(SZmask,1));
    y=cat(1,y,c(SZmask,2));
    z=cat(1,z,c(SZmask,1)*0+ii-1);
end
x=x(2:end);
y=y(2:end);
z=z(2:end);
toc

%% find coordinates
sz=round(psfsigma*6+1);

fprintf('making subregions...\n')
[in_sub t l]=cMakeSubregions(y,x,z,sz,single(in));
```

186

```matlab
nt = size(in,3);

if nargout<5
    clear in
end

fprintf('fitting subregions...\n')

%clear GPUgaussMLE
[x y N_all bg_all s lax lay li lb ls idiv]=GPUgaussMLE(permute(single(in_sub),[2 1 3]),psfsigma,10,1);
[tmp tmp tmp tmp s]=GPUgaussMLE(permute(single(in_sub),[2 1 3]),psfsigma,10,2);

x=x+l;
y=y+t;

figure;hist(N_all,200)
xlabel('Photons/frame')
ylabel('Counts')

figure;hist(idiv,200)
xlabel('idiv')
ylabel('Counts')

figure;hist(s,200)
xlabel('Sigma')
ylabel('Counts')

clear in_sub


%% Connecting the coordinates

LAcutoff=psfsigma/3;

mask=N_all>Ncutoff;
mask=mask&(idiv>iDiv);
mask=mask&(sigmarange(1)<s);
mask=mask&(sigmarange(2)>s);
mask=mask&(sqrt(lax)<LAcutoff);
mask=mask&(sqrt(lay)<LAcutoff);
mask=mask&( (x-l)>0);
mask=mask&( (x-l)<6*psfsigma+1);
mask=mask&( (y-t)>0);
mask=mask&( (y-t)<6*psfsigma+1);
```

```matlab
x=x(mask);
y=y(mask);
z=z(mask);
n=N_all(mask);
s=s(mask);

merit=idiv(mask);
bg=bg_all(mask);
lax=lax(mask);
lay=lay(mask);

%prepare arrays for connectcoords.c

clear x_arr size_arr y_arr n_arr merit_arr z_arr
zold=1;
size_arr(1)=0;
for nn=1:size(x,1)
    if z(nn)+1>zold;
        zold=z(nn)+1;
        size_arr(zold)=1;
    else
        size_arr(zold)=size_arr(zold)+1;
    end
    t=z(nn)+1;
    num=size_arr(zold);
    x_arr(num,t)=x(nn);
    y_arr(num,t)=y(nn);
    z_arr(num,t)=z(nn);
    n_arr(num,t)=n(nn);
    merit_arr(num,t)=merit(nn);
end

fprintf('connecting coordinates...\n')
if exist('x_arr')
    %     save preConnectcoords
    tic
    [X Y V M I ID]=connectcoords(double(x_arr),double(y_arr),size_arr,D,...

double(n_arr),double(merit_arr),maxjump,maxTjump,goodframes,diffcutoff1,diffcutoff2);
    toc
else
    warning('no single molucules found');
    varargout{1}=0;
    varargout{2}=0;
    varargout{3}=0;
```

```matlab
        varargout{4}=0;
        varargout{5}=0;
        varargout{6}=0;
        varargout{7}=0;
        return
end

%% Identifying connected tracks with found values
clear BG LAx LAy Sigma
BG=zeros(size(X));
LAx=zeros(size(X));
LAy=zeros(size(X));
AN=zeros(size(X));
ABG=zeros(size(X));
Sigma=zeros(size(X));

fprintf('identifying coordinates and matching accuracies...\n')
for nn=1:size(X,1)
    for tt=1:size(X,2)
        if ID(nn,tt)>0
            for jj=1:size(x,1)
                if (X(nn,tt)==x(jj))&(Y(nn,tt)==y(jj))
                    BG(nn,tt)=bg(jj);
                    LAx(nn,tt)=lax(jj); %these are variances
                    LAy(nn,tt)=lay(jj); %these are variances
                    AN(nn,tt)=li(jj);
                    ABG(nn,tt)=lb(jj);
Sigma=zeros(size(X));
                end
            end
        end
    end
end

LA=cat(3,sqrt(LAx+LAy),sqrt(LAx),sqrt(LAy),sqrt(AN),sqrt(ABG));

%% Giving outputs

if size(X,2)<nt
    X(:,T)=0;
    Y(:,T)=0;
    V(:,T)=0;
    M(:,T)=0;
    I(:,T)=0;
    LA(:,T,:)=0;
    Sigma(:,T)=0;
```

```matlab
end

c=cat(3,X,Y);

if nargout>6
    if exist('I')
        fprintf('making color overlay...\n')
        gs=dip_image(stretch(GaussianSeries(c,[size(in,1)
size(in,2)],psfsigma,1,I)),'uint8');
        rd=dip_image(stretch(in),'uint8');
        varargout{6}=joinchannels('RGB',gs,rd);
    end
end

varargout{1}=c;
varargout{2}=I;
varargout{3}=V;
varargout{4}=M;
varargout{5}=LA; %these are stds
varargout{6}=Sigma;

fprintf('GPUSPT finished\n')

%%
%% Diffusion Analysis
resdir='Z:\Shal\SPT Data\GroupedData_A431_Final\HMM Final\HMM EGF\';
datapath=resdir;
filestring='*.HMMData';
Files=dir([datapath filestring]);
sigma=1.0720e-001;
inc=0;
deltaT=2;
for jj = 1:length(Files)
    filename = Files(jj).name;
    load([datapath filename],'-mat');
    try
        if isfield(HMM_Data,'raw_ch1_tracks')
            for hh=1:size(HMM_Data.raw_ch1_tracks,1)
                track=HMM_Data.raw_ch1_tracks(hh,:,:);
                v=HMM_Data.ch1_valids(hh,:);
                for ii=1:deltaT:size(track,2)-deltaT
                    p1=ii;
                    p2=ii+deltaT;
                    x=track(:,:,1);
                    y=track(:,:,2);
                    if v(1,p1) && v(1,p2)
```

```matlab
                inc=inc+1;
                r2(inc) = ((x(:,p1)-x(:,p2))^2) + ((y(:,p1)-y(:,p2))^2);
            end
            close all
        end
        clear track v x y p1 p2 sz
    end
  end
catch
end
end
r2sort=sort(r2,2,'ascend');
rmask=r2sort<4; %This filter could be used to remove jumps of greater than 1.5 pixels
... still a question of why we get these at all
r2sort=r2sort(rmask);
r2_1=size(r2sort,2);
rystep=(1:length(r2sort))/length(r2sort);
save([resdir '\Pr2Results'],'r2','r2sort','rystep');

%Two component fit for all data:
rTCopts=fitoptions('Method','Nonlinear','StartPoint',[.5.2.1],'Lower',[0,0,0],'Upper',[1,10,1
0]);
%Schutz, et al., BJ, V73, 1997:
rTCftype=fittype('1-((a.*exp(-x./b))+((1-a).*exp(-
x./c)))','options',rTCopts,'coeff',{'a','b','c'},'indep','x','depen','y');
[rTCresults, rTCgoodnessL]=fit((r2sort)',rystep',rTCftype);

rTCc_1=coeffvalues(rTCresults);
rTCalpha_1=rTCc_1(1);
rTCdr1_1=rTCc_1(2);
rTCdr2_1=rTCc_1(3);
rTCrmse_1=rTCgoodnessL.rmse;
rTCFitResult=1-((rTCalpha_1.*exp(-r2sort./rTCdr1_1))+((1-rTCalpha_1).*exp(-
r2sort./rTCdr2_1)));

rTCDout1_1 = (rTCdr1_1-(4*(sigma^2)))/(4*deltaT);
rTCDout2_1 = (rTCdr2_1-(4*(sigma^2)))/(4*deltaT);
rTCD1um_1 = rTCDout1_1*20*0.267^2;
rTCD2um_1 = rTCDout2_1*20*0.267^2;

%All data plotting
rdTC=figure;
semilogx(squeeze(r2sort),squeeze(rystep),'go')
hold on
semilogx(squeeze(r2sort),rTCFitResult,'--b','LineWidth',2)
```

```matlab
hold off
xlabel('(r^2) (pix)')
ylabel('P(r^2)')
legend('Data','Fit')
title('Two Component Fit for All P(r^2) Data')
hold off

saveas(rdTC,[resdir 'rTCPr2'],'fig');
saveas(rdTC,[resdir 'rTCPr2'],'jpg');

pause(2);
close all

%%
%% HMM Simulations
function varargout = GPUSPT(varargin)

d = struct('menu','HMM',...
    'display','HMM Simulation',...
    'inparams',struct('name',{'sz','N','T','D','IntDis','Pint','Tau','retrack'},...
    'description',{'Region Size','Particles per Channel','Frames',...
    'Diffustion Const. (pixels^2/frame)','Interaction Distance','Interaction Probability',...
    'Interaction Lifetime','Track Image Data'},...
    'type',      {'array','array','array','array','array','array','array','array'},...
    'dim_check', {0,0,0,0,0,0,0,0},...
    'range_check',{[],[],[],[],[],[],[],[]},...
    'required',   {0,0,0,0,0,0,0,0},...
    'default',    {32,10,100,1,.25,.5,20,0}...
    ),...
    'outparams',struct('name',{'Tau_found','Tau_Matrix','LogP','Traj_raw',...
    'Traj_noise','Traj_found','im1','im2','coloroverlay'},...
    'description',{'Found Lifetime','Calculated Tau_on,Tau_off',...
    'Log Probability','Simulated Trajectories','Sim Traj. + noise','Tracked Traj.'...
    'image 1','image 2','coloroverlay'},...
    'type',{'array','array','array','array','arrray','array','image','image','image'}...
    )...
    );
if nargin == 1
    s = varargin{1};
    if ischar(s) & strcmp(s,'DIP_GetParamList')
        varargout{1} = d;
        return
    end
end
try
    [sz,N,T,D,IntDis,Pint,Tau,retrack] = getparams(d,varargin{:});
```

192

```matlab
catch
    if ~isempty(paramerror)
        error(paramerror)
    else
        error(firsterr)
    end
end

Pblinkon=.2;
Pblinkoff=.1;
LA=.1;
PSFSigma=1;

[tracks,ntracks,series,I]                                              =
InteractingParticles(sz,2*N,D,T,'Reflecting',IntDis,1/Tau,Pint,Pblinkon,Pblinkoff,LA,0);

Ltracks=tracks(1:N,:,:);
Rtracks=tracks(N+1:end,:,:);
LI=I(1:N,:);
RI=I(N+1:end,:);
Lt = cGaussianSeries(Ltracks,LI,PSFSigma,sz,sz);
Rt = cGaussianSeries(Rtracks,RI,PSFSigma,sz,sz);
nL=noise(1+Lt*(PSFSigma/LA)^2,'poisson');
nR=noise(1+Rt*(PSFSigma/LA)^2,'poisson');
co=joinchannels('RGB',nL,nR);
```

```matlab
%%
clear t1 t2 Lvcell Rvcell sigmas1 sigmas2
t1{1}=Ltracks;
t2{1}=Rtracks;
Lvcell{1}=LI;
Rvcell{1}=RI;
sigmas1{1}=LA*ones(N,T);
sigmas2{1}=LA*ones(N,T);
minpath=10;
L=4;

[X1 X2 Y1 Y2 PairID V1 V2 S1 S2 startframe endframe pairlength] =
Preprocess(t1,t2,Lvcell,Rvcell,sigmas1,sigmas2,minpath,L);

PMatrix                                                              =
Pmatrix(X1,X2,Y1,Y2,PairID,V1,V2,S1,S2,startframe,endframe,pairlength,IntDis,L);
```

```matlab
%% try plots
dT=10.^(0:.05:3.5);
clear MLarray
```

193

```matlab
for Tau_oninc=1:length(dT)
    for Tau_offinc=1:length(dT)
        Tau_BF_test=dT(Tau_oninc);
        Tau_BB_test=dT(Tau_offinc);
        [Tau_BF_test Tau_BB_test];
        [lnP]=Ponly_PODHMM(PMatrix,Tau_BF_test,Tau_BB_test,L,startframe,endframe);
        MLarray(Tau_oninc,Tau_offinc)=lnP;
    end

end

[tmp id1]=max(MLarray);
[tmp id2]=max(tmp);

found_Tau_BF=dT(id1(id2))
found_Tau_BB=dT(id2)

figure;semilogx(dT,(MLarray(:,id2)))

xlabel('Tau_{BF}')
figure;semilogx(dT,(MLarray(id1(id2),:)))
xlabel('Tau_{BB}')
hold on

%%
X=repmat(dT',[1 length(dT)]);
Y=repmat(dT,[length(dT) 1]);

figure
mesh(X,Y,exp(MLarray-max(max(MLarray))))
%mesh(X,Y,exp(MLarray))
xlabel('\tau_{on}','fontsize',18)
ylabel('\tau_(Diermeier et al.)','fontsize',18)
zlabel('Normalized Likelihood','fontsize',14)
%axis([0 1000 0 1000 max(max(MLarray))-2 max(max(MLarray))])
set(gca,'Yscale','log')
set(gca,'Xscale','log')

function varargout = HMM_GenSimData(varargin)

d = struct('menu','HMM',...
    'display','HMM Simulation',...

'inparams',struct('name',{'OutFile','OutDir','Condition','sz','N','T','D','IntDis','PixelSize','TimeStep','Pint','Tau'},...
```

```matlab
    'description',{'Output    File','Output    Data    Directory','Condition    ID','Region
Size','Particles per Channel','Frames',...
    'Diffustion    Const.    (pixels^2/frame)','Interaction    Distance    (nm)','PixelSize
(microns)','TimeStep (s)','Interaction Probability',...
    'Interaction Lifetime'},...
    'type',
{'outfile','indir','string','array','array','array','array','array','array','array','array'},...
    'dim_check',  {0,0,0,0,0,0,0,0,0,0,0,0,0},...
    'range_check',{'*.HMMData','*.mat',[],[],[],[],[],[],[],[],[],[]},...
    'required',   {0,0,0,0,0,0,0,0,0,0,0,0,0},...
    'default',    {'','','Sim',64,10,100,.01,30,16/60,.05,.5,20}...
    ),...
    'outparams',struct('name',{'HMM_Data'},...
    'description',{'HMM Data Structure'},...
    'type',{'strct'}...
    )...
    );
if nargin == 1
    s = varargin{1};
    if ischar(s) & strcmp(s,'DIP_GetParamList')
        varargout{1} = d;
        return
    end
end
try
    [OutFile,OutDir,Conditions,sz,N,T,D,IntDis,PixelSize,TimeStep,Pint,Tau]           =
getparams(d,varargin{:});
catch
    if ~isempty(paramerror)
        error(paramerror)
    else
        error(firsterr)
    end
end


%% Generate Data
Pblinkon=.2;
Pblinkoff=.1;
LA=.1;
PSFSigma=1;
N_Photons=200;
bg=5;

n_sigma=PSFSigma/sqrt(N_Photons);
```

```
%convert to pixels and frames
IntDis=IntDis/1000/PixelSize
D=D/PixelSize^2*TimeStep


[tracks,ntracks,series,I]                                                              =
InteractingParticles(sz,2*N,D,T,'Reflecting',IntDis,1/Tau,Pint,Pblinkon,Pblinkoff,LA,0);

Ltracks=tracks(1:N,:,:);
Rtracks=tracks(N+1:end,:,:);
LI=I(1:N,:);
RI=I(N+1:end,:);
Lt = cGaussianSeries(Ltracks,LI,PSFSigma,sz,sz);
Rt = cGaussianSeries(Rtracks,RI,PSFSigma,sz,sz);
nL=noise(bg+Lt*N_Photons,'poisson');
nR=noise(bg+Rt*N_Photons,'poisson');
```

```
%% Save Data
sequence=cat(1,nL,nR);
st=max(findstr(OutFile,'\'))+1;
en=max(findstr(OutFile,'.'))-1;
fn=[OutFile(st:en) '.mat'];
save([OutDir '\' fn],'sequence');
```

```
%% Link Data
HMM_Data.TreeDir=[OutDir '\'];
HMM_Data.DataFile=fn;
HMM_Data.BGFile='';
HMM_Data.Bead_Align='';
HMM_Data.SaveDir=[OutDir '\'];
HMM_Data.Bead_Gain='';
HMM_Data.PixelSize=PixelSize;
HMM_Data.TimeStep=TimeStep;
HMM_Data.DataConditions=Conditions;

HMM_Data.ch1_tracks=Ltracks+randn(size(Ltracks))*n_sigma;
HMM_Data.ch1_intensities=LI;
HMM_Data.ch1_valids=LI;
HMM_Data.ch1_LA=ones(N,T)*n_sigma;

HMM_Data.ch2_tracks=Rtracks+randn(size(Ltracks))*n_sigma;
HMM_Data.ch2_intensities=RI;
HMM_Data.ch2_valids=RI;
HMM_Data.ch2_LA=ones(N,T)*n_sigma;

%information included for new tracking functions
```

```
HMM_Data.ch_bin=[1 1];
HMM_Data.Dconvert = 1/PixelSize^2*TimeStep;
HMM_Data.FigDir=[HMM_Data.SaveDir 'figures\'];
```

```
%% Calculate Gain and Background

HMM_Data.BGImage=squeeze(sequence(:,:,0)*0);
HMM_Data.CCDGain=1;
```

```
%% Calculate Shift
sz=size(sequence);
a=newim(sz(1:2));
a=(4+xx(a))/16==round((4+xx(a))/16)&(4+yy(a))/16==round((4+yy(a))/16);
a=gaussf(a);
a=cat(1,a,a);
a=noise(a*1000)
options=set_im_transformOptions;
options = set_im_transformOptions(options,'meritcutoff',.9);
tform = im_transform_gauss(a,options);
options=set_im_transformOptions(options,'tform');
HMM_Data.tform=tform;
close all
```

```
%% Write output

save(OutFile, 'HMM_Data');

varargout{1}=HMM_Data;
```

```
%%
%% HMM Analysis
%Using DS values for the lowest lnP result for each condition

%If error: ??? Reference to non-existent field 'shifted_ch2_tracks':
HMM_Data.raw_ch2_tracks=zeros(0,1000,2)
HMM_Data.ch2_intensities=zeros(0,1000)
HMM_Data.ch2_valids=zeros(0,1000)
HMM_Data.ch2_LA=zeros(0,1000)
HMM_Data.ch2_sigma=zeros(0,1000)
HMM_Data.shifted_ch2_tracks=zeros(0,1000,2)
tmp=max(strfind(HMM_Data.DataFile,'\'));
if isempty(tmp) tmp=0; end
tmp=tmp+1;
save([HMM_Data.SaveDir HMM_Data.DataFile(tmp:end-4) '.HMMData'] , 'HMM_Data');
```

197

```matlab
%%Example: analysis of EGF data, A431 cells
%%2-State HMM analysis of candidate pairs
datadir='Z:\Shal\SPT Data\GroupedData_A431_Final\HMM Final\';
IntDis=100; %nm (overlay error)+(probe separation in a dimer)
L=1; %micron.  Analysis is restricted to frames where seperation is less than L
minOLF=10; %frames. Minimum number of overlapping valid frames of two tracks for
inclusion in analysis
minTL=50; %frames.  Tracks must have valid points seperated by this value or larger or
are excluded
DC=.5; %duty cycle.  Tracks must have a (valid frames)/(track length) ratio greater than
DC
appThresh=.2;%micron Tracks must get this close at least once to be included
minOLT=10; %frames. Minimum number of overlapping frames (valid or invalid) of two
tracks for inclusion in analysis

%%EGF
HMM_PreProcessData = HMM_PreProcess([datadir 'HMM EGF\'],'QD EGF',[datadir
'HMM EGF\EGF.HMMPP'],IntDis,L,minOLF,minTL,DC,minOLT,appThresh);
[Tau_BB,Tau_BF,MLarray]        =        HMM_FindLifetimes([datadir        'HMM
EGF\EGF.HMMPP'],[datadir 'HMM EGF\']);
HMM_PreProcessData = HMM_FindDimers([datadir 'HMM EGF\EGF.HMMPP'],0,0)
HMM_PreProcessData = HMM_LifetimeDist([datadir 'HMM EGF\EGF.HMMPP'],[datadir
'HMM EGF\'])
HMM_PlotCandidates([datadir        'HMM        EGF\EGF.HMMPP'],[datadir        'HMM
EGF\CandidatePairsEGF\'])

function varargout = HMM_PreProcess(varargin)
%Written by Shalini Low-Nam and Keith Lidke

conditions ={'QD EGF','QD Nanobody','QD EGF + PD','QD Nanobody + PD',...
   'QD Nanobody + dEGF','QD Nanobody + dEGF + PD','QD EGF + dEGF',...
   'QD EGF + dEGF + PD','QD EGF + QD VhH','QD EGF + QD VhH +
PD','Sim','QD625',...
   'QD IgE','QD IgE DNP(0.01ug/ml)','QD IgE PP2(10uM)','QD IgE DNP(0.1ug/ml)
PP2(10uM)'};

d = struct('menu','HMM',...
   'display','HMM Pre-Process Data',...
   'inparams',struct('name',{'HMM_DataDir','DataConditions','OutFile',...
   'IntDis','L','MinOverlap','MinPath','DutyCycle','MinTime','D_Thresh'},...
   'description',{'HMM DataFile Directory','Data Conditions','OutPutFile',...
   'Max Dimer Separation (nm)','Analysis Threshold (microns)','Min Overlapping Valid
Frames',...
   'Min Traj Length (frames)','Duty Cycle','Min Overlapping Time (Frames)','Close
Approach Threshold (microns)'},...
   'type',      {'indir','option','outfile','array','array','array','array','array','array','array'},...
```

```matlab
        'dim_check',  {0,0,0,0,0,0,0,0,0,0},...
        'range_check',{'*.HMMData',conditions,'*.HMMPP',[],[],[],[],[],[],[]},...
        'required',   {0,0,0,0,0,0,0,0,0,0},...
        'default',    {'',conditions{1},'',30,3,10,50,0.5,20,0.2}...
        ),...
        'outparams',struct('name',{'HMM_PreProcessData'},...
        'description',{'HMM PreProcessed Data Structure'},...
        'type',{'strct'}...
        )...
        );
if nargin == 1
    s = varargin{1};
    if ischar(s) & strcmp(s,'DIP_GetParamList')
        varargout{1} = d;
        return
    end
end
try
    [HMM_DataDir,DataConditions,OutFile,...
        IntDis,L,MinOverlap,MinPath,DutyCycle,MinTime,D_Thresh]                    =
getparams(d,varargin{:});
catch
    if ~isempty(paramerror)
        error(paramerror)
    else
        error(firsterr)
    end
end
```

%% Make a list of files to process

```matlab
f=dir([HMM_DataDir '\*.HMMData']);

Files=[];
cnt=1;
switch DataConditions
    case 'All'
        for ii=1:size(f,1)
            Files(Paez et al.)=f(ii).name;
        end
    otherwise
        for ii=1:size(f,1)
            load([HMM_DataDir '\' f(ii).name],'-mat');
            if strmatch(HMM_Data.DataConditions,DataConditions,'exact')
                Files{cnt}=f(ii).name;
                cnt=cnt+1;
```

199

```matlab
        end
    end
end

if isempty(Files)
    warning('no files with that condition are found \n');
    varargout{1}=[];
    return
end

%% Process Files

Nfiles=size(Files,2);

PMatrix=cell(0,0);
StartFrame=cell(0,0);
EndFrame=cell(0,0);
PairID=cell(0,0);
FileID=cell(0,0);
for nn=1:Nfiles
    fprintf('Processing File: %s \n',Files{nn})
    load([HMM_DataDir '\' Files{nn}],'-mat');
    [PMatrix{nn} StartFrame{nn} EndFrame{nn} PairID{nn}]=PP(HMM_Data,...

DutyCycle,MinTime,L/HMM_Data.PixelSize,MinOverlap,MinPath,IntDis/HMM_Data.Pixe
lSize/1000,D_Thresh/HMM_Data.PixelSize);

    FileID{nn}=[HMM_DataDir '\' Files{nn}];

    Npairs=size(PMatrix{nn},1);

    if isempty(PMatrix{nn})
        warning('no interactions found in the following data set:')
        [HMM_DataDir '\' Files{nn}]
    else
        fprintf('Interactions found between : \n')
        for nf=1:Npairs
            fprintf('ch1: %d   ch2: %d \n',PairID{nn}(nf,1), PairID{nn}(nf,2))
        end
        fprintf('\n')
    end
end

HMM_PreProcessData.PMatrix=PMatrix;
HMM_PreProcessData.StartFrame=StartFrame;
HMM_PreProcessData.EndFrame=EndFrame;
```

```matlab
HMM_PreProcessData.PairID=PairID;
HMM_PreProcessData.FileID=FileID;
HMM_PreProcessData.D_Thresh=D_Thresh;
HMM_PreProcessData.IntDis=IntDis/HMM_Data.PixelSize/1000; %in pixels
HMM_PreProcessData.L=L/HMM_Data.PixelSize; %in pixels
HMM_PreProcessData.MinOverlap=MinOverlap;
HMM_PreProcessData.MinPath=MinPath;
HMM_PreProcessData.DutyCycle=DutyCycle;
HMM_PreProcessData.MinTime=MinTime;

save([OutFile],'HMM_PreProcessData');

varargout{1}=HMM_PreProcessData;

end

function                     [PMatrix                   StartFrame                  EndFrame
PairID]=PP(HMM_Data,DutyCycle,MinTime,L,MinOverlap,MinPath,IntDis,D_Thresh)
% this calculates the pmatrix for 1 data set

PMatrix=[];
StartFrame=[];
EndFrame=[];
PairID=[];
FileID=[];

if isfield(HMM_Data,'raw_ch1_tracks')

    Nframes=size(HMM_Data.raw_ch1_tracks,2);
    t1=HMM_Data.raw_ch1_tracks;
    %t2=HMM_Data.ch2_tracks; %changed by SLow-Nam; April 26, 2010,  to
    %accomodate transformed ch2 tracks
    t2=HMM_Data.shifted_ch2_tracks;
    v1=HMM_Data.ch1_valids;
    v2=HMM_Data.ch2_valids;
    s1=HMM_Data.ch1_LA;
    s2=HMM_Data.ch2_LA;
    %temp hack
    v1=logical(t1(:,:,1));
    v2=logical(t2(:,:,1));

    Ntracks_1=size(t1,1);
    Ntracks_2=size(t2,1);
    num=1;

    for nn1=1:Ntracks_1
```

201

```matlab
        sf1=find(v1(nn1,:),1); %find start frame
        ef1=max(find(v1(nn1,:))); %find end frame
        if isempty(sf1); continue; end
        if (ef1-sf1)<MinTime;continue;end %rule out short tracks
        if  (sum(v1(nn1,sf1:ef1))/(ef1-sf1))<DutyCycle;continue;end  %rule out low duty
cycle tracks

        for nn2=1:Ntracks_2
            sf2=find(v2(nn2,:),1); %find start frame
            ef2=max(find(v2(nn2,:))); %find end frame
            if isempty(sf2); continue; end
            if (ef2-sf2)<MinTime;continue;end %rule out short tracks
            if  (sum(v2(nn2,sf2:ef2))/(ef2-sf2))<DutyCycle;continue;end %rule out low duty
cyle tracks

            validmask=(v1(nn1,:).*v2(nn2,:))==1;
            x1=t1(nn1,:,1);
            y1=t1(nn1,:,2);
            x2=t2(nn2,:,1);
            y2=t2(nn2,:,2);

            d=sqrt((x2(validmask)-x1(validmask)).^2+(y2(validmask)-y1(validmask)).^2);

            if min(d)> D_Thresh; continue; end %rule out tracks that don't get close enough

            if sum(d<L)< MinOverlap; continue; end %rule out tracks that don't overlap
enough


            %now find start and end frames of the interaction
            dcandidate=sqrt((x1-x2).^2+(y1-y2).^2);
            mask=(dcandidate<=L).*validmask;
            sf=find(mask,1);
            ef=max(find(mask));
            T = ef- sf;
            if T < MinPath; continue; end %rule out tracks that don't overlap for enough
frames

            for tt=sf:ef  %loop only startframe:endframe
                if v1(nn1,tt) && v2(nn2,tt)
                    d=sqrt((x1(tt)-x2(tt))^2+(y1(tt)-y2(tt))^2);
                    if d<=L
                      %PMatrix(num,tt)=Pbr1r2(x1(tt),x2(tt),y1(tt),y2(tt),max([s1(nn1,tt)
.01]),max([s2(nn2,tt)]),IntDis,L);
                        PMatrix(num,tt)=P_dimer(x1(tt),x2(tt),y1(tt),y2(tt),max([s1(nn1,tt)
                        .01]),max([s2(nn2,tt)]),IntDis);
```

202

```matlab
            end
          end
        end

        PairID(num,:)=[nn1,nn2];
        StartFrame(num)=sf;
        EndFrame(num)=ef;

        num=num+1;
      end
    end
    if (~isempty(PMatrix))&(size(PMatrix,2)<Nframes) %gaurantee PMatrix is length of
tracks
      PMatrix(end,Nframes)=0;
    end

else
    warning('No ch1 tracks in this data set')
    pause(0.5)
    return
end
end

function varargout = HMM_FindLifetimes(varargin)

d = struct('menu','HMM',...
    'display','HMM Find Lifetimes',...
    'inparams',struct('name',{'HMM_PreProcessFile','OutDir'},...
    'description',{'HMM PreProcess File','Output Directory'},...
    'type',       {'infile','indir'},...
    'dim_check',  {0,0},...
    'range_check',{'*.HMMPP','*.HMMParams'},...
    'required',   {0,0},...
    'default',    {'',''}...
    ),...
    'outparams',struct('name',{'Tau_BB','Tau_BF','MLarray'},...
    'description',{'Modified HMM Data Structure'},...
    'type',{'strct'}...
    )...
    );
if nargin == 1
    s = varargin{1};
    if ischar(s) & strcmp(s,'DIP_GetParamList')
      varargout{1} = d;
      return
    end
```

203

```matlab
end
try
    [HMM_PreProcessFile, OutDir] = getparams(d,varargin{:});
catch
    if ~isempty(paramerror)
        error(paramerror)
    else
        error(firsterr)
    end
end


load(HMM_PreProcessFile,'-mat');

dT=10.^(0:.1:5);
%dT=10.^(0:.05:3.5);
clear MLarray
for Tau_oninc=1:length(dT)
    for Tau_offinc=1:length(dT)
        Tau_BF_test=dT(Tau_oninc);
        Tau_BB_test=dT(Tau_offinc);
        [Tau_BF_test Tau_BB_test];
        [lnP]=PODHMM(HMM_PreProcessData,Tau_BF_test,Tau_BB_test);
        MLarray(Tau_oninc,Tau_offinc)=lnP;
    end
end
[tmp id1]=max(MLarray);
[tmp id2]=max(tmp);

found_Tau_BF=dT(id1(id2))
found_Tau_BB=dT(id2)

figure;semilogx(dT,(MLarray(:,id2)))

xlabel('Tau_{BF}')
figure;semilogx(dT,(MLarray(id1(id2),:)))
xlabel('Tau_{BB}')
hold on

X=repmat(dT',[1 length(dT)]);
Y=repmat(dT,[length(dT) 1]);

%old mesh plotting:
% figure
% mesh(X,Y,exp(MLarray-max(max(MLarray))))
% %mesh(X,Y,exp(MLarray))
```

204

```matlab
% xlabel('\tau_{on}','fontsize',18)
% ylabel('\tau_(Diermeier et al.)','fontsize',18)
% zlabel('Normalized Likelihood','fontsize',14)
% %axis([0 1000 0 1000 max(max(MLarray))-2 max(max(MLarray))])
% set(gca,'Yscale','log')
% set(gca,'Xscale','log')

figure
surfc(X,Y,exp(MLarray-max(max(MLarray))))
set(gca,'zdir','reverse')
%colormap bone
axis([0 1000 0 1000 -0.1 1])
xlabel('\tau_{on}','fontsize',18)
ylabel('\tau_(Diermeier et al.)','fontsize',18)
zlabel('Normalized Likelihood','fontsize',14)
%axis([0 1000 0 1000 max(max(MLarray))-2 max(max(MLarray))])
set(gca,'Yscale','log')
set(gca,'Xscale','log')

HMM_PreProcessData.found_Tau_BB=found_Tau_BB;
HMM_PreProcessData.found_Tau_BF=found_Tau_BF;
HMM_PreProcessData.MLarray=MLarray;

%save(HMM_PreProcessFile,'-mat');
save(HMM_PreProcessFile,'HMM_PreProcessData')

varargout{1}=found_Tau_BB;
varargout{2}=found_Tau_BF;
varargout{3}=MLarray;


function lnP=PODHMM(HMM_PreProcessData,Tau_BF,Tau_BB)

N=size(HMM_PreProcessData.PMatrix,2); %Number of files to analyze


RegionSize=HMM_PreProcessData.L;

lnP=0;
for ii=1:N
    %fprintf ('Analyzing file %d of %d \n',ii,N)

    pm_all=HMM_PreProcessData.PMatrix(Paez et al.);

    for pp=1:size(pm_all,1) %pairs in file
```

```matlab
        pm=pm_all(pp,:);

        validframes=find(pm)';

        Frames=size(validframes,1); %valid time frames.

        if ~Frames;continue;end

        clear f alpha;
        alpha=1;

        f=zeros([2 Frames]);
        f(:,1)=[1-pm(1) pm(1)];
        alpha=zeros([1 Frames]);
        P=zeros(2,2);
        for ttid=2:Frames
            tt=validframes(ttid);

            frame=validframes(ttid);
            pframe=validframes(ttid-1);
            deltat=frame-pframe;

            P(1,1)=1-pm(tt);
            P(2,2)=pm(tt);

            HMM(1,1)=1-(1-exp(-deltat/Tau_BF)); %free to free
            HMM(2,1)=(1-exp(-deltat/Tau_BF));   %free to bound
            HMM(1,2)=(1-exp(-deltat/Tau_BB));   %bound to free
            HMM(2,2)=exp(-deltat/Tau_BB);       %bound to bound

            T_DHMM=P*HMM;

            tmp=T_DHMM*f(:,ttid-1);
            alpha(ttid)=sum(sum(tmp));
            f(:,ttid)=tmp/alpha(ttid);
        end

        lnP=lnP+sum(sum(log(alpha(2:end-2))));
    end

end

function varargout = HMM_FindDimers(varargin)

d = struct('menu','HMM',...
    'display','HMM Find Dimers',...
```

```matlab
  'inparams',struct('name',{'HMM_PreProcessFile','Tau_BB','Tau_BF'},...
  'description',{'HMM PreProcess File','Tau off (0 for HMMPP value)','Tau on (0 for
HMMPP value)'},...
  'type',      {'infile','array','array'},...
  'dim_check', {0,0,0},...
  'range_check',{'*.HMMPP',[],[]},...
  'required',  {0,0,0},...
  'default',   {'',0,0}...
  ),...
  'outparams',struct('name',{'HMM_PreProcessData'},...
  'description',{'HMM_PreProcessData Structure'},...
  'type',{'strct'}...
  )...
  );
if nargin == 1
   s = varargin{1};
   if ischar(s) & strcmp(s,'DIP_GetParamList')
      varargout{1} = d;
      return
   end
end
try
   [HMM_PreProcessFile,Tau_BB,Tau_BF] = getparams(d,varargin{:});
catch
   if ~isempty(paramerror)
      error(paramerror)
   else
      error(firsterr)
   end
end

load(HMM_PreProcessFile,'-mat');
N=size(HMM_PreProcessData.PMatrix,2); %Number of files to analyze

if ~(Tau_BB)
   Tau_BB=HMM_PreProcessData.found_Tau_BB;
end

if ~(Tau_BF)
   Tau_BF=HMM_PreProcessData.found_Tau_BF;
end

Nstates=2; %(free, bound)

for ii=1:N %loop over files
   %fprintf ('Analyzing file %d of %d \n',ii,N)
```

207

```matlab
pm_all=HMM_PreProcessData.PMatrix(Paez et al.);
States=zeros(size(pm_all,1),size(pm_all,2));
Pout=0;
for pp=1:size(pm_all,1) %pairs in file

    pm=pm_all(pp,:);
    validframes=find(pm)';
    Frames=size(validframes,1); %valid time frames
    if ~Frames;continue;end

    clear Traj
    Traj(:,1)=(0:Nstates-1); %state space trajectory, grows to Nstates*T
    P_old=ones(Nstates,1);

    for ttid=2:Frames
        tt=validframes(ttid);

        frame=validframes(ttid);
        pframe=validframes(ttid-1);
        deltat=frame-pframe;

        P(1,1)=1-pm(tt);
        P(2,1)=pm(tt);


        HMM(1,1)=1-(1-exp(-deltat/Tau_BF)); %free to free
        HMM(2,1)=(1-exp(-deltat/Tau_BF));   %free to bound
        HMM(1,2)=(1-exp(-deltat/Tau_BB));   %bound to free
        HMM(2,2)=exp(-deltat/Tau_BB);       %bound to bound

        tmpTraj=Traj;

        for ss=0:Nstates-1 %looping over states at time t (current states)
            tmp=P_old.*HMM(:,ss+1).*P;
            [Ptmp id]=max(tmp);
            P_new(ss+1,1)=Ptmp;
            tmpTraj(ss+1,1:ttid-1)=Traj(id,:);
            tmpTraj(ss+1,ttid)=id-1;
        end
        Traj=tmpTraj;
        P_old=P_new;
    end

    [Pout(pp) id]=max(P_old);
    States(pp,logical(pm))=Traj(id,:);
```

```matlab
    end
    StateMatrix(Paez et al.)=States;
    PViterbi(Paez et al.)=Pout;
  end
  HMM_PreProcessData.StateMatrix=StateMatrix;
  HMM_PreProcessData.PViterbi=PViterbi;

  varargout{1}=HMM_PreProcessData;
  save(HMM_PreProcessFile,'-mat');

function varargout = HMM_LifetimeDist(varargin)

d = struct('menu','HMM',...
   'display','HMM Lifetime Distributions',...
   'inparams',struct('name',{'HMM_PreProcessFile','Out_Dir'},...
   'description',{'HMM PreProcess File','Output Directory'},...
   'type',        {'infile','indir'},...
   'dim_check',   {0,0},...
   'range_check',{'*.HMMPP','*.*'},...
   'required',    {0,0},...
   'default',     {'',''}...
   ),...
   'outparams',struct('name',{'HMM_PreProcessData'},...
   'description',{'HMM_PreProcessData structure'},...
   'type',{'strct'}...
   )...
   );
if nargin == 1
   s = varargin{1};
   if ischar(s) & strcmp(s,'DIP_GetParamList')
      varargout{1} = d;
      return
   end
end
try
   [HMM_PreProcessFile,OutDir] = getparams(d,varargin{:});
catch
   if ~isempty(paramerror)
      error(paramerror)
   else
      error(firsterr)
   end
end


load(HMM_PreProcessFile,'-mat');
```

```matlab
tmp=max(strfind(HMM_PreProcessFile,'\'));
fnbase=HMM_PreProcessFile(tmp+1:end-6);


SM=HMM_PreProcessData.StateMatrix;

Nfiles=size(SM,2);
cnt=1;
for nf=1:Nfiles
   sm=SM(Lund et al.);
   pm=HMM_PreProcessData.PMatrix(Lund et al.);
   shf=zeros([size(pm,1) size(pm,2)]); %create matrix for state with holes filled
   for nn=1:size(pm,1)
      s=sm(nn,:);
      if (sum(s))==0;continue;end
      v=logical(pm(nn,:));
      state=0;
      for tt=1:max(find(v))
         if v(tt)&(s(tt))&(~state);sf=tt;end %this is the start of a dimer
         if (v(tt)&(~s(tt))&state)|((tt==max(find(v)))&state) %dimer ends at this condition
            StateLength(cnt,1)=tt-sf; %lifetime
            StateLength(cnt,2)=nf;%File ID
            StateLength(cnt,3:4)=HMM_PreProcessData.PairID(Lund et al.)(1,:);
            cnt=cnt+1;
         end
         if v(tt);state=s(tt);end
         shf(nn,tt)=state;
      end
   end
   if sum(sum(shf));%dipshow(shf)
      %joinchannels('RGB',shf,sm)
   end
   FilledStates(Lund et al.)=shf;
end

if cnt==1
   StateLength=[];
else
   [Thist Thistbins]=hist(StateLength(:,1),20)

%%find fits to histogram
%changed 06.17.10 by Shal to accomodate no interactions found
f_Atau=inline('mse(data,x(1)*exp(-t/x(2)))','x','t','data');
f_A=inline('mse(data,x(1)*exp(-t/tau))','x','t','tau','data');
options=optimset('display','off');
```

```matlab
X0=[Thist(1) Thistbins(end)/2]';
Atau=fminsearch(f_Atau,X0,options,Thistbins,Thist);
X0=[Thist(1)];
t_hmm=HMM_PreProcessData.found_Tau_BB;
A=fminsearch(f_A,X0,options,Thistbins,t_hmm,Thist);

model_fithist=Atau(1)*exp(-Thistbins/Atau(2));
model_hmm=A*exp(-Thistbins/t_hmm);

h=figure
bar(Thistbins,Thist,'k','linewidth', 2)
hold on
plot(Thistbins,model_fithist,'r','linewidth',2)
plot(Thistbins,model_hmm,'g','linewidth',2)

xlabel('Dimer Event Lifetime (frames)','Fontsize', 16)
ylabel('Number of Events','Fontsize',16)

s1=sprintf('Fit to Histogram. tau=%g frames',Atau(2))
s2=sprintf('HMM Model. tau=%g frames',t_hmm)
legend({'Data',s1,s2})

title(fnbase)

saveas(h, [OutDir '\' fnbase '_LifetimeDist.jpg'], 'jpg');
end
%% save back to file

HMM_PreProcessData.FilledStates=FilledStates;
HMM_PreProcessData.StateLength=StateLength;

save(HMM_PreProcessFile,'HMM_PreProcessData');

varargout{1}=HMM_PreProcessData;

function varargout = HMM_PlotCandidates_test(varargin)
%HMM_PlotCandidates(preprocessfile,resdir)
%This function will take the HMM_PreProcess files (of the type *.HMMPP) and make
3D trajectory
%plot and separation distance plot of the candidate pairs.
%Images will be saved (to directory 'resdir') to view later.
%
%written by Diane Lidke and Shalini Low-Nam
%April 15, 2010
%
%Example call of this function:
```

```matlab
%HMM_PlotCandidates('Z:\Shal\EGFDimerExamples\test.HMMPP','Z:\Shal\EGFDimer
Examples\CandidatePairs\');

%%Setup for DIPimage menu
d = struct('menu','HMM',...
    'display','HMM Plot Candidates',...
    'inparams',struct('name',{'HMM_DataFile','Out_Dir'},...
    'description',{'HMM PreProcess File','Output Directory'},...
    'type',      {'infile','indir'},...
    'dim_check',  {0,0},...
    'range_check',{'*.HMMPP','*.*'},...
    'required',   {0,0},...
    'default',    {'',''}...
    ),...
    'outparams',struct('name',{'tracklengths','ratios'},...
    'description',{'Track Lengths','Ratios'},...
    'type',{'strct'}...
    )...
    );
if nargin == 1
    s = varargin{1};
    if ischar(s) & strcmp(s,'DIP_GetParamList')
        varargout{1} = d;
        return
    end
end
try
    [HMM_PreProcessFile,OutDir] = getparams(d,varargin{:});
catch
    if ~isempty(paramerror)
        error(paramerror)
    else
        error(firsterr)
    end
end
%% Load PreProcess file and make ResultsDir
HMM_PreProcessFile=varargin{1};
load(HMM_PreProcessFile,'-mat');
resdir=OutDir;
mkdir(resdir);

numfile=size(HMM_PreProcessData.FileID, 2);


%% 3D plot of all tracks in ch1(r) and ch2(g)
%plot candidate pairs 3D trajectory + label
%ch = red, QD655;  ch2 = green, QD585
```

```matlab
sz=0;
for hh=1:numfile  %loop through each file
    tmp=max(strfind(HMM_PreProcessData.FileID{hh},'\'));

    fname = HMM_PreProcessData.FileID{hh};
    load([fname],'-mat');
    basename=fname(tmp+1:end-8);

    h(1,3) = figure;
    ah = gca;

    pair=HMM_PreProcessData.PairID{hh};
    numpairs=size(pair,1);
    d=zeros(numpairs,1000);
    state=HMM_PreProcessData.StateMatrix{hh};
    dimer=HMM_PreProcessData.FilledStates{hh};
    for ii=1:numpairs %size(ch,1)
        ch1spot=pair(ii,1);
        ch2spot=pair(ii,2); %%%THERE NEEDS TO BE A CHECK FOR SHIFTED
TRACKS!!
        xch1=HMM_Data.raw_ch1_tracks(ch1spot,:,1);
        ych1=HMM_Data.raw_ch1_tracks(ch1spot,:,2);

        s1=logical(xch1(:,:)); %find the valid points of trajectory 1
        tmps1=find(s1,1); %start of trajectory 1
        tmpe1=max(find(s1)); %end of trajectory 1
        l1=tmpe1-tmps1+1; %length of trajectory 1

        xch2=HMM_Data.shifted_ch2_tracks(ch2spot,:,1);
        ych2=HMM_Data.shifted_ch2_tracks(ch2spot,:,2);
    %       xch2=HMM_Data.ch2_tracks(ch2spot,:,1);
    %       ych2=HMM_Data.ch2_tracks(ch2spot,:,2);

        s2=logical(xch2(:,:)); %find the valid points of trajectory 2
        tmps2=find(s2,1); %start of trajectory 2
        tmpe2=max(find(s2)); %end of trajectory 2
        l2=tmpe2-tmps2+1; %length of trajectory 2

        intensities1(ii,:)=HMM_Data.ch1_intensities(ch1spot,:); %For bleedthrough check
        intensities2(ii,:)=HMM_Data.ch2_intensities(ch2spot,:);

        valid=dimer(ii,:); %valids of when dimer

        hsvline(squeeze(xch1),squeeze(ych1),HMM_Data.TimeStep,h(1,3),2,1,[],[],[],[],[1  0
0],[],[],1);
```

213

```matlab
    hold on
    hsvline(squeeze(xch2),squeeze(ych2),HMM_Data.TimeStep,h(1,3),2,1,[],[],[],[],[0 1
0],[],[],1);
    hold on
    xlabel('X Coordinate')
    ylabel('Y Coordinate')
    zlabel('Time (s)')

    if sum(state(ii,:))>0
        dimerextent=sum(dimer(ii,:));
        sz=sz+1;
        tracklengths(sz,:)=[hh pair(ii,1) pair(ii,2) l1 l2 dimerextent];


hsvline(squeeze(xch1).*valid,squeeze(ych1).*valid,HMM_Data.TimeStep,h(1,3),2,1,1.5,[
],[],[],[1 0 0]*.3,[],'o',1);
        hold on

hsvline(squeeze(xch2).*valid,squeeze(ych2).*valid,HMM_Data.TimeStep,h(1,3),2,1,1.5,[
],[],[],[0 1 0]*.3,[],'d',1);  %.*logical(state(ii,:))
        hold on

        set(findall(allchild(gca),'type','line'),'markersize',0.3)

    else
        hold on
    end

    text(xch1(find(logical(xch1),1)),...
        ych1(find(logical(ych1),1)),...
        find(logical(xch1),1)*HMM_Data.TimeStep,num2str(ch1spot));

    text(xch2(find(logical(xch2),1)),...
        ych2(find(logical(ych2),1)),...
        find(logical(xch2),1)*HMM_Data.TimeStep,num2str(ch2spot));

    axis tight
end

hold off
title(basename)
axis tight
saveas(h(1,3),[resdir basename '_3D' ],'fig');

for nn=1:numpairs %Focal Drift Plots with State
    ch1spot=pair(nn,1);
```

```matlab
        ch2spot=pair(nn,2);

        figure
        trace=dimer(nn,:);

        x1=[0.05:.05:50];
        y1=trace;
        hl1 = line(x1,y1,'Color',[0 1 0]*0.6,'linewidth',5);
        ax1 = gca;
        set(ax1,'XColor',[0 1 0]*0.3,'YColor',[0 1 0]*0.3);
        axis([0 50 0 1.05]);
        xlabel('Time (s)')
        ylabel('State')

        sigma1=HMM_Data.ch1_sigma(ch1spot,:);
        sigma2=HMM_Data.ch2_sigma(ch2spot,:);
        ax2 = axes('Position',get(ax1,'Position'),...
            'XAxisLocation','top',...
            'YAxisLocation','right',...
            'Color','none',...
            'XColor','k','YColor','k');
        ylabel('Sigma (\mu m)')
        x2=[0.05:.05:50];
        y2=sigma1;
        z2=sigma2;
        svalids1=logical(sigma1);
        svalids2=logical(sigma2);
        hl2 = line(x2(svalids1),y2(svalids1).*0.267,'Color','r','Parent',ax2,'linewidth',0.7);
        hl3 = line(x2(svalids2),z2(svalids2).*0.267,'Color','g','Parent',ax2,'linewidth',0.7);
        hold off
        title('Sigmas of found dimers');
        saveas(gcf, [resdir basename '_Sigma_ch1_' num2str(ch1spot) '_ch2_'
num2str(ch2spot)], 'jpg');

        close all
        clear trace
    end

    for mm=1:numpairs %Focal Drift Plots with Distance
        ch1spot=pair(mm,1);
        ch2spot=pair(mm,2);

        xch1=HMM_Data.raw_ch1_tracks(ch1spot,:,1);
        ych1=HMM_Data.raw_ch1_tracks(ch1spot,:,2);

        xch2=HMM_Data.shifted_ch2_tracks(ch2spot,:,1);
```

215

```matlab
        ych2=HMM_Data.shifted_ch2_tracks(ch2spot,:,2);
%         xch2=HMM_Data.ch2_tracks(ch2spot,:,1);
%         ych2=HMM_Data.ch2_tracks(ch2spot,:,2);

        figure

        d(mm,:)=sqrt((xch1-xch2).^2+(ych1-ych2).^2).*logical(xch1).*logical(xch2);
        d=(d(mm,:).*0.267);
        x1=[0.05:.05:50];
        y1=d;
        dvalids=logical(d);
        hl1 = line(x1(dvalids),y1(dvalids),'Color','b','linewidth',1);
        ax1 = gca;
        set(ax1,'XColor',[0 0 1],'YColor',[0 0 1]);
        axis([0 50 0 1.5]);
        xlabel('Time (s)')
        ylabel('Distance (\mu m)')

        hold on
        sigma1=HMM_Data.ch1_sigma(ch1spot,:);
        sigma2=HMM_Data.ch2_sigma(ch2spot,:);
        ax2 = axes('Position',get(ax1,'Position'),...
           'XAxisLocation','top',...
           'YAxisLocation','right',...
           'Color','none',...
           'XColor','k','YColor','k');
        %axis([0 50 0 1.5]);
        ylabel('Sigma (\mu m)')
        x2=[0.05:.05:50];
        y2=sigma1;
        z2=sigma2;
        svalids1=logical(sigma1);
        svalids2=logical(sigma2);
        hl2 = line(x2(svalids1),y2(svalids1).*0.267,'Color','r','Parent',ax2,'linewidth',0.7);
        hl3 = line(x2(svalids2),z2(svalids2).*0.267,'Color','g','Parent',ax2,'linewidth',0.7);
        hold off
        title('Sigmas and Distance');

        saveas(gcf, [resdir basename '_Sigma_and_Distance_ch1_' num2str(ch1spot)
'_ch2_' num2str(ch2spot)], 'fig');
        close all

    end

    for nn=1:numpairs %Distance Plots
        ch1spot=pair(nn,1);
```

216

```matlab
    ch2spot=pair(nn,2); %%THERE NEEDS TO BE A CHECK FOR SHIFTED
TRACKS!!

    xch1=HMM_Data.raw_ch1_tracks(ch1spot,:,1);
    ych1=HMM_Data.raw_ch1_tracks(ch1spot,:,2);

%       xch2=HMM_Data.ch2_tracks(ch2spot,:,1);
%       ych2=HMM_Data.ch2_tracks(ch2spot,:,2);
    xch2=HMM_Data.shifted_ch2_tracks(ch2spot,:,1);
    ych2=HMM_Data.shifted_ch2_tracks(ch2spot,:,2);

    figure

    trace=dimer(nn,:);

    x1=[0.05:.05:50];
    y1=trace;
    hl1 = line(x1,y1,'Color',[0 1 0]*0.6,'linewidth',5);
    ax1 = gca;
    set(ax1,'XColor',[0 1 0]*0.3,'YColor',[0 1 0]*0.3);
    axis([0 50 0 1.05]);
    xlabel('Time (s)')
    ylabel('State')

    d(nn,:)=sqrt((xch1-xch2).^2+(ych1-ych2).^2).*logical(xch1).*logical(xch2);
    d=(d(nn,:).*0.267);
    ax2 = axes('Position',get(ax1,'Position'),...
       'XAxisLocation','top',...
       'YAxisLocation','right',...
       'Color','none',...
       'XColor','k','YColor','k');
    ylabel('Distance (\mu m)')
    x2=[0.05:.05:50];
    y2=d;
    dvalids=logical(d);
    hl2 = line(x2(dvalids),y2(dvalids),'Color','b','Parent',ax2,'linewidth',1);

    hold on
    ID=0.1; %a horizontal line for the specified interaction distance
    line([0.05;50],[ID;ID],'Color','m','linewidth',0.3,'LineStyle','--')
    hold off
    title('Distance between QDs of found dimers');

    saveas(gcf, [resdir basename '_D_ch1_' num2str(ch1spot) '_ch2_'
num2str(ch2spot)], 'jpg');
    close all
```

217

```matlab
        clear trace
    end

%     for ff=1:numpairs %Intensity plots to check for bleedthrough
%     (simultaneous blinking)
%         ch1spot=pair(ff,1);
%         ch2spot=pair(ff,2);
%         figure
%         plot(intensities1(ff,:),'color',[1 0 0],'linewidth',1)
%         hold on
%         plot(intensities2(ff,:),'color',[0 1 0],'linewidth',1)
%         xlabel('Frame number')
%         ylabel('Intensity')
%             saveas(gcf, [resdir basename 'Intensities_ch1_' num2str(ch1spot) '_ch2_'
num2str(ch2spot)], 'jpg');
%         close all
%     end

    for ll=1:numpairs %Localization accuracy plots
        ch1spot=pair(ll,1);
        ch2spot=pair(ll,2);
        LA1=HMM_Data.ch1_LA(ch1spot,:);
        LA2=HMM_Data.ch2_LA(ch2spot,:);
        figure
        plot(LA1(logical(LA1))*0.267,'color',[1 0 0],'linewidth',1)
        hold on
        plot(LA2(logical(LA2))*0.267,'color',[0 1 0],'linewidth',1)
        xlabel('Frame number')
        ylabel('Localization Accuracy (\mu m)')
        title('Localization Accuracy of Candidate Trajectories');
        saveas(gcf,    [resdir    basename    '_LA_ch1_'    num2str(ch1spot)    '_ch2_'
num2str(ch2spot)], 'jpg');
        close all
    end

    for pp=1:numpairs %P Matrix with Filled States
        ch1spot=pair(pp,1);
        ch2spot=pair(pp,2);
        P=HMM_PreProcessData.PMatrix{hh};

        figure
        trace=dimer(pp,:);

        x1=[0.05:.05:50];
        y1=trace;
        hl1 = line(x1,y1,'Color',[0 1 0]*0.6,'linewidth',5);
```

218

```matlab
        ax1 = gca;
        set(ax1,'XColor',[0 1 0]*0.3,'YColor',[0 1 0]*0.3)
        axis([0 50 0 1.05]);
        xlabel('Time (s)')
        ylabel('State')

        x2=[0.05:.05:50];
        y2=P(pp,:);
        ax2 = axes('Position',get(ax1,'Position'),...
            'XAxisLocation','top',...
            'YAxisLocation','right',...
            'Color','none',...
            'XColor','k','YColor','k');
        hl2            =            line(x2(logical(y2)),y2(logical(y2)),'Color',[0          1
1]*0.8,'Parent',ax2,'linewidth',0.9);
        ylabel('Probability')
        title('Probability of found interactions');
        saveas(gcf,   [resdir   basename   '_PMatrix_ch1_'   num2str(ch1spot)   '_ch2_'
num2str(ch2spot)], 'jpg');
        close all
        clear trace
    end
    clear tmp d fname basename

end


%%determine ratios of dimer duration to track length
if exist('tracklengths')
    ratio=zeros(size(tracklengths,1),4);
    for rr=1:size(tracklengths,1)
        pair1(rr)=tracklengths(rr,2);
        pair2(rr)=tracklengths(rr,3);
        ratio1(rr)=(tracklengths(rr,6)/tracklengths(rr,4))*100;
        ratio2(rr)=(tracklengths(rr,6)/tracklengths(rr,5))*100;
        ratio(rr,:)=[pair1(rr) pair2(rr) ratio1(rr) ratio2(rr)];
        clear pair1 pair2 ratio1 ratio2
    end
end
try
    varargout{1}=tracklengths;
    varargout{2}=ratio;
    save([resdir 'CandidateTrackLengths.mat'],'tracklengths','ratio');
catch
end

%%3-State HMM analysis of candidate pairs
```

219

```matlab
% datadir='Z:\Shal\SPT Data\GroupedData_A431_Final\HMM Final\';
% IntDis=50; %nm (overlay error)+(probe separation in a dimer)
% L=1; %micron.  Analysis is restricted to frames where separation is less than L
% DomainSize=250; %nm based on observation of excursion-and-return distance
% minOLF=10; %frames. Minimum number of overlapping valid frames of two tracks for
inclusion in analysis
% minTL=50; %frames.  Tracks must have valid points separated by this value or larger
or are excluded
% DC=.5; %duty cycle.  Tracks must have a (valid frames)/(track length) ratio greater
than DC
% appThresh=.2;%micron Tracks must get this close at least once to be included
% minOLT=10; %frames. Minimum number of overlapping frames (valid or invalid) of
two tracks for inclusion in analysis

%%EGF
for DS=150
    for ID=50
        datadir='Z:\Shal\SPT Data\GroupedData_A431_Final\HMM Final\';
        L=1; %micron.  Analysis is restricted to frames where separation is less than L
        minOLF=10; %frames. Minimum number of overlapping valid frames of two tracks
for inclusion in analysis
        minTL=50; %frames.  Tracks must have valid points separated by this value or
larger or are excluded
        DC=.5; %duty cycle.  Tracks must have a (valid frames)/(track length) ratio greater
than DC
        appThresh=.2;%micron Tracks must get this close at least once to be included
        minOLT=10; %frames. Minimum number of overlapping frames (valid or invalid) of
two tracks for inclusion in analysis
        HMM_PreProcessData = HMM_PreProcessStates([datadir 'HMM EGF\'],'QD
EGF',[datadir 'HMM EGF\EGF_3state_DD' num2str(DS) 'nm_ID' num2str(ID)
'nm.HMMPP'],ID,DS,L,minOLF,minTL,DC,minOLT,appThresh);
        [HMM_PreProcessData K_found K_found_err] = HMM_FindRates([datadir 'HMM
EGF\EGF_3state_DD' num2str(DS) 'nm_ID' num2str(ID) 'nm.HMMPP']);
        clear HMM_PreProcessData
    end
end
HMM_PreProcessData = HMM_FindStates([datadir 'HMM EGF\EGF_3state_DD'
num2str(DS) 'nm_ID' num2str(ID) 'nm.HMMPP']);
HMM_PreProcessData = HMM_StatesDist([datadir 'HMM EGF\EGF_3state_DD'
num2str(DS) 'nm_ID' num2str(ID) 'nm.HMMPP'],[datadir 'HMM EGF\EGF_3state_DD'
num2str(DS) 'nm_ID' num2str(ID) 'nm.HMMPP']);
HMM_PlotCandidates_3state([datadir 'HMM EGF\EGF_3state_DD' num2str(DS)
'nm_ID' num2str(ID) 'nm.HMMPP'],[datadir 'HMM
EGF\CandidatePlotsFinalTest_3state_DD' num2str(DS) 'nm_ID' num2str(ID) 'nm\'],1)
```

```matlab
datapath='Z:\Shal\SPT Data\GroupedData_A431_Final\HMM Final\HMM UNM HeLa EGF\';
ppfilestring='EGF_3state_DD150nm_ID50nm.HMMPP';
resdir=datapath;
HMM_StatesHist(datapath,ppfilestring,resdir)
clear

uiopen('Z:\Shal\SPT Data\GroupedData_A431_Final\HMM Final\HMM UNM HeLa EGF\EGF_3state_DD150nm_ID50nm.HMMPP',1)
EGF=HMM_PreProcessData.StateLength;
EGF=sort(EGF); %if there are events of 50 s, extra line needed
EGF=EGF./20;
edges=0:1:50;
N_EGF=histc(EGF,edges)
figure; bar(N_EGF,'b');

function varargout = HMM_PreProcessStates(varargin)

conditions ={'QD EGF','QD Nanobody','QD EGF + PD','QD Nanobody + PD',...
    'QD Nanobody + dEGF','QD Nanobody + dEGF + PD','All','QD EGF + QD VhH',...
    'QD Neu','QD rH','QD IgE','QD IgE DNP(0.01ug/ml)','QD IgE PP2(10uM)',...
    'QD IgE DNP(0.1ug/ml) PP2(10uM)','QD IgE + DNP(1ug/ml)','QD IgE DNP(1ug/ml)',...
    'QD IgE + DNP(0.01ug/ml)','QD IgE DNP(0.01ug/ml)','QD IgE + DNP(0.1ug/ml)',...
    'QD IgE DNP(0.1ug/ml)','QD IgE + DNP(0.01ug/ml) PP2(10uM)','QD IgE + DNP(0.1ug/ml) PP2(10uM)',...
    'QD IgE DNP(0.01ug/ml) PP2(10uM)','QD rH + QD EGF','QD rH + QD EGF + PD','QD Neu + Lap30min'};

d = struct('menu','HMM',...
    'display','HMM Pre-Process Data',...
    'inparams',struct('name',{'HMM_DataDir','DataConditions','OutFile',...
    'IntDis','DomainSize','L','MinOverlap','MinPath','DutyCycle','MinTime','D_Thresh'},...
    'description',{'HMM DataFile Directory','Data Conditions','OutPutFile',...
    'Max Dimer Separation (nm)','Domain Size (nm)','Analysis Threshold (microns)','Min Overlapping Valid Frames',...
    'Min Traj Length (frames)','Duty Cycle','Min Overlapping Time (Frames)','Close Approach Threshold (microns)'},...
    'type',
{'indir','option','outfile','array','array','array','array','array','array','array','array'},...
    'dim_check', {0,0,0,0,0,0,0,0,0,0,0},...
    'range_check',{'*.HMMData',conditions,'*.HMMPP',[],[],[],[],[],[],[],[]},...
    'required', {0,0,0,0,0,0,0,0,0,0,0},...
    'default', {'',conditions{1},'',30,100,3,10,50,0.5,20,0.2}...
    ),...
    'outparams',struct('name',{'HMM_PreProcessData'},...
    'description',{'HMM PreProcessed Data Structure'},...
```

```
      'type',{'strct'}...
   )...
   );
if nargin == 1
   s = varargin{1};
   if ischar(s) & strcmp(s,'DIP_GetParamList')
      varargout{1} = d;
      return
   end
end
try
   [HMM_DataDir,DataConditions,OutFile,...
      IntDis,DomainSize,L,MinOverlap,MinPath,DutyCycle,MinTime,D_Thresh]          =
getparams(d,varargin{:});
catch
   if ~isempty(paramerror)
      error(paramerror)
   else
      error(firsterr)
   end
end

_____

%% Make a list of files to process

f=dir([HMM_DataDir '\*.HMMData']);

Files=[];
cnt=1;
switch DataConditions
   case 'All'
      for ii=1:size(f,1)
         Files(Paez et al.)=f(ii).name;
      end
   otherwise
      for ii=1:size(f,1)
         load([HMM_DataDir '\' f(ii).name],'-mat');
         if strmatch(HMM_Data.DataConditions,DataConditions,'exact')
            Files{cnt}=f(ii).name;
            cnt=cnt+1;
         end
      end
end

if isempty(Files)
   warning('no files with that condition are found \n');
   varargout{1}=[];
```

222

```matlab
        return
end

%% Process Files

Nfiles=size(Files,2);

StartFrame=cell(0,0);
EndFrame=cell(0,0);
PairID=cell(0,0);
FileID=cell(0,0);

for nn=1:Nfiles
    fprintf('Processing File: %s \n',Files{nn})
    load([HMM_DataDir '\' Files{nn}],'-mat');
    if isfield(HMM_Data,'raw_ch1_tracks')

        [P_states{nn}        V_states{nn}        StartFrame{nn}        EndFrame{nn}
PairID{nn}]=PP(HMM_Data,...
            DutyCycle,MinTime,L/HMM_Data.PixelSize,MinOverlap,MinPath,...

IntDis/HMM_Data.PixelSize/1000,DomainSize/HMM_Data.PixelSize/1000,D_Thresh/H
MM_Data.PixelSize);

        FileID{nn}=[HMM_DataDir '\' Files{nn}];

        Npairs=size(P_states{nn},3);

        if isempty(P_states{nn})
            warning('no interactions found in the following data set:')
            [HMM_DataDir '\' Files{nn}]
        else
            fprintf('Interactions found between : \n')
            for nf=1:Npairs
                fprintf('ch1: %d   ch2: %d \n',PairID{nn}(nf,1), PairID{nn}(nf,2))
            end
            fprintf('\n')
        end
    else
        warning('no trajectories in data set')
        continue
    end
end

HMM_PreProcessData.StartFrame=StartFrame;
HMM_PreProcessData.EndFrame=EndFrame;
```

223

```matlab
HMM_PreProcessData.PairID=PairID;
HMM_PreProcessData.FileID=FileID;
HMM_PreProcessData.D_Thresh=D_Thresh;
HMM_PreProcessData.IntDis=IntDis/HMM_Data.PixelSize/1000; %in pixels
HMM_PreProcessData.L=L/HMM_Data.PixelSize; %in pixels
HMM_PreProcessData.MinOverlap=MinOverlap;
HMM_PreProcessData.MinPath=MinPath;
HMM_PreProcessData.DutyCycle=DutyCycle;
HMM_PreProcessData.MinTime=MinTime;

HMM_PreProcessData.Nstates=3;
HMM_PreProcessData.P_states=P_states;
HMM_PreProcessData.V_states=V_states;
HMM_PreProcessData.DomainSize=DomainSize/HMM_Data.PixelSize/1000;        %in
pixels

save([OutFile],'HMM_PreProcessData');

varargout{1}=HMM_PreProcessData;

end


function                [P            Vout           StartFrame            EndFrame
PairID]=PP(HMM_Data,DutyCycle,MinTime,L,MinOverlap,MinPath,IntDis,DomainSize,D
_Thresh)
%Written by Shalini Low-Nam and Keith Lidke
%this calculates the pmatrix for 1 data set
P=[];
Vout=[];
StartFrame=[];
EndFrame=[];
PairID=[];
FileID=[];

Nframes=size(HMM_Data.raw_ch1_tracks,2);

%all sizes in pixels, frames
t1=HMM_Data.raw_ch1_tracks;
%t2=HMM_Data.ch2_tracks; %for data transformed during tracking
t2=HMM_Data.shifted_ch2_tracks; %this should be the shifted tracks, common
coordinate registration
v1=HMM_Data.ch1_valids;
v2=HMM_Data.ch2_valids;
s1=HMM_Data.ch1_LA;
s2=HMM_Data.ch2_LA;
```

224

```
Diff=HMM_Data.Dconvert;
OverlayError=HMM_Data.tform.error.fre; %in pixels

%temp hack
v1=logical(v1(:,:,1));
v2=logical(v2(:,:,1));

Ntracks_1=size(t1,1);
Ntracks_2=size(t2,1);
num=1;

P_bound=inline('1./S2.*exp(-d.^2./(2*S2)).*d','d','S2');
P_free=inline('2/L^2*d','d','L');
P_freeD=inline('r/(2*pi*S2)*.01*sum(                        exp(-r^2/(2*S2)-
d^2/(2*S2)+r*d/S2*sin((0:.01:2*pi))))','r','d','S2');

for nn1=1:Ntracks_1
    sf1=find(v1(nn1,:),1); %find start frame
    ef1=max(find(v1(nn1,:))); %find end frame
    if isempty(sf1); continue; end
    if (ef1-sf1)<MinTime;continue;end %rule out short tracks
    if (sum(v1(nn1,sf1:ef1))/(ef1-sf1))<DutyCycle;continue;end %rule out low duty cycle
tracks

    for nn2=1:Ntracks_2
        sf2=find(v2(nn2,:),1); %find start frame
        ef2=max(find(v2(nn2,:))); %find end frame
        if isempty(sf2); continue; end
        if (ef2-sf2)<MinTime;continue;end %rule out short tracks
        if (sum(v2(nn2,sf2:ef2))/(ef2-sf2))<DutyCycle;continue;end %rule out low duty cyle
tracks

        validmask=(v1(nn1,:).*v2(nn2,:))==1;
        x1=t1(nn1,:,1);
        y1=t1(nn1,:,2);
        x2=t2(nn2,:,1);
        y2=t2(nn2,:,2);

        d=sqrt((x2(validmask)-x1(validmask)).^2+(y2(validmask)-y1(validmask)).^2);

        if min(d)> D_Thresh; continue; end %rule out tracks that don't get close enough
        if sum(d<L)< MinOverlap; continue; end %rule out tracks that don't overlap enough

        %now find start and end frames of the interaction
        dcandidate=sqrt((x1-x2).^2+(y1-y2).^2);
        mask=(dcandidate<=L).*validmask;
```

225

```matlab
sf=find(mask,1);
ef=max(find(mask));
T = ef- sf;
if T < MinPath; continue; end %rule out tracks that don't overlap for enough frames

D_array=zeros(Nframes,1);
Valids=zeros(Nframes,1);
for tt=sf:ef  %loop only startframe:endframe
   if v1(nn1,tt) && v2(nn2,tt)
      d=sqrt((x1(tt)-x2(tt))^2+(y1(tt)-y2(tt))^2);
      if d<=L
         D_array(tt)=d;
         Valids(tt)=1;
      end
   end
end

%Calculate Probalities
%localization errors are sqrt(sx^2+sy^2)
IDs=find(Valids);
S2_1=1/2*s1(nn1,IDs).^2+1/2*s2(nn2,IDs).^2+OverlayError.^2+IntDis.^2;
S2_2=1/2*s1(nn1,IDs).^2+1/2*s2(nn2,IDs).^2+OverlayError.^2+DomainSize.^2;

%index is for current, with a past valid
ID_now=IDs(2:end);
ID_past=IDs(1:end-1);
delt=ID_now-ID_past;
d_past=D_array(IDs(1:end-1));
d_now=D_array(IDs(2:end));

S2_3=1/2*s1(nn1,ID_past).^2+1/2*s2(nn2,ID_past).^2+...
   1/2*s1(nn1,ID_now).^2+1/2*s2(nn2,ID_now).^2+...
   OverlayError.^2+2*Diff*delt';

P1=P_bound(D_array(IDs),S2_1');
P2=P_bound(D_array(IDs),S2_2');
clear P3; P3(1)=P_free(D_array(IDs(1)),L);

for ii=2:length(d_now)+1;P3(ii)=P_freeD(d_now(ii-1),d_past(ii-1),S2_3(ii-1));end

P1out=zeros(Nframes,1);
P2out=zeros(Nframes,1);
P3out=zeros(Nframes,1);

P1out(IDs)=P1;
P2out(IDs)=P2;
```

226

```matlab
        P3out(IDs)=P3;

        %[D_array(1:10) P1out(1:10) P2out(1:10) P3out(1:10)]
        Vout(:,num)=Valids;

        P(:,:,num)=cat(2,P1out,P2out,P3out);

        PairID(num,:)=[nn1,nn2];
        StartFrame(num)=sf;
        EndFrame(num)=ef;

        num=num+1;
    end
end
end

function varargout = HMM_FindRates(varargin)

d = struct('menu','HMM',...
    'display','HMM Find Lifetimes',...
    'inparams',struct('name',{'HMM_PreProcessFile'},...
    'description',{'HMM PreProcess File'},...
    'type',      {'infile'},...
    'dim_check',  {0},...
    'range_check',{'*.HMMPP'},...
    'required',   {0},...
    'default',    {''}...
    ),...
    'outparams',struct('name',{'HMM_PreProcessData','K_found','K_found_err'},...
    'description',{'Modified HMM Data Structure','Found k matrix','precision of k matrix'},...
    'type',{'strct','array','array'}...
    )...
    );
if nargin == 1
    s = varargin{1};
    if ischar(s) & strcmp(s,'DIP_GetParamList')
        varargout{1} = d;
        return
    end
end
try
    [HMM_PreProcessFile] = getparams(d,varargin{:});
catch
    if ~isempty(paramerror)
        error(paramerror)
    else
```

227

```
        error(firsterr)
    end
end

load(HMM_PreProcessFile,'-mat');

%get number of states
N=HMM_PreProcessData.Nstates;
_____

%% Use fminsearch to maximize likelihood
options=optimset('TolX',10e-8,'MaxFunEvals',10e8,'MaxIter',10e8,'Display','iter');
func=@PODHMM; %this points to the function that will be minimized

X0=repmat(.001,[N*(N-1)  1]); %these  are  the  starting  guesses;  value  of  X0=0.001
decided 08.19.2010
LB=repmat(0,[N*(N-1) 1]);
UB=repmat(1,[N*(N-1) 1]);
[out]=fminsearch(func,X0,options,HMM_PreProcessData,N); %original
%[out]=lsqnonlin(func,X0,LB,UB,options,HMM_PreProcessData,N); %PJC

out=abs(out);

mask=~eye(N);
K=zeros(N,N);
K(mask)=out;

% find errors
%1: calculate Hessian:
sz=N*(N-1);
H=zeros(sz,sz);
deltaf=.05; %use a 5 percent change around found k value
mindeltaf=10e-8;
for ii=1:sz
    for jj=1:sz
        deltaii=max(deltaf*out(ii),mindeltaf);
        deltajj=max(deltaf*out(jj),mindeltaf);

        %measure slope wrt ii at two positions of jj
        K_in1=out;
        K_in2=out;
        K_in1(ii)=K_in1(ii)-deltaii/2;
        K_in2(ii)=K_in2(ii)+deltaii/2;
        K_in1(jj)=K_in1(jj)-deltajj/2;
        K_in2(jj)=K_in2(jj)-deltajj/2;
        s1=1/deltaii*(PODHMM(K_in2,HMM_PreProcessData,N)-
PODHMM(K_in1,HMM_PreProcessData,N));
```

```matlab
    %s1 = sum(s1); %PJC

    K_in1=out;
    K_in2=out;
    K_in1(ii)=K_in1(ii)-deltaii/2;
    K_in2(ii)=K_in2(ii)+deltaii/2;
    K_in1(jj)=K_in1(jj)+deltajj/2;
    K_in2(jj)=K_in2(jj)+deltajj/2;
    s2=1/deltaii*(PODHMM(K_in2,HMM_PreProcessData,N)-
PODHMM(K_in1,HMM_PreProcessData,N));
    %s2 = sum(s2); %PJC

    H(ii,jj)=1/deltajj*(s2-s1);
  end
end
K_err=sqrt(diag(inv(H)));
HMM_PreProcessData.K_matrix_found=K
HMM_PreProcessData.K_matrix_found_err=K_err
HMM_PreProcessData.K_matrix_found_Hessian=H;

HMM_PreProcessData.lnP=PODHMM(out,HMM_PreProcessData,N); %this  calculates
the lnP at the found k values

save(HMM_PreProcessFile,'-mat');

varargout{1}=HMM_PreProcessData;
varargout{2}=K;
varargout{3}=K_err;


function lnP=PODHMM(K_vector,HMM_PreProcessData,N)
%K_vector must be a vector for fminsearch. Size is N*(N-1). Convert back to matrix
%N: number of states

mask=~eye(N);
K=zeros(N,N);
K(mask)=K_vector;

%if(min(min(K)))<0; warning('negative rate constant');end;
K=abs(K);

%disp(K_vector) %original

Nfiles=size(HMM_PreProcessData.P_states,2); %Number of files to analyze

RegionSize=HMM_PreProcessData.L;
```

```matlab
lnP=0; %original
for ii=1:Nfiles
    %fprintf ('Analyzing file %d of %d \n',ii,N) %original

    P_states=HMM_PreProcessData.P_states(Paez et al.); %probability of each state in
each timestep
    V_states=HMM_PreProcessData.V_states(Paez et al.); %indicates valid time frames
for analysis

    if isempty(P_states);continue;end

    for pp=1:size(P_states,3) %pairs in file

        VFrames=sum(V_states(:,pp)); %valid time frames
        if ~VFrames;continue;end

        %prepare input for HMM_lnP
        Frames=size(P_states,1);
        T=(1:Frames)';
        mask=logical(V_states(:,pp));
        T=T(mask); %times for valid analyis
        P=P_states(mask,:,pp);
        [lnP_pair]=HMM_lnP(P,T,K);
        lnP=lnP+lnP_pair;
    end
end
lnP=-lnP;

function varargout = HMM_FindStates(varargin)

d = struct('menu','HMM',...
    'display','HMM Find States',...
    'inparams',struct('name',{'HMM_PreProcessFile','K'},...
    'description',{'HMM PreProcess File','k vector (0 for HMMPP value)'},...
    'type',      {'infile','array'},...
    'dim_check',  {0,0},...
    'range_check',{'*.HMMPP',[]},...
    'required',   {0,0},...
    'default',    {'',0}...
    ),...
    'outparams',struct('name',{'HMM_PreProcessData'},...
    'description',{'HMM_PreProcessData Structure'},...
    'type',{'strct'}...
    )...
    );
```

230

```matlab
if nargin == 1
   s = varargin{1};
   if ischar(s) & strcmp(s,'DIP_GetParamList')
      varargout{1} = d;
      return
   end
end
try
   [HMM_PreProcessFile,K] = getparams(d,varargin{:});
catch
   if ~isempty(paramerror)
      error(paramerror)
   else
      error(firsterr)
   end
end

load(HMM_PreProcessFile,'-mat');
Nfiles=size(HMM_PreProcessData.P_states,2); %Number of files to analyze

if ~(K(1))
   K_matrix=HMM_PreProcessData.K_matrix_found;
end

StateMatrix{Nfiles}=[];
PViterbi{Nfiles}=[];


for ii=1:Nfiles %loop over files
   %fprintf ('Analyzing file %d of %d \n',ii,N)

   P_states=HMM_PreProcessData.P_states(Paez et al.); %probability of each state in
each timestep
   V_states=HMM_PreProcessData.V_states(Paez et al.); %indicates valid time frames
for analysis
   K_matrix=HMM_PreProcessData.K_matrix_found;   %matrix of rate constants
(k_from,to)
   N=size(K,1);

   if isempty(P_states);
      continue;
   end

   Npairs=size(P_states,3);%pairs in file
   Frames=size(V_states,1);
   States=zeros(Frames,Npairs);
```

```matlab
    Pout=zeros(Npairs,1);
    for pp=1:Npairs

        VFrames=sum(V_states(:,pp)); %valid time frames
        if ~VFrames;continue;end

        %prepare input for HMM_Viterbi
        Frames=size(P_states,1);
        T=(1:Frames)';
        T=T(logical(V_states(:,pp))); %times for valid analyis
        mask=repmat(V_states(:,pp),[1 N])>0;
        tmp=P_states(:,:,pp);
        P=reshape(tmp(mask),[sum(V_states(:,pp)) N]);

        [States(logical(V_states(:,pp)),pp) Pout(pp)]=HMM_Viterbi(P,T,K_matrix);
    end
    StateMatrix(Paez et al.)=States;
    PViterbi(Paez et al.)=Pout;
end
HMM_PreProcessData.StateMatrix=StateMatrix;
HMM_PreProcessData.PViterbi=PViterbi;

varargout{1}=HMM_PreProcessData;
save(HMM_PreProcessFile,'-mat');

end

function [States Pout]=HMM_Viterbi(P,T,K)
%HMM_Viterbi: Finds the most likely states of a Markov series
%
%INPUT:
%   P: A (Frames x N) probability matrix
%   T: Each element is a (Frames x 1) time array
%   K: NxN Matrix.  Rate constants for state transitions
%OUTPUT:
%   States: Mx1 Cell array.  Each element is a Tx1 State array.
%state are 1 based indexed

N=size(K,1);
Tsteps=size(T,1);

%intialize
Traj(:,1)=(1:N); %state space trajectory, grows to Nstates*T
P_old(1,:)=P(1,:);

%first index-from, second index-to
```

```matlab
for tt=2:Tsteps %loop over frames
    deltat=T(tt)-T(tt-1);
    HMM=K*deltat;
    HMM(eye(size(HMM,1))==1)=0;
    HMM(eye(size(HMM,1))==1)=1-sum(HMM,2);
    tmpTraj=Traj;

    %find best way to get to each current state
    for ss=1:N %looping over states at time t (current states)
        tmp=P_old.*HMM(:,ss)'.*P(tt,:);
        [Ptmp id]=max(tmp);
        P_new(ss)=Ptmp;
        tmpTraj(ss,1:tt-1)=Traj(id,:);
        tmpTraj(ss,tt)=id;
    end
    Traj=tmpTraj;
    P_old=P_new/sum(P_new);

    [Pout id]=max(P_old);
    States=Traj(id,:);
end

function varargout = HMM_StatesDist(varargin)
%This function fills state information for the 3-state HMM (similar to
%HMM_LifetimeDist for 2-state model)
%Written by Shalini Low-Nam

d = struct('menu','HMM',...
    'display','HMM Lifetime Distributions',...
    'inparams',struct('name',{'HMM_PreProcessFile','Out_Dir'},...
    'description',{'HMM PreProcess File','Output Directory'},...
    'type',      {'infile','indir'},...
    'dim_check',  {0,0},...
    'range_check',{'*.HMMPP','*.*'},...
    'required',   {0,0},...
    'default',    {'',''}...
    ),...
    'outparams',struct('name',{'HMM_PreProcessData'},...
    'description',{'HMM_PreProcessData structure'},...
    'type',{'strct'}...
    )...
    );
if nargin == 1
    s = varargin{1};
    if ischar(s) & strcmp(s,'DIP_GetParamList')
        varargout{1} = d;
```

```matlab
            return
        end
    end
try
    [HMM_PreProcessFile,OutDir] = getparams(d,varargin{:});
catch
    if ~isempty(paramerror)
        error(paramerror)
    else
        error(firsterr)
    end
end

%%
load(HMM_PreProcessFile,'-mat');

Nfiles=size(HMM_PreProcessData.P_states,2);

HMM_PreProcessData.StateMatrix{Nfiles}=[]; %In case the size of the StateMatrix does
not match that of P_states;
%commented out for simulations
SM=HMM_PreProcessData.StateMatrix;
PM=HMM_PreProcessData.P_states;

tmp=max(strfind(HMM_PreProcessFile,'\'));
fnbase=HMM_PreProcessFile(tmp+1:end-6);

cnt=1;
for nf=1:Nfiles
    sm=SM(Lund et al.);
    if sum(size(sm))==0
        FilledStates(Lund et al.)=[];
        continue
    else
        pm=PM(Lund et al.);
        shf=zeros([size(pm,1) size(pm,3)]); %create matrix for state with holes filled
        for nn=1:size(pm,3) %loop over number of candidate pairs
            s=sm(:,nn);
            if (sum(s))==0 %if there are no states; these are filled with state 3
                shf=3.*ones([size(pm,1) size(pm,3)]); %commented out new
                continue;
            end
            v=logical(pm(:,1,nn));
            state=s(1,:);
            for tt=1:max(find(v))
                if v(tt)&s(tt)&(~state) %start of a state
```

```
                sf=tt;
                state=s(tt); %which state has begun at sf
            end
            if    v(tt)&(~s(tt))&state|((tt==max(find(v)))&state)    %for    plotting    lifetimes;
currently incomplete
                ef=tt;
                %StateLength=ef-sf; %commented out for simulations
            end
            if v(tt);
                state=s(tt);
            end
            shf(tt,nn)=state;
        end
        shf(shf==0)=3; %replace any remaining zeros with 3
    end
    FilledStates(Lund et al.)=shf;
  end
end
```

```
%% save back to file

HMM_PreProcessData.FilledStates=FilledStates;
% HMM_PreProcessData.StateLength=StateLength;

save(HMM_PreProcessFile,'HMM_PreProcessData');

varargout{1}=HMM_PreProcessData;

function varargout = HMM_PlotCandidates_3state(varargin)
%HMM_PlotCandidates_3state(preprocessfile,resdir)
%This function will take the HMM_PreProcess files (of the type *.HMMPP) and make
3D trajectory
%plot and separation distance plot of the candidate pairs.
%Images will be saved (to directory 'resdir') to view later.
%
% input:
%  HMM_DataFile: HMM PreProcess File of the format .HMMPP
%  Out_Dir: path for saving plots
%  plot_flag: if 0 don't make plot else make plot. Default 1.
%
% output:
% Images will be saved (to directory 'Out_Dir') to view later.
%
%updated by Shalini Low-Nam
%July 14, 2010
%
```

235

```matlab
%Example call of this function:
%HMM_PlotCandidates('Z:\Shal\EGFDimerExamples\test.HMMPP','Z:\Shal\EGFDimer
Examples\CandidatePairs\');

%%Setup for DIPimage menu
d = struct('menu','HMM',...
   'display','HMM Plot Candidates',...
   'inparams',struct('name',{'HMM_DataFile','Out_Dir','plot_flag'},...
   'description',{'HMM PreProcess File','Output Directory','plot flag'},...
   'type',       {'infile','indir','boolean'},...
   'dim_check',  {0,0,0},...
   'range_check',{'*.HMMPP','*.*',[]},...
   'required',   {0,0,0},...
   'default',    {'','',1}...
   ),...
   'outparams',struct('name',{'tracklengths','ratios'},...
   'description',{'Track Lengths','Ratios'},...
   'type',{'strct'}...
   )...
   );
if nargin == 1
   s = varargin{1};
   if ischar(s) & strcmp(s,'DIP_GetParamList')
      varargout{1} = d;
      return
   end
end
try
   [HMM_PreProcessFile,OutDir,plot_flag] = getparams(d,varargin{:});
catch
   if ~isempty(paramerror)
      error(paramerror)
   else
      error(firsterr)
   end
end
%% Load PreProcess file and make ResultsDir
HMM_PreProcessFile=varargin{1};
load(HMM_PreProcessFile,'-mat');
resdir=OutDir;
mkdir(resdir);

numfile=size(HMM_PreProcessData.FileID, 2);


%% 3D plot of all tracks in ch1(r) and ch2(g)
%plot candidate pairs 3D trajectory + label
```

236

```matlab
%ch1 = red, QD655;  ch2 = green, QD585

for hh=1:numfile  %loop through each file
    try
        tmp=max(strfind(HMM_PreProcessData.FileID{hh},'\'));

        fname = HMM_PreProcessData.FileID{hh};
        load([fname],'-mat');
        basename=fname(tmp+1:end-8);
        if plot_flag
            h(1,3) = figure;
            ah = gca;

            pair=HMM_PreProcessData.PairID{hh};
            numpairs=size(pair,1);
            d=zeros(numpairs,1000);

            state=HMM_PreProcessData.FilledStates{hh}; %should be FILLEDSTATES
            dimer=state'==1; %where dimer state found
            domain=state'==2; %where domain state found
            free=state'==3; %where free state found

            for ii=1:numpairs %size(ch,1)
                ch1spot=pair(ii,1);
                ch2spot=pair(ii,2); %%THERE NEEDS TO BE A CHECK FOR SHIFTED
TRACKS!!
                xch1=HMM_Data.raw_ch1_tracks(ch1spot,:,1);
                ych1=HMM_Data.raw_ch1_tracks(ch1spot,:,2);

                s1=logical(xch1(:,:)); %find the valid points of trajectory 1
                tmps1=find(s1,1); %start of trajectory 1
                tmpe1=max(find(s1)); %end of trajectory 1
                l1=tmpe1-tmps1+1; %length of trajectory 1

                xch2=HMM_Data.shifted_ch2_tracks(ch2spot,:,1);
                ych2=HMM_Data.shifted_ch2_tracks(ch2spot,:,2);

                s2=logical(xch2(:,:)); %find the valid points of trajectory 2
                tmps2=find(s2,1); %start of trajectory 2
                tmpe2=max(find(s2)); %end of trajectory 2
                l2=tmpe2-tmps2+1; %length of trajectory 2

%               intensities1(ii,:)=HMM_Data.ch1_intensities(ch1spot,:); %For bleedthrough
check
%               intensities2(ii,:)=HMM_Data.ch2_intensities(ch2spot,:);
```

237

```matlab
            valid1=dimer(ii,:); %valids of when dimer
            valid2=domain(ii,:);


hsvline(squeeze(xch1),squeeze(ych1),HMM_Data.TimeStep,h(1,3),2,1,[],[],[],[],[1        0
0],[],[],1);
            hold on

hsvline(squeeze(xch2),squeeze(ych2),HMM_Data.TimeStep,h(1,3),2,1,[],[],[],[],[0        1
0],[],[],1);
            hold on
            xlabel('X Coordinate')
            ylabel('Y Coordinate')
            zlabel('Time (s)')

            if sum(dimer(ii,:))>0 %blue; dimer
                dimerextent=sum(dimer(ii,:));

hsvline(squeeze(xch1).*valid1,squeeze(ych1).*valid1,HMM_Data.TimeStep,h(1,3),2,1,1.
5,[],[],[],[0 0 1],[],'o',1);
                hold on

hsvline(squeeze(xch2).*valid1,squeeze(ych2).*valid1,HMM_Data.TimeStep,h(1,3),2,1,1.
5,[],[],[],[0 0 1],[],'d',1);  %.*logical(state(ii,:))
                hold on
                set(findall(allchild(gca),'type','line'),'markersize',2)
            else
                hold on
                if sum(domain(ii,:))>0 %purple; domain
                    domainextent=sum(domain(ii,:));

hsvline(squeeze(xch1).*valid2,squeeze(ych1).*valid2,HMM_Data.TimeStep,h(1,3),2,1,1.
5,[],[],[],[1 0 1]*0.7,[],'o',1);
                    hold on

hsvline(squeeze(xch2).*valid2,squeeze(ych2).*valid2,HMM_Data.TimeStep,h(1,3),2,1,1.
5,[],[],[],[1 0 1]*0.7,[],'d',1);  %.*logical(state(ii,:))
                    hold on
                    set(findall(allchild(gca),'type','line'),'markersize',2)
                else
                    hold on
                end
            end

            text(xch1(find(logical(xch1),1)),...
                ych1(find(logical(ych1),1)),...
```

238

```matlab
        find(logical(xch1),1)*HMM_Data.TimeStep,num2str(ch1spot));

    text(xch2(find(logical(xch2),1)),...
        ych2(find(logical(ych2),1)),...
        find(logical(xch2),1)*HMM_Data.TimeStep,num2str(ch2spot));

    title(basename)
    axis tight
    saveas(h(1,3),[resdir basename '_3D' ],'fig');
end

for nn=1:numpairs %Distance Plots
    ch1spot=pair(nn,1);
    ch2spot=pair(nn,2);

    xch1=HMM_Data.raw_ch1_tracks(ch1spot,:,1);
    ych1=HMM_Data.raw_ch1_tracks(ch1spot,:,2);

    xch2=HMM_Data.shifted_ch2_tracks(ch2spot,:,1);
    ych2=HMM_Data.shifted_ch2_tracks(ch2spot,:,2);

    state=HMM_PreProcessData.FilledStates{hh};

    figure
    d(nn,:)=sqrt((xch1-xch2).^2+(ych1-ych2).^2).*logical(xch1).*logical(xch2);
    d=(d(nn,:).*0.267);
    ax1 = gca;
    set(ax1,'XColor',[0 0 0],'YColor',[0 0 0]);
    axis([0 50 0 3.05]);
    xlabel('Time (s)')
    ylabel('Distance (\mu m)')
    x1=[0.05:.05:50];
    y1=d;
    dvalids=logical(d);
    hl1 = line(x1(dvalids),y1(dvalids),'Color','k','Parent',ax1,'linewidth',0.5);
    axis([0 50 0 max(d)+0.05]);
    hold on

    path=state(:,nn)';
    ax2 = axes('Position',get(ax1,'Position'),...
        'XAxisLocation','top',...
        'YAxisLocation','right',...
        'Color','none',...
        'XColor','k','YColor','k');
    ylabel('State')
    for pp=1:size(state,1)-1
```

```matlab
                seg1=path(:,pp);
                seg2=path(:,pp+1);
                x2=[0.05:.05:50];
                if seg1==seg2
                    if seg1&&seg2==2
                        c=[1 0 1]*0.7;l=3; %domain %magenta
                    end
                    if seg1&&seg2==1
                        c=[0 0 1];l=3; %dimer %blue
                    end
                    if seg1&&seg2==3
                        c=[1 0 0];l=3; %free %red
                    end
                else
                    c=[0 1 0]*0.8; l=0.75; %dk green
                end
                hl2 = line([x2(pp) x2(pp+1)],[seg1 seg2],'Color',c,'linewidth',l);
                hold on
            end
            axis([0 50 0.95 3.05]);
            hold off

            title('Distance between found interactions');

            saveas(gcf,  [resdir   basename   '_D_ch1_'   num2str(ch1spot)   '_ch2_'
num2str(ch2spot)], 'jpg');
            clear d state
            close all
            clear path
        end
    end
  catch
  end
end

%%
% try
%    varargout{1}=tracklengths;
%    varargout{2}=ratio;
%    save([resdir 'CandidateTrackLengths.mat'],'tracklengths','ratio');
% catch
% end

function h = HMM_StatesHist(datapath,ppfilestring,resdir)
% Generate histogram of dimers, using HMM_PreProcessData.FilledStates
% Similar to HMM_LifetimeDist for 2-state HMM
```

240

```matlab
%
% h = HMM_StatesHist(datapath,filestring,ppfilestring,resdir,deltaT)
%
% INPUTS
% OUTPUT
%
% Written by Shalini Low-Nam
% August 2010

%% Example:
% datapath='Z:\Shal\SPT Data\GroupedData_A431_Final\HMM Final\HMM EGF\';
% ppfilestring='EGF_3state_DD150nm_ID50nm.HMMPP';
% resdir=datapath;
% HMM_StatesHist(datapath,ppfilestring,resdir)
%% Determine Lengths of Dimers
T=1000;

ppFile=dir([datapath ppfilestring]);
HMM_PreProcessFile=([datapath ppfilestring]);

load([datapath ppFile.name],'-mat'); %load HMM_PreProcessData file

tmp=max(strfind(HMM_PreProcessFile,'\'));
fnbase=HMM_PreProcessFile(tmp+1:end-6);

FS=HMM_PreProcessData.FilledStates;

Nfiles=size(FS,2);
cnt=1;
multi=1;
for nf=1:Nfiles %Loop over number of files
    fprintf('Analyzing File: %d of %d\n',nf,Nfiles)
    if size(FS(Lund et al.),1) == 0
        fprintf('No interactions; proceeding to next data set ...\n')
        continue
    end
    s=FS(Lund et al.);
    mask=s==1;
    ds=s.*mask;
    for ii=1:size(FS(Lund et al.),2) %Loop over number of pairs
        dimers=ds(:,ii);
        [a]=find(dimers); %Find all dimers within dataset
        if size(a,1) ~= 0
            if size(a,1) ~= (a(end,1)-a(1,1))+1
                for mm=1:size(find(diff(a)>1))+1 %Loop over number of multiple dimers
                    z=(find(diff(a)>1));
```

241

```matlab
                if mm == 1
                    sf=a(1,1);
                    ef=a(min(find(diff(a)>1)));
                    Multi(multi,1)=ef-sf+1;
                    multi=multi+1;
                else
                    sfm=a(z(mm-1,1)+1,1);
                    if mm+1 <= size(find(diff(a)>1),1)+1
                        efm=a(z(mm,1),1); %could exceed mm
                    else
                        efm=a(end,1);
                    end
                    Multi(multi,1)=efm-sfm+1;
                    multi=multi+1;
                    clear sf ef sfm efm
                end
            end
        else
            SingleDimer(cnt,1)=size(a,1)+1; %Length of single dimer events
            cnt=cnt+1;
        end
    end
    end
    clear s mask ds
end
%% Graph results
if multi == 1
    Multi=[];
end
if cnt == 1
    SingleDimer=[];
else
    StateLength=[Multi ; SingleDimer];
    [Thist Thistbins]=hist(StateLength(:,1),20); %Histogram in frames
    h=figure;
    bar(Thistbins,Thist,'k','linewidth', 2);
    %axis([0 50 0 160]); %To plot all conditions on same axes
    xlabel('Dimer Event Lifetime (frames)','Fontsize', 16);
    ylabel('Number of Events','Fontsize',16);
    title('Distribution of Dimer Lifetimes - 3 State HMM','Fontsize',16);
    saveas(h,[resdir 'DimerDistribution_frames'],'fig');
    saveas(gcf, [resdir 'DimerDistribution_frames'], 'jpg');
    [Thists Thistbinss]=hist(StateLength(:,1)./20,20); %Histogram in seconds
    hs=figure;
    bar(Thistbinss,Thists,'k','linewidth', 2);
    %axis([0 50 0 160]); %To plot all conditions on same axes
```

242

```matlab
    xlabel('Dimer Event Lifetime (seconds)','Fontsize', 16);
    ylabel('Number of Events','Fontsize',16);
    title('Distribution of Dimer Lifetimes - 3 State HMM','Fontsize',16);
    saveas(hs,[resdir 'DimerDistribution_seconds'],'fig');
    saveas(gcf, [resdir 'DimerDistribution_seconds'], 'jpg');
%     close all
end
%% Save StateLength back to HMMPP file
HMM_PreProcessData.StateLength=StateLength;
save(HMM_PreProcessFile,'HMM_PreProcessData');

varargout{1}=HMM_PreProcessData;

%%Diffusion by state
datapath='Z:\Shal\SPT Data\GroupedData_A431_Final\HMM Final\HMM UNM HeLa
EGF\';
filestring='EGF*.HMMData';
ppfilestring='EGF*.HMMPP';
resdir=[datapath 'Pr2Results_deltaT2\'];
mkdir(resdir);
sigma=1.0720e-001;
Pr2_3State(datapath,filestring,ppfilestring,resdir,2,sigma)

function  h  =  Pr2_3State(datapath,filestring,ppfilestring,resdir,deltaT,sigma)%fittype-
option for one, two, or immobile component fitting
% Generate P(r2) as in de Keijzer et al., JCS 2008
%
% h = Pr2_3State(datapath,filestring,ppfilestring,resdir,deltaT,sigma)
%
% Inputs are location of trajectories, delta T, 1 or 2 component fit, sigma
% DeltaT is in frames (not time step)
% Read in tracks & valids
%
% INPUTS
%   datapath - string; path to files of type .HMMData
%   filestring - string of the type 'EGF*.HMMData'
%   ppfilestring - string of the type 'EGF*.HMMPP'
%   resdir - results directory where fit results and plots are saved
%   deltaT - step size for jumps to be calculated
% OUTPUT
%  h - handle for cpa figure
%
% Written by Shalini Low-Nam
% August 2010

%% Input examples:
```

```
% datapath='Z:\Shal\SPT Data\GroupedData_A431_Final\HMM Final\HMM EGF\';
% filestring='EGF*.HMMData';
% ppfilestring='EGF*.HMMPP';
% resdir=[datapath 'Pr2Results_deltaT2\'];
% mkdir(resdir);
% sigma=1.0720e-001;
% Pr2_3State(datapath,filestring,ppfilestring,resdir,deltaT,sigma)
```
_____
```
%% Calculate jump sizes and fitting
%calculate jump size for specific bin of deltaT
fprintf('Determining Square Displacements ...\n')
inc=0; idinc=0; finc=0; ddinc=0; dinc=0;  %counters for free, domain, and dimer states
clear r2sort ystep

Files=dir([datapath filestring]);
ppFile=dir([datapath ppfilestring]);
load([datapath ppFile.name],'-mat'); %load HMM_PreProcessData file
Nfiles=size(HMM_PreProcessData.P_states,2); %Number of files to analyze

HMM_PreProcessData.FilledStates{Nfiles}=[]; %In case the size of the FilledStates
does not match that of P_states

for jj = 1:length(Files)
    fprintf('Analyzing File: %d of %d\n',jj,length(Files))
    filename = Files(jj).name;
    load([datapath filename],'-mat'); %load HMM_Data file
    state=HMM_PreProcessData.FilledStates{jj};
    pair=HMM_PreProcessData.PairID{jj};
    if size(pair)==0
        continue
    end
    fpair=unique(pair(:,1)); %!!This will remove QD655 trajectory numbers that are
repeated; it will not matter for this analysis, but should not be used for any 2-channel
analyses
    ss=1; %this must be reset to one for each new HMM_Data file
    try
        if isfield(HMM_Data,'raw_ch1_tracks')
            for hh=1:size(HMM_Data.raw_ch1_tracks,1)
                track=HMM_Data.raw_ch1_tracks(hh,:,:);
                v=HMM_Data.ch1_valids(hh,:);
                if fpair(ss,1)==hh; %if the track is a candidate track
                    v1=v.*(state(:,ss)');
                    ss=ss+1;
                    for ii=1:deltaT:size(track,2)-deltaT
                        p1=ii;
                        p2=ii+deltaT;
```

```matlab
                    x=track(:,:,1);
                    y=track(:,:,2);
                    if v1(1,p1)==v1(1,p2)
                        if v1(1,p1)== 1 %r2 values for dimers
                            dinc=dinc+1;
                            dr2(dinc) = ((x(:,p1)-x(:,p2))^2) + ((y(:,p1)-y(:,p2))^2);
                        end
                        if v1(1,p1)== 2 %r2 values for domain-confined receptors
                            ddinc=ddinc+1;
                            ddr2(ddinc) = ((x(:,p1)-x(:,p2))^2) + ((y(:,p1)-y(:,p2))^2);
                        end
                        if v1(1,p1)== 3 %r2 values for free receptors
                            idinc=idinc+1;
                            fr2(idinc) = ((x(:,p1)-x(:,p2))^2) + ((y(:,p1)-y(:,p2))^2);
                        end
                    else
                        if v(1,p1) && v(1,p2) %r2 values for monomers in candidate tracks
                            finc=finc+1;
                            mr2(finc) = ((x(:,p1)-x(:,p2))^2) + ((y(:,p1)-y(:,p2))^2);
                        end
                    end
                    close all
                end
                clear track x y p1 p2 v1
            else %for all other tracks, treat as monomers
                for kk=1:deltaT:size(track,2)-deltaT
                    p1=kk;
                    p2=kk+deltaT;
                    x=track(:,:,1);
                    y=track(:,:,2);
                    if v(1,p1) && v(1,p2)
                        inc=inc+1;
                        r2(inc) = ((x(:,p1)-x(:,p2))^2) + ((y(:,p1)-y(:,p2))^2);
                    else
                    end
                    close all
                end
                clear track v x y p1 p2
            end
        end
    else
        fprintf('No tracks; continuing with next ...\n')
        continue
    end
catch
end
```

```matlab
end

if idinc == 0
    fr2=[];
end
if finc == 0
    mr2=[];
end
if inc == 0
    r2=[];
end
m_r2=[fr2 mr2 r2]; %concatenate all monomer r2 values

if dinc == 0
    d_r2=[];
    save([resdir '\Pr2FittingResults_Dimer_Domain_Monomer'],'m_r2','dd_r2');
else
    d_r2=dr2;
    save([resdir '\Pr2FittingResults_Dimer_Domain_Monomer'],'m_r2','d_r2');
end
if ddinc == 0
    dd_r2=[];
    save([resdir '\Pr2FittingResults_Dimer_Domain_Monomer'],'m_r2','d_r2');
else
    dd_r2=ddr2;
    save([resdir '\Pr2FittingResults_Dimer_Domain_Monomer'],'m_r2','dd_r2','d_r2');
end

load([resdir '\Pr2FittingResults_Dimer_Domain_Monomer.mat'])

%Remove jumps greater than 2 pixels (r^2=4)
mr2sort=sort(m_r2,2,'ascend');
mmask=mr2sort<4; %This filter could be used to remove jumps of greater than 1.5
pixels ... still a question of why we get these at all
mr2sort=mr2sort(mmask);
mr2=size(mr2sort,2);
ddr2sort=sort(dd_r2,2,'ascend');
ddmask=ddr2sort<4; %This filter could be used to remove jumps of greater than 1.5
pixels ... still a question of why we get these at all
ddr2sort=ddr2sort(ddmask);
ddr2=size(ddr2sort,2);
dr2sort=sort(d_r2,2,'ascend');
dmask=dr2sort<4; %This filter could be used to remove jumps of greater than 1.5 pixels
... still a question of why we get these at all
dr2sort=dr2sort(dmask);
dr2=size(dr2sort,2);
```

```matlab
mystep=(1:length(mr2sort))/length(mr2sort);
ddystep=(1:length(ddr2sort))/length(ddr2sort);
dystep=(1:length(dr2sort))/length(dr2sort);

%%Combined r2
clear r2
r2=[m_r2,d_r2,dd_r2];
rr2sort=sort(r2,2,'ascend');
rmask=rr2sort<4; %This filter could be used to remove jumps of greater than 1.5 pixels
... still a question of why we get these at all
rr2sort=rr2sort(rmask);
rr2=size(rr2sort,2);
rystep=(1:length(rr2sort))/length(rr2sort);
```

```matlab
%% Two component fits
%Two component fit for monomer data:
mTCopts=fitoptions('Method','Nonlinear','StartPoint',[.5                     .2
.1],'Lower',[0,0,0],'Upper',[1,10,10]);
%Schutz, et al., BJ, V73, 1997:
mTCftype=fittype('1-((a.*exp(-x./b))+((1-a).*exp(-
x./c)))','options',mTCopts,'coeff',{'a','b','c'},'indep','x','depen','y');
[mTCresults, mTCgoodnessL]=fit((mr2sort)',mystep',mTCftype);

mTCc=coeffvalues(mTCresults);
mTCalpha=mTCc(1);
mTCdr1=mTCc(2);
mTCdr2=mTCc(3);
mTCrmse=mTCgoodnessL.rmse;
mTCFitResult=1-((mTCalpha.*exp(-mr2sort./mTCdr1))+((1-mTCalpha).*exp(-
mr2sort./mTCdr2)));

%get confidence interval (95% is default)
mTC_CI=confint(mTCresults);
mTC_alpha_CI=mTC_CI(:,1);
mTC_dr1_CI=mTC_CI(:,2);
mTC_dr2_CI=mTC_CI(:,3);

%Two component fit for domain data:
ddTCopts=fitoptions('Method','Nonlinear','StartPoint',[.5                     .2
.1],'Lower',[0,0,0],'Upper',[1,10,10]);
%Schutz, et al., BJ, V73, 1997:
ddTCftype=fittype('1-((a.*exp(-x./b))+((1-a).*exp(-
x./c)))','options',ddTCopts,'coeff',{'a','b','c'},'indep','x','depen','y');
[ddTCresults, ddTCgoodnessL]=fit((ddr2sort)',ddystep',ddTCftype);
```

247

```matlab
ddTCc=coeffvalues(ddTCresults);
ddTCalpha=ddTCc(1);
ddTCdr1=ddTCc(2);
ddTCdr2=ddTCc(3);
ddTCrmse=ddTCgoodnessL.rmse;
ddTCFitResult=1-((ddTCalpha.*exp(-ddr2sort./ddTCdr1))+((1-ddTCalpha).*exp(-
ddr2sort./ddTCdr2)));

%get confidence interval (95% is default)
ddTC_CI=confint(ddTCresults);
ddTC_alpha_CI=ddTC_CI(:,1);
ddTC_dr1_CI=ddTC_CI(:,2);
ddTC_dr2_CI=ddTC_CI(:,3);

%Two component fit for dimer data:
dTCopts=fitoptions('Method','Nonlinear','StartPoint',[.5                              .2
.1],'Lower',[0,0,0],'Upper',[1,10,10]);
%Schutz, et al., BJ, V73, 1997:
dTCftype=fittype('1-((a.*exp(-x./b))+((1-a).*exp(-
x./c)))','options',dTCopts,'coeff',{'a','b','c'},'indep','x','depen','y');
[dTCresults, dTCgoodnessL]=fit((dr2sort)',dystep',dTCftype);

dTCc=coeffvalues(dTCresults);
dTCalpha=dTCc(1);
dTCdr1=dTCc(2);
dTCdr2=dTCc(3);
dTCrmse=dTCgoodnessL.rmse;
dTCFitResult=1-((dTCalpha.*exp(-dr2sort./dTCdr1))+((1-dTCalpha).*exp(-
dr2sort./dTCdr2)));

%get confidence interval (95% is default)
dTC_CI=confint(dTCresults);
dTC_alpha_CI=dTC_CI(:,1);
dTC_dr1_CI=dTC_CI(:,2);
dTC_dr2_CI=dTC_CI(:,3);

%Two component fit for all data:
rTCopts=fitoptions('Method','Nonlinear','StartPoint',[.5                              .2
.1],'Lower',[0,0,0],'Upper',[1,10,10]);
%Schutz, et al., BJ, V73, 1997:
rTCftype=fittype('1-((a.*exp(-x./b))+((1-a).*exp(-
x./c)))','options',rTCopts,'coeff',{'a','b','c'},'indep','x','depen','y');
[rTCresults, rTCgoodnessL]=fit((rr2sort)',rystep',rTCftype);

rTCc=coeffvalues(rTCresults);
rTCalpha=rTCc(1);
```

```
rTCdr1=rTCc(2);
rTCdr2=rTCc(3);
rTCrmse=rTCgoodnessL.rmse;
rTCFitResult=1-((rTCalpha.*exp(-rr2sort./rTCdr1))+((1-rTCalpha).*exp(-
rr2sort./rTCdr2)));

%get confidence interval (95% is default)
rTC_CI=confint(rTCresults);
rTC_alpha_CI=rTC_CI(:,1);
rTC_dr1_CI=rTC_CI(:,2);
rTC_dr2_CI=rTC_CI(:,3);
```
_____

```
%% Convert results to um^2/s and save in a table
%Solve for D using: D=(MSD-(4*(sigma^2)))/(4*deltaT)
mTCDout1 = (mTCdr1-(4*(sigma^2)))/(4*deltaT);
mTCDout2 = (mTCdr2-(4*(sigma^2)))/(4*deltaT);
mTCD1um=mTCDout1*20*0.267^2;
mTCD2um=mTCDout2*20*0.267^2;
mTC_dr1_CI_LB=((mTC_dr1_CI(1,1)-(4*(sigma^2)))/(4*deltaT))*20*0.267^2;      %lower
and upper bounds for 95% confidence interval in units of um^2/s
mTC_dr1_CI_UB=((mTC_dr1_CI(2,1)-(4*(sigma^2)))/(4*deltaT))*20*0.267^2;
mTC_dr2_CI_LB=((mTC_dr2_CI(1,1)-(4*(sigma^2)))/(4*deltaT))*20*0.267^2;
mTC_dr2_CI_UB=((mTC_dr2_CI(2,1)-(4*(sigma^2)))/(4*deltaT))*20*0.267^2;
% Dmr2=((median(mr2sort)-(4*(sigma^2)))/(4*deltaT))*(20*(.267^2))

ddTCDout1 = (ddTCdr1-(4*(sigma^2)))/(4*deltaT);
ddTCDout2 = (ddTCdr2-(4*(sigma^2)))/(4*deltaT);
ddTCD1um=ddTCDout1*20*0.267^2;
ddTCD2um=ddTCDout2*20*0.267^2;
ddTC_dr1_CI_LB=((ddTC_dr1_CI(1,1)-(4*(sigma^2)))/(4*deltaT))*20*0.267^2;      %lower
and upper bounds for 95% confidence interval in units of um^2/s
ddTC_dr1_CI_UB=((ddTC_dr1_CI(2,1)-(4*(sigma^2)))/(4*deltaT))*20*0.267^2;
ddTC_dr2_CI_LB=((ddTC_dr2_CI(1,1)-(4*(sigma^2)))/(4*deltaT))*20*0.267^2;
ddTC_dr2_CI_UB=((ddTC_dr2_CI(2,1)-(4*(sigma^2)))/(4*deltaT))*20*0.267^2;
% Dddr2=((median(ddr2sort)-(4*(sigma^2)))/(4*deltaT))*(20*(.267^2))

dTCDout1 = (dTCdr1-(4*(sigma^2)))/(4*deltaT);
dTCDout2 = (dTCdr2-(4*(sigma^2)))/(4*deltaT);
dTCD1um=dTCDout1*20*0.267^2;
dTCD2um=dTCDout2*20*0.267^2;
dTC_dr1_CI_LB=((dTC_dr1_CI(1,1)-(4*(sigma^2)))/(4*deltaT))*20*0.267^2; %lower and
upper bounds for 95% confidence interval in units of um^2/s
dTC_dr1_CI_UB=((dTC_dr1_CI(2,1)-(4*(sigma^2)))/(4*deltaT))*20*0.267^2;
dTC_dr2_CI_LB=((dTC_dr2_CI(1,1)-(4*(sigma^2)))/(4*deltaT))*20*0.267^2;
dTC_dr2_CI_UB=((dTC_dr2_CI(2,1)-(4*(sigma^2)))/(4*deltaT))*20*0.267^2;
% Ddr2=((median(dr2sort)-(4*(sigma^2)))/(4*deltaT))*(20*(.267^2))
```

249

```matlab
rTCDout1 = (rTCdr1-(4*(sigma^2)))/(4*deltaT);
rTCDout2 = (rTCdr2-(4*(sigma^2)))/(4*deltaT);
rTCD1um=rTCDout1*20*0.267^2;
rTCD2um=rTCDout2*20*0.267^2;
rTC_dr1_CI_LB=((rTC_dr1_CI(1,1)-(4*(sigma^2)))/(4*deltaT))*20*0.267^2; %lower and
upper bounds for 95% confidence interval in units of um^2/s
rTC_dr1_CI_UB=((rTC_dr1_CI(2,1)-(4*(sigma^2)))/(4*deltaT))*20*0.267^2;
rTC_dr2_CI_LB=((rTC_dr2_CI(1,1)-(4*(sigma^2)))/(4*deltaT))*20*0.267^2;
rTC_dr2_CI_UB=((rTC_dr2_CI(2,1)-(4*(sigma^2)))/(4*deltaT))*20*0.267^2;
% Rdr2=((median(rr2sort)-(4*(sigma^2)))/(4*deltaT))*(20*(.267^2))


clear excelPr2
excelPr2(1,1) = {'Pr2 Summary:'};
excelPr2(2,1)                    =                    {'Monomer'};excelPr2(3,1:11)                =
{'N','Alpha_LB','Alpha','Alpha_UB','D1CI_LB','D1','D1CI_UB','D2CI_LB','D2','D2CI_UB','
RMSE'};
excelPr2(2,13)                   =                    {'Domain'};excelPr2(3,13:23)               =
{'N','Alpha_LB','Alpha','Alpha_UB','D1CI_LB','D1','D1CI_UB','D2CI_LB','D2','D2CI_UB','
RMSE'};
excelPr2(2,25)                   =                    {'Dimer'};excelPr2(3,25:35)               =
{'N','Alpha_LB','Alpha','Alpha_UB','D1CI_LB','D1','D1CI_UB','D2CI_LB','D2','D2CI_UB','
RMSE'};
excelPr2(2,37)              =              {'All              Data'};excelPr2(3,37:47)               =
{'N','Alpha_LB','Alpha','Alpha_UB','D1CI_LB','D1','D1CI_UB','D2CI_LB','D2','D2CI_UB','
RMSE'};
excelPr2(4,1:11)                                                                              =
{mr2,mTC_alpha_CI(1,1),mTCalpha,mTC_alpha_CI(2,1),mTC_dr1_CI_LB,mTCD1um,
mTC_dr1_CI_UB,mTC_dr2_CI_LB,mTCD2um,mTC_dr2_CI_UB,mTCrmse};
excelPr2(4,13:23)                                                                            =
{ddr2,ddTC_alpha_CI(1,1),ddTCalpha,ddTC_alpha_CI(2,1),ddTC_dr1_CI_LB,ddTCD1u
m,ddTC_dr1_CI_UB,ddTC_dr2_CI_LB,ddTCD2um,ddTC_dr2_CI_UB,ddTCrmse};
excelPr2(4,25:35)                                                                            =
{dr2,dTC_alpha_CI(1,1),dTCalpha,dTC_alpha_CI(2,1),dTC_dr1_CI_LB,dTCD1um,dTC
_dr1_CI_UB,dTC_dr2_CI_LB,dTCD2um,dTC_dr2_CI_UB,dTCrmse};
excelPr2(4,37:47)                                                                            =
{rr2,rTC_alpha_CI(1,1),rTCalpha,rTC_alpha_CI(2,1),rTC_dr1_CI_LB,rTCD1um,rTC_dr1
_CI_UB,rTC_dr2_CI_LB,rTCD2um,rTC_dr2_CI_UB,rTCrmse};
xlswrite([resdir 'Pr2_FitData.xls'], excelPr2);

fprintf('Two Component Fitting Complete!\n')
%% TC plotting
%Monomer plotting
hmTC=figure;
semilogx(squeeze(mr2sort),squeeze(mystep),'ko')
hold on
```

250

```matlab
semilogx(squeeze(mr2sort),mTCFitResult,'--r','LineWidth',2)

hold off
xlabel('(r^2) (pix)')
ylabel('P(r^2)')
legend('Data','Fit')
title('Two Component Fit for Monomer P(r^2) Data')
hold off

saveas(hmTC,[resdir 'mTCPr2' ],'fig');
saveas(hmTC,[resdir 'mTCPr2' ],'jpg');

%Domain plotting
hddTC=figure;
semilogx(squeeze(ddr2sort),squeeze(ddystep),'co')
hold on
semilogx(squeeze(ddr2sort),ddTCFitResult,'--m','LineWidth',2)

hold off
xlabel('(r^2) (pix)')
ylabel('P(r^2)')
legend('Data','Fit')
title('Two Component Fit for Domain P(r^2) Data')
hold off

saveas(hddTC,[resdir 'ddTCPr2' ],'fig');
saveas(hddTC,[resdir 'ddTCPr2' ],'jpg');

%Dimer plotting
hdTC=figure;
semilogx(squeeze(dr2sort),squeeze(dystep),'go')
hold on
semilogx(squeeze(dr2sort),dTCFitResult,'--b','LineWidth',2)

hold off
xlabel('(r^2) (pix)')
ylabel('P(r^2)')
legend('Data','Fit')
title('Two Component Fit for Dimer P(r^2) Data')
hold off

saveas(hdTC,[resdir 'dTCPr2' ],'fig');
saveas(hdTC,[resdir 'dTCPr2' ],'jpg');

%Composite
hTC=figure;
```

```matlab
semilogx(squeeze(mr2sort),squeeze(mystep),'ko')
hold on
semilogx(squeeze(mr2sort),mTCFitResult,'--r','LineWidth',2)
hold on
semilogx(squeeze(ddr2sort),squeeze(ddystep),'co')
hold on
semilogx(squeeze(ddr2sort),ddTCFitResult,'--m','LineWidth',2)
hold on
semilogx(squeeze(dr2sort),squeeze(dystep),'go')
hold on
semilogx(squeeze(dr2sort),dTCFitResult,'--b','LineWidth',2)
hold off
xlabel('(r^2) (pix)')
ylabel('P(r^2)')
legend('Monomer Data','Monomer Fit','Domain Data','Domain Fit','Dimer Data','Dimer Fit')
title('Two Component Fit for P(r^2) Data')
hold off
axis([1*10^-7 1*10^1 0 1]);

saveas(hTC,[resdir 'TCPr2' ],'fig');
saveas(hTC,[resdir 'TCPr2' ],'jpg');

%All data plotting
rdTC=figure;
semilogx(squeeze(rr2sort),squeeze(rystep),'go')
hold on
semilogx(squeeze(rr2sort),rTCFitResult,'--b','LineWidth',2)

hold off
xlabel('(r^2) (pix)')
ylabel('P(r^2)')
legend('Data','Fit')
title('Two Component Fit for All P(r^2) Data')
hold off

saveas(rdTC,[resdir 'rTCPr2' ],'fig');
saveas(rdTC,[resdir 'rTCPr2' ],'jpg');

pause(2);
close all
```

```matlab
%%
```

_____

```matlab
%% Figures for manuscripts
%%Tracks on raw data (example from VhH+PD since receptors experience
%%greater excursion)
%Pair ID = 108; Spots ch1=16, ch2=13
%Raw Data
load('Z:\Shal\SPT Data\GroupedData_A431_Final\VhH_PD\100108\Chamber2\VhH_3fold-2010-1-8-15-37.mat')
%Left Side (655)
%Right Side (585)
clear L
clear Ru
clear series
series=squeeze(sequence);
im=series;
[ch1,ch2] = splitImage(im,5,[1 1],0);
L=ch1(:,:,999);
mask=max(L);
L=joinchannels('RGB',mask.*L,L,mask.*L);
dipshow(L,[370000,900000]); %use dipmapping to show only magenta for single molecules
hm=gca;
scaleLine(hm,2,0.267,[115 140],[1 1 1],3) %2 um scale bar on all figure one DAQ images

Ru=ch2(:,:,999);
mask=max(Ru);
Ru=joinchannels('RGB',Ru,mask.*Ru,Ru);
dipshow(Ru,[285000,430000]); %use dipmapping to show only green for single molecules
hg=gca;
scaleLine(hg,2,0.267,[115 140],[1 1 1],3)

save(['Z:\Shal\Manuscripts\erbB1HomodimerLifetimes_Science\Figure1RawChannels'],'L','Ru');

%%SPT Jump Correlation
%To do SPTJC on a single movie
resultsdir='C:\Users\slow-nam\Desktop\ExEGFtracks\';
Lfiles=dir([resultsdir 'trackinfo_L_*']);
Rstracksfiles=dir([resultsdir 'Rstracks_trackinfo_*']);
Rfiles=dir([resultsdir 'trackinfo_Ru_*']);
SPTJCdir='C:\Users\slow-nam\Desktop\ExEGFtracks\SPTJC\';
mkdir(SPTJCdir);
```

253

```matlab
shiftvector=[0 0]';
cutoff=0.5;
binsize=.05;
pixelsize=0.067;

for nn=1:size(Lfiles,1)%data series
    L=load([resultsdir Lfiles(nn).name]);
    R=load([resultsdir Rfiles(nn).name]);
    Rs=load([resultsdir Rstracksfiles(nn).name]);

    if length(size(L.tracks))==2
        continue
    end

    R.valids=repmat(R.valids,[1 1 2]);
    TracksI{nn}=Rs.Rstracks.*R.valids;
    TracksII{nn}=L.tracks;
end

%%call SPTJumpCorrelation
% shiftvector=[0 0]';
% cutoff=10;
% binsize=.1;
% pixelsize=.1;
for nn=1:size(Lfiles,1)%data series
[Data_all{nn}]=SPTJumpCorrelation(TracksI{nn},TracksII{nn},cutoff,binsize,pixelsize,shif
tvector);
end

%[Data_all{nn}
c]=SPTJumpCorrelation(L_tracks{3}(3,:,:),R_tracks{3}(9,:,:),cutoff,binsize,pixelsize,shiftv
ector)
bin_num=round(cutoff/binsize);
cutoff=bin_num*binsize;
X=linspace(0,cutoff,bin_num);


for n=1:bin_num-1
    cnt(n)=0;
    Parameter=[0 0];
    Parameter2=[0 0];
    Parameter3=[0 0];
    Y(n)=0;
    E(n)=0;
```

254

```matlab
    for nn=1:size(Lfiles,1)%Nsets
        Data=Data_all{nn};

        for m=1:size(Data,1)
            if X(n)<=Data(m,3)&&Data(m,3)<X(n+1)
                cnt(n)=cnt(n)+1;
                Parameter(cnt(n))=Data(m,12);
                Parameter2(cnt(n))=sqrt(Data(m,6)^2+Data(m,7)^2);
                Parameter3(cnt(n))=Data(m,10);

                cnt(n)=cnt(n)+1;
                Parameter(cnt(n))=Data(m,13);
                Parameter2(cnt(n))=sqrt(Data(m,8)^2+Data(m,9)^2);
                Parameter3(cnt(n))=Data(m,11);

            end
        end
    end

    %Y is getting larger than X
    if cnt(n)>0
        %take average of each interval
        Y(n)=mean(Parameter);
        Y2(n)=mean(Parameter2);
        Y3(n)=mean(Parameter3);
        %calculate std. error of the mean NOTE:2 type of std. which one is
        %better.
        E(n)=std(Parameter)/sqrt(cnt(n));
        E2(n)=std(Parameter2)/sqrt(cnt(n));
        E3(n)=std(Parameter3)/sqrt(cnt(n));
    end
end

%shift x over by half a bin size.  this will plot values within a bin at a
%centered point
X=X+binsize/2;
X=X(1:end-1);

X=X(cnt>0);
Y=Y(cnt>0);
Y2=Y2(cnt>0);
Y3=Y3(cnt>0);
E=E(cnt>0);
E2=E2(cnt>0);
E3=E3(cnt>0);
```

255

```matlab
sz=1;
figure
if(sz>0)
   hold on
   errorbar(X,Y,E)
   name = ['Graph of Uncorrelated Jump Distance'];

   title(name)
   xlabel('Seperation Distance (\mum)')
   ylabel('Average Correlation (\mum)')

   errorbar(X,Y2,E2,'r')
   %errorbar(X,Y3,E3,'g')
   legend('uncorrelated jump distance','jump magnitude')
   %legend('uncorrelated jump distance','jump magnitude','jump to center of mass')
   hold off
end

%To perform SPTJC for a condition (all movies)
topdir='Z:\Shal\SPT Data\GroupedData_erbB3\erbB3\'
cutoff=2;
binsize=0.05;

%EGF
SPTdirs={[topdir 'HMM EGF\']};
figDir=[topdir 'HMM EGF\SPTJumpCorrelation'];
if ~exist(figDir,'dir')
    mkdir(figDir)
end
conditions{1}='QD EGF';

[jumpResults condIdx cnt h]=SPTJumpCorrelation(SPTdirs,cutoff,binsize,conditions);

conditions=conditions{1};
saveas(gca,[figDir '\SPTJC_' conditions],'fig');
saveas(gca,[figDir '\SPTJC_' conditions],'jpg');

close all
clear jumpResults condIdx cnt h SPTdirs figDir conditions

function        [jumpResults        condIdx        cnt        h        unCorrelatedJD
JumpMagnitude]=SPTJumpCorrelation(SPTdirs,cutoff,binsize,conditions,jumpResults,c
ondIdx)
% SPTJUMPCORRELATION    compute jump correlation for files in specifed directories
%
```

```
%                    [jumpResults    condIdx    cnt    h    unCorrelatedJD
JumpMagnitude]=SPTJumpCorrelation(SPTdirs,cutoff,binsize,conditions,jumpResults,c
ondIdx)
%
%
%
% INPUTS:
%   SPTdirs: cell array of directories containing '*.SPTData' or '*.HMMData'
%          data files for which to compute the jump correlation
%   cutoff: Max separation distance for analysis in microns
%   binsize: jump binsize in microns
%   conditions: DataConditions in SPTData or HMMData files for which compute
%            the jump correlation. Conditions are used for plot titles.
%            Leave empty to perform single jump correlation analysis
%            for all files.
%   jumpResults: optional input. 'jumpResults' output from previous call to
%            SPTJumpCorrelation. If nargin > 4 then only plot results
%   condIdx: 'condIdx' output from previous call to SPTJumpCorrelation.
%            Required if input jumpResults.
%   unCorrelatedJD: cell array of all calculated uncorrelated jump distance
%                Each cell is for the corresponding condition
%   JumpMagnitude:
% OUTPUTS:
%   jumpResults: cell array of matrices with 13 columns and rows equal to the number
of
%      times particles came within the cutoff distance. Each cell
%      corresponds to a different data file/movie.
%    [i j S COM(1) COM(2) J1(1) J1(2) J2(1) J2(2) J1_COM J2_COM D1(1) D2(1) t]
%      Above is the layout of a row of the Data Matrix.
%      i is the particle from TracksI that was involved in the interaction
%      j is the particle from TracksII that was involved in the interaction
%      S is the seperation distance between the two particles.
%      The others are mentioned below in the DESCRIPTION section with ...(1)
%      meaning the x-axis and ...(2) meaning the y-axis.
%   condIdx: vector with same size as jumpResults cell array. Each
%            element contains the index of the input 'conditions' that
%            correspond to the jumpResults in the cell array.
%   cnt: cell array with size of conditions. each cell contains a vector
%      with the number of events in each bin
%   h: vector of figure handles
%
% NOTE: Only works for 2 channel data
%
% Written by Jonas Anderson
% Revised by Shalini Low-Nam and Keith Lidke, 2009
% Updated by Pat Cutler July 2010
```

```
%
% DESCRIPTION
%
% This function will take two color data as input and search for correlations
% between the two data sets.
%
% First the function looks at a track from TracksI and compares it with all
% tracks in TracksII.  If two tracks are found below the user specified cutoff,
% calculations are performed to measure correlations between the tracks.
%
% These calculations involve finding the seperation distance, the center of
% mass (COM), the jump vector(J1,J2), the jump toward the COM (J1_COM,
% J2_COM), and the uncorrelated jump distance (D1,D2).
%
% The jump vector has magnitude that is the length a particle
% jumps between consecutive time frames and points in the direction of the jump.
% J1 is the jump vector of a track in TracksI while J2 is for TracksII.
%
% Jump toward the COM is similar to the Jump vector except the lenght and
% direction are calculated in relation to the COM.
%
% The uncorrelated jump distance is a measure of correlation between J1 and
% J2.  If the two tracks make similar (correlated) jumps, the uncorrelated
% jump distance will be small.
%
% After the quantities of interest are calculated and saved to the Data matrix
% intervals are defined based on seperation distance.
% Each interval is defined by user input (binsize) and the range is 0 to user input
(cutoff).
% Each interaction between particles that happened when the seperation
% distance was in the specified interval is added together.  Then the
% average of all the interactions that occured in this interval is taken.
% This same process is repeated for each interval.  Finally, error bars are
% calculated using Standard Error of the Mean (sigma/sqrt(N)).
%
% A similar process of is used for the Jump vectors.
%
% These are all plotted and output.
%
%


%SPT Jump Correlation
%July 22, 2010
%Making SPTJC compatible with new HMM and SPT data structures
%Shalini Low-Nam and Pat Cutler
```

```matlab
%% perform jump correlation analysis on each data set

disp('SPTJumpCorrelation Started')

if nargin < 4
    conditions = [];
end

if nargin < 5
    condIdx = [];
    for ii = 1:length(SPTdirs)
        disp(['Checking directory ' SPTdirs(Paez et al.)])
        Files_SPT = dir([SPTdirs(Paez et al.) '\*.SPTData']); % find SPTData files in single directory
        Files_HMM = dir([SPTdirs(Paez et al.) '\*.HMMData']); % find SPTData files in single directory
        Files = [Files_SPT Files_HMM];
        for jj = 1:length(Files)
            temp = load([SPTdirs(Paez et al.) '\' Files(jj).name],'-mat'); % load data file
            if isfield(temp,'SPT_Data') % identify SPTData files
                Data = temp.SPT_Data;
            else if isfield(temp,'HMM_Data') % identify HMMData files
                    HMMcheck = 1;
                    Data = temp.HMM_Data;
                end
            end
            if ~isempty(conditions)
                if ~isempty(find(strcmp(Data.DataConditions,conditions),1))
                    condIdx(ii,jj) = find(strcmp(Data.DataConditions,conditions)); % determine conditions for SPTData file
                else
                    condIdx(ii,jj) = 0;
                end
            else
                condIdx(ii,jj) = 1; % if no conditions specified group everything together
            end
            if condIdx(ii,jj)
                disp(['computing jumpCorrelation for ' Files(jj).name])
                if isfield(Data,'shifted_ch2_tracks')
                    jumpResults{ii,jj}                                            = jumpCorrelation(Data.raw_ch1_tracks,Data.shifted_ch2_tracks,cutoff,binsize,Data.Pixel Size);
                else
                    try
```

259

```matlab
                jumpResults{ii,jj}                                                    =
jumpCorrelation(Data.raw_ch1_tracks,Data.ch2_tracks,cutoff,binsize,Data.PixelSize,Da
ta(1).tform);
                catch
                end
            end
        else
            jumpResults{ii,jj} = [];
        end
    end
  end
else if nargin ~= 6
    error('SPTJumpCorrelation: if "jumpResults" input "condIdx" input also required')
  end
end

jumpResults = jumpResults(:);
condIdx = condIdx(:);


uniqueCondIdx = unique(condIdx);

if isempty(conditions)
  disp('Making jumpCorrelation plot')
  [cnt{1},unCorrelatedJD{1},JumpMagnitude{1},JumpCOM{1},h(1)]                         =
plotJumpDistance(cutoff,binsize,jumpResults,conditions);
else
  for ii = uniqueCondIdx'
    if ii
      disp(['Making jumpCorrelation plots for ' conditions(ii)])
      [cnt(Paez    et    al.),unCorrelatedJD(Paez    et    al.),JumpMagnitude(Paez    et
al.),JumpCOM(Paez et al.),h(ii)] = plotJumpDistance(cutoff,binsize,jumpResults(condIdx
== ii),conditions(Paez et al.));
    end
  end
end

disp('SPTJumpCorrelation Finished')

%
% Plot results for jump distance for each condition
%
function                  [cnt,unCorrelatedJD,JumpMagnitude,JumpCOM,h]                  =
plotJumpDistance(cutoff,binsize,jumpResults,conditions)

bin_num=round(cutoff/binsize);
```

260

```matlab
cutoff=bin_num*binsize;
X=linspace(0,cutoff,bin_num);

for n=1:bin_num-1
    cnt(n)=0;
    unCorrelatedJD{n}=[0 0];
    JumpMagnitude{n}=[0 0];
    JumpCOM{n}=[0 0];
    Y(n)=0;
    E(n)=0;

    for nn=1:length(jumpResults) %Nsets
        if ~isempty(jumpResults{nn})
            for m = 1:size(jumpResults{nn},1)
                if X(n)<=jumpResults{nn}(m,3)&&jumpResults{nn}(m,3)<X(n+1)
                    cnt(n)=cnt(n)+1;
                    unCorrelatedJD{n}(cnt(n))=jumpResults{nn}(m,12);  % uncorrelated jump
Distance

JumpMagnitude{n}(cnt(n))=sqrt(jumpResults{nn}(m,6)^2+jumpResults{nn}(m,7)^2);
                    JumpCOM{n}(cnt(n))=jumpResults{nn}(m,10);

                    cnt(n)=cnt(n)+1;
                    unCorrelatedJD{n}(cnt(n))=jumpResults{nn}(m,13);

JumpMagnitude{n}(cnt(n))=sqrt(jumpResults{nn}(m,8)^2+jumpResults{nn}(m,9)^2);
                    JumpCOM{n}(cnt(n))=jumpResults{nn}(m,11);

                end
            end
        end
    end

    %Y is getting larger than X
    if cnt(n)>0
        %take average of each interval
        Y(n)=mean(unCorrelatedJD{n});
        Y2(n)=mean(JumpMagnitude{n});
        Y3(n)=mean(JumpCOM{n});
        %calculate std. error of the mean NOTE:2 type of std. which one is
        %better.
        E(n)=std(unCorrelatedJD{n})/sqrt(cnt(n));
        E2(n)=std(JumpMagnitude{n})/sqrt(cnt(n));
        E3(n)=std(JumpCOM{n})/sqrt(cnt(n));
    end
end
```

261

```matlab
%shift x over by half a bin size.  this will plot values within a bin at a
%centered point
X=X+binsize/2;
X=X(1:end-1);

X=X(cnt>0);
Y=Y(cnt>0);
Y2=Y2(cnt>0);
Y3=Y3(cnt>0);
E=E(cnt>0);
E2=E2(cnt>0);
E3=E3(cnt>0);

sz=1;
% h = figure; %commented out by SL-N and SS 12.20.10
if(sz>0)
    %    errorbar_tick(H,W,T) adjust the width of error bars with handle H.
    %     The input W is given in the units of the current x-axis.
    %     The input T is the 'LineWidth' of the errorbar
    figure;
    hold on
    h=errorbar(X,Y,E)
    name = ['Graph of Uncorrelated Jump Distance (' conditions ')'];
    errorbar_tick(h,100)  %Added 12.20.10 by SL-N and SS; change the second
parameter (smaller = wider)

    title(name)
    xlabel('Separation Distance (\mum)')
    ylabel('Average Correlation (\mum)')

    h=errorbar(X,Y2,E2,'r')
    errorbar_tick(h,100)
    %errorbar(X,Y3,E3,'g')
    legend('uncorrelated jump distance','jump magnitude')
    %legend('uncorrelated jump distance','jump magnitude','jump to center of mass')
    hold off
end

%
% compute jump correlation for individual data set
%
function jumpResults = jumpCorrelation(TracksI,TracksII,cutoff,binsize,pixelsize,tform)

if nargin > 5  % shift tracks2 if tform is given
    tempX = TracksII(:,:,1);
```

```matlab
        tempY = TracksII(:,:,2);
        [tempX1,tempY1] = point_transform(tempX(:),tempY(:),tform);
        tempX1(~tempX) = 0;
        tempY1(~tempY) = 0;
        TracksII(:,:,1) = reshape(tempX,[size(TracksII,1) size(TracksII,2)]);
        TracksII(:,:,2) = reshape(tempY,[size(TracksII,1) size(TracksII,2)]);
end

% scale tracks by pixelsize
TracksI=TracksI*pixelsize;
TracksII=TracksII*pixelsize;

bin_num=round(cutoff/binsize);
cutoff=bin_num*binsize;
timesteps=size(TracksI,2);
sz=0;
for i=1:size(TracksI,1)
    for j=1:size(TracksII,1)
        for t=1:timesteps-1
            % check if two tracks are close, if so check for correlation
            % make zero condition applys to t and t+1 tracks
            if  TracksI(i,t,1)&&TracksII(j,t,1)
                if TracksI(i,t+1,1)&&TracksII(j,t+1,1)
                    if                           (sqrt((TracksI(i,t,1)-TracksII(j,t,1)).^2+(TracksI(i,t,2)-
TracksII(j,t,2)).^2)<=cutoff)
                        sz=sz+1;
                        %seperation distance
                        S=sqrt((TracksI(i,t,1)-TracksII(j,t,1)).^2+(TracksI(i,t,2)-TracksII(j,t,2)).^2);
                        %calculate center of mass (x and y)
                        COM = (1/2)*squeeze(TracksII(j,t,:)+TracksI(i,t,:));
                        %define jump vectors
                        J1=squeeze((TracksI(i,t+1,:)-TracksI(i,t,:)));
                        J2=squeeze((TracksII(j,t+1,:)-TracksII(j,t,:)));

                        %define jump vectors to COM
                        j1tocom=COM-squeeze(TracksI(i,t,:));
                        j2tocom=COM-squeeze(TracksII(j,t,:));
                        J1_COM=dot(J1,j1tocom/norm(j1tocom));
                        J2_COM=dot(J2,j2tocom/norm(j2tocom));
                        %define uncorrelated jump distance
                        D1=norm(J1-J1*dot(J1,J2/norm(J1)/norm(J2)));
                        D2=norm(J2-J2*dot(J2,J1/norm(J1)/norm(J2)));
                        %save data
                        jumpResults(sz,:)=[i j S COM(1) COM(2) J1(1) J1(2) J2(1) J2(2)
J1_COM J2_COM D1(1) D2(1) t];
                    end
```

263

```matlab
            end
        end
      end
    end
end

if ~exist('jumpResults','var')
    jumpResults = [];
end


%%State trace examples
%%1 to 2 to 1 oscillations:
%%Results directory, filestring, and raw data
resdir                                                              =
'Z:\Shal\Manuscripts\erbB1HomodimerLifetimes_Science\SupportingFigures\StateExam
ples\';
basename = 'EGF_12-16-11-46_ch1_8_ch2_19';
%EGF figure for 12-16-11-46
%Ch1:8; Ch2:19
%Raw data:
load('Z:\Shal\SPT Data\091216\EGF_A431_NPR-2009-12-16-11-46.mat')
%Raw channels:
load('Z:\Shal\SPT          Data\091216\Chamber1\Ru_EGF_A431_NPR-2009-12-16-11-
46.mat')
load('Z:\Shal\SPT Data\091216\Chamber1\L_EGF_A431_NPR-2009-12-16-11-46.mat')
%HMM_Data file:
uiopen('Z:\Shal\SPT          Data\GroupedData_A431_Final\HMM          Final\HMM
EGF\EGF_A431_NPR-2009-12-16-11-46.HMMData',1)

%Color overlay
load('Z:\Shal\SPT Data\091216\Chamber1\ColorOverlays\co_L_EGF_A431_NPR-2009-
12-16-11-46.mat')

%Color overlay of both trajectories on one image (movie)
HMMDataFile   =   'Z:\Shal\SPT   Data\GroupedData_A431_Final\HMM   Final\HMM
EGF\EGF_A431_NPR-2009-12-16-11-46.HMMData';
tracks = [8;19];
pix = 8;
scaleline = 0.5;
getframes = 1;
tailpoints = 1;
zm = 4;
fps = 20;
plotTracks = [1 1];
overlayChannels = [1 1];
```

264

```
magenta = 1;

dataRep = 4;
CreateAVI = 'GaussFilterScaleMagenta';
Coloroverlay                                                              =
SPT_CreateOverlay(HMMDataFile,tracks,pix,scaleline,getframes,tailpoints,zm,dataRep,
CreateAVI,fps,plotTracks,overlayChannels,magenta)

dataRep = 3;
CreateAVI = 'GaussFilterMagenta';
Coloroverlay                                                              =
SPT_CreateOverlay_Threshold(HMMDataFile,tracks,pix,scaleline,getframes,tailpoints,z
m,dataRep,CreateAVI,fps,plotTracks,overlayChannels,magenta)

%Frames for stills
load('Z:\Shal\SPT Data\091216\Chamber1\ColorOverlays\co_L_EGF_A431_NPR-2009-
12-16-11-46.mat')
g=co{2}; %extract 585 data
r=co{1}; %extract 655 data
g=g(5:21,91:107,130:end);
r=r(5:21,91:107,130:end);
gcrop=g(:,:,:); %crop frames
rcrop=r(:,:,:); %crop frames
gout=gaussf(gcrop,[0.7 0.7 0],'best') %crop frames
rout=gaussf(rcrop,[0.7 0.7 0],'best') %crop frames
cropco=joinchannels('RGB',stretch(rout),stretch(gout),stretch(rout))
%stills: Frames 0,70,293,316,371,427,615,695,833
x=833;
gframe=cropco{2}; %extract 585 data
rframe=cropco{1}; %extract 655 data
gcropframe=gframe(:,:,x) %crop frames
rcropframe=rframe(:,:,x) %crop frames
cropcoframe=joinchannels('RGB',rcropframe,gcropframe,rcropframe)
a=squeeze(cropcoframe);
[out,barlength] = scalebar(a,0.267,'bottomright','hor',0.5,0)

%3-D plot for fluctuating interactions
load('Z:\Shal\SPT        Data\GroupedData_A431_Final\HMM        Final\HMM
EGF\EGF_A431_NPR-2009-12-16-11-46.HMMData','-mat')

xch1=HMM_Data.raw_ch1_tracks(8,:,1);
ych1=HMM_Data.raw_ch1_tracks(8,:,2);

s1=logical(xch1(:,:)); %find the valid points of trajectory 1
tmps1=find(s1,1); %start of trajectory 1
tmpe1=max(find(s1)); %end of trajectory 1
```

```matlab
l1=tmpe1-tmps1+1; %length of trajectory 1

xch2=HMM_Data.shifted_ch2_tracks(19,:,1);
ych2=HMM_Data.shifted_ch2_tracks(19,:,2);

s2=logical(xch2(:,:)); %find the valid points of trajectory 2
tmps2=find(s2,1); %start of trajectory 2
tmpe2=max(find(s2)); %end of trajectory 2
l2=tmpe2-tmps2+1; %length of trajectory 2

h(1,3) = figure;
ah = gca;
hsvline(squeeze(xch1),squeeze(ych1),HMM_Data.TimeStep,h(1,3),2,1,3,[],[],[],[1    0
1],[],[],1);
hold on
hsvline(squeeze(xch2),squeeze(ych2),HMM_Data.TimeStep,h(1,3),2,1,3,[],[],[],[0    1
0],[],[],1);
hold on
xlabel('X Coordinate')
ylabel('Y Coordinate')
zlabel('Time (s)')

saveas(gcf, [resdir basename '_3D'], 'jpg');
saveas(gcf, [resdir basename '_3D'], 'fig');

%2-State Distance and State Plot
uiopen('Z:\Shal\SPT          Data\GroupedData_A431_Final\HMM          Final\HMM
EGF\2StateResults_ID100\EGF.HMMPP',1)
dimer=HMM_PreProcessData.FilledStates{109};

nn=3;
figure
d(nn,:)=sqrt((xch1-xch2).^2+(ych1-ych2).^2).*logical(xch1).*logical(xch2);
d=(d(nn,:).*0.267);
ax1 = gca;
set(ax1,'XColor',[0 0 0],'YColor',[0 0 0]);
axis([0 50 0 3.05]);
% xlabel('Time (s)')
% ylabel('Distance (\mu m)')
x1=[0.05:.05:50];
y1=d;
dvalids=logical(d);
hl1 = line(x1(dvalids),y1(dvalids),'Color','k','Parent',ax1,'linewidth',0.5);
axis([0 50 0 max(d)+0.05]);
hold on
```

266

```matlab
ID=0.1; %a horizontal line for the specified interaction distance
line([0.05;50],[ID;ID],'Color','m','linewidth',2,'LineStyle','--')

hold on
n=3; %pair number
trace=dimer(n,:);
ax2 = axes('Position',get(ax1,'Position'),...
    'XAxisLocation','top',...
    'YAxisLocation','right',...
    'Color','none',...
    'XColor','k','YColor','k');
x2=[0.05:.05:50];
y2=trace;
hl2 = line(x2,y2,'Color',[0 1 0]*0.6,'linewidth',3);
ax2 = gca;
set(ax2,'XColor','k','YColor','k');
axis([0 50 0 1.05]);
% xlabel('Time (s)')
% ylabel('State')
hold off

title('Distance between QDs of found dimers');

saveas(gcf, [resdir basename '_D_2state'], 'jpg');
saveas(gcf, [resdir basename '_D_2state'], 'fig');

%3-State Distance and State Plot
load('Z:\Shal\SPT          Data\GroupedData_A431_Final\HMM          Final\HMM
EGF\EGF_3state_DD150nm_ID50nm.HMMPP','-mat')
state=HMM_PreProcessData.FilledStates{109};

nn=3; %which PairID element
figure
d(nn,:)=sqrt((xch1-xch2).^2+(ych1-ych2).^2).*logical(xch1).*logical(xch2);
d=(d(nn,:).*0.267);
ax1 = gca;
set(ax1,'XColor',[0 0 0],'YColor',[0 0 0]);
axis([0 50 0 3.05]);
xlabel('Time (s)')
ylabel('Distance (\mu m)')
x1=[0.05:.05:50];
y1=d;
dvalids=logical(d);
hl1 = line(x1(dvalids),y1(dvalids),'Color','k','Parent',ax1,'linewidth',0.5);
axis([0 50 0 max(d)+0.05]);
hold on
```

```matlab
path=state(:,nn)';
ax2 = axes('Position',get(ax1,'Position'),...
    'XAxisLocation','top',...
    'YAxisLocation','right',...
    'Color','none',...
    'XColor','k','YColor','k');
ylabel('State')
for pp=1:size(state,1)-1
    seg1=path(:,pp);
    seg2=path(:,pp+1);
    x2=[0.05:.05:50];
    if seg1==seg2
        if seg1&&seg2==2
            c=[1 0 1]*0.7;l=3; %domain %magenta
        end
        if seg1&&seg2==1
            c=[0 0 1];l=3; %dimer %blue
        end
        if seg1&&seg2==3
            c=[1 0 0];l=3; %free %red
        end
    else
        c=[0 1 0]*0.8; l=0.75; %dk green
    end
    hl2 = line([x2(pp) x2(pp+1)],[seg1 seg2],'Color',c,'linewidth',l);
    hold on
end

hold on
path=state(:,nn)';
ID=-0.02; %timeline
for pp=1:size(state,1)-1
    seg1=path(:,pp);
    seg2=path(:,pp+1);
    x2=[0.05:.05:50];
    if seg1==seg2
        if seg1&&seg2==2
            c=[1 0 1]*0.7;l=10; %domain %magenta
        end
        if seg1&&seg2==1
            c=[0 0 1];l=10; %dimer %blue
        end
        if seg1&&seg2==3
            c=[1 0 0];l=10; %free %red
        end
    end
```

268

```matlab
            end
        hl2 = line([x2(pp) x2(pp+1)],[ID ID],'Color',c,'linewidth',l);
        hold on
    end
end
axis([0 50 -0.055 2.75]);

title('Distance between found interactions');

saveas(gcf, [resdir basename '_D_state'], 'jpg');
saveas(gcf, [resdir basename '_D_state'], 'fig');

%Distance Only
%D between particles, with correction for pixel size
figure
d=sqrt((xch1-xch2).^2+(ych1-ych2).^2).*logical(xch1).*logical(xch2);
d=(d.*0.267);
ax1 = gca;
set(ax1,'XColor',[0 0 0],'YColor',[0 0 0]);
axis([0 50 0 3.05]);
xlabel('Time (s)')
ylabel('Distance (\mu m)')
x1=[0.05:.05:50];
y1=d;
dvalids=logical(d);
hl1 = line(x1(dvalids),y1(dvalids),'Color','k','Parent',ax1,'linewidth',2);
axis([0 50 0 max(d)+0.05]);

hold on
ID=0.06; %a horizontal line for the specified interaction distance
line([0.05;50],[ID;ID],'Color','m','linewidth',2,'LineStyle','--')
hold off

function h = HMM_DvsLifetime(datapath,filestring,ppfilestring,resdir,deltaT)
% Generate P(r2) as in de Keijzer et al., JCS 2008
%
% h = HMM_DvsLifetime(datapath,filestring,ppfilestring,resdir,deltaT)
%
% Inputs are location of trajectories, delta T, 1 or 2 component fit, sigma
% DeltaT is in frames (not time step)
% Read in tracks & valids
%
% INPUTS
%   datapath - String; path to files of type .HMMData
%   filestring - String of the type '*.HMMData'
%   ppfilestring - String of the type '*.HMMPP'
%   resdir - Results directory where fit results and plots are saved
```

```matlab
%   deltaT - Step size for jumps to be calculated
% OUTPUT
%   h - Handle for figure
%
% Written by Shalini Low-Nam
% August 2010

%_____
%% Input example:
% datapath='Z:\Shal\SPT Data\GroupedData_A431_Final\HMM Final\HMM EGF\';
% filestring='EGF*.HMMData';
% ppfilestring='*.HMMPP';
% resdir=[datapath 'DvsLifetime\'];
% mkdir(resdir);
%_____
%% Determine Lengths of Dimers
T=1000;
ppFile=dir([datapath ppfilestring]);
HMM_PreProcessFile=([datapath ppfilestring]);

load([datapath ppFile.name],'-mat'); %load HMM_PreProcessData file

tmp=max(strfind(HMM_PreProcessFile,'\'));
fnbase=HMM_PreProcessFile(tmp+1:end-6);

FS=HMM_PreProcessData.FilledStates; %states of interactions

Nfiles=size(FS,2);
Files=dir([datapath filestring]);
cnt=1;
multi=1;

deltaT=2; %calculate jump size for specific bin of deltaT
inc=0;sdinc=0;sz=1;sdsz=1;
clear sdr2 r2sort ystep Firstr2 Multir2

Firstr2=[];
Multir2=[];

%%
for nf=1:Nfiles %Loop over number of files
    fprintf('Analyzing File: %d of %d\n',nf,Nfiles)
    filename = Files(nf).name;
    load([datapath filename],'-mat'); %load HMM_Data file
    pair=HMM_PreProcessData.PairID(Lund et al.);

    if size(FS(Lund et al.),1) == 0
        fprintf('No interactions; proceeding to next data set ...\n')
```

```matlab
        continue
    end

    for pp=1:size(FS(Lund et al.),2) %Loop over number of pairs
        ch1spot=pair(pp,1);
        xch1=HMM_Data.raw_ch1_tracks(ch1spot,:,1);
        ych1=HMM_Data.raw_ch1_tracks(ch1spot,:,2);
        v1=HMM_Data.ch1_valids(ch1spot,:);

        s=FS(Lund et al.);
        mask=s==1;
        ds=s.*mask;
        dimers=ds(:,pp);
        [a]=find(dimers); %Find all dimers within dataset
        if size(a,1) ~= 0
            if size(a,1) ~= (a(end,1)-a(1,1))+1
                for mm=1:size(find(diff(a)>1))+1 %Loop over number of multiple dimers
                    z=(find(diff(a)>1));
                    if mm == 1
                        sf=a(1,1);
                        ef=a(min(find(diff(a)>1)));
                        Multi(multi,1)=ef-sf+1;
                        multi=multi+1;
                        for ii=sf:deltaT:ef-deltaT
                            p1=ii;
                            p2=ii+deltaT;
                            if v1(1,p1)&&v1(1,p2)
                                inc=inc+1;
                                Multir2(inc,1) = (xch1(:, p1)-xch1(:, p2))^2 + (ych1(:, p1)-ych1(:,
p2))^2;
                            end
                        end
    %                    meanr2(sz,:)=[median(Multir2) (ef-sf+1)];
                        meanr2(sz,:)=[mean(Multir2) (ef-sf+1)];
                        sz=sz+1;
                    else
                        sfm=a(z(mm-1,1)+1,1);
                        if mm+1 <= size(find(diff(a)>1),1)+1
                            efm=a(z(mm,1),1); %could exceed mm
                        else
                            efm=a(end,1);
                        end
                        Multi(multi,1)=efm-sfm+1;
                        multi=multi+1;
                        for ii=sfm:deltaT:efm-deltaT
                            p1=ii;
```

```matlab
                    p2=ii+deltaT;
                    if v1(1,p1)&&v1(1,p2)
                       inc=inc+1;
                       Multir2(inc,1) = (xch1(:, p1)-xch1(:, p2))^2 + (ych1(:, p1)-ych1(:,
p2))^2;
                    end
                 end
%                    meanr2(sz,:)=[median(Multir2) (efm-sfm+1)];
                 meanr2(sz,:)=[mean(Multir2) (efm-sfm+1)];
                 sz=sz+1;
                 Multir2 = []; %PJC 9-21-10
                 inc = 0; %PJC 9-21-10
                 clear sf ef sfm efm
              end
           end
        end

     end
  end
  clear ch1spot xch1 ych1 v1 s mask ds dimers a
  for rr=1:size(FS(Lund et al.),2) %Loop over number of pairs %This is happening
multiple times! should only be done once!
     ch1spot=pair(rr,1);
     xch1=HMM_Data.raw_ch1_tracks(ch1spot,:,1);
     ych1=HMM_Data.raw_ch1_tracks(ch1spot,:,2);
     v1=HMM_Data.ch1_valids(ch1spot,:);

     s=FS(Lund et al.);
     mask=s==1;
     ds=s.*mask;
     dimers=ds(:,rr);
     [a]=find(dimers); %Find all dimers within dataset
     if size(a,1) ~= 0
        if size(a,1) == (a(end,1)-a(1,1))+1
           SingleDimer(cnt,1)=size(a,1)+1; %Length of single dimer events
           cnt=cnt+1;
           for jj=a(1,1):deltaT:a(end,1)-deltaT
              p1=jj;
              p2=jj+deltaT;
              if v1(1,p1)&&v1(1,p2)
                 sdinc=sdinc+1;
                 sdr2(sdinc,1) = (xch1(:, p1)-xch1(:, p2))^2 + (ych1(:, p1)-ych1(:, p2))^2;
              end
           end
%              sdmeanr2(sdsz,:)=[median(sdr2) (a(end,1)-a(1,1)+1)];
           sdmeanr2(sdsz,:)=[mean(sdr2) (a(end,1)-a(1,1)+1)];
```

272

```matlab
                sdr2=[];
                sdinc = 0; %PJC 9-21-10
                sdsz=sdsz+1;
            else
                continue
            end
        end
    end
    clear a
    end
    clear s mask ds
end

if sz==1 %PJC 9-21-10
    Firstr2=[];
    Multir2=[];
    meanr2=[];
    fmeanr2=sdmeanr2;
    fmeanr2=[meanr2;sdmeanr2];
    save([resdir '\DvsLifetime'],'meanr2','sdmeanr2','fmeanr2');
else
    fmeanr2=[meanr2;sdmeanr2];
    save([resdir '\DvsLifetime'],'meanr2','sdmeanr2','fmeanr2');
end

%% Plot
a=figure
axis([0 50 0 0.3]);
plot(fmeanr2(:,2)./20,fmeanr2(:,1),'bo')
xlabel('Length of Dimer (seconds)')
ylabel('Average r^2 (pix^2)')
title('Mean r^2 for All Dimers')
saveas(a,[resdir '\DvsLifetime_AllDimers' ],'fig');
saveas(a,[resdir '\DvsLifetime_AllDimers' ],'tif');

b=figure
axis([0 50 0 0.3]);
plot(meanr2(:,2)./20,meanr2(:,1),'ko')
hold on
plot(sdmeanr2(:,2)./20,sdmeanr2(:,1),'mo')
xlabel('Length of Dimer (seconds)')
ylabel('Average r^2 (pix^2)')
legend('Multiple Dimer Events','Single Dimer Event')
title('Mean r^2 for Dimers')
saveas(b,[resdir '\DvsLifetime_DimersByType' ],'fig');
saveas(b,[resdir '\DvsLifetime_DimersByType' ],'tif');
close all
```
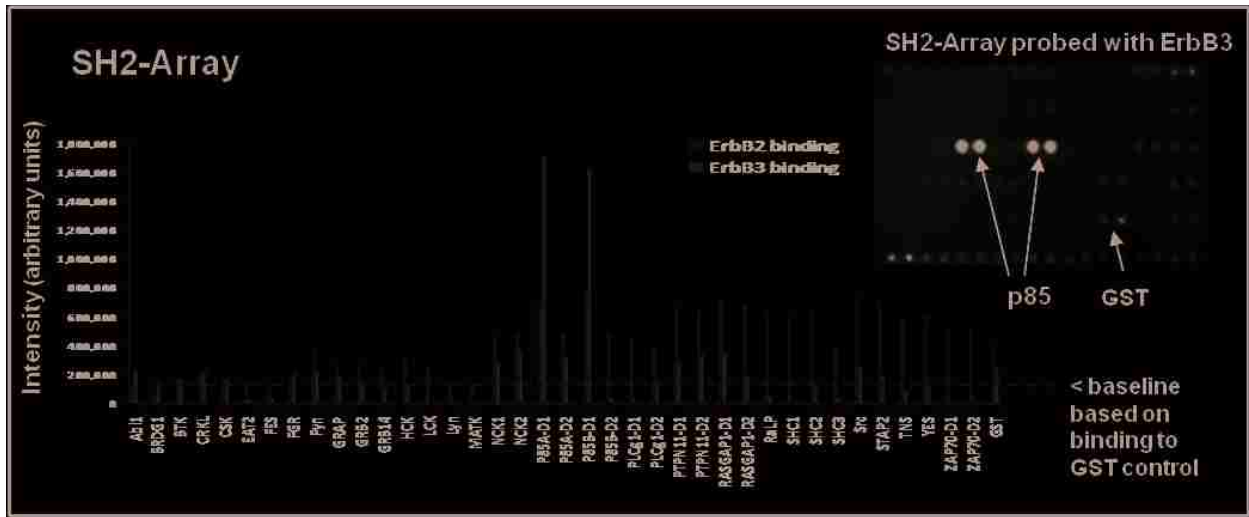
273

Supplemental Figure 4.1. Results from a TranSignal phosphotyrosine profiling (SH2) array. SKBR3 cell lysates were prepared from cells after 2 min HRG stimulation (12 nM). SH2 array membranes were incubated with cell lysates, sequentially probed with 1° antibodies for erbB3 or erbB2 and HRP-conjugated 2° antibodies, and chemiluminescence was detected using the ECL method. Quantitative data were acquired using a Genegenome densitometer and plotted for each kinase. ErbB3-specific binding was only detected for p85, a known binding partner of erbB3. An array probed with erbB3 is shown (inset).
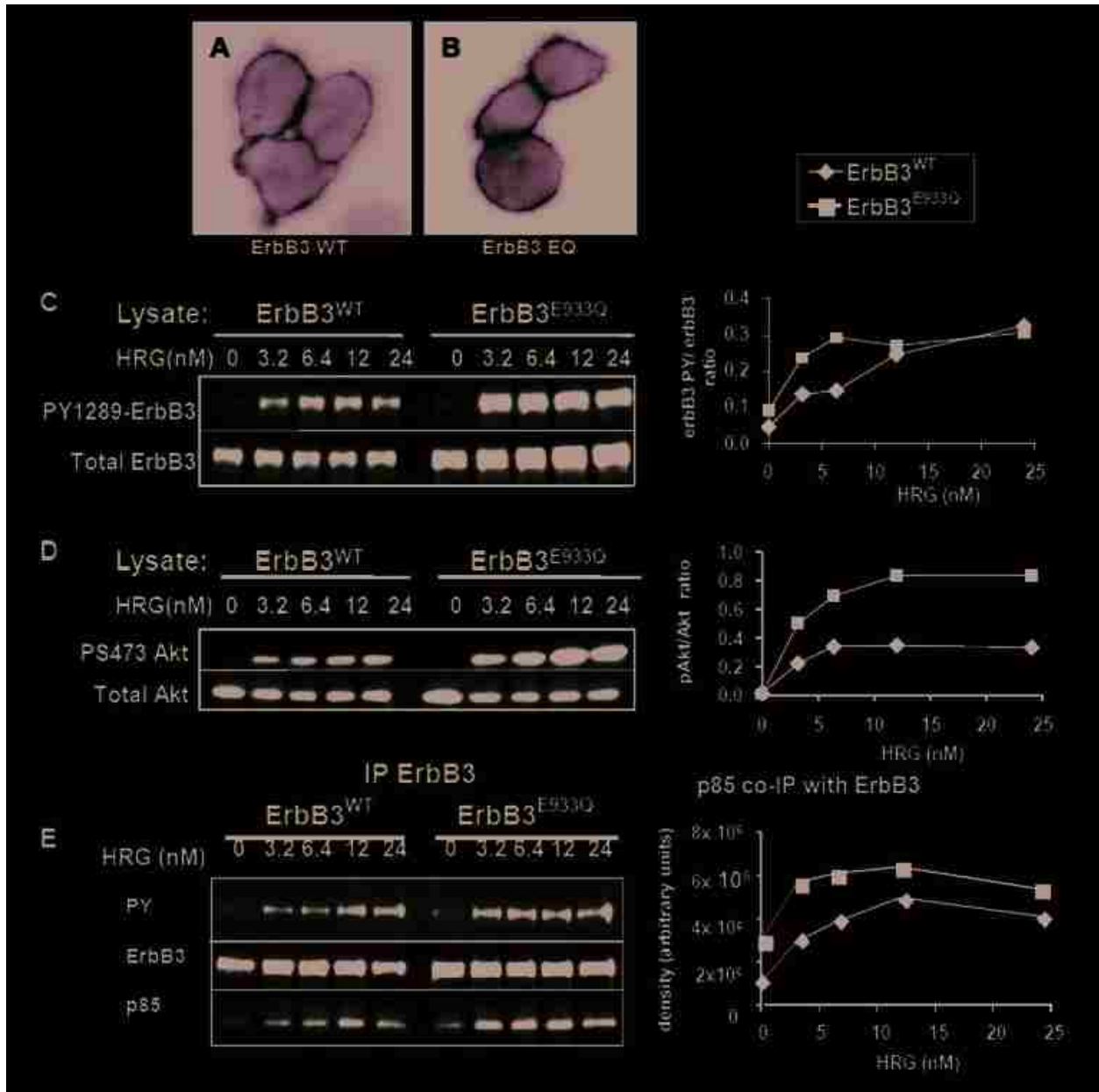
Supplemental Figure 4.2. In addition to enhancing kinase activity, the E933Q gain-of-function mutation enhances sensitivity of erbB3 to low doses of ligand. All data was collected from CHO cells stably expressing either erbB3^{WT}-mCit or erbB3^{E933Q}-mCit as indicated. (**A,B**) Fluorescence microscopy images showing transfected CHO cells expressed erbB3-mCit at the cell membrane. (**C**) Western blots of total lysates from CHO transfectants after cells were treated with varying concentrations of HRG. Blots were probed with antibodies for phospho-or total erbB3. ErbB3 tyrosine phosphorylation

(PY1289) was maximal at low doses of HRG in cells expressing erbB3^{E933Q}-mCit. (**D**) Akt, the major downstream target of erbB3, showed similarly enhanced phosphorylation in E933Q transfectants at low HRG doses. (**E**) Co-precipation of the p85 subunit of PI 3-Kinase is also maximal at low doses of HRG in cells expressing the gain-of-function mutant. Band intensities for blots in **C**, **D** and **E** were quantified and the ratio of phospho-protein to total protein (**C,D**) or relative band intensity (**E**) was plotted with respect to HRG concentration in the graphs on the right.
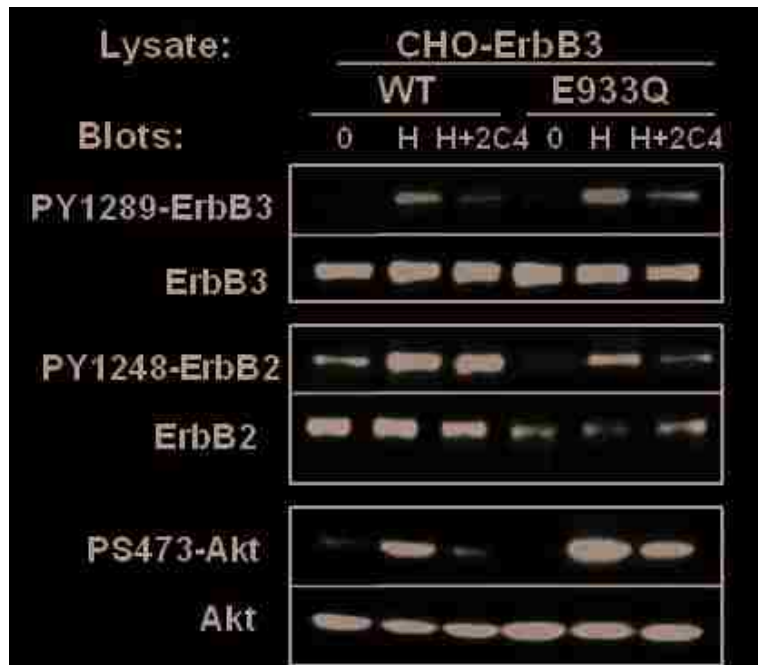
Supplemental Figure 4.3. Effect of 2C4 treatment on CHO cells transfected with ErbB3^{WT}-mCit or ErbB3^{E933Q}-mCit. Western blot of total lysates from CHO cells expressing ErbB3^{WT}-mCit or ErbB3^{E933Q}-mCit treated with 12 nM HRG, 2C4 or both as labeled above. Treatment with 2C4 reduces both ErbB3^{WT} –mCit and ErbB3^{E933Q}-mCit phosphorylation, but ErbB3^{E933Q} -mCit has a higher level of residual ErbB3 and Akt phosphorylation after treatment.
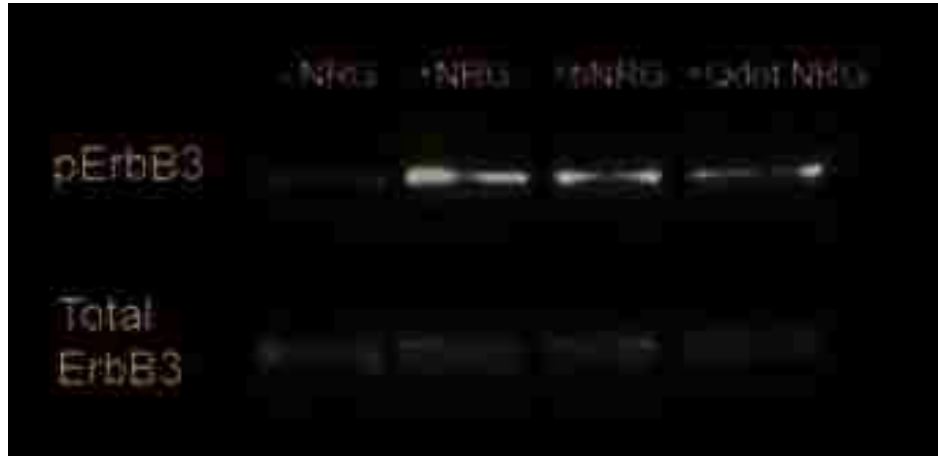
Supplemental Figure 4.4. Biotinylated HRG (bHRG) and QDot-HRG activate ErbB3 as well as unmodified HRG. SKBR3 cells were serum-starved for 4 hours and then stimulated for 2 min. with 12 nM HRG, biotinylated NRG or NRG conjugated to QDs. All 3 conditions show increased phospho-ErbB3. Total ErbB3 was used as a loading control
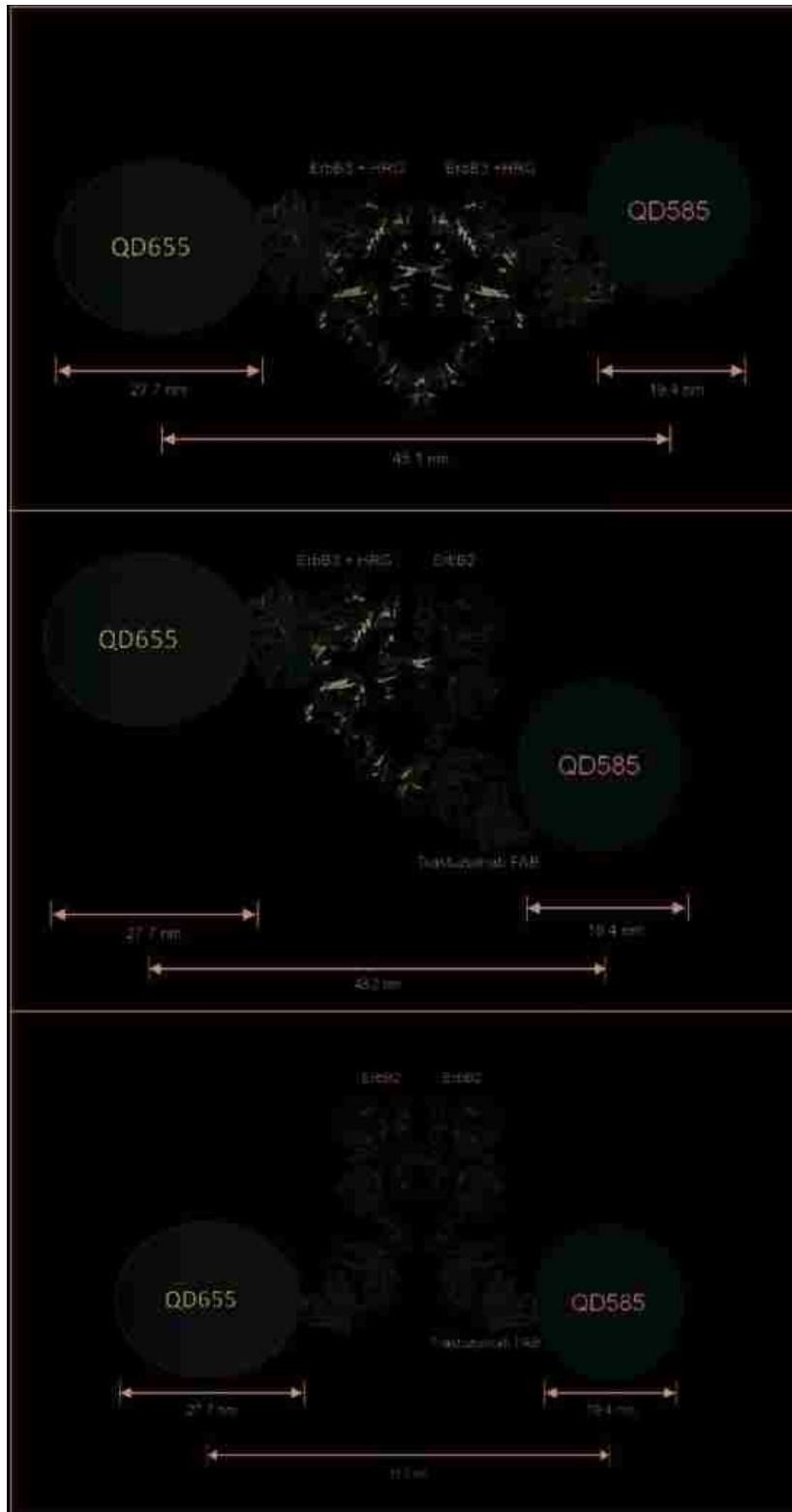
Supplemental Figure 4.5. Estimated distance from the center of QD pairs in heterodimer and homodimers. Structural information for ErbB1 dimer distances (and

ligand, ErbB2 and its FAB antibody, and reported Qdot diameters (Antelman, 2009) was used to estimate the distance between pairs of quantum dots, an important parameter for image analysis. Note that QD655 is not spherical and the longest diameter for the QD655 was used thus the calculations give an upper estimate of the Qdot distances in a dimer. **A** ErbB3 homodimer distance between Qdots. The model is based on the EGFR homodimer crystal structure (along with calculations suggesting that ErbB3 homodimer distances would be comparable (Warren et al, 2006). **B** ErbB2/ErbB3 heterodimer. Distances are based on the crystal structure of the Trastuzumab FAB bound to domain IV of the ErbB2 extracellular region (Cho et al, 2003). W e assumed rotation of Domain IV to allow dimerization.
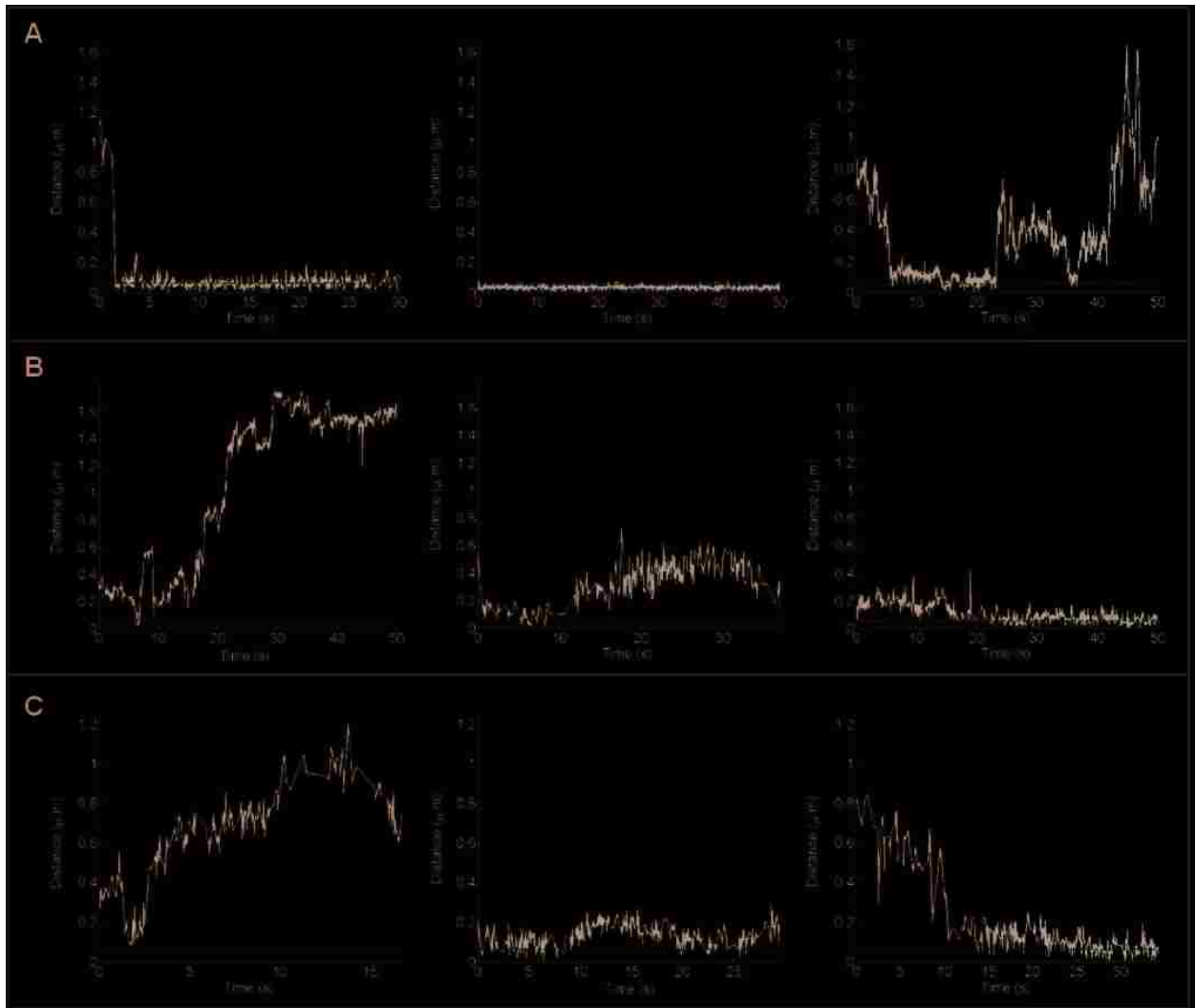
Supplemental Figure 4.6. Distanct plots of candidate pairs from single particle tracking. A) ErbB3 homodimer candidates based on separation distances between two color HRG/HRG QDot tracking have long periods where pairs are at or near the estimated dimer distance. B) ErbB2/ErbB3 heterodimer candidates (HRG/Trastuzumab Qdots) generally approach the estimated dimer distance and then separate quickly. Rare instances show receptors staying together for longer time periods. C) ErbB2 dimer candidates (two-color Trastuzumab Qdots) generally show short interactions with an occasional pair cstaying together for longer time periods. The purple line indicates the estimated distance between two Qdots in a given dimer based on distances shown in Supplemental Figure 4.

APPENDIX F – REPORTED ERBB KINETICS

Cell Line	Technique	EGFR-type	Association Constant	Dissociation Constant	Citation
A431 human epithelial carcinoma extract	Quantitative glutaraldehyde crosslinking and Quantitative Immunoblotting	Intact erbB1		2 pM	Sherrill and Kyte, 1996
Chinese Hamster Ovary	Small Angle X-ray Scattering (SAXS) to measure ligand binding kinetics	sEGFR		$3E5\ M^{-1}$	Lemmon, et al., 1997
Rat Hepatocytes	Quantitative Immunoblotting and Computational modeling	Intact erbB1	$1E^{-2}\ nM^{-1}s^{-1}$	$1E^{-2}\ s^{-1}$	Kholodenko, et al., 1999
	Analytical ultracentrifugation	sEGFR		$1.2 \pm 2.6\ \mu M$	Dawson, et al., 2005
	Computational modeling	Intact erbB1	$1E^{-2}\ nM^{-1}s^{-1}$	$1E^{-2}\ s^{-1}$	Shankaran, et al., 2006 (based on Kholodenko, et al., 1999)
A431 human epithelial carcinoma	Computational modeling	Intact erbB1	1.07047 $(\#*s/simspace)^{-1}$	$0.167\ s^{-1}$	Hsieh, et al., 2008

- sEGFR – secreted extracellular domain of erbB1
- Based on a model for dimerization that is ligand-activation dependent (in a 2:2 stoichiometric ratio)
- Lemmon rate parameter is based on equilibrium model of dimerization
- Dawson paper used TGFα as erbB1 ligand
- Number of receptors per cell covers a few orders of magnitude

References

Adams, C. W., Allison, D. E., Flagella, K., Presta, L., Clarke, J., Dybdal, N., McKeever, K., and Sliwkowski, M. X., 2006: Humanization of a recombinant monoclonal antibody to produce a therapeutic HER dimerization inhibitor, pertuzumab. *Cancer Immunol Immunother,* 55: 717-727.

Agus, D. B., Akita, R. W., Fox, W. D., Lewis, G. D., Higgins, B., Pisacane, P. I., Lofgren, J. A., Tindell, C., Evans, D. P., Maiese, K., Scher, H. I., and Sliwkowski, M. X., 2002: Targeting ligand-activated ErbB2 signaling inhibits breast and prostate tumor growth. *Cancer Cell,* 2: 127-137.

Anderson, C. M., Georgiou, G. N., Morrison, I. E., Stevenson, G. V., and Cherry, R. J., 1992: Tracking of cell surface receptors by fluorescence digital imaging microscopy using a charge-coupled device camera. Low-density lipoprotein and influenza virus receptor mobility at 4 degrees C. *J Cell Sci,* 101 (Pt 2): 415-425.

Andrews, N. L., Lidke, K. A., Pfeiffer, J. R., Burns, A. R., Wilson, B. S., Oliver, J. M., and Lidke, D. S., 2008: Actin restricts FcepsilonRI diffusion and facilitates antigen-induced receptor immobilization. *Nat Cell Biol,* 10: 955-963.

Andrews, N. L., Pfeiffer, J. R., Martinez, A. M., Haaland, D. M., Davis, R. W., Kawakami, T., Oliver, J. M., Wilson, B. S., and Lidke, D. S., 2009: Small, mobile FcepsilonRI receptor aggregates are signaling competent. *Immunity,* 31: 469-479.

Ariotti, N., Liang, H., Xu, Y., Zhang, Y., Yonekubo, Y., Inder, K., Du, G., Parton, R. G., Hancock, J. F., and Plowman, S. J., 2010: Epidermal growth factor receptor activation remodels the plasma membrane lipid environment to induce nanocluster formation. *Mol Cell Biol,* 30: 3795-3804.

Arndt-Jovin, D. J., Lidke, D. S., Lidke, K. A., Rieger, B., and Jovin, T. M., 2006: Quantum dots shed light on processes in living cells. *Proceedings of SPIE.*

Beausang, J. F., Zurla, C., Manzo, C., Dunlap, D., Finzi, L., and Nelson, P. C., 2007: DNA looping kinetics analyzed using diffusive hidden Markov model. *Biophys J,* 92: L64-66.

Beerli, R. R., Graus-Porta, D., Woods-Cook, K., Chen, X., Yarden, Y., and Hynes, N. E., 1995: Neu differentiation factor activation of ErbB-3 and ErbB-4 is cell specific and displays a differential requirement for ErbB-2. *Mol Cell Biol,* 15: 6496-6505.

Blakely, B. T., Rossi, F. M., Tillotson, B., Palmer, M., Estelles, A., and Blau, H. M., 2000: Epidermal growth factor receptor dimerization monitored in live cells. *Nat Biotechnol,* 18: 218-222.

Boni-Schnetzler, M. and Pilch, P. F., 1987: Mechanism of epidermal growth factor receptor autophosphorylation and high-affinity binding. *Proc Natl Acad Sci U S A,* 84: 7832-7836.

Burgess, A. W., Cho, H. S., Eigenbrot, C., Ferguson, K. M., Garrett, T. P., Leahy, D. J., Lemmon, M. A., Sliwkowski, M. X., Ward, C. W., and Yokoyama, S., 2003: An open-and-shut case? Recent insights into the activation of EGF/ErbB receptors. *Mol Cell,* 12: 541-552.

Campiglio, M., Ali, S., Knyazev, P. G., and Ullrich, A., 1999: Characteristics of EGFR family-mediated HRG signals in human ovarian cancer. *J Cell Biochem,* 73: 522-532.

Carraway, K. L., 3rd, Sliwkowski, M. X., Akita, R., Platko, J. V., Guy, P. M., Nuijens, A., Diamonti, A. J., Vandlen, R. L., Cantley, L. C., and Cerione, R. A., 1994: The erbB3 gene product is a receptor for heregulin. *J Biol Chem,* 269: 14303-14306.

Carter, P., Presta, L., Gorman, C. M., Ridgway, J. B., Henner, D., Wong, W. L., Rowland, A. M., Kotts, C., Carver, M. E., and Shepard, H. M., 1992: Humanization of an anti-p185HER2 antibody for human cancer therapy. *Proc Natl Acad Sci U S A,* 89: 4285-4289.

Chan, C. and Gill, G. N., 1996: Mutational analysis of the nucleotide binding site of the epidermal growth factor receptor and v-Src protein-tyrosine kinases. *J Biol Chem,* 271: 22619-22623.

Chapman-Smith, A. and Cronan, J. E., Jr., 1999: Molecular biology of biotin attachment to proteins. *J Nutr,* 129: 477S-484S.

Cheezum, M. K., Walker, W. F., and Guilford, W. H., 2001: Quantitative comparison of algorithms for tracking single fluorescent particles. *Biophys J,* 81: 2378-2388.

Chen, Y., Yang, B., and Jacobson, K., 2004: Transient confinement zones: a type of lipid raft? *Lipids,* 39: 1115-1119.

Cho, H. S., Mason, K., Ramyar, K. X., Stanley, A. M., Gabelli, S. B., Denney, D. W., Jr., and Leahy, D. J., 2003: Structure of the extracellular region of HER2 alone and in complex with the Herceptin Fab. *Nature,* 421: 756-760.

Chung, I., Akita, R., Vandlen, R., Toomre, D., Schlessinger, J., and Mellman, I., 2010: Spatial control of EGF receptor activation by reversible dimerization on living cells. *Nature,* 464: 783-787.

Churchman, L. S., Okten, Z., Rock, R. S., Dawson, J. F., and Spudich, J. A., 2005: Single molecule high-resolution colocalization of Cy3 and Cy5 attached to macromolecules measures intramolecular distances through time. *Proc Natl Acad Sci U S A,* 102: 1419-1423.

Clayton, A. H., Walker, F., Orchard, S. G., Henderson, C., Fuchs, D., Rothacker, J., Nice, E. C., and Burgess, A. W., 2005: Ligand-induced dimer-tetramer transition during the activation of the cell surface epidermal growth factor receptor-A multidimensional microscopy analysis. *J Biol Chem,* 280: 30392-30399.

Dahan, M., Levi, S., Luccardini, C., Rostaing, P., Riveau, B., and Triller, A., 2003: Diffusion dynamics of glycine receptors revealed by single-quantum dot tracking. *Science,* 302: 442-445.

Daumas, F., Destainville, N., Millot, C., Lopez, A., Dean, D., and Salome, L., 2003: Confined diffusion without fences of a g-protein-coupled receptor as revealed by single particle tracking. *Biophys J,* 84: 356-366.

Dawson, J. P., Berger, M. B., Lin, C. C., Schlessinger, J., Lemmon, M. A., and Ferguson, K. M., 2005: Epidermal growth factor receptor dimerization and

activation require ligand-induced conformational changes in the dimer interface. *Mol Cell Biol,* 25: 7734-7742.

de Keijzer, S., Serge, A., van Hemert, F., Lommerse, P. H., Lamers, G. E., Spaink, H. P., Schmidt, T., and Snaar-Jagalska, B. E., 2008: A spatially restricted increase in receptor mobility is involved in directional sensing during Dictyostelium discoideum chemotaxis. *J Cell Sci,* 121: 1750-1757.

De Meyts, P., 2008: The insulin receptor: a prototype for dimeric, allosteric membrane receptors? *Trends Biochem Sci,* 33: 376-384.

Dehmelt, L. and Bastiaens, P. I., 2010: Spatial organization of intracellular communication: insights from imaging. *Nat Rev Mol Cell Biol,* 11: 440-452.

Dhand, R., Hiles, I., Panayotou, G., Roche, S., Fry, M. J., Gout, I., Totty, N. F., Truong, O., Vicendo, P., Yonezawa, K., and et al., 1994: PI 3-kinase is a dual specificity enzyme: autoregulation by an intrinsic protein-serine kinase activity. *EMBO J,* 13: 522-533.

Diagaradjane, P., Orenstein-Cardona, J. M., Colon-Casasnovas, N. E., Deorukhkar, A., Shentu, S., Kuno, N., Schwartz, D. L., Gelovani, J. G., and Krishnan, S., 2008: Imaging epidermal growth factor receptor expression in vivo: pharmacokinetic and biodistribution characterization of a bioconjugated quantum dot nanoprobe. *Clin Cancer Res,* 14: 731-741.

Diermeier, S., Horváth, G., Knuechel-Clarke, R., Hofstaedter, F., Szöllosi, J., and Brockhoff, G., 2005: Epidermal growth factor receptor coexpression modulates susceptibility to Herceptin in HER2/neu overexpressing breast cancer cells via specific erbB-receptor interaction and activation. *Experimental Cell Research,* 304: 604-619.

Douglass, A. D. and Vale, R. D., 2005: Single-molecule microscopy reveals plasma membrane microdomains created by protein-protein networks that exclude or trap signaling molecules in T cells. *Cell,* 121: 937-950.

Dumoulin, M., Conrath, K., Van Meirhaeghe, A., Meersman, F., Heremans, K., Frenken, L. G., Muyldermans, S., Wyns, L., and Matagne, A., 2002: Single-domain antibody fragments with high conformational stability. *Protein Sci,* 11: 500-515.

Ehrensperger, M. V., Hanus, C., Vannier, C., Triller, A., and Dahan, M., 2007: Multiple association states between glycine receptors and gephyrin identified by SPT analysis. *Biophys J,* 92: 3706-3718.

Engelman, J. A., Zejnullahu, K., Mitsudomi, T., Song, Y., Hyland, C., Park, J. O., Lindeman, N., Gale, C. M., Zhao, X., Christensen, J., Kosaka, T., Holmes, A. J., Rogers, A. M., Cappuzzo, F., Mok, T., Lee, C., Johnson, B. E., Cantley, L. C., and Janne, P. A., 2007: MET amplification leads to gefitinib resistance in lung cancer by activating ERBB3 signaling. *Science,* 316: 1039-1043.

Fabian, M. A., Biggs, W. H., 3rd, Treiber, D. K., Atteridge, C. E., Azimioara, M. D., Benedetti, M. G., Carter, T. A., Ciceri, P., Edeen, P. T., Floyd, M., Ford, J. M., Galvin, M., Gerlach, J. L., Grotzfeld, R. M., Herrgard, S., Insko, D. E., Insko, M. A., Lai, A. G., Lelias, J. M., Mehta, S. A., Milanov, Z. V., Velasco, A. M., Wodicka,

L. M., Patel, H. K., Zarrinkar, P. P., and Lockhart, D. J., 2005: A small molecule-kinase interaction map for clinical kinase inhibitors. *Nat Biotechnol,* 23: 329-336.

Ferguson, K. M., Berger, M. B., Mendrola, J. M., Cho, H. S., Leahy, D. J., and Lemmon, M. A., 2003: EGF activates its receptor by removing interactions that autoinhibit ectodomain dimerization. *Mol Cell,* 11: 507-517.

Ferguson, K. M., 2008: Structure-based view of epidermal growth factor receptor regulation. *Annu Rev Biophys,* 37: 353-373.

Forney, G. D., 1973: Viterbi algorithm. *Proceedings of the IEEE,* 61: 268-278.

Franklin, M. C., Carey, K. D., Vajdos, F. F., Leahy, D. J., de Vos, A. M., and Sliwkowski, M. X., 2004: Insights into ErbB signaling from the structure of the ErbB2-pertuzumab complex. *Cancer Cell,* 5: 317-328.

Fry, D. W., Kraker, A. J., McMichael, A., Ambroso, L. A., Nelson, J. M., Leopold, W. R., Connors, R. W., and Bridges, A. J., 1994: A specific inhibitor of the epidermal growth factor receptor tyrosine kinase. *Science,* 265: 1093-1095.

Gadella, T. W., Jr. and Jovin, T. M., 1995: Oligomerization of epidermal growth factor receptors on A431 cells studied by time-resolved fluorescence imaging microscopy. A stereochemical model for tyrosine kinase receptor activation. *J Cell Biol,* 129: 1543-1558.

Graus-Porta, D., Beerli, R. R., Daly, J. M., and Hynes, N. E., 1997: ErbB-2, the preferred heterodimerization partner of all ErbB receptors, is a mediator of lateral signaling. *EMBO J,* 16: 1647-1655.

Guy, P. M., Platko, J. V., Cantley, L. C., Cerione, R. A., and Carraway, K. L., 3rd, 1994: Insect cell-expressed p180erbB3 possesses an impaired tyrosine kinase activity. *Proc Natl Acad Sci U S A,* 91: 8132-8136.

Haase, P., 1995: Spatial pattern analysis in ecology based on Ripley's K-function: Introduction and methods of edge correction. *journal of Vegetation Science,* 6: 575-582.

Harmsen, M. M. and De Haard, H. J., 2007: Properties, production, and applications of camelid single-domain antibody fragments. *Appl Microbiol Biotechnol,* 77: 13-22.

Hellyer, N. J., Kim, M. S., and Koland, J. G., 2001: Heregulin-dependent activation of phosphoinositide 3-kinase and Akt via the ErbB2/ErbB3 co-receptor. *J Biol Chem,* 276: 42153-42161.

Hofman, E. G., Ruonala, M. O., Bader, A. N., van den Heuvel, D., Voortman, J., Roovers, R. C., Verkleij, A. J., Gerritsen, H. C., and van Bergen En Henegouwen, P. M., 2008: EGF induces coalescence of different lipid rafts. *J Cell Sci,* 121: 2519-2528.

Hofman, E. G., Bader, A. N., Voortman, J., Van den Heuvel, D. J., Sigismund, S., Verkleij, A. J., Gerritsen, H. C., and Van Bergen En Henegouwen, P. M., 2010: Ligand-induced epidermal growth factor receptor (EGFR) oligomerization is kinase-dependent and enhances internalization. *J Biol Chem.*

Holliger, P. and Hudson, P. J., 2005: Engineered antibody fragments and the rise of single domains. *Nat Biotechnol,* 23: 1126-1136.

Howarth, M., Chinnapen, D. J., Gerrow, K., Dorrestein, P. C., Grandy, M. R., Kelleher, N. L., El-Husseini, A., and Ting, A. Y., 2006: A monovalent streptavidin with a single femtomolar biotin binding site. *Nat Methods,* 3: 267-273.

Hsieh, M. Y., Yang, S., Raymond-Stinz, M. A., Steinberg, S., Vlachos, D. G., Shu, W., Wilson, B., and Edwards, J. S., 2008: Stochastic simulations of ErbB homo and heterodimerisation: potential impacts of receptor conformational state and spatial segregation. *IET Syst Biol,* 2: 256-272.

Hubbard, S. R., 2004: Juxtamembrane autoinhibition in receptor tyrosine kinases. *Nat Rev Mol Cell Biol,* 5: 464-471.

Ichinose, J., Murata, M., Yanagida, T., and Sako, Y., 2004: EGF signalling amplification induced by dynamic clustering of EGFR. *Biochem Biophys Res Commun,* 324: 1143-1149.

Jeong, E. G., Soung, Y. H., Lee, J. W., Lee, S. H., Nam, S. W., Lee, J. Y., and Yoo, N. J., 2006: ERBB3 kinase domain mutations are rare in lung, breast and colon carcinomas. *Int J Cancer,* 119: 2986-2987.

Jonas, M., Yao, Y., So, P. T., and Dewey, C. F., Jr., 2006: Detecting single quantum dot motion with nanometer resolution for applications in cell biology. *IEEE Trans Nanobioscience,* 5: 246-250.

Jura, N., Endres, N. F., Engel, K., Deindl, S., Das, R., Lamers, M. H., Wemmer, D. E., Zhang, X., and Kuriyan, J., 2009a: Mechanism for activation of the EGF receptor catalytic domain by the juxtamembrane segment. *Cell,* 137: 1293-1307.

Jura, N., Shan, Y., Cao, X., Shaw, D. E., and Kuriyan, J., 2009b: Structural analysis of the catalytically inactive kinase domain of the human EGF receptor 3. *Proc Natl Acad Sci U S A,* 106: 21608-21613.

Kani, K., Warren, C. M., Kaddis, C. S., Loo, J. A., and Landgraf, R., 2005: Oligomers of ERBB3 have two distinct interfaces that differ in their sensitivity to disruption by heregulin. *J Biol Chem,* 280: 8238-8247.

Keating, E., Nohe, A., and Petersen, N. O., 2008: Studies of distribution, location and dynamic properties of EGFR on the cell surface measured by image correlation spectroscopy. *Eur Biophys J,* 37: 469-481.

Kholodenko, B. N., Demin, O. V., Moehren, G., and Hoek, J. B., 1999: Quantification of Short Term Signaling by the Epidermal Growth Factor Receptor. *Journal of Biological Chemistry,* 274: 30169-30181.

Klein, P., Mattoon, D., Lemmon, M. A., and Schlessinger, J., 2004: A structure-based model for ligand binding and dimerization of EGF receptors. *Proc Natl Acad Sci U S A,* 101: 929-934.

Kusumi, A., Sako, Y., and Yamamoto, M., 1993: Confined Lateral Diffusion of Membrane Receptors as Studied by Single Particle Tracking (Nanovid

Microscopy). Effects of Calcium-Induced Differentiation in Cultured Epithelial Cells. *Biophysical Journal,* 65: 2021-2040.

Landgraf, R. and Eisenberg, D., 2000: Heregulin reverses the oligomerization of HER3. *Biochemistry,* 39: 8503-8511.

Larkin, M. A., Blackshields, G., Brown, N. P., Chenna, R., McGettigan, P. A., McWilliam, H., Valentin, F., Wallace, I. M., Wilm, A., Lopez, R., Thompson, J. D., Gibson, T. J., and Higgins, D. G., 2007: Clustal W and Clustal X version 2.0. *Bioinformatics,* 23: 2947-2948.

Lee, J. W., Soung, Y. H., Seo, S. H., Kim, S. Y., Park, C. H., Wang, Y. P., Park, K., Nam, S. W., Park, W. S., Kim, S. H., Lee, J. Y., Yoo, N. J., and Lee, S. H., 2006: Somatic mutations of ERBB2 kinase domain in gastric, colorectal, and breast carcinomas. *Clin Cancer Res,* 12: 57-61.

Lemmon, M. A., Treutlein, H. R., Adams, P. D., Brunger, A. T., and Engelman, D. M., 1994: A dimerization motif for transmembrane alpha-helices. *Nat Struct Biol,* 1: 157-163.

Lemmon, M. A., Bu, Z., Ladbury, J. E., Zhou, M., Pinchasi, D., Lax, I., Engelman, D. M., and Schlessinger, J., 1997: Two EGF molecules contribute additively to stabilization of the EGFR dimer. *EMBO J,* 16: 281-294.

Lemmon, M. A. and Schlessinger, J., 2010: Cell signaling by receptor tyrosine kinases. *Cell,* 141: 1117-1134.

Lidke, D. S., Nagy, P., Heintzmann, R., Arndt-Jovin, D. J., Post, J. N., Grecco, H. E., Jares-Erijman, E. A., and Jovin, T. M., 2004: Quantum dot ligands provide new insights into erbB/HER receptor-mediated signal transduction. *Nat Biotechnol,* 22: 198-203.

Lidke, D. S., Lidke, K. A., Rieger, B., Jovin, T. M., and Arndt-Jovin, D. J., 2005a: Reaching out for signals: filopodia sense EGF and respond by directed retrograde transport of activated receptors. *J Cell Biol,* 170: 619-626.

Lidke, D. S. and Wilson, B. S., 2009: Caught in the act: quantifying protein behaviour in living cells. *Trends Cell Biol,* 19: 566-574.

Lidke, K., Rieger, B., Jovin, T., and Heintzmann, R., 2005b: Superresolution by localization of quantum dots using blinking statistics. *Opt Express,* 13: 7052-7062.

Lidke, K. A., Rieger, B., Lidke, D. S., and Jovin, T. M., 2005c: The role of photon statistics in fluorescence anisotropy imaging. *IEEE Trans Image Process,* 14: 1237-1245.

Lillemeier, B. F., Pfeiffer, J. R., Surviladze, Z., Wilson, B. S., and Davis, M. M., 2006: Plasma membrane-associated proteins are clustered into islands attached to the cytoskeleton. *Proc Natl Acad Sci U S A,* 103: 18992-18997.

Liu, H. Y. and Vu, T. Q., 2007: Identification of quantum dot bioconjugates and cellular protein co-localization by hybrid gel blotting. *Nano Lett,* 7: 1044-1049.

Lund, K. A., Lazar, C. S., Chen, W. S., Walsh, B. J., Welsh, J. B., Herbst, J. J., Walton, G. M., Rosenfeld, M. G., Gill, G. N., and Wiley, H. S., 1990: Phosphorylation of the epidermal growth factor receptor at threonine 654 inhibits ligand-induced internalization and down-regulation. *J Biol Chem,* 265: 20517-20523.

Macdonald, J. L. and Pike, L. J., 2008: Heterogeneity in EGF-binding affinities arises from negative cooperativity in an aggregating system. *Proc Natl Acad Sci U S A,* 105: 112-117.

Mattoon, D., Klein, P., Lemmon, M. A., Lax, I., and Schlessinger, J., 2004: The tethered configuration of the EGF receptor extracellular domain exerts only a limited control of receptor function. *Proc Natl Acad Sci U S A,* 101: 923-928.

Metzger, H., 1992: Transmembrane signaling: the joy of aggregation. *J Immunol,* 149: 1477-1487.

Michalet, X., Pinaud, F. F., Bentolila, L. A., Tsay, J. M., Doose, S., Li, J. J., Sundaresan, G., Wu, A. M., Gambhir, S. S., and Weiss, S., 2005: Quantum dots for live cells, in vivo imaging, and diagnostics. *Science,* 307: 538-544.

Monsey, J., Shen, W., Schlesinger, P., and Bose, R., Her4 and Her2/neu tyrosine kinase domains dimerize and activate in a reconstituted in vitro system. *J Biol Chem,* 285: 7035-7044.

Moriki, T., Maruyama, H., and Maruyama, I. N., 2001: Activation of preformed EGF receptor dimers by ligand-induced rotation of the transmembrane domain. *J Mol Biol,* 311: 1011-1026.

Murase, K., Fujiwara, T., Umemura, Y., Suzuki, K., Iino, R., Yamashita, H., Saito, M., Murakoshi, H., Ritchie, K., and Kusumi, A., 2004: Ultrafine membrane compartments for molecular diffusion as revealed by single molecule techniques. *Biophys J,* 86: 4075-4093.

Muyldermans, S., Cambillau, C., and Wyns, L., 2001: Recognition of antigens by single-domain antibody fragments: the superfluous luxury of paired domains. *Trends Biochem Sci,* 26: 230-235.

Nagy, P., Claus, J., Jovin, T. M., and Arndt-Jovin, D. J., 2010: Distribution of resting and ligand-bound ErbB1 and ErbB2 receptor tyrosine kinases in living cells using number and brightness analysis. *Proc Natl Acad Sci U S A,* 107: 16524-16529.

Nehilla, B. J., Vu, T. Q., and Desai, T. A., 2005: Stoichiometry-dependent formation of quantum dot-antibody bioconjugates: a complementary atomic force microscopy and agarose gel electrophoresis study. *J Phys Chem B,* 109: 20724-20730.

Nirmal, M., Norris, D. J., Kuno, M., Bawendi, M. G., Efros, A. L., and Rosen, M., 1995: Observation of the "Dark exciton" in CdSe quantum dots. *Phys Rev Lett,* 75: 3728-3731.

Orr, G., Hu, D., Ozcelik, S., Opresko, L. K., Wiley, H. S., and Colson, S. D., 2005: Cholesterol dictates the freedom of EGF receptors and HER2 in the plane of the membrane. *Biophys J,* 89: 1362-1373.

Owen, D. M., Lanigan, P. M., Dunsby, C., Munro, I., Grant, D., Neil, M. A., French, P. M., and Magee, A. I., 2006: Fluorescence lifetime imaging provides enhanced contrast when imaging the phase-sensitive dye di-4-ANEPPDHQ in model membranes and live cells. *Biophys J,* 90: L80-82.

Paez, J. G., Janne, P. A., Lee, J. C., Tracy, S., Greulich, H., Gabriel, S., Herman, P., Kaye, F. J., Lindeman, N., Boggon, T. J., Naoki, K., Sasaki, H., Fujii, Y., Eck, M. J., Sellers, W. R., Johnson, B. E., and Meyerson, M., 2004: EGFR mutations in lung cancer: correlation with clinical response to gefitinib therapy. *Science,* 304: 1497-1500.

Pawson, T., 2004: Specificity in signal transduction: from phosphotyrosine-SH2 domain interactions to complex cellular systems. *Cell,* 116: 191-203.

Pons, T., Uyeda, H. T., Medintz, I. L., and Mattoussi, H., 2006: Hydrodynamic dimensions, electrophoretic mobility, and stability of hydrophilic quantum dots. *J Phys Chem B,* 110: 20308-20316.

Rabiner, L. R., 1989: A Tutorial on Hidden Markov Models and Selected Applications in Speech Recognition. *Proceedings of the IEEE,* 77: 257-286.

Red Brewer, M., Choi, S. H., Alvarado, D., Moravcevic, K., Pozzi, A., Lemmon, M. A., and Carpenter, G., 2009: The juxtamembrane region of the EGF receptor functions as an activation domain. *Mol Cell,* 34: 641-651.

Reynolds, A. R., Tischer, C., Verveer, P. J., Rocks, O., and Bastiaens, P. I., 2003: EGFR activation coupled to inhibition of tyrosine phosphatases causes lateral signal propagation. *Nat Cell Biol,* 5: 447-453.

Roovers, R. C., Laeremans, T., Huang, L., De Taeye, S., Verkleij, A. J., Revets, H., de Haard, H. J., and van Bergen en Henegouwen, P. M., 2007: Efficient inhibition of EGFR signaling and of tumour growth by antagonistic anti-EFGR Nanobodies. *Cancer Immunol Immunother,* 56: 303-317.

Roullier, V., Clarke, S., You, C., Pinaud, F., Gouzer, G. G., Schaible, D., Marchi-Artzner, V., Piehler, J., and Dahan, M., 2009: High-affinity labeling and tracking of individual histidine-tagged proteins in live cells using Ni2+ tris-nitrilotriacetic acid quantum dot conjugates. *Nano Lett,* 9: 1228-1234.

Ruhe, J. E., Streit, S., Hart, S., Wong, C. H., Specht, K., Knyazev, P., Knyazeva, T., Tay, L. S., Loo, H. L., Foo, P., Wong, W., Pok, S., Lim, S. J., Ong, H., Luo, M., Ho, H. K., Peng, K., Lee, T. C., Bezler, M., Mann, C., Gaertner, S., Hoefler, H., Iacobelli, S., Peter, S., Tay, A., Brenner, S., Venkatesh, B., and Ullrich, A., 2007: Genetic alterations in the tyrosine kinase transcriptome of human cancer cell lines. *Cancer Res,* 67: 11368-11376.

Saffarian, S., Li, Y., Elson, E. L., and Pike, L. J., 2007: Oligomerization of the EGF receptor investigated by live cell fluorescence intensity distribution analysis. *Biophys J,* 93: 1021-1031.

Sako, Y., Minoghchi, S., and Yanagida, T., 2000: Single-molecule imaging of EGFR signalling on the surface of living cells. *Nat Cell Biol,* 2: 168-172.

289

Saxton, M. J. and Jacobson, K., 1997: Single-particle tracking: applications to membrane dynamics. *Annu Rev Biophys Biomol Struct,* 26: 373-399.

Schlessinger, J., 2002: Ligand-induced, receptor-mediated dimerization and activation of EGF receptor. *Cell,* 110: 669-672.

Schutz, G. J., Schindler, H., and Schmidt, T., 1997: Single-molecule microscopy on model membranes reveals anomalous diffusion. *Biophys J,* 73: 1073-1080.

Sergina, N. V., Rausch, M., Wang, D., Blair, J., Hann, B., Shokat, K. M., and Moasser, M. M., 2007: Escape from HER-family tyrosine kinase inhibitor therapy by the kinase-inactive HER3. *Nature,* 445: 437-441.

Shankaran, H., Wiley, H. S., and Resat, H., 2006: Modeling the effects of HER/ErbB1-3 coexpression on receptor dimerization and biological response. *Biophys J,* 90: 3993-4009.

Sharma, V., Wang, Q., and Lawrence, D. S., 2008: Peptide-based fluorescent sensors of protein kinase activity: design and applications. *Biochim Biophys Acta,* 1784: 94-99.

Sherrill, J. M. and Kyte, J., 1996: Activation of Epidermal Growth Factor Receptor by Epidermal Growth Factor. *Biochemistry,* 35: 5705-5718.

Shi, F., Telesco, S. E., Liu, Y., Radhakrishnan, R., and Lemmon, M. A., 2010: ErbB3/HER3 intracellular domain is competent to bind ATP and catalyze autophosphorylation. *Proc Natl Acad Sci U S A,* 107: 7692-7697.

Sierke, S. L., Cheng, K., Kim, H. H., and Koland, J. G., 1997: Biochemical characterization of the protein tyrosine kinase homology domain of the ErbB3 (HER3) receptor protein. *Biochem J,* 322 (Pt 3): 757-763.

Simson, R., Sheets, E. D., and Jacobson, K., 1995: Detection of temporary lateral confinement of membrane proteins using single-particle tracking analysis. *Biophys J,* 69: 989-993.

Singer, S. J. and Nicolson, G. L., 1972: The fluid mosaic model of the structure of cell membranes. *Science,* 175: 720-731.

Smith, C. S., Joseph, N., Rieger, B., and Lidke, K. A., 2010: Fast, single-molecule localization that achieves theoretically minimum uncertainty. *Nat Methods,* 7: 373-375.

Soung, Y. H., Lee, J. W., Kim, S. Y., Wang, Y. P., Jo, K. H., Moon, S. W., Park, W. S., Nam, S. W., Lee, J. Y., Yoo, N. J., and Lee, S. H., 2006: Somatic mutations of the ERBB4 kinase domain in human cancers. *Int J Cancer,* 118: 1426-1429.

Tada, H., Higuchi, H., Wanatabe, T. M., and Ohuchi, N., 2007: In vivo real-time tracking of single quantum dots conjugated with monoclonal anti-HER2 antibody in tumors of mice. *Cancer Res,* 67: 1138-1144.

Uyemura, T., Takagi, H., Yanagida, T., and Sako, Y., 2005: Single-molecule analysis of epidermal growth factor signaling that leads to ultrasensitive calcium response. *Biophys J,* 88: 3720-3730.

Verveer, P. J., Wouters, F. S., Reynolds, A. R., and Bastiaens, P. I., 2000: Quantitative imaging of lateral ErbB1 receptor signal propagation in the plasma membrane. *Science,* 290: 1567-1570.

Viterbi, A. J., 1967: Error Bounds for Convolutional Codes and an Asymptotically Optimum Decoding Algorithm. *IEEE Transactions on Information Theory,* IT-13: 260-269.

Wang, Y., Pennock, S., Chen, X., and Wang, Z., 2002: Endosomal signaling of epidermal growth factor receptor stimulates signal transduction pathways leading to cell survival. *Mol Cell Biol,* 22: 7279-7290.

Webb, S. E., Roberts, S. K., Needham, S. R., Tynan, C. J., Rolfe, D. J., Winn, M. D., Clarke, D. T., Barraclough, R., and Martin-Fernandez, M. L., 2008: Single-molecule imaging and fluorescence lifetime imaging microscopy show different structures for high- and low-affinity epidermal growth factor receptors in A431 cells. *Biophys J,* 94: 803-819.

Whitson, K. B., Whitson, S. R., Red-Brewer, M. L., McCoy, A. J., Vitali, A. A., Walker, F., Johns, T. G., Beth, A. H., and Staros, J. V., 2005: Functional effects of glycosylation at Asn-579 of the epidermal growth factor receptor. *Biochemistry,* 44: 14920-14931.

Wieduwilt, M. J. and Moasser, M. M., 2008: The epidermal growth factor receptor family: biology driving targeted therapeutics. *Cell Mol Life Sci,* 65: 1566-1584.

Wilson, B. S., Pfeiffer, J. R., and Oliver, J. M., 2000: Observing FcepsilonRI signaling from the inside of the mast cell membrane. *J Cell Biol,* 149: 1131-1142.

Wilson, B. S., Steinberg, S. L., Liederman, K., Pfeiffer, J. R., Surviladze, Z., Zhang, J., Samelson, L. E., Yang, L. H., Kotula, P. G., and Oliver, J. M., 2004: Markers for detergent-resistant lipid rafts occupy distinct and dynamic domains in native membranes. *Mol Biol Cell,* 15: 2580-2592.

Wilson, B. S., Pfeiffer, J. R., Raymond-Stintz, M. A., Lidke, D., Andrews, N., Zhang, J., Yin, W., Steinberg, S., and Oliver, J. M., 2007: Exploring membrane domains using native membrane sheets and transmission electron microscopy. *Methods Mol Biol,* 398: 245-261.

Wofsy, C., Goldstein, B., Lund, K., and Wiley, H. S., 1992: Implications of epidermal growth factor (EGF) induced egf receptor aggregation. *Biophys J,* 63: 98-110.

Xiao, Z., Zhang, W., Yang, Y., Xu, L., and Fang, X., 2008: Single-molecule diffusion study of activated EGFR implicates its endocytic pathway. *Biochem Biophys Res Commun,* 369: 730-734.

Yamabhai, M. and Anderson, R. G., 2002: Second cysteine-rich region of epidermal growth factor receptor contains targeting information for caveolae/rafts. *J Biol Chem,* 277: 24843-24846.

Yang, S., Raymond-Stintz, M. A., Ying, W., Zhang, J., Lidke, D. S., Steinberg, S. L., Williams, L., Oliver, J. M., and Wilson, B. S., 2007: Mapping ErbB receptors on

breast cancer cell membranes during signal transduction. *J Cell Sci,* 120: 2763-2773.

Yarden, Y. and Sliwkowski, M. X., 2001: Untangling the ErbB signalling network. *Nat Rev Mol Cell Biol,* 2: 127-137.

Zhang, H., Berezov, A., Wang, Q., Zhang, G., Drebin, J., Murali, R., and Greene, M. I., 2007: ErbB receptors: from oncogenes to targeted cancer therapies. *J Clin Invest,* 117: 2051-2058.

Zhang, J., Leiderman, K., Pfeiffer, J. R., Wilson, B. S., Oliver, J. M., and Steinberg, S. L., 2006a: Characterizing the topography of membrane receptors and signaling molecules from spatial patterns obtained using nanometer-scale electron-dense probes and electron microscopy. *Micron,* 37: 14-34.

Zhang, X., Gureasko, J., Shen, K., Cole, P. A., and Kuriyan, J., 2006b: An allosteric mechanism for activation of the kinase domain of epidermal growth factor receptor. *Cell,* 125: 1137-1149.

Zidovetzki, R., Bartholdi, M., Arndt-Jovin, D., and Jovin, T. M., 1986: Rotational dynamics of the Fc receptor for immunoglobulin E on histamine-releasing rat basophilic leukemia cells. *Biochemistry,* 25: 4397-4401.

292